




INSTITUT DE CIÈNCIES
DEL MAR DE BARCELONA

CONSEJO SUPERIOR DE
INVESTIGACIONES CIENTÍFICAS

UNIVERSITAT POLITÈCNICA
DE CATALUNYA

# *BIOGEOCHEMICAL MODELLING OF UPPER OCEAN SULFUR DYNAMICS AND ITS IMPACT ON CLOUD FORMING AEROSOLS*

Sergio M. Vallina

Memoria per optar al títol de Doctor en Ciències del Mar en el *Departament d'Enginyeria Hidráulica, Martíma I Ambiental* per la Universitat Politécnica de Catalunya (UPC), sota la direcció del Dr. Rafel Simó a l'Institut de Ciències del Mar de Barcelona - Consejo Superior de Investigaciones Científicas (ICM - CSIC).

Barcelona, 31 d'Octubre de 2006

# Agradecimientos

Llegar a realizar una tesis doctoral requiere que varios factores confluyan: tener motivación, que te den la oportunidad de trabajar, que surja la creatividad, y que haya un poquito de suerte. La persona que ha hecho posible que esa receta se haya mantenido el tiempo necesario para que yo haya llegado a este nuevo punto de inflexión en mi vida es Rafel Simó. Mi amigo Simó. Por tu capacidad de liderazgo sin nunca querer imponer a la fuerza tus ideas, por tu enorme capacidad intelectual desprovista de arrogancia, por tu aún más enorme calidad humana y emocional, te admiro. Confiaste en mí sin conocerme, me diste la libertad de movimiento justa, siempre me has tratado de tú a tú en nuestras conversaciones científicas (y no científicas), y siempre has sido justo al valorar mi trabajo. Cuando creías que había hecho algo bien me lo decías con ilusión; cuando creías que me había quedado por debajo lo que esperabas, me lo decías sin hundirme. Eso me ha permitido sacar lo mejor de mí mismo. Gracias a tu manera de ser y de dirigirme la tesis, nunca he tenido miedo de arriesgar. Para mí eres el 'jefe' perfecto. Gracias de todo corazón.

Desde un punto de vista profesional he tenido también el apoyo de varias otras personas. Jordi Dachs me siguió muy de cerca el trabajo y contribuyó con sus grandes ideas. Elena Jurado compartió conmigo datos y programas Matlab (además de alguna cervecita). Evilio del Río ha sido como mi Dios-Linux personal; no se que hubiera sido de mí sin su inestimable ayuda. Además me cae muy bien. Antonio Turiel me sorprendió con su inteligencia (él juega en otra liga) y su disponibilidad para con el común de los mortales. Y Jordi Soler; nunca he entendido del todo su salto 'cuántico' da la quantum-physics al ecosystem-modelling, supongo que Heisenberg tiene algo que ver... Pero a mi me vino muy bien pues lo freí a preguntas. Gracias por estar siempre disponible. También me gustaría agradecer a Carles Pedrós-Alió sus audaces respuestas a mis tontas preguntas. Y el que no se haya enfadado conmigo porque al final nunca abordara el tema de algoritmos para la producción bacteriana como le prometí al principio... Por último le tengo que dar las gracias más sinceras a un magnifico profesor (el mejor) de la universidad que es, en cierto modo, la causa última de que yo haya llegado hasta aquí. Jose Miguel Pacheco Castelao fue quien me enseñó que las matemáticas podían ser útiles para entender los ecosistemas. Eso cambió mi visión y me hizo querer dirigirme hacia la modelización y el análisis de datos. Él ha sido por tanto una persona clave en mi (aún corta) carrera. Desde entonces hemos guardado una amistad personal y profesional. Ojalá dure muchos años más...

Fuera de nuestras fontreras me gustaría agradecer (aunque no me van a entender!) a varias personas que me han permitido trabajar con ellos, pero sobretodo me permitieron aprender de ellos. Trabajé muy agusto bajo la supervisión de Ekaterina Popova (NOC, UK). Una persona encantadora. Tuvo un bébé al poco de llegar yo y me dejó su despacho para mí solo sin ningún problema. Siguió mi trabajo por email con una eficiencia que ya querrían tener algunos estudiantes de sus supervisores viéndolos en persona. Y puedo decir sin dudar que es con

ella que aprendí a hacer modelos de ecosistema. Tom Anderson (NOC, UK) ha sido con el que mantenido desde entonces más contacto profesional por tener intereses comunes y le agradezco, entre otras cosas, haberme hecho pensar en cuál debe ser la dirección a seguir por la siguiente generación de modelos. Aún sigo pensando... Albert Gabric (Griffith Univ., Aus.) me permitió trabajar con él en un lugar tan agradable como Brisbane. Se ocupó de mí como si fuera su estudiante. Es un tipo excelente. Pero al final con el que más interaccioné fue con su ex-estudiante Roger Cropp (Griffith Univ., Aus.). Un gran científico. Y sobre todo una gran persona. Gracias Roger. Por último agradecer a Corinne Le Quéré (UEA, UK) permitirme trabajar en su grupo durante mi última estancia en el extranjero de la tesis. Ese primer contacto se acabó transformado en un segundo más serio, ya que he empezado un Post-Doc con ella...

Pero bueno, en última instancia la investigación es una profesión más bien solitaria... Y uno no es de piedra. En los cuatro años de vida que se dedican a 'la tesis' hay épocas buenas, épocas no tan buenas, y épocas definitivamente malas. Es ahí donde muchas personas pasan a jugar un papel fundamental. Especialmente importante es el ambiente que se respira en el lugar de trabajo. Lo que se podría llamar el 'habiente de los pasillos'. Esos contactos más o menos esporádicos, pero del día a día, que acaban teniendo una gran influencia en tu estado de ánimo y motivación para trabajar y socializar. Lástima que el ICM sea tan grande como para no tener espacio en estas pocas páginas para agradecer individualmente a todos los que lo merecen. Perdonadme aquellos que saben que les tengo una gran estima pero que no aparezcan en estas líneas por despiste...

Ante todo me gustaría agradecer a mis companer@s de despacho su gran compañerismo. Sus nombres son: Cristina Roldán, Gisela Llaveria, Oscar Guadayol, Mariona Segura, Nagore Sampedro y Sonia Quijano. Cristina, no se si eres consciente de tener un 'alma' especial. Yo te considero un ángel sobre esta tierra. Da gusto conversar contigo; proyectas una paz interior, una serenidad y bondad que, simplemente, son muy difíciles de encontrar. Gracias por ser como eres. Gisela, compañera de últimas horas de despacho. Menos mal que estabas cuando ya no quedaba ni el apuntador y así tenía a alguien con el que convensar en las pausas. Anda que no te he dado la tabarra a veces!. Gracias Oscar por ser un amigo diario, por tener esa actitud ante la vida tan inteligente, con dosis de filosofía, por todas esas conversaciones serias o triviales que hemos mantenido, y por tu humor un tanto ácido que siempre se agradece. Mariona, aunque cambiaste de despacho al poco de llegar yo para irte tan lejos como al de al lado, eres una de los nuestros. El 'proyecto pecera' fue una gran idea; y aún envidio que mientras que a mí se me murieron los dos peces que tuve, el tuyo aguantó de todo!. Gracias también por hablarme regularmente en catalán y así permitirme practicarlo sin aplicar esa máxima que es 'la ley del mínimo esfuerzo', tan clásica en los castellano-hablantes. Nagore, tú eras 'la vecina de justo al lado', siempre te tenía a mano para preguntarte cualquier cosa y siempre me contestabas con buen humor. Gracias por tu paciencia y nunca enfadarte conmigo aunque te okupara a veces toda la mesa con mis carpetas, o te robara el cable de consexión a internet. Y finalmente, Sonia. La 'madre' del grupo,

que en realidad era una 'hermana' más. No se por qué siempre te hacían gracia mis chistes, aunque fueran malos, y eso hacía que me sintiera libre para seguir haciendo el payaso. Una suerte haber compartido contigo estos últimos años. Ah! y mil gracias por las fotos del día de la defensa; si no es por tí no hubiera tenido ni una sola foto de recuerdo!. Mi madre aún las está esperando...

Dentro del 'Planeta de los Becarios' hay algunos con los que he tenido más contacto que con otros, pero afortunadamente, con todos los que he tenido la oportunidad de compartir algo me han demostrado ser grandes personas y compañeros. Sin ellos esto habría sido mucho más duro. Su proximidad me ha ayudado enormemente. Me han hecho sentirme querido, que es de las cosas más importantes y necesarias para ser feliz. Entre ellos merece una mención especial, como no podía ser de otra manera, Enric Pallàs ('El Nen' para los amigos). Compañero de casa y universidad en Las Palmas de Gran Canaria, volvimos a coincidir en Barcelona por azar. Con él he pasado desde horas de serio estudio y estrés en epoca de exámenes, hasta noches míticas hasta el amanecer, pasando por conversaciones eternas de cualquier tema o silencios contemplativos. Pienso que digo una obviedad al afirmar que Enric tiene un no-se-que, una magia personal e innanta, que le hace despuntar en todo lo que hace y enriquecer todo lo que toca, incluidos los seres humanos. Es una persona a la que quiero y admiro como a un hermano. Su compañía durante todos estos años me ha hecho aprender mucho sobre el mundo y sobre mí mismo; me ha hecho mejor persona. Otros dos grandes amigos son también Kintxo y Baptiste Mourre. La hora de ir a comer cada día los cuatro juntos a la UPF era especial. La mejor pausa del día. Sobre todo el tea-time en la cafetería Ycaria. A Kintxo le conocía de vista en la universidad. Todo el mundo le quería y respetaba, pero a mí esas barbas de paisano me intimidaban!. Nunca hablé con él. Luego cuando le conocí de verdad ya en el ICM descubrí que es un amor como persona, todo corazón. Y Baptiste, igual. Desprende bondad y buen 'karma' desde el primer día que le conoces. Gracias por habermelo ofrecido cada día.

Otro despacho especial para mí fue el de 'las chicas' (Cristina Linares, Dacha Atienza, Laura Alonso, Maria Vila). Entraba y salía como si fuera el mío. A Cristina la conozco un poco menos, pero siempre me cayó muy bien. De Dacha que voy a decir, que es un cielo. Gracias por el pez 'tiburon' que me regalaste. Lastima que se muriera tan rápido... Todavía recuerdo llegar corriendo al despacho porque esa noche había soñado que el pobre moría atacado por los peces zebra y... joder! me lo encontre muerto y medio comido!. Vaya shock. Laurita, mi favorita. Conecté contigo desde el primer día. Después de hablar contigo siempre me sentía mejor. Tienes un don. Y Maria; no podía haber tenido una compañera de tesis mejor. Siempre activa, motivándome y haciéndome creer que todo me iba salir cojonudo cuando yo dudaba... T'estimo molt noia. Entre tanto apareció el relevo generacional, las simpáticas Violeta Saló y Arancha Lana. Lástima que la maternidad de Violeta y el poco tiempo que hace que llego Arancha hizo que no me diera tiempo a conocerlas un poco más.

Luego está el grupo de amigos que aunque no veía a diario (eso de que estuvieran en la primera planta no ayudaba...) son importantes para mi. Sus bonitos nombre son: Andrés Gutiérrez (el capitán); Begoña Vendrell (un hada...), Itziar Lekunberri (aupa!), Laura Gomez (encantadora), Gorka Merino (ese esfuerzo!) y María Pastor (Heidiii...!). Deciros a todos que os quiero y os voy a echar mucho de menos. No me puedo olvidar de varias personas muy especiales: Karolos, Luisa, Ramón, Solenne (los 'ADN people'); y Valentí Sallares y Alcinoe Calaorrano (para mí, la pareja perfecta). Nos cononcemos tanto ya que casi sobran las palabras. Habeis estado ahí desde el principio hasta el final. Sois mis grandes amigos y os adoro.

Por supuesto hay mucha más gente con la que he compartido pequeños-grandes momentos. Conversaciones ligeras pero divertidas, saludos de pasillo repetidos a lo largo del día, y día tras día. Alguien que cada vez que nos cruzábamos me regalaba una sonrisa de esas que te animan para todo el día era Francesc Pagès. La noticia de su muerte me afecto mucho. Dondequiera que estés te doy las gracias... Quiero agredecer especialmente a Josep Lluis Pelegrí. Fue profesor mío durante la universidad y ya entonces todos sabíamos la gran persona que es. Diría más, es una de las mejores personas que he conocido en mi vida. Y conmigo se ha portado siempre de una manera impecable. No tengo más que halagos para él. Me gustaría agradecer a Pep Gasol, por su sentido del humor y cordialidad. A Celia Marrasé, a la que podía saludar desde la ventana, porque siempre me daba un rato de conversación muy entretenido. También a Lluïsa Cros, que es la amabilidad personificada. Gracias igualmente a Mikel Latasa y Renate Scharek por su buen humor y buen rollo. Ah! y a Isabel Palomera, con la que quedé 'suplente' en mi primer intento de obtener una FPI. Siempre ha sido muy agradable conmigo y le tengo mucho aprecio. También le tengo un aprecio especial a Evarist Vazquez. Lo empezé a conocer, más alla del simple hola-y-adiós, a partir del ASLO'2005 en Santiago (que risas con él!) y desde entonces cada día me cae mejor. Otro risas, el Sergi Rosi!. Me parto con él. Un gran tipo. Dos grandes persona, que siempre me sonríen, son Dolors Vaqué y Laura Arín. Asimismo quisiera agradecer su mera presencia cotidiana, por lo bien que me caen, a Covadonga Orejas, Carles Pelejero y Eva Calvo, Jaime Piera, y Ramón Massana. Sois gente con algo especial. También me gustaría agradecer a Miquel Alcaraz, quien siempre ha sido un caballero, que aquel desliz que cometí no presentandome al Tribunal Único del DEA no terminara en suspenso monumental... Por último, mis más sinceros agradecimientos para las siguientes personas porque son gente sana a la que aprecio de corazón: Albert Reñé, Andrea Gori, Cristina Romera, Clara Ruiz, Ero, Estela Romero, Eva Flo, Georgios Tsounis, Ida Fiorillo, Irene Forn, Maricel Auladell, Thomas Lefort, Vanessa Balagué (la que mejor viste del ICM)...

Estoy seguro de que, aunque he intentado incluir a todos los que de una u otra manera han estado a mi lado durante la realización de esta tesis, he dejado a muchos sin citar expresamente. Yo nunca he sido alguien con memoria de elefante y es fácil que se me hayan despistado nombres. Ellos saben que les aprecio y le pido perdon por no dejarlo por escrito...

A todos y todas: GRACIAS.

*A mi hermana Bibiana...*

# Resumen

La hipótesis de CLAW establece que un incremento en la radiación solar o de los flujos de calor hacia el océano puede producir una respuesta biogeoquímica para contrarrestar el incremento de temperatura o radiación solar. Este mecanismo de retroalimentación se produciría en varios pasos: primero, habría un incremento de la concentración de dimetilsulfuro disuelto en la superficie del océano ($DMS_w$) y por tanto de su emisión a la atmósfera; segundo, como consecuencia de la oxidación del DMS en la atmósfera se produciría un incremento de la producción de núcleos de condensación de nubes (CCN) de origen biogénico ($CCN_{bio}$); tercero, gracias al incremento en CCN se aumentaría el albedo de las nubes. Por tanto, se ha sugerido que el DMS da lugar a un efecto refrigerante sobre los flujos radiativos de la Tierra a través de su efecto sobre la formación y las propiedades ópticas de las nubes de la troposfera oceánica. Dicho mecanismo de retroalimentación se ha propuesto que puede actuar como un proceso natural que podría contrarrestar en parte el Calentamiento Global de origen antropogénico. Esta hipótesis, aunque sugestiva, es muy especulativa y algunos de sus postulados principales continúan sin haber sido probados. En este estudio se pretende contribuir al conocimiento actual del ciclo del azufre biogénico marino y de su impacto potencial en el clima en base a abordar algunas preguntas que permanecen sin respuesta con respecto a la hipótesis de CLAW. El factor climático que gobierna la producción oceánica de DMS, el impacto de la oxidación atmosférica del DMS en los CCN, y el potencial de DMS para contrarrestar el Calentamiento Global son investigados en profundidad basándose en modelización y en el anánlisis de datos. Se ha desarrollado un modelo en una dimensión (1D) de la dinámica del DMS (bautizado 'DMOS') y se acopló a un modelo de ecosistema pelágico pre-existente que simulaba explícitamente el bucle microbiano. El modelo se aplica al Mar de los Sargazos para intentar explicar qué proceso dirige la estacionalidad del DMS. Se realizaron una serie de experimentos (virtuales) con el modelo a partir de activar o desactivar algunos de los procesos presentes en DMOS. Las simulaciones obtenidas de clorofila-a, dimetilsulfoniopropionato (DMSP; el precursor del DMS), así como las concentraciones de DMS se comparan con perfiles verticales de las mismas variables medidos *in-situ* durante los años 1992 y 1993. La exudación de DMS por parte del fitoplancton como respuesta a altos niveles de radiación solar aparece como el proceso clave, sin el cual el modelo no es capaz de simular correctamente el DMS ni reproducir la 'DMS summer-paradox'. El análisis de una base de datos global de DMS así como de series temporales de DMS en lugares específicos (la Bahía de Blanes y el Mar de los Sargazos) reveló que la radiación solar recibida en la capa de mezcla oceánica (o SRD) es el factor climático que parece dirigir la dinámica del DMS. Desde un punto de vista global pero teniendo en cuenta la distribución espacial, el análisis de mapas globales mensuales climatológicos de SRD y DMS muestran que el acoplamiento estacional entre SRD y DMS es muy alto en la gran mayoría de la superficie oceánica, sin importar la latitud, temperatura o biomasa de fitoplancton. A partir de estos resultados se ha obtenido una ecuación predictiva diagnóstica que relaciona la concentración de DMS con la SRD. El análisis estadístico de datos globales, procedentes

de modelos o satélites, de varias variables océnicas y atmosféricas sugiere que la oxidación del DMS puede ser una fuente mayoritaria de CCN en regiones oceánicas lejos de fuentes continentales de aerosoles (ej. Océano Sur, Océano Pacífico Subtropical), especialmente en verano, cuando la eficiencia de la oxidación del DMS es más elevada. Partículas pequeñas de spray marino (SS), aunque desde un punto de vista cuantitativo son importantes, no parecen contribuir a la estacionalidad de los CCN en Océano Sur, que es una región donde la producción de SS es de las más elevadas del mundo debido a la presencia constante de fuertes vientos. El SS parece más bien conformar una concentración de fondo de CCN más o menos constante. La diferencias observadas entre la estacionalidad del viento y de la fracción fina de aerosoles apoyan estas conclusiones. Aunque en regiones oceánicas con aire limpio el DMS parece controlar la estacionalidad de los CCN y su contribución a la concentración de CCN puede llegar hasta el 80-100%, a escala global la estimación de la contribución del DMS a los CCN está entorno al 30%. Dos modelos diagnósticos del DMS, obtenidos de análisis globales, para los que la profundidad de la capa de mezcla (MLD) es un parámetro clave, se aplican a campos globales de MLD y clorofila-a simulados con un modelo de tres dimensiones (3D) de circulación general oceánica (OGCM) acoplado a un modelo biogeoquímico. Un incremento del 50% de la cantidad de $CO_2$ atmosférica se usa como forzamiento del OGCM, al mismo tiempo que una simulación control donde no hay dicha perturbación corre en paralelo. De esta manera se estima la respuesta de la producción oceánica del DMS debido al Calentamiento Global. Los resultados muestran un incremento del DMS, especialmente en verano, cuando un incremento en el albedo de las nubes sería más efectivo para refrigerar la Tierra. Sin embargo, el incremento es tan débil (globalmente un 1.2%) que difícilmente puede ser relevante en comparación con el forzamiento radiativo debido al incremento de los gases de efecto invernadero. Ésto contrasta con con la variabilidad estacional del DMS (un incremento del 1000-2000% de invierno a verano). Se sugiere que el mecanismo de retroalimentación 'SRD - DMS - nubes - albedo del Planeta' propuesto por la hipótesis de CLAW no es un mecanismo termorregulador a largas escalas temporales sino más bien un mecanismo estacional que contribuye a regular las dosis de radiación que llegan a la biosfera de la Tierra.

# Abstract

The CLAW hypothesis postulates that an increase in solar irradiance or in the heat flux to the ocean can trigger a biogeochemical response to counteract the associated increase in temperature and available sunlight. This natural (negative) feedback mechanism would be based on a multi-step response: first, an increase in seawater dimethylsulfide concentrations ($DMS_w$) and then its fluxes to the atmosphere ($DMS_{flux}$); second, an increase in the atmospheric cloud condensation nuclei (CCN) burden as a consequence of DMS oxidation to form biogenic CCN ($CCN_{bio}$); third, an increase in cloud albedo due to higher CCN numbers. Therefore, DMS is suggested to exert a cooling effect on the Earth radiative budget through its involvement in the formation and optical properties of tropospheric clouds over the ocean. Such a feedback has been regarded as a potential natural mechanism that might partly counteract anthropogenic Global Warming. This hypothesis, although suggestive, is highly speculative and some of its main postulates remain unproved. In this study we sought to contribute to the current knowledge of the oceanic biogenic sulfur cycle and its potential impact on climate by addressing some relevant open questions regarding the CLAW hypothesis. The climatic factor that drives oceanic DMS production, the impact of DMS oxidation on atmospheric CCN, and the potentiality of DMS to counteract Global Warming are investigated in detail based on modeling and data analyses. A new one-dimensional (1D) model of DMS dynamics (DMOS) is developed and coupled to a pre-existing ecological model that explicitly simulates the microbial-loop. The model is applied to the Sargasso Sea in order to explain what drives DMS seasonality. We have conducted a series of modeling experiments where some of the DMOS sulfur paths are turned 'off' or 'on', and the results on chlorophyll-a, dimethylsulfoniopropionate (DMSP; the DMS precursor) and DMS concentrations have been compared with the vertical profiles of these same variables measured during the years 1992 through 1993. Solar-induced DMS exudation by phytoplankton outstands as the process without which the model is unable to produce realistic DMS simulations and reproduce the DMS summer-paradox. The analysis of a global DMS database as well as local DMS time-series (Blanes Bay and Sargasso Sea) have revealed that it is the solar radiation dose in the upper mixed layer (or SRD) the climatic factor that seems to drive DMS dynamics. With a spatially resolved perspective, our analysis of globally derived SRD and DMS climatologies shows that the seasonal couplings between SRD and DMS are very tight and widespread over the Global Ocean, irrespective of latitude, temperature, and phytoplankton biomass. From these results, we have been able to obtain a global predictive diagnostic equation that relates DMS concentrations to the SRD. Statistical analyses of satellite and model-derived global data of several oceanic and atmospheric variables suggest that DMS oxidation can indeed be a major source of CCN over oceanic regions far from continental aerosol sources (eg. Southern Ocean, Subtropical South Pacific), especially in summer when the oxidation efficiency of DMS is the highest. Small sea-salt (SS) aerosols, although quantitatively important, do not seem to control CCN seasonality over the Southern Ocean, a region were SS production is amongst the highest of the world due to the constant presence of strong

winds. Rather, they appear to conform a fairly constant background of CCN. Differences in the seasonalities of wind speed and the small-mode fraction of aerosols support these conclusions. Although over clean-air oceanic regions DMS seems to control CCN seasonality and its contribution to CCN numbers is estimated to up to 80-100%, over a global scale, estimated current DMS contribution to total CCN numbers is about 30%. Two globally-derived DMS diagnostic models for which the mixing layer depth (MLD) is a key parameter, are applied to global fields of MLD and chlorophyll-a simulated with a three-dimensional (3D) Ocean General Circulation Model (OGCM) coupled to a biogeochemistry model. A 50% increase of atmospheric $CO_2$ is used to force the OGCM, and an unperturbed control is run in parallel. By this means we estimate the response of the DMS-producing pelagic ocean to Global Warming. Our results show a net global increase in DMS, specially in summer when an increase in cloud albedo will be more effective in cooling the Earth. This increase, however, is so weak (globally 1.2%) that it can hardly be relevant as compared with the radiative forcing of the increase of greenhouse gases. This contrasts with the seasonal variability of DMS (1000-2000% summer-to-winter ratio). We suggest that the 'SRD - DMS - clouds - Earth albedo' feedback proposed by the CLAW hypothesis is not a long-term thermostatic system but rather a seasonal mechanism that contributes to regulate the solar radiation doses reaching the Earth's biosphere.

# Contents

CHAPTER 1

# Introduction

*Research has to be a game,*
*because only by playing are we happy.*

*(Ramón Margalef)*

## 1.1 Background

The Gaia theory (*Lovelock and Margulis*, 1974; *Lovelock*, 1979) postulates that life on Earth drives the global cycling of its basic elements (mainly carbon, oxygen, hydrogen, nitrogen, phosphorus, and sulfur) and thereby affects the environment in which life develops. This results in the promotion and sustain of climate conditions favorable for life itself. Earth is thus viewed as a self-regulated 'super-organism' or 'macro-ecosystem', where the biosphere is the modulating force. The biosphere is defined as the presence of life on land and in the oceans. Therefore, according to Gaia the composition and functioning of the four major components of the Earth's surface (lithosphere, hydrosphere, atmosphere, and biosphere) would be constantly interconnected and in co-evolution (*Lovelock*, 1988) as a single entity that has been also called 'ecosphere' (see Figure 1.1). This would be a (non-closed) living complex system where all its components (either biotic or abiotic) are connected through feedback mechanisms in such a way that stability of the whole system emerges. This is known as 'homoeostasis' (*Lovelock and Margulis*, 1974). Through these feedback mechanisms, the ecosphere would be able to sustain itself within a state of low entropy (high order) that is stable and at the same time it is far from thermodynamic equilibrium (maximum entropy, maximum disorder). For this to occur, a constant input of energy is needed; such an energy source is essentially provided by the Sun.

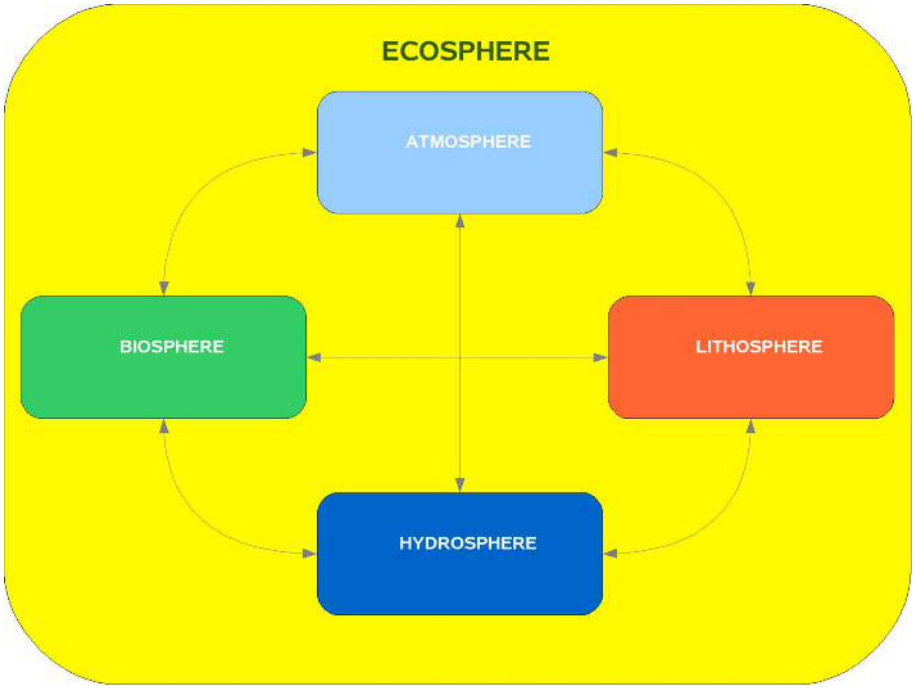


Fig. 1.1: The four major components of the Earth's surface: lithosphere, hydrosphere, atmosphere, and biosphere

The global cycling of matter and energy in the ecosphere is known as 'global biogeochemical cycles'. In this context, it has been proposed that the production of biogenic sulfur in the ocean and its emission into the atmosphere may be directly related to Earths' climate regulation (*Charlson et al.*, 1987). This has been called the CLAW hypothesis after the authors' initials,

with a clear reference to the phonetics of the word 'cloud'. For a cloud to form in the troposphere (lower layer of the atmosphere that occupies from the surface up to a height of 8 km over the poles and 16 km over the tropics) a supply of 'cloud condensation nuclei' (CCN) is required besides water vapor (*Cox*, 1997). CCN are small hygroscopic particles onto which atmospheric water vapor condenses to form cloud droplets, small non-precipitating water drops, usually of less than 0.2 mm. Without CCN clouds cannot form.

Clouds play an important role in the Earth radiative budget, mainly through their shading effect, which reduces the amount of short-wave solar radiation arriving to the Earth's surface (*Charlson et al.*, 1987) (compare Figure 1.2 and Figure 1.3 to better appreciate the global importance of cloud's shading in the Earth). That is, they increase the 'albedo' of the planet: the fraction of total solar incident radiation that is reflected back to space. Globally, it is estimated that clouds directly reflect ≈20% of solar incident radiation (*Kiehl and Trenberth*, 1997) (Figure 1.4). Given that the atmosphere is mostly heated from the bottom by the long-wave radiation emitting surface, more reflective (whiter) clouds result in less atmospheric warming, i.e., Earth cooling. Cloud reflectivity (albedo) depends on the amount and size of cloud droplets (*Twomey*, 1974) and therefore on the amount of CCN (see below). On the other hand, clouds also retain part of the long-wave (warming) radiation coming up from the Earth surface (*Kaufman et al.*, 2002). That is, clouds have two opposite effects on Earth's temperature. In this regard we should note that there are several (main) types of clouds, and part of the typology depends on their altitude in the atmosphere: low, middle, and high altitude clouds. Two thirds of the oceans are covered by low altitude clouds, that have a high albedo and a low absorption of infra-red radiation. These clouds occur at the top of the marine boundary layer, and their formation and persistence are regulated by the supply of CCN from below or, to a lesser extent, from the adjacent free troposphere.

Over oceanic regions far from continents, where particle that can act as CCN are scarce, a major CCN source is dimethylsulfide (DMS) (*Charlson et al.*, 1987; *Ayers et al.*, 1997a; *Vallina and Simó*, 2007b). DMS is a reduced sulfur compound of biological origin, which occurs dissolved in the surface ocean (see below). Since DMS is always supersaturated in seawater, there is a constant sea-to-air emission of DMS following Henry's law (*Liss and Mervilat*, 1986; *Nightingale et al.*, 2000). In the atmosphere, DMS is oxidized by free radicals (mainly the hydroxyl radical, OH, and the nitrate radical) (*Hynes et al.*, 1986; *Stark et al.*, 2007) to sulfur dioxide ($SO_2$) and/or methanesulfonate acid (MSA) (*Cox*, 1997). In the presence of water, $SO_2$ undergoes aqueous oxidation to form small drops of sulfuric acid ($H_2SO_2$) which, after water evaporation, become atmospheric sulfate particles. These particles contribute to the atmospheric sulfate burden as 'non-sea-salt sulfates' (nss-$SO_4$), which are distinct from sulfate particles with their origin in sea salts. Aerosols formed by 'gas-to-particle' conversion, such as those from DMS-to-sulfate oxidation, are particularly small, generally in the range of 0.1 to 1 ∝m in diameter (*Ayers et al.*, 1997a; *Jourdain and Legrand*, 2001), which is the optimal size range for CCN. MSA can also undergo gas-to-particle nucleation to produce CCN (*Cox*, 1997; *Jourdain and Legrand*, 2001),

yet they are less abundant compared to sulfate CCN. Conversely, sulfate particles derived from the drying of the sea spray risen by wind friction and wave breaking are mostly larger and then much less efficient as CCN.

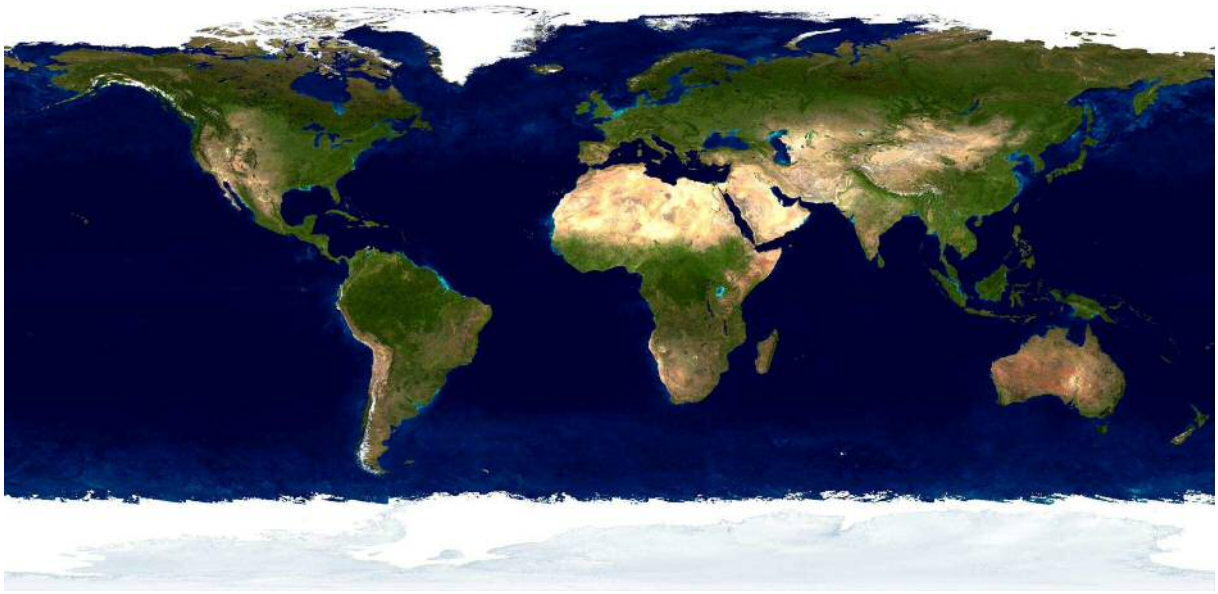

Fig. 1.2: The Earth free of clouds. Credit: NASA

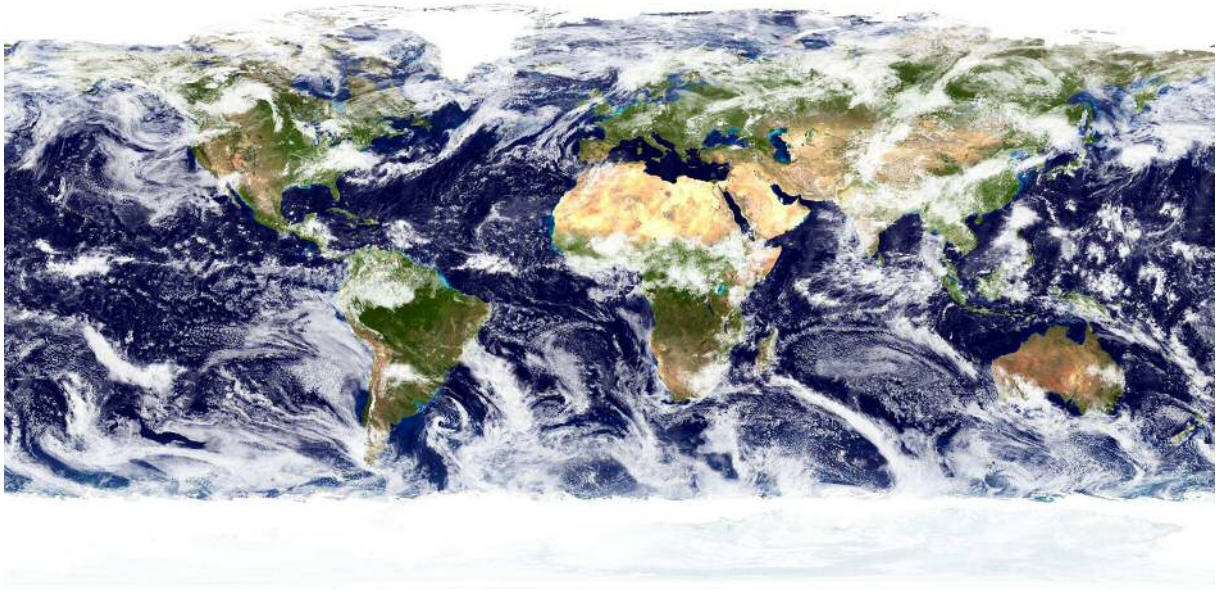

Fig. 1.3: The Earth covered by clouds. Credit: NASA

The CLAW hypothesis postulates that a rise of the Earth's temperature and/or the surface solar irradiance would trigger a biogeochemical response consisting of an increase of oceanic DMS production and concentration, its flux to the atmosphere and, therefore, CCN numbers over the ocean (*Charlson et al.*, 1987). The increase of CCN numbers would have two major impacts on clouds. First, it would increase the amount of cloud-droplets per unit of volume inside the clouds, with a consequent increase of the 'optical density' or 'optical depth' of the clouds, giving rise to a higher cloud albedo. This is called the 'first indirect effect' or 'Twomey's effect'

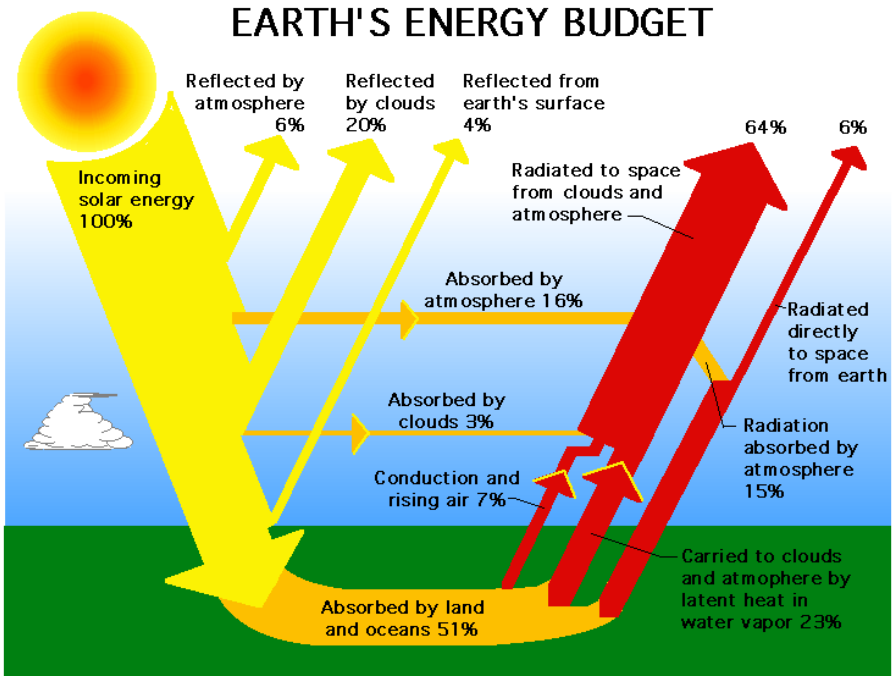


Fig. 1.4: The Earth's energy budget. Credit: NASA

(*Twomey*, 1974). The second impact is related to cloud lifetime. In case of low CCN concentrations, water vapor condensates on fewer particles that grow to bigger cloud droplets and become rain drops. The cloud takes shorter to precipitate and disappear. On the other hand, in the presence of higher CCN concentrations, water condensation distributes onto many more particles that become small cloud-droplets. The cloud takes longer to precipitate as rain, and contribute longer to atmospheric albedo. This is the 'second indirect effect' of clouds on climate or 'Albrecth effect' (*Albrecht*, 1989). An increase of cloud optical density combined with longer cloud lifetimes reduce the amount of solar radiation at the surface and induce a cooling of the Planet's temperature. If such cooling made oceanic DMS concentrations decrease, the feedback loop would close (see Figure 1.5). The CLAW hypothesis, hence, suggests that the Earth's ecosphere responds to climatic fluctuations (e.g. in temperature or solar radiation) in a way that tends to counteract the fluctuation. This is known in thermodynamics as the 'LeChatelier-Braun principle': if a system in equilibrium experiences a perturbation that moves the system away from the equilibrium, the system response is to oppose the change in order to minimize its effects (*Gladyshev*, 1997). The CLAW hypothesis is a clear example of one of the potential feedback mechanisms that may be acting to stabilize the ecosphere.

One consequence derived from this proposed feedback mechanism is that the global increase of Earth temperature resulting from human activities, especially from the emission of green-house effect gases like carbon dioxide ($CO_2$), may be compensated to a certain extent through the increase of DMS production and its cooling effect (*Charlson et al.*, 1987). This suggestion has drawn great interest from the scientific community to study the global sulfur cycle at all scales (*Simó*, 2001, 2004). This research has yielded around $\approx$1500 scientific articles in the field (*Ayers and Cainey*, 2007). With most of them contributing small pieces of the big jigsaw (*Malin*,

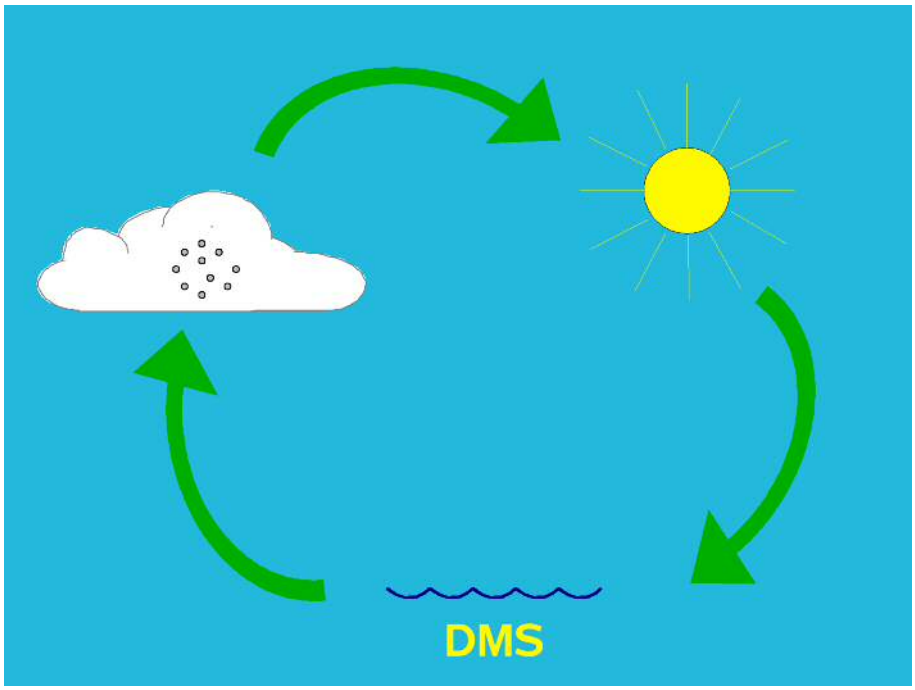


Fig. 1.5: Schematic diagram of the CLAW hypothesis

2006), the ultimate goal of the DMS research community is to evaluate if the main postulates of the CLAW are fulfilled.

The DMS precursor is 'dimethylsulfoniopropionate' (DMSP), which is produced by many species of phytoplankton (*Keller et al.*, 1989). The classes *Prymnesiophyceae* (also called *Haptophyceae*, which include the coccolithophores and small flagellates) and *Dinophyceae* (dinoflagellates), as well as some *Crysophyceae*, show the highest intracellular levels of DMSP. On the other hand, *Bacillariophyceae* (diatoms), *Cryptophyceae* and *Cyanophyceae* (cyanobacteria; prokaryotic phytoplankton) are low or null DMSP producers (*Keller et al.*, 1989; *Keller and Korjeff-Bellows*, 1996). *Phaeocystis* (Prymnesiophyte) and *Emiliania huxleyi* (Primnesiophyte; coccolithophore) are among the best studied taxa, because high amounts of DMSP and DMS are found during blooms of these phytoplankters (*Matrai and Keller*, 1993; *Matrai et al.*, 1995). The Southern Ocean, North Atlantic and the Bering Sea are among their preferred niches (*Keller et al.*, 1989; *Brown and Yoder*, 1994; *DiTullio et al.*, 2000; *Boyd*, 2002; *Iglesias-Rodríguez et al.*, 2002; *Archer et al.*, 2002; *Wulff and Wängberg*, 2004). The levels of intracellular DMSP do not only vary between phytoplankton species but also within each species, depending on the physiological state of the cell (*Keller and Korjeff-Bellows*, 1996; *Stefels*, 2000; *Sunda et al.*, 2002). DMSP has been suggested to play several roles in the cell, such as osmoregulation (regulate salinity changes by acting as a compatible solute), cryoprotection (protect from freezing by stabilizing proteins), control of excess of fixed carbon (by being exuded in conditions of low nutrient concentrations), antioxidant protection (by scavenging harmful oxygen radicals), and involvement as a methyl-donor in metabolic reactions (*Kirst et al.*, 1991; *Stefels*, 2000; *Sunda et al.*, 2002). Intracellular DMSP (also called particulate DMSP, DMSPp) is released to the surrounding aquatic environment (as dissolved DMSP, DMSPd) by three main processes: cell

lysis due to phytoplankton non-grazing mortality (also called natural mortality); cell lysis due to grazing by higher trophic levels (zooplankton) or by viral infection; and active exudation. Passive release by diffusion through the cell membrane is low (*Groene*, 1995; *Stefels*, 2000; *Yoch*, 2002). Also, an important fraction of the DMSPp ingested by zooplankton may be eventually excreted as DMSPd (*Simó*, 2004). Therefore, the difference between DMSPp and DMSPd is not chemical (since they are exactly the same substance) but related to where the substance is located (inside the cell or dissolved in seawater, respectively).

The conversion of DMSP into DMS is mediated by the enzyme DMSP-lyase, which has been found in marine heterotrophic bacterioplankton as well as in DMSP-producing phytoplankton species (*Groene*, 1995; *Niki et al.*, 2000; *Yoch*, 2002; *Zubkov et al.*, 2002). DMSPd is a major source of reduced sulfur for heterotrophic bacteria (*Kiene and Linn*, 2000; *Yoch*, 2002), so that bacterial DMS production is secondary (usually less than 10% of the DMSPd consumed) (*Kiene*, 1996; *Kiene and Linn*, 2000). Nevertheless bacterial DMS production represents a very important source of DMS, generally seen as its main source (*Kiene*, 1992; *Yoch*, 2002). Recent works have questioned this fact and pointed to phytoplankton themselves as another important DMS source, at least under some environmental and physiological conditions (*Niki et al.*, 2000). Most remarkably, it has been suggested that DMSP, DMS and the product of DMS oxidation dimethylsulfoxide (DMSO) conform an antioxidant chain reaction system inside the cells that efficiently scavenge the OH radicals produced as photosynthesis subproducts under oxidative stress conditions (*Sunda et al.*, 2002). More specifically, in axenic cultures under high doses of ultraviolet radiation (UVR) it was observed that the intracellular concentrations of DMSP and DMS increased by up to 100% and 3500%, respectively (*Sunda et al.*, 2002). Also, on the basis of field data analysis, it has been suggested that DMS seasonality is mostly driven by the direct exudation of DMS from phytoplankton cells rather than by bacterial activity on DMSPd (*Toole and Siegel*, 2004). However, there are no studies with *in-situ* measurements of such phytoplankton DMS production in the oceans.

A challenging observation that adds more confusion but also opens interesting questions, is the fact that at low and mid latitudes (which comprise the largest proportion of the global ocean's surface) DMS seasonality is in anti-phase with the seasonality of phytoplankton biomass and primary production (PP) (*Simó and Pedros-Allió*, 1999a; *Uher et al.*, 2000; *Vallina et al.*, 2006; *Vila-Costa et al.*, 2008). This translates into significant negative correlations between DMS and chlorophyll-a (CHL) concentrations in the upper mixed layer (*Toole and Siegel*, 2004). That is, in these regions the annual maximum of CHL and PP is generally observed from late winter to spring (when DMS concentrations are low), while the annual maximum of DMS occurs in mid summer (when CHL and PP are in their annual minimum due to water column stratification and subsequent nutrient limitation). This has been called the 'DMS-summer-paradox' (*Simó and Pedros-Allió*, 1999a) because it seemed counter-intuitive that DMS does not follow the same seasonal variation as phytoplankton, the biological source of its precursor. This appeared to somehow contradict one of the original postulates of the CLAW hypothesis, that

temperature and/or solar radiation increases would be followed by increases in PP and phytoplankton biomass, which would lead to increased DMS. Only in high latitude and deep mixed regions (like the Southern Ocean and the subpolar North Atlantic), CHL and DMS are tightly coupled over seasonal scales (*Gabric et al.*, 1996; *Ayers and Gillett*, 2000; *Vallina et al.*, 2006). Also, at the shorter and smaller scales of DMSP-producing phytoplankton blooms (which usually occupy confined regions and last for few days) good positive correlations are found between DMS and CHL concentrations (*Matrai and Keller*, 1993; *Matrai et al.*, 1995; *Archer et al.*, 2002).

Within this context, from the analysis of a global DMS data-base (with 15,000 data points), *Simó and Dachs* (2002) derived a (double) empirical equation that allows prediction of surface DMS concentrations from known CHL concentrations and the depth of the mixed layer (MLD) at any site in the global ocean. Interestingly, over ≈85% of the ocean's surface (mainly open ocean regions at low and mid latitudes) DMS concentrations can be successfully estimated only with the MLD. Only over the remaining ≈15% (mainly coastal areas or open ocean regions at high latitudes, where the highest CHL concentrations are found) both CHL and MLD are needed to estimate DMS. These authors suggested that the MLD acts as an integrative parameter of the several processes involved in DMS dynamics (*Simó and Pedros-Allió*, 1999a). For example, shallow mixed layers will expose both bacteria and phytoplankton to high UVR doses. It has been reported that UVR can both inhibit bacterial sulfur consumption (*Slezak et al.*, 2001) and increase phytoplanktonic DMS production (*Sunda et al.*, 2002), so, shallow mixed layers would favor higher DMS concentrations. In highly productive regions, on the other hand, the inclusion of CHL in the algorithm allows for taking into account biomass-related DMS production during blooms.

DMS undergoes three major loss processes in the ocean: bacterial consumption, photolysis, and emission to the atmosphere (ventilation). Their relative importance varies in the short-term (*Simó and Pedros-Allió*, 1999b; *Merzouk et al.*, 2004, 2006) and seasonally (*Toole and Siegel*, 2004; *Vila-Costa et al.*, 2008), and especially with depth. In the first meter ventilation dominates; in the first 20m photolysis dominates; and in the first 60m biological consumption dominates (*Kieber et al.*, 1996). Contrary to DMSPd, it seems that not all groups of heterotrophic bacteria use DMS but rather only some specialized taxa (*Vila-Costa et al.*, 2006a). Regarding DMS 'photolysis' this notation is not strictly correct because DMS does not absorb photons at wavelengths longer than 260nm (*Toole et al.*, 2003). It is through an indirect mechanism that DMS photo-oxidizes: free radical production upon the photolysis of chromophoric dissolved organic matter (CDOM), which then react to oxidize DMS to DMSO, sulfate, and other unknown products (*Toole et al.*, 2003). Ventilation of DMS is a function of the sea surface temperature (SST) and wind speed (*Nightingale et al.*, 2000). Globally, it is estimated at ≈25 Tg per year (*Chapman et al.*, 2002), which represents about a third of the global anthropogenic sulfur emissions (≈70 Tg per year; mostly in the form of $SO_2$) (*Smith et al.*, 2001). In spite of this huge amount of sulfur being emitted annually from the ocean, DMS ventilation is rather a minor fraction (about

a 3% (*Vila-Costa et al.*, 2006a)) of total phytoplankton DMSP production; that is, the most of the marine biogenic sulfur production is recycled and remineralized within the pelagic food-web.

## 1.2 Open questions

After almost 20 years of intensive research, our knowledge of the mechanisms involved in the marine sulfur cycle, from DMSP and DMS production/consumption at the cellular level to atmospheric DMS oxidation, has largely improved (*Simó*, 2001, 2004). However, important gaps remain in our understanding of all these steps. In consequence, it has not yet been possible to prove unequivocally that the feedback mechanism proposed by the CLAW hypothesis actually occurs, and least of all if it may serve to alleviate anthropogenic global warming. It is not even sure that the CLAW hypothesis is experimentally testable (hence demonstrable) (*Cropp*, 2002).

For example, it is still unknown if the main factor that would trigger an increase of oceanic DMS production would be temperature or solar radiation (or both). Also, it is still an open question if the dominant biological source of DMS in seawater is bacterial cleavage of DMSPd or phytoplankton direct DMS release. Thus, the causes for the DMS-summer-paradox are still uncertain; although several mechanisms have been suggested, which one is the key one (or whether it is a combination of all of them) has not been elucidated (*Simó*, 2001). The main hypotheses in consideration by researchers to explain why DMS usually accumulates in summer are three: *i*) it results from increased zooplankton grazing upon DMSP-rich phytoplankton (*Dacey and Wakeham*, 1986; *Steinke et al.*, 2002b), *ii*) it results from inhibition of bacterial DMS consumption by high UVR doses (UVR damages DNA, affects bacterial activity, and reduces sulfur consumption) (*Simó and Pedros-Alliό*, 1999a; *Slezak and Herndl*, 2003; *Toole et al.*, 2006), *iii*) it results from an increase of phytoplankton 'direct' exudation due to UVR- and low nutrient-induced oxidative stress (appealing to the antioxidant function of DMSP and DMS) (*Simó and Pedros-Alliό*, 1999a; *Sunda et al.*, 2002; *Toole and Siegel*, 2004). The latest studies are pointing towards the importance of the third mechanism, although by now they are no more than well founded speculations.

Another unresolved point is whether the potential contribution of DMS oxidation products to the CCN burden may be significant at a global scale, given that nowadays anthropogenic emissions dominate among atmospheric sulfur sources, particularly in the northern hemisphere. Even in regions of the southern hemisphere far from continents the importance of biogenic sulfur for CCN formation has been questioned (*Murphy et al.*, 1998). Sea salt (SS) from marine spray, although forming basically supramicron size aerosols, is also found in the submicron size fraction and therefore potentially contributes to CCN (*O'Dowd et al.*, 1997; *Murphy et al.*, 1998). Another identified source of submicron marine aerosols is organic compounds lifted from the surface ocean (*Novakov and Penner*, 1993; *O'Dowd et al.*, 2004; *Meskhidze and Nenes*, 2006).

There are also high uncertainties regarding the efficiency at which CCN can affect the albedo and lifetime of clouds because cloud droplet formation is a very complex process that depends on many factors (e.g. aerosols chemical composition and size, amount of water vapor) (*Andreae and Crutzen*, 1997). In the context of the CLAW hypothesis, it is particularly uncertain which would be the (potential) reduction of surface solar irradiance due to DMS. Although, as stated above, the global contribution of DMS to the atmospheric $SO_4$ burden has been modeled at 30%, this does not necessarily mean that DMS is contributing 30% of the total $SO_4$-induced radiative forcing on climate; the contribution could be less due to non-linearities in the climate system and due to the near-saturation state that may result from high anthropogenically-derived CCN loads (*Gondwe et al.*, 2004). A modeling study estimated that the solar energy returned back to space by $SO_4$ aerosols from DMS origin is globally -0.03 W $m^{-2}y^{-1}$, i.e., an order of magnitude lower than the estimated global radiative forcing of anthropogenic $SO_4$ (-0.4 W $m^{-2}y^{-1}$). Another modeling study estimated that a 100% increase in DMS fluxes to the atmosphere would result in 25% reduction of the current incident solar radiation (*Jones et al.*, 2001). It has to be noticed, though, that these modeling approximations to the relative role of biogenic and anthropogenic sulfate aerosols in radiative forcing face the challenge of representing accurately the coupled transport-chemistry behavior of the atmosphere. This is important because of the sort-lived nature of sulfate aerosols, which follow limited dispersion in the global atmosphere. Thus, their contribution to CCN formation and radiative forcing is not dependent upon the absolute emission rates only but also on the spatial distribution of the emission sources (*Langner et al.*, 1992). Most of the continental sulfur emissions never reach the remote open ocean, where biogenic emissions, even though of smaller magnitude, become more important (*Falkowski et al.*, 1992). Frequent long-range transport episodes of continental haze over the central ocean, however, can result in overloads of CCN-like particles, so that no new CCN from biogenic sulfur can be formed. In any case, DMS may have had a far more significant global influence on climate in the pre-industrial Earth (*Gondwe et al.*, 2004).

Another open question that has not yet been addressed specifically concerns the operation time scale of the hypothetical CLAW feedback. Assuming that the climate-stabilizing mechanisms proposed by CLAW do actually operate, which is their temporal scale of actuation?. In the discussion of their original paper, (*Charlson et al.*, 1987) combined several scales, from seasonal to glacial/interglacial. If we are to assess the potential of DMS to alleviate global warming, it is fundamental to learn about the time scale at which the feedback mechanism is the most efficient.

And finally, from a broader research view, one of the more intriguing and hard to answer questions is: what has driven such a feedback mechanism throughout evolution? What are the selection pressures that act for a feedback like this to emerge? Since the origin of DMS is to be found in DMSP production by algae, the genes encoding for DMSP synthesis, which are (probably) shared by all producers, must have been selected long time ago in a common ancestor. *Charlson et al.* (1987) speculated about two independent origins: one in coastal zones, re-

lated to algal stress due to high salinity and another one in the open ocean surface related to algal nitrogen deficiency or UVR-induced stress. In any of the cases, would the protective benefit derived from cloudiness enhancement be high enough for the algae as to evolutionarily select/preserve those genes? Or, is it rather a 'neutral' selection, where volatile sulfur production is neither a disadvantage nor an advantage (and then the genes were not eliminated throughout evolution)? Further questions arise from these: How today's climate would have been different without DMS as a source of CCN? If DMS loses its role in cloud formation because of anthropogenic sulfur, how will this affect oceanic phytoplankton and the evolution of DMSP-production genes?

In view of the fact that phytoplankton themselves is not the only source of DMS, that this results from complex interaction in food-webs, and that any climatic benefit from DMS production will be shared by all organisms (including competitors), *Simó* (2001) suggested that the selective pressure was not climatic but rather acted on the important intracellular roles of DMSP, which benefit directly the producer. According to this, DMS would be a secondary 'by-product' of DMSP metabolism in the food-web, whose production is enhanced in conditions of higher irradiance. This by-product 'accidentally' plays a role in reducing solar irradiance. Should DMS have had a detrimental role for marine microbiota, phytoplankton DMSP production would have disappeared through evolution. This view of a life by-product accidentally generating an emerging feedback (*Simó*, 2001) goes along with the notion that many biogeochemical feedbacks of the Earth system are based on life wastes (*Volk*, 1998). To me, however, this explanation is not fully satisfactory if we seek to establish a causal relationship between biosphere and climate; their co-evolution implies necessarily a selective pressure of climate on the biosphere. All these are really 'major questions', probably impossible to answer with our current knowledge of how the ecosphere in which we live operates and evolve. Certainly, these questions go far beyond the scope of this thesis.

## 1.3 Ph.D Thesis objetives and outline

The memory of this Ph.D Thesis contains five central chapters in scientific-article format (introduction; data and methodology; results and discussion; conclusion), plus a general introduction (current chapter) and general conclusions (last chapter). Some of the information given in this general introduction may appear repeated in some of the central chapters.

**The study was aimed to make a contribution to the knowledge of the oceanic biogenic sulfur cycle and its potential impact on climate. It covers spatial scales going from the local to regional and global, as well as temporal scales from seasonal to inter-annual and inter-decadal.**

The work was performed on the bases of informatic tools only (basically MatLab and ForTran programming) with the goal at modeling biogeochemical processes relevant for DMSP/DMS dynamics, as well as statistical analyses of *in-situ*, satellite and model data with the object to evaluate the feasibility of the CLAW hypothesis. None of the data used have been obtained by the author. In most cases the data are public and freely available through the 'World Wide Web' (Internet); in the other cases they have been generated by members of the work team and/or by collaborators.

**Chapter 2** reports the development of a one-dimensional (1D) model that is capable to simulate the DMS-summer-paradox. The study is focused in the Sargasso Sea, since a study site in this region has been extensively sampled and an important data-base of both physical and biological variables (among them CHL, DMSPp, DMSPd and DMS) is available. A dynamic model (mechanistic model, based on partial differential equations) has been developed in order to simulate the annual cycle of biogenic sulfur and the organisms involved (phytoplankton, zooplankton and bacteria). A sulfur (DMSP/DMS) cycle model was conceived and coupled to a pre-existing ecosystem model (*Anderson and Pondaven*, 2003). The coupled ecosystem-DMSP/DMS model is one-dimensional (it is vertical-depth resolved), where physical processes (turbulent diffusion) are prescribed in a diagnostic way (*Cropp et al.*, 2004). By testing several scenarios, the processes that appear as the most important to explain the DMS seasonality and the summer-paradox are sought. Also, the relative importance of all the processes relevant to DMS dynamics is assessed.

**Chapter 3** is aimed at assessing if CCN seasonality over the Southern Ocean is controlled by oceanic biota through DMS production, emission and oxidation. The Southern Ocean was chosen because it is a region weakly impacted by continental sources of aerosols. CHL is used in this particular case as a proxy for DMS since over this region both variables are tightly coupled. This allows a longer temporal coverage (3 years, from 2002 to 2004) of monthly means, necessary for a deep analysis. The study is mainly based on statistical analyses of contemporary satellite data of CHL, the fine fraction of aerosols (ETA), and CCN, together with model output fields of atmospheric OH concentrations, rainfall amounts, and wind speeds. A first analysis seeks for lineal relationships between the variables in order to resolve what drives CCN production (either biogenic emissions or sea salt) and CCN losses (wet deposition by rain washout). A second analysis, based on an 'effective' multi-linear model (statistic, not based on differential equations but on averaged data), addresses the relative importance of the source and loss terms. Finally, an estimate of the relative contribution of biogenic CCN to total CCN numbers over the Southern Ocean is given.

**Chapter 4** addresses two of the main postulates of the CLAW hypothesis: *i)* if an increase of the solar radiation dose in the oceanic upper mixed layer (UML), or SRD, gives rise to DMS concentration increases; *ii)* if an increase of oceanic DMS gives rise to an increase of CCN numbers. The two questions are studied at the scale of the global ocean (spatially resolved) making use

of climatological data of surface solar radiation, MLD, DMS (concentration and fluxes), OH, MSA, ETA and CCN. In a first analysis, global maps of seasonal correlations between the variables of interest are obtained. In a second analysis, a linear relationship between an estimate of DMS oxidation and CCN numbers is derived for the Southern Ocean, and it is extrapolated to the rest of the global ocean. By this means an estimate of the biogenic contribution to CCN in regions of the global ocean is achieved.

**Chapter 5** seeks to better elucidate which variable (phytoplankton biomass, temperature, solar radiation) drives DMS dynamics, and to look deeply into the hypothesis that the solar radiation dose in the UML might be the main factor that controls DMS seasonality at a global scale. To do so, climatological data of CHL and SST, *in-situ* or climatological data of MLD, and *in-situ* data of DMS concentrations are analyzed from a local perspective (Sargasso Sea, Blanes Bay) as well as globally. The study looks for a direct and 'universal' relationship between the solar radiation dose DMS concentrations in the UML. The focus is not on the seasonal couplings as in Chapter 4, where the spatially resolved seasonal correlations did not take into account the absolute value of the variables but only their co-variation. Instead, the goal is to show if, globally, higher doses of solar radiation dose are associated with higher DMS concentrations.

Finally, in **Chapter 6** by applying both the obtained relationship (Chapter 5) as a DMS diagnostic model, as well as the diagnostic model proposed by *Simó and Dachs* (2002), to MLD predicted by a three-dimensional (3D) global ocean general circulation model (OGCM) for the year 2061, an estimate of the potential increase in DMS in response to global warming is obtained. The results are discussed for their implications for the CLAW hypothesis. Arguments about the most probable time scale at which the proposed DMS-climate feedback operates are presented.

CHAPTER 2

# A dynamic model of oceanic sulfur (DMOS) applied to the Sargasso Sea: Simulating the dimethylsulfide (DMS) summer-paradox

*The secret of creativity is*
*knowing how to hide your sources.*

*(Albert Einstein)*

# A dynamic model of oceanic sulfur (DMOS) applied to the Sargasso Sea: Simulating the dimethylsulfide (DMS) summer-paradox


ABSTRACT

A new one-dimensional model of DMSP/DMS dynamics (DMOS) is developed and applied to the Sargasso Sea in order to explain what drives the observed dimethylsulfide (DMS) summer-paradox: a summer DMS concentration maximum concurrent with a minimum in the biomass of phytoplankton, the producers of the DMS precursor dimethylsulfoniopropionate (DMSP). Several mechanisms have been postulated to explain this mismatch: a succession in phytoplankton species composition towards higher relative abundances of DMSP producers in summer; inhibition of bacterial DMS consumption by ultra-violet radiation (UVR); and direct DMS production by phytoplankton due to UVR-induced oxidative stress. None of these hypothetical mechanisms, except for the first one, has been tested with a dynamic model. We have coupled a new sulfur cycle model that incorporates the latest knowledge on DMSP/DMS dynamics to a pre-existing nitrogen/carbon-based ecological model that explicitly simulates the microbial-loop. This allows the role of bacteria in DMS production and consumption to be represented and quantified. The main improvements of DMOS with respect to previous DMSP/DMS models are the explicit inclusion of: solar-radiation inhibition of bacterial sulfur uptakes; DMS exudation by phytoplankton caused by solar-radiation-induced stress; and uptake of dissolved DMSP by phytoplankton. We have conducted a series of modeling experiments where some of the DMOS sulfur paths are turned 'off' or 'on', and the results on chlorophyll-a, bacteria, DMS, and DMSP (particulate and dissolved) concentrations have been compared with climatological data of these same variables. The simulated rate of sulfur cycling processes are also compared with the scarce data available from previous works. All processes seem to play a role in driving DMS seasonality. Among them, however, solar-radiation-induced DMS exudation by phytoplankton stands out as the process without which the model is unable to produce realistic DMS simulations and reproduce the DMS summer-paradox.



S. M. Vallina, R. Simó, T. R. Anderson, A. Gabric, R. Cropp, & J. M. Pacheco (2008)
*J. Geophys. Res. - Biogeosciences*, 113, G01009, doi: 10.1029/2007JG000415

## 2.1 Introduction

The oceanic sulfur cycle, believed to be an important part of the Earth biogeochemical system because of its potential for climate regulation (*Charlson et al.*, 1987; *Andreae and Crutzen*, 1997), has received considerable attention in the last two decades. However, owing to the complexity of the cycle, in which the whole microbial food web is involved (*Simó*, 2001), some important features regarding its seasonal dynamics remain largely unexplained. Phytoplankton are the primary producers of dimethylsulfoniopropionate (DMSP), the biochemical precursor of dimethylsulfide (DMS), a volatile compound that is ubiquitous in the global surface ocean. Emission of oceanic DMS to the atmosphere (*Bates et al.*, 1992; *Kettle and Andreae*, 2000) is thought to contribute to non-sea-salt sulfate (nss-$SO_4$) production and cloud condensation nuclei (CCN) formation (*Charlson et al.*, 1987; *Andreae and Crutzen*, 1997; *Vallina et al.*, 2007a). The amount of atmospheric CCN is linked to cloud albedo and therefore to the Earth radiative budget (*Twomey*, 1974; *Albrecht*, 1989; *Kaufman et al.*, 2002). In this regard, a negative feedback between oceanic DMS production and Earth albedo has been postulated (*Charlson et al.*, 1987).

Intracellular DMSP (also called particulate DMSP or DMSPp) is released to the water as dissolved DMSP (DMSPd) during phytoplankton cell lysis by natural (non-grazing) mortality, zooplankton grazing and virus attacks (*Groene*, 1995; *Yoch*, 2002; *Steinke et al.*, 2002b). However, the amount of DMSPp varies among phytoplankton groups (*Keller et al.*, 1989; *Keller and Korjeff-Bellows*, 1996) as well as with the physiological state of the cells within each group (*Keller and Korjeff-Bellows*, 1996; *Stefels*, 2000; *Sunda et al.*, 2002; *Bucciarelli and Sunda*, 2003; *Slezak and Herndl*, 2003). DMSP may also be exuded by phytoplankton living cells as an overflow of energy (*Groene*, 1995; *Stefels*, 2000). The conversion of DMSP to DMS is mediated by DMSP-lyase, an enzyme that has been found in DMSP-producing phytoplankton groups as well as in numerous groups of DMSP-consuming bacteria (*Groene*, 1995; *Yoch*, 2002; *Zubkov et al.*, 2002; *Niki et al.*, 2000; *Wolfe et al.*, 2002; *Steinke et al.*, 2002a). Until recently it was believed that the majority of DMS production was due to zooplankton grazing on phytoplankton and bacterial activity on DMSPd (*Levasseur et al.*, 1996; *Dacey et al.*, 1998; *González et al.*, 1999). However, recent studies suggest that the role of phytoplankton DMS production has been overlooked (*Simó and Pedros-Alló*, 1999a; *Niki et al.*, 2000; *Wolfe et al.*, 2002; *Sunda et al.*, 2002; *Toole and Siegel*, 2004; *Toole et al.*, 2006). Under conditions of high UV radiation stress or severe nutrient limitation it seems that phytoplankton may be responsible of an important fraction of the total DMS production (*Stefels and van Leeuwe*, 1998; *Wolfe et al.*, 2002; *Sunda et al.*, 2002). Most groups of oceanic bacteria are able to undertake DMSPd consumption (from which only a small fraction is cleaved to DMS plus acrylate, the rest being demethylated to other forms of sulfur (*Groene*, 1995; *Yoch*, 2002; *Kiene and Linn*, 2000)). DMS is consumed as a carbon source mostly by some methylotrophic bacteria (*Kiene and Bates*, 1990; *Kiene*, 1992, 1993; *Bates et al.*, 1994; *Wolfe et al.*, 1999; *Simó et al.*, 2000; *Yoch*, 2002; *Zubkov et al.*, 2004; *Vila-Costa et al.*,

2006a) or converted to dimethylsulfoxide (DMSO) with energy gain by unknown bacteria (*Vila-Costa et al.*, 2006a; *del Valle et al.*, 2007). The other major sinks of DMS are photolysis by UV (a process mediated by photosynthesizer substances) (*Brimblecombe and Shooter*, 1986; *Brugger et al.*, 1998; *Toole et al.*, 2003; *Kieber et al.*, 1996) and emission to the atmosphere (*Kettle and Andreae*, 2000). Also, it has been recently discovered that non DMSP-producing phytoplankton are also able to take up DMSPd, potentially reducing the amount of DMSPd available for bacteria degradation and its conversion to DMS (*Vila-Costa et al.*, 2006b).

Both DMSP and DMS are an integral part of the dissolved organic matter (DOM) pool. The oceanic cycles of DOM and organic sulfur are therefore thought to be tightly coupled (*Vézina*, 2004). DMSPd appears to be the main source of sulfur (S) for bacteria (*Kiene et al.*, 1999; *Kiene and Linn*, 2000; *Yoch*, 2002; *Zubkov et al.*, 2001, 2002), although it is also a source of carbon (C) (*Yoch et al.*, 1997; *Zubkov et al.*, 2001; *Yoch*, 2002). On the other hand, DMS is mainly a source of carbon and energy, sulfate and DMSO being the primary fate of sulfur from bacterial consumption of DMS (*Vila-Costa et al.*, 2006a; *del Valle et al.*, 2007). DMS dynamics are therefore regulated by a complex interplay of biotic and abiotic processes where phytoplankton, zooplankton and bacteria are believed to have a prominent role.

With the aim at gaining a better understanding on the processes governing the oceanic sulfur cycle, several dynamic (i.e. mechanistic) models of DMSP/DMS have been developed in the last decade or so (*Gabric et al.*, 1993; *Lawrence*, 1993; *van den Berg et al.*, 1996; *Laroche et al.*, 1999; *Jodwalis et al.*, 2000; *Archer et al.*, 2002; *Lefèvre et al.*, 2002; *Chu et al.*, 2004). These models usually consist of two submodels: a nitrogen based one (N-cycle) characterizing the ecosystem, and a sulfur based one (S-cycle) of the DMSP/DMS dynamics (*Vézina*, 2004). These two submodels are coupled but without feedbacks between them: the N-cycle affects the S-cycle, but not viceversa (*Vézina*, 2004). Most of these models do not, however, include a characterization of the microbial loop, that is, an explicit representation of bacteria, bacterivory, and the DOM cycle. This is due to the fact that the first ecosystem models did not give sufficient relevance to the microbial loop.

However, in recent years, bacteria and DOM dynamics have gained relative importance in ecosystem models and it has been shown that their inclusion is fundamental in order to obtain realistic simulations of the seasonal cycles of the model state variables (*Spitz et al.*, 2001). In the Sargasso Sea, for example, most of the carbon cycling is through the microbial loop (*Steinberg et al.*, 2001, and references therein). The DMSP/DMS model of *Archer et al.* (2002) (which is based on the ERSEM ecosystem model (*Baretta et al.*, 1995)) is the only ecosystem model to additionally incorporate bacteria and DOM dynamics. Although the model of *Gabric et al.* (1993) incorporated bacteria as part of the N-cycle, bacteria were not explicitly represented in the S-cycle. Rather, bacterial effects on DMSP and DMS concentrations were parameterized as constant rates, independently of their evolution in the N-cycle. This is probably due to the fact that the N-cycle of Gabric's model (which is based on *Moloney et al.* (1986)) does not

include DOM dynamics, such that predicted bacteria display "catastrophic behaviour", being close to zero for much of the time (*Cropp*, 2002; *Cropp et al.*, 2004). Variations in bacterial sulfur demand have been suggested to affect DMS production, so that if DMSPd is in excess of bacterial requirements for sulfur, a larger proportion of the DMSPd taken up could be converted to DMS (*Kiene et al.*, 1999). Therefore, *Cropp* (2002) recommends that a priority for the next generation of DMSP/DMS models is the inclusion of a realistic microbial loop. Similar conclusions were reported by other authors (*Lefèvre et al.*, 2002; *Le Clainche et al.*, 2004; *Vézina*, 2004).

Another significant problem with most of the current DMSP/DMS models is the difficulty of decoupling DMS dynamics from that of phytoplankton. It has been observed that DMS peaks in summer at tropical, subtropical and low temperate latitudes, a time when chlorophyll-a (CHL, a common proxy for phytoplankton biomass) is at its annual minimum (*Simó and Pedros-Allió*, 1999a; *Uher et al.*, 2000; *Toole and Siegel*, 2004; *Vallina et al.*, 2006; *Vila-Costa et al.*, 2008). This finding has been dubbed the *DMS summer-paradox* (*Simó and Pedros-Allió*, 1999a). Several mechanisms have been proposed to explain it, such as a succession in phytoplankton species composition towards high DMSPp producers, inhibition of bacterial DMS consumption by high UV, and a higher (direct) production of DMS from phytoplankton cells due to UV stress (*Simó and Pedros-Allió*, 1999a; *Sunda et al.*, 2002; *Toole and Siegel*, 2004). Most of these potential explanations have not as yet been tested in models. The model of *Lefèvre et al.* (2002) and the parameterization used by *Gabric et al.* (2005) are the sole examples of including a variable sulfur to nitrogen (S:N) phytoplankton internal quota as a function of light in order to account for a shift in species composition and/or a change in phytoplankton physiological state. This allowed a higher degree of decoupling between DMS and CHL in these models. It was, however, shown by *Le Clainche et al.* (2004) for the Sargasso Sea (using the same model as *Lefèvre et al.* (2002) but coupled to a dynamic turbulent scheme) that the seasonality of modelled DMS was lower than that of DMS observations and the summer maximum was underestimated.

In this work we present a Dynamic Model of Oceanic Sulfur (DMOS) which is based on a modified version of the ecosystem model (N/C-cycles) developed by *Anderson and Pondaven* (2003) (hereafter A&P'03). It has an explicit representation of bacteria and DOM dynamics, and is adapted for the Sargasso Sea using data collected during the Bermuda Atlantic Time-series Study (BATS) (*Steinberg et al.*, 2001). We have coupled a new S-cycle to it that incorporates the latest knowledge of DMSP/DMS dynamics. Model complexity was progressively increased in order to test several of the hypotheses generally used to explain the DMS summer-paradox. The performance of the model in simulating annual cycles of concentrations, fluxes and turnover rates of the sulfur variables is analyzed.

## 2.2 Data and Methodology

### 2.2.1 Sargasso Sea data

The Sargasso Sea is located in the subtropical West North Atlantic and represents an oligotrophic open ocean region where the DMS summer-paradox is readily observable (*Dacey et al.*, 1998; *Toole and Siegel*, 2004). Phytoplankton seasonality is regulated by physical processes which drive the deep nutrient entrainment in the upper layers during winter and spring, followed by nutrient depletion in summer due to a strong stratification of the water column (*Goericke and Welschmeyer*, 1998; *DuRand et al.*, 2001; *Steinberg et al.*, 2001). The dominant phytoplankton groups are prokariotic picophytoplankton (Prochlorococcus and Synechococcus) and eukariotic phytoplankton (Prymnesiophytes, Pelagophytes) (*Goericke and Welschmeyer*, 1998; *DuRand et al.*, 2001; *Steinberg et al.*, 2001). Diatoms are not a dominant group, although rare episodic blooms have been observed (*Steinberg et al.*, 2001). Dinoflagellates are also represented as a low percentage of the phytoplankton community (*Goericke and Welschmeyer*, 1998; *Steinberg et al.*, 2001). The mixed layer depth (MLD) has a marked seasonal cycle with values from $\approx$200m to less than 10m in summer (*Steinberg et al.*, 2001; *Spitz et al.*, 2001) and the sea surface temperature (SST) varies from $\approx$20°C in winter to $\approx$28°C in summer (*Steinberg et al.*, 2001).

During the Bermuda Atlantic Time-series Study, station BATS (31.75°N, 64.17°W) was sampled for vertically resolved profiles of CHL and bacteria (along with many other physical and biological variables) approximately monthly from 1989. Data are available at the BATS database (http://bats.bbsr.edu/). Hydrostation-S (32.17°N, 64.50°W) has been sampled for vertically resolved profiles of DMSPp, DMSPd and DMS approximately biweekly from 1992 to 1994 (*Dacey et al.*, 1998; *Toole and Siegel*, 2004). Using these depth resolved time series we have constructed two-dimensional (2D; time and depth) climatologies of CHL and bacteria (more than 10 years of data, from 1989 to 2000) as well as DMSPp, DMSPd and DMS (three years of data, from 1992 to 1994). The methodology used for building the climatology was as follows. All measured profiles were merged by month. Then, for each month, a $6^{th}$ degree polynomial regression was used to fit the cloud of data, obtaining a single depth-resolved profile per month. Finally the resulting monthly profiles were interpolated in time, generating 2D (time, depth) plots with a resolution of 1day x 1m. To be consistent, model results were also interpolated in depth and averaged in time to obtain the same 1day x 1m resolution (see section 2.3). DMSPd did not display a clear repeated seasonal pattern over the sampling period (*Dacey et al.*, 1998) and therefore the obtained climatology has to be viewed with some caution. On the other hand, DMSPp and DMS showed a much clearer seasonal cycle (*Dacey et al.*, 1998).

### 2.2.2 Model description

The A&P'03 ecosystem model includes a detailed characterization of the microbial loop. It incorporates a complex description of the DOM cycle and explicitly includes heterotrophic bacteria as a state variable. The treatment of DOM includes dual currencies, nitrogen (DON) and carbon (DOC). Since DMSP and DMS are part of the DOM, and therefore they share many of their processes (such as bacterial uptake and degradation), a DMSP/DMS model including a detailed microbial loop is fundamental (*Vézina*, 2004). We thus coupled our S-cycle model to the A&P'03 N/C-cycles, calling this coupled ecosystem-DMSP/DMS model 'DMOS' (Dynamic Model of Oceanic Sulfur). The new S-cycle model contains important improvements like the explicit representation of bacterial activity in the sulfur cycle (including for the first time UV inhibition of bacterial sulfur uptake), a time-varying DMS exudation term from phytoplankton (due to UV stress) as well as an uptake of DMSPd for phytoplankton. In a manner similar to *Archer et al.* (2002), we include nonlinear kinetics for sulfur uptake (other models use linear relationships (*Vézina*, 2004)).

One of the advantages of including bacteria explicitly in DMSP/DMS models is that it is then possible to evaluate the relative contributions of phytoplankton and bacteria to the DMS production, this being one of the important unanswered questions concerning the biogeochemistry of DMS (*Yoch*, 2002). Further, the DMS-yield of the whole food web (total DMS production / total DMSP consumption), which is a very sensitive parameter in DMSP/DMS models (*Lefèvre et al.*, 2002; *Vézina*, 2004; *Le Clainche et al.*, 2004; *Cropp et al.*, 2004) is not prescribed as an a-priori parameter: it is now an output of the model (see section 2.3). The full set of DMOS equations is described in Appendix A (section 2.5). Model parameters are listed in Table 2.1. An schematic diagram of DMOS model is shown in Figure 2.1.

### 2.2.3 N/C-cycles

The model contains single state variables for phytoplankton (eq(2.1)), zooplankton (eq(2.2)) and heterotrophic bacteria (eq(2.3)), two nutrient pools (nitrate (eq(2.4)) and ammonium (eq(2.5))), labile and semilabile DON and DOC (eqs(2.6-2.9)), detritus (eqs(2.10-2.12)), dissolved inorganic carbon (DIC, eq(2.13)) and alkalinity (eq(2.14)). CHL (eq(2.15)) is calculated for phytoplankton N at each time step based upon *Geider et al.* (1997) as in *Spitz et al.* (2001), permitting comparison with field data. Phytoplankton primary production (eq(2.19)) is controlled by light (eq(2.22)) (*Walsh et al.*, 2001) and temperature (eq(2.21)) (*Eppley*, 1972), affecting the specific growth rate (eq(2.20)), as well as by nutrient availability (eq(2.25)) (*Spitz et al.*, 2001). Phytoplankton losses are due to zooplankton grazing (eq(2.29)), natural mortality (eq(2.55)) and vertical sinking (eq(2.80)). Zooplankton graze upon phytoplankton, bacteria and soft detritus (eqs(2.29-2.32)). Zooplankton production (eq(2.37) or eq(2.39)), ammonium excretion

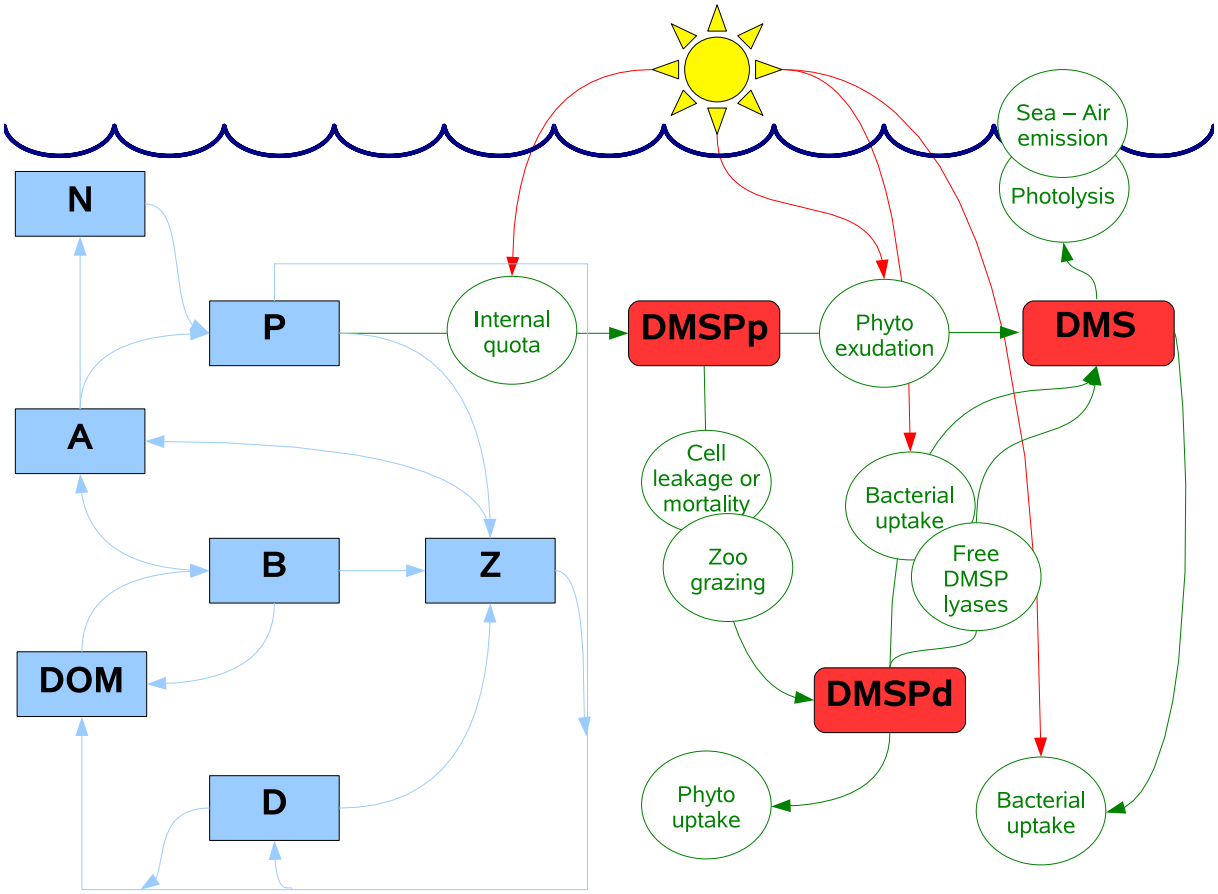


Fig. 2.1: Schematic diagram of DMOS model. On the left side is shown the ecosystem submodel: (N/C-cycles; mmol $m^{-3}$) A = ammonium, N = nitrates, P = phytoplankton, B = bacteria, Z = zooplankton, DOM = dissolved organic matter (can be either nitrogen based or carbon based, and labile or semilabile), D = detritus (can be either nitrogen based or carbon based). Note that the modeled cycling of dissolved organic matter and detritus has been purposely simplified in this diagram as a generic DOM and D pools for clarity; a more detailed scheme of the ecosystem submodel can be found in (*Anderson and Pondaven*, 2003). On the right side is shown the DMSP/DMS submodel (S-cycle; mmol $m^{-3}$): DMSPp = particulated dimethylsulfoniopropionate, DMSPd = dissolved dimethylsulfoniopropionate, DMS = dimethylsulfide. The red lines comming from the sun refers to the S-cycle processes directly affected by solar radiation in DMOS model that has been tested by the five modelling experiments performed.

| Parameter | Symbol | Value | Unit |
|---|---|---|---|
| Phyto. max. specific growth rate | $\propto_P^{max}$ | 3.7 | $(d^{-1})$ |
| Phyto. saturating irradiance | $I_s$ | 60 | $(W\ m^{-2})$ |
| Phyto. half-sat. for $NO_3^=$ uptake | $k_P^N$ | 0.15 | $(mmolN\ m^{-3})$ |
| Phyto. half-sat. for $NH_4^+$ uptake | $k_P^A$ | 0.05 | $(mmolN\ m^{-3})$ |
| Phyto. $NH_4^+$ inhibition parameter | $\psi$ | 1.5 | $(mmolN^{-1})$ |
| Phyto. leakage fraction | $\gamma_1$ | 0.05 | $(adim)$ |
| Phyto. DOC exudation parameter | $\gamma_2$ | 0.34 | $(adim)$ |
| Phyto. specific mortality rate | $m_P$ | 0.045 | $(d^{-1})$ |
| Phyto. mortality losses to DOM | $\varepsilon$ | 0.34 | $(adim)$ |
| Phyto. sinking rate | $\lvert\vec{w_P}\rvert$ | 0.05 | $(m\ d^{-1})$ |
| Phyto. C:N ratio | $\theta_{P_{c:n}}$ | 6.625 | $(mmolC\ mmolN^{-1})$ |
| Phyto. $CaCO_3$:C ratio | $\theta_{Ca}$ | 0.10 | $(mmolC\ mmolC^{-1})$ |
| Phyto. max. CHL:C ratio | $\theta_{chl}^m$ | 0.041 | $(mgCHL\ mgC-1)$ |
| Phyto. initial slope of P-I curve | $\alpha_{chl}$ | 1.0 | $(mgC\ mgCHL^{-1}\ (W\ m^{-2})^{-1}\ d^{-1})$ |
| Phyto. molecular weight of Carbon | $C_{mw}$ | 12 | $(mgC\ mmolC^{-1})$ |
| Phyto. min. S:N internal quota | $\theta_{P_{s:n}}^{min}$ | 0.044 | $(mmolS\ mmolN^{-1})$ |
| Phyto. max. S:N internal quota | $\theta_{P_{s:n}}^{max}$ | 0.220 | $(mmolS\ mmolN^{-1})$ |
| Phyto. max. DMS specific exudation rate | $\gamma_s^{max}$ | 0.25 | $(d^{-1})$ |
| Phyto. fraction of DMSPd consumers | $\alpha_P$ | 0.1 | $(adim)$ |
| Phyto. free DMSP-lyase activity | $f$ | 0.01 | $(d^{-1})$ |
| Zoo. max. specific ingestion rate | $g$ | 3.2 | $(d^{-1})$ |
| Zoo. N assim. efficiency | $\beta_n$ | 0.75 | $(adim)$ |
| Zoo. C assim. efficiency | $\beta_c$ | 0.65 | $(adim)$ |
| Zoo. C net growth efficiency | $\omega_Z$ | 0.8 | $(adim)$ |
| Zoo. half-sat. const. for N ingestion | $k_g$ | 0.75 | $(mmolN\ m^{-3})$ |
| Zoo. grazing preference upon Phyto. | $p_P$ | 1/3 | $(adim)$ |
| Zoo. grazing preference upon Bact. | $p_B$ | 1/3 | $(adim)$ |
| Zoo. grazing preference upon Det. | $p_D$ | 1/3 | $(adim)$ |
| Zoo. C:N ratio | $\theta_{Z_{c:n}}$ | 5.5 | $(mmolC\ mmolN^{-1})$ |
| Zoo. messy feeding losses to DOM | $\phi$ | 0.23 | $(adim)$ |
| Zoo. max. specific mortality rate | $m_Z$ | 0.3 | $(d^{-1})$ |
| Zoo. half-sat. const. for mortality | $k_Z$ | 0.2 | $(mmolN\ m^{-3})$ |
| Zoo. mortality fraction going to DOM | $\Omega_{dom}$ | 0.38 | $(adim)$ |
| Zoo. mortality fraction going to $NH_4^+$ | $\Omega_A$ | 0.33 | $(adim)$ |
| Zoo. mortality fraction going to Detritus-N | $\Omega_{D_n}$ | 0.29 | $(adim)$ |
| Zoo. mortality fraction going to Detritus-C | $\Omega_{D_c}$ | 0.46 | $(adim)$ |
| Zoo. mortality fraction going DIC | $\Omega_{DIC}$ | 0.16 | $(adim)$ |
| Zoo. DMSPp ingestion: fraction converted to DMSPd | $\alpha_1$ | 0.7 | $(adim)$ |
| Bact. max. Lc/$NH_4^+$ and sulfur uptake | $\propto_B^{max}$ | 13.3 | $(d^{-1})$ |
| Bact. max. Sc hydrolysis | $\propto_{Sc}$ | 4 | $(d^{-1})$ |
| Bact. half-sat. const. for $NH_4^+$ uptake | $k_A$ | 0.5 | $(mmolN\ m^{-3})$ |
| Bact. half-sat. const. for Lc uptake | $k_{Lc}$ | 25 | $(mmolC\ m^{-3})$ |
| Bact. half-sat. const. for Sc hydrolysis | $k_{Sc}$ | 417 | $(mmolC\ m^{-3})$ |
| Bact. max. inhibition by UV of nutrient uptake | $\phi_{inhib}^{max}$ | 0.75 | $(adim)$ |
| Bact. specific nitrification rate | $\nu$ | 0.03 | $(d^{-1})$ |
| Bact. C gross growth efficiency | $\omega_B$ | 0.17 | $(adim)$ |
| Bact. specific mortality rate | $m_B$ | 0.04 | $(d^{-1})$ |
| Bact. C:N ratio | $\theta_{B_{c:n}}$ | 5.1 | $(mmolC\ mmolN^{-1})$ |
| Bact. S:C ratio | $\theta_{B_{s:c}}$ | 1/250 | $(mmolS\ mmolC^{-1})$ |
| Bact. fraction of DMS consumers | $\alpha_B$ | 0.20 | $(adim)$ |
| Bact. half-sat. const. for DMSPd uptake | $k_{DMSPd}$ | 0.01 | $(mmolS\ m^{-3})$ |
| Bact. half-sat. const. for DMS uptake | $k_{DMS}$ | 0.01 | $(mmolS\ m^{-3})$ |
| Bact. DMSPd excess uptake: fraction converted to DMS | $\alpha_2$ | 0.1 | $(adim)$ |
| Labile fraction of DOM produced | $\delta_1$ | 0.7 | $(adim)$ |
| Labile fraction of Phyto. extra-DOC exudation | $\delta_2$ | 0.4 | $(adim)$ |
| Detrital-N breakdown rate | $m_{D_n}$ | 0.055 | $(d^{-1})$ |
| Detrital-C breakdown rate | $m_{D_c}$ | 0.04 | $(d^{-1})$ |
| Detrital-$CaCO_3$ dissolution rate | $m_{D_h}$ | 0.05 | $(d^{-1})$ |
| Detrital sinking rate | $\lvert\vec{w_{D_i}}\rvert$ | 0.05 | $(m\ d^{-1})$ |
| Irradiance max. | $I_{max}$ | 150 | $(W\ m^{-2})$ |
| Irradiance min. | $I_{min}$ | 45 | $(W\ m^{-2})$ |
| Irradiance threshold | $I^*$ | 25 | $(W\ m^{-2})$ |
| Irradiance attenuation due to water | $k_w$ | 0.04 | $(m^{-1})$ |
| Irradiance attenuation due to Phyto. self-sheding | $k_p$ | 0.03 | $(m^2\ mmolN^{-1})$ |
| Max. specific DMS photolysis rate | $k_{photo}^{max}$ | 0.15 | $(d^{-1})$ |
| Max. turbulent diffusion | $kz_{max}$ | 250 | $(m^2\ d^{-1})$ |
| Min. turbulent diffusion | $kz_{min}$ | 1 | $(m^2\ d^{-1})$ |
| Max. sea temperature (changes each day) | $st_{max}$ | SST | $(^\circ C)$ |
| Min. sea temperature | $st_{min}$ | 19 | $(^\circ C)$ |
| Steepness of the pycnocline | $r$ | -20 | $(adim)$ |

Table 2.1: List of DMOS parameters

(eq(2.38) or eq(2.40)), and respiration (eq(2.41)) are calculated according to a stoichiometric model (*Anderson and Hessen*, 1995; *Anderson and Pondaven*, 2003). Zooplankton mortality is assumed to occur in the form of a quadratic Michaelis-Menten equation (eq(2.56)). This is a classical way of parameterizing both natural mortality and grazing by higher predators (which are not explicitly modelled). Bacteria production, excretion and respiration (eqs(2.47-2.52)) are calculated from elemental stoichiometry (*Anderson*, 1992; *Anderson and Williams*, 1998; *Anderson and Pondaven*, 2003). Labile DOC and DON are the primary growth substrates, with ammonium supplementing DON when the ratio DOC/DON (C:N ratio of DOM) is high. Uptake of labile DOC and DON and the maximum potential uptake of ammonium are described in eqs(2.42-2.44). Bacteria either take up or regenerate ammonium at any one time depending on the availability of DOC and DON (eq(2.47)), an upper limit of ammonium uptake being given by eq(2.44). The fraction of DOC taken up not used for balanced (C:N) growth is respired (eq(2.49) or eq(2.52)). Bacteria loss terms are zooplankton grazing (eq(2.30)) and natural mortality (eq(2.57)).

The main sink for nutrients is phytoplankton uptake (eq(2.19)), ammonium also being lost to the nitrate pool via nitrification at constant rate (see second term on eq(2.5)). The DOM pools are produced by phytoplankton leakage, excretion and exudation, zooplankton messy feeding, phytoplankton and bacterial natural mortality, and non-carbonate detrital breakdown (eqs(2.58-2.59)). The semilabile DOM pool is converted to labile DOM due to the action of exoenzymes by bacteria (eqs(2.53-2.54)). Phytoplankton exudation of DOC is directly proportional to primary production (see eq(2.28)). Non-carbonate (or soft) detritus (eqs(2.10-2.11)) arises from zooplankton egestion as well as phytoplankton and zooplankton mortality, and is lost by zooplankton grazing (eqs(2.31-2.32)), breakdown, and vertical sinking (eq(2.80)). The carbonate (or hard) detritus (eq(2.12)) originates from the contribution of carbonate-forming (e.g. organisms such as coccolithophores to primary production). This is parameterized assuming a constant $CaCO_3$:C ratio for phytoplankton (see Table 2.1). The carbonate fraction of total detritus is variable (*Anderson and Pondaven*, 2003). DIC (eq(2.13)) is consumed by phytoplankton (for soft tissue and carbonate production, and also as additional carbon fixed as DOC), and returned by zooplankton and bacteria respiration as well as zooplankton mortality. Other return pathways, such as breakdown of carbonate detritus (eq(2.60)), occur via cycling of DOC. Exchange of $CO_2$ with the atmosphere can also be estimated ($F_{atm}$ term in eq(2.13)) although it is not necessary for our purposes. Parameterization of alkalinity (eq(2.14)) is performed according to the stoichiometry described in *Broecker and Peng* (1982).

### 2.2.4 S-cycle

DMSPp (eq(2.16)) production by phytoplankton is modelled by using a sulfur/nitrogen (S:N) internal quota ($\theta_{P_{s:n}}$ parameter, see Table 2.1). $\theta_{P_{s:n}}$ is allowed to vary as function of light intensity following *Lefèvre et al.* (2002) (eqs(2.63-2.64)). Since the model has only one generic phyto-

plankton group, this method permits an implicit simulation of a shift in species composition towards high DMSPp producers in summer and/or a shift in phytoplankton physiological state (*Lefèvre et al.*, 2002), one of the proposed explanations of the DMS summer-paradox (*Dacey et al.*, 1998; *Simó and Pedros-Alliό*, 1999a). DMSPp is released to the water as DMSPd (eq(2.17)) due to phytoplankton leakage and natural mortality as well by zooplankton grazing. It is assumed that 70% of the grazed DMSPp is recovered in the dissolved phase (*Levasseur et al.*, 2004; *Simó*, 2004). The DMSPd losses are bacterial (eq(2.68)) and phytoplankton uptake (eq(2.67)) as well as cleavage to DMS by free DMSP-lyases (as in *Archer et al.* (2002)). Bacterial uptake is a well known sink for DMSPd since this compound is a major source of reduced sulfur for apparently most of marine bacteria (*Kiene and Linn*, 2000; *Yoch*, 2002; *Zubkov et al.*, 2002; *Vila et al.*, 2004; *Vila-Costa et al.*, 2007). A close seasonal correlation between DMSP assimilation by bacteria and bacterial heterotrophic production (measured as leucine incorporation) has been observed recently in a Mediterranean coastal site (*Vila-Costa*, 2006). We therefore assumed that DMSPd consumption is proportional to the total bacterial community in the model. On the other hand, various phytoplankton take up DMSPd such as diatoms, Synechococcus and Prochlorococcus, these all being low or non DMSP producers (*Vila-Costa et al.*, 2006b; *Malmstrom et al.*, 2004). With current uncertainties regarding what fraction of total phytoplankton biomass is able to take up DMSPd and at what rates, we considered that this process is carried out by 10% of the phytoplankton (see parameter $\alpha_P$ in Table 2.1).

In the model, DMS (eq(2.18)) production has 3 sources: cleavage from DMSPd by bacteria (eqs(2.71-2.72)) and free DMSP-lyases (3th term in eq(2.18)) as well as direct exudation by phytoplankton (eq(2.65)). The total amount of sulfur required by bacteria for balanced (C:S) growth (also called bacterial sulfur demand) (*Kiene and Linn*, 2000) is given by eq(2.70). If the DMSPd taken up is in excess of bacterial sulfur demand (no S-limitation), a fraction ($\alpha_2$, see Table 2.1) of this sulfur excess is cleaved to DMS (eq(2.71)), the remainder being converted to other forms of sulfur (e.g. sulfates via the methanethiol pathway) (*Kiene*, 1996; *Kiene and Linn*, 2000; *Kiene et al.*, 2000). It has been observed experimentally that bacterial production of methanethiol dominates over DMS production (*Kiene*, 1996; *Kiene and Linn*, 2000; *Zubkov et al.*, 2002). Bacterial DMS-yield rarely goes beyond 10%. Recent works found a range between 2 and 12% (*Slezak* pers. comm.). Similar values were reported by *Kiene and Linn* (2000) and *Zubkov et al.* (2002) (6-12%). Therefore $\alpha_2$ is assumed to be small (10%) (*Kiene and Linn*, 2000; *Niki et al.*, 2000). On the other hand, if the DMSPd taken up by bacteria is lower than the requirement for balanced (C:S) growth (S-limitation), DMS is not produced (eq(2.72)) because sulfur is fixed exclusively into proteins.

Phytoplankton direct exudation of DMS has been assumed to be constant and very small in some models (e.g. *Gabric et al.* (1993); *Chu et al.* (2004)), with many models not even including it as a process. Recent field research have however suggested that phytoplankton is likely an important source of DMS, mainly under high UV stress (*Toole and Siegel*, 2004; *Toole et al.*, 2006; *Vila-Costa et al.*, 2008). In support of these findings, the work of *Sunda et al.* (2002) showed

increases up to 3500% in the amount of DMS per unit cell volume in phytoplankton cultures exposed to high doses of UV-A. They proposed that DMS acts as an efficient hydroxyl radical scavenger, i.e. as an intracellular antioxidant under conditions of high UV exposure. In the model, therefore, direct exudation of DMS was made a function of light intensity (first fraction in eq(2.66)), although the level of phytoplankton activity is also taken into account (second fraction in eq(2.66)).

There is only one biological loss for DMS, namely its uptake by bacteria (eq(2.69)). The complete phylogeny of marine DMS-consuming bacteria is not known, but a recent study has shown that the use of DMS as a C source seems mostly restricted to some methylotrophic bacteria (*Vila-Costa et al.*, 2006a), yet DMS consumption as a source of energy by unknown bacteria (conversion to DMSO without use of the C) might be more common (*del Valle et al.*, 2007). Therefore DMS consumption seems to be not as widespread a process among bacterioplankton as DMSPd utilisation (*Vila-Costa et al.*, 2006a). Thus, we assumed that only a fraction (20%, see parameter $\alpha_B$ in Table 2.1) of the generic pool of modelled bacteria acts as a sink for DMS. The other two sinks for DMS in the model are photolysis and emission to the atmosphere. Photolysis is assumed to be solely a function of light intensity (eq(2.73)) although in reality it is a process mediated by chromophoric DOM (or CDOM) (*Brimblecombe and Shooter*, 1986; *Brugger et al.*, 1998; *Toole et al.*, 2003), which is not modelled in the current version of DMOS. DMS emission to the atmosphere (eq(2.75)) is parameterized with the gas transfer model of *Nightingale et al.* (2000) (eqs(2.76-2.78)) using climatological (1992-1994) surface wind speed ($U$, m $s^{-1}$) from the NCEP/NCAR Reanalysis Project (provided by the NOAA-CIRES Climate Diagnostics Center). Monthly data were interpolated in time and smoothed to generate daily values.

Regarding the bacterial uptake of nutrients (either labile DON/DOC or $NH_4^+$) and sulfur (either DMSPd or DMS), the model includes a light inhibition parameter that influences the specific rate of bacterial uptake (eq(2.45)). This parameter accounts for the well known effect of UVR upon bacterial heterotrophic activity and bacterial DMSP/DMS consumption (*Herndl et al.*, 1993; *Slezak et al.*, 2001; *Toole et al.*, 2006). We assume a maximum inhibition of bacterial uptake of 75% (see $\phi_{inhib}^{max}$ in Table 2.1) (*Slezak et al.*, 2001; *Toole et al.*, 2006).

### 2.2.5 Physical frame and forcings

The biogeochemical model is embedded in a one-dimensional (1D) vertical physical frame. The model therefore neglects horizontal transport processes and takes into account only vertical processes, i.e. advection (eq(2.80)) and diffusion (eq(2.81)), which are considered the main driving forces of ecosystem dynamics in the upper ocean (*Eigenheer et al.*, 1996; *Denman and na*, 1999). As in the models of *Lefèvre et al.* (2002) and *Cropp et al.* (2004), vertical mixing in the current version of DMOS is parameterized using a prescribed turbulent diffusion coefficient ($kz$, Table 2.1) following the approach used by *Cropp et al.* (2004). Coefficient $kz$ is generated

using a sigmoid equation (eq(2.82)) and climatological MLD data (*Levitus*, 1982). As a result the maximum diffusion ($kz_{max}$) occurs in the upper mixed layer (UML) and the minimum diffusion ($kz_{min}$) occurs below the UML. In between, $kz$ decreases from $kz_{max}$ to $kz_{min}$ as dictated by the parameter $r$ (Table 2.1) which defines the steepness of the pycnocline (*Cropp et al.*, 2004). The same sigmoid function (eq(2.82)) is used to generate the vertical temperature profiles, the only difference being that the maximum value for temperature is the sea surface temperature (SST) which varies seasonally, instead of being constant as for diffusion. SST data for the Sargasso Sea were obtained from a climatology (1971-2000, NOAA-CIRES Climate Diagnostics Center). Monthly data were interpolated in time and smoothed to generate daily values.

Light in the model ($I_z$, W $m^{-2}$) is defined as daily averaged photosynthetic available radiation (PAR). Daily values of PAR at the surface ($I_0$) of the Sargasso Sea were obtained after interpolating in time and smoothing a SeaWiFS climatology (from years 2002 to 2004). Light decays with depth ($z$, in metres) following an exponential function (eq(2.23)) that depends on water and phytoplankton. In the current version of DMOS we wanted to explore if the observed DMS seasonality could be simulated through the inclusion of light-driving processes, with the assumption that UVR is the forcing behind these processes (e.g. bacterial inhibition, phytoplankton stress), yet bacterial inhibition of sulfur uptakes has been also described to occur under PAR (*Slezak et al.*, 2001). PAR seasonality can be used as a proxy for UVR seasonality, UVR being a constant fraction of PAR. Given that all the parameterizations used to account for UVR-driven processes are based on the term $\frac{I_z}{I_{max}}$, the constant fraction cancels out and we are just left with a non-dimensional term representing UVR that varies between 0 and 1. While UVR attenuates faster in the water column than PAR, the UVR driving processes affecting DMS production may operate at higher depths. It has been described that organisms need some time for recovering after being exposed to high UVR doses (*Toole et al.*, 2006). Therefore when they escape from the UV zone (i.e. by sinking and/or turbulent diffusion) they may keep a 'memory' of the stress deeper in the water column. Nevertheless, exploring the use of an explicit wavelength-resolved UVR formulation, with the inclusion of CDOM as a state variable, is desirable and will be object of future research.

The model domain is from 0 to 200m with a vertical resolution of 2.5m. Initial conditions (in mmol $m^{-3}$) are constant profiles for all variables: 0.1 for phytoplankton, zooplankton and bacteria; 2.0 for nitrates; 0.5 for ammonium and labile DON; 24 for labile DOC; 2100 for TIC; 2375 for alkalinity; 0.16 for chlorophyll-a; 0.013 for DMSPp; 0.1 for DMSPd and DMS; and zero for the remaining variables. The boundary conditions are zero-flux in order to conserve mass (with the exception of sulfur since DMS emission in the upper top grid is allowed). A mass-conservative ecosystem model is desirable so that the biotic pools do not eventually run out of nutrients (*Spitz et al.*, 2001; *Cropp et al.*, 2004). An accumulation of dying phytoplankton and detritus in the bottom boundary due to vertical sinking occurs, which implies that DOM increases and finally that $NH_4^+$ and $NO_3^=$ (from $NH_4^+$ nitrification) also accumulates. This simulates the observed presence of high $NO_3^=$ levels deep in the water column at BATS (*Steinberg et al.*, 2001). During winter, the

MLD reaches the bottom and the strong mixing carry some of this nutrients pool to the UML, generating the vernal phytoplankton bloom (see section 2.3). In order to reach an equilibrium state, the model was ran for 10 years (with a time step of 0.005 days) prior to the analysis of the results. Previous tests without seasonal forcings showed that the model reaches a 'stable node' equilibrium, indicating that the model does not have unwanted internal dynamics (e.g. oscillations) and that the seasonal changes are driven by the seasonal forcings.

## 2.3 Results and Discussion

The model successfully reproduces bacteria (Figure 2.2) and CHL (Figure 2.3) distributions, capturing the winter/spring phytoplankton bloom in surface and the deep chlorophyll maximum (DCM) during summer months (Figure 2.3) as well as the development of a sub-surface maximum (40-60m depth) of bacteria from late spring to early fall (Figure 2.2). Modeled values of bacteria concentrations are, however, about a half those of the data. This is because the model only simulates active bacteria, while the data includes both active and non-active bacteria (*Anderson and Pondaven*, 2003). The vernal phytoplankton bloom is triggered by the entrainment of deep nutrients. In contrast, nutrients are depleted in summer leading to lowest phytoplankton biomass in surface waters. Deeper in the water column, the presence of higher concentrations of nutrients along with light in sufficient quantity for primary production results in the formation of a DCM. Bacteria distributions mainly result from the interplay of DOM release by phytoplankton and the inhibition of bacterial DOM uptake by high solar radiation doses during summer.

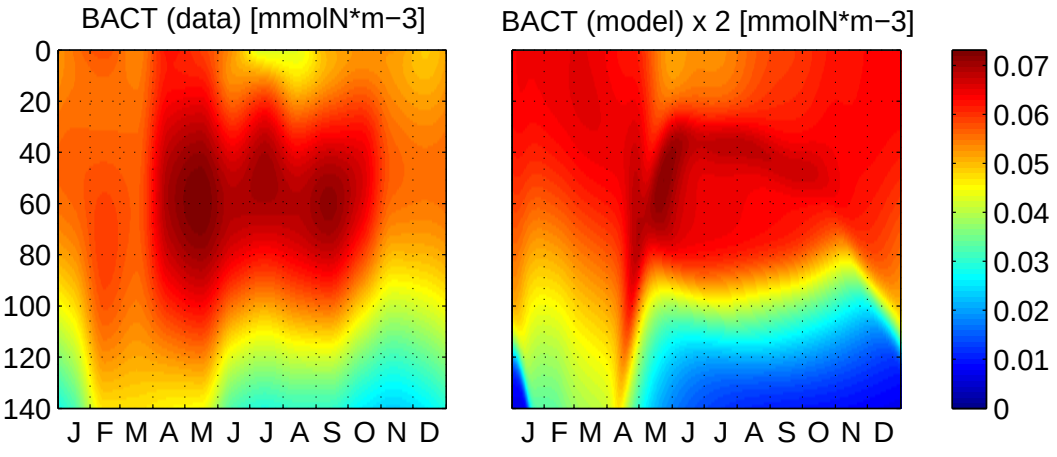


Fig. 2.2: 2D (time, depth) plots of bacteria (mmolN $m^{-3}$) from climatological *in-situ* data (left panel) and DMOS model results (right panel). Conversion from bacterial counts ($10^8$ cells $kg^{-1}$, BATS data) to mmolN $m^{-3}$ was done using a conversion factor of 0.0118 (mmolN $m^{-3}$ / $10^8$ cells $kg^{-1}$), which was obtained assuming that bacterial cells have 7.2 fgC $cell^{-1}$ (*Gundersen et al.*, 2002) and a C:N molar ratio of 5.1 (Table 2.1). Note that simulated bacteria are scaled up by a factor of 2 for the sake of visual comparison against data.

| Process affecting S-cycle | ExpA | ExpB | ExpC | ExpD | ExpE |
|---|---|---|---|---|---|
| Phyto. S:N ratio shift by UV: | NO | **YES** | **YES** | **YES** | **YES** |
| Bact. inhibition by UV: | NO | NO | **YES** | **YES** | **YES** |
| Phyto. DMSPd consumption: | NO | NO | NO | **YES** | **YES** |
| Phyto. DMS production by UV: | NO | NO | NO | NO | **YES** |

Table 2.2: Model experiments

## 2.3.1 Model experiments

In order to gain some insight into the processes that are most relevant for explaining the observed seasonality of DMS in the Sargasso Sea, and therefore what drives the DMS summer-paradox, we conducted several model experiments turning 'off' or 'on' various DMOS sulfur paths. This exercise was undertaken in a sequence of steps, starting from the simplest characterization of the S-cycle and increasing complexity in a stepwise fashion until realistic simulations were obtained. The first scenario excluded all of the processes usually cited in the literature to explain the DMS summer-paradox, namely shift in the S:N ratio of phytoplankton, inhibition of bacterial uptake by UV light, phytoplankton uptake of DMSPd, and phytoplankton exudation of DMS under UV stress. Each of these processes was then added one after the other (see Table 2.2). Simulations for each of the experiments (A, B, C, D, E; Table 2.2) are compared with observations for the Sargasso Sea observations (0-140m) in Figures 2.3-2.7. Note that, for the sake of visual comparison of model results against data, in each figure the colorbar range of the variables vary according to the maximum value (either model or data).

### 2.3.1.1 Experiment A

In this experiment there is no seasonal increase in the S:N ratio of phytoplankton (therefore $\theta_{P_{s:n}}$ is constant and equal to 0.13 mmolS mmolN$^{-1}$, the middle value between $\theta^{min}_{P_{s:n}}$ and $\theta^{max}_{P_{s:n}}$ ), UV induces neither bacterial inhibition of semilabile-DOM/$NH_4^+$ and sulfur uptake (DMSPd and DMS) nor phytoplankton stress-driven DMS production, and phytoplankton does not to take up DMSPd. Modelled DMSPp, DMSPd and DMS closely follow the predicted CHL distribution, all displaying maximum values in winter/spring and minima in summer/fall (Figure 2.3). The main differences between DMSPp and CHL are due to the variability of CHL as a response of the levels of light intensity. This constancy between sulfur species and CHL is not observed in the data. Further, DMSPp maximum values are slightly underestimated while DMS values are highly underestimated. We must conclude that this experiment is not capturing at all the main processes controlling oceanic sulfur dynamics.

#### 2.3.1.2 Experiment B

In contrast to the previous experiment, a variable S:N internal quota in phytoplankton was now added in order to parameterize a seasonal change in species composition towards high DMSPp producers and/or a change in phytoplankton physiological state due to higher UV doses (*Sunda et al.*, 2002; *Slezak and Herndl*, 2003). Results are shown in Figure 2.4. The simulations for DMSPp are improved in comparison to the first experiment. However the modelled DMSPp maximum in spring takes place earlier than observed (by about one month, similar to what was observed by (*Le Clainche et al.*, 2004)) and DMSPd distributions correlate too closely with DMSPp, a feature not observed in the field (*Dacey et al.*, 1998). DMSPp simulations are also clearly overestimated during summer. Therefore, the parameterization of the S:N ratio as a function of light, although better than using a constant value, is far from being perfect. There is a need to explore other ways of modeling DMSPp concentrations, e.g., by including in the model several phytoplankton groups with specific S:N internal quotas. On the other hand, DMS values are again severely underestimated and, although a summer maximum is now predicted, it is deeper in the water column and smaller in magnitude than seen in the observations. Furthermore, predicted DMS in surface waters does not display the summer maximum seen in the observations, but rather shows a spring maximum. It therefore appears that inclusion of a variable the S:N ratio of phytoplankton in the model can not on its own account for the observed seasonality of DMS nor explain the DMS summer-paradox.

#### 2.3.1.3 Experiment C

Next, the inhibition of bacterial uptake of nutrients (semilabile-DOM/$NH_4^+$) and sulfur (DMSPd and DMS) by solar radiation was added to the model (*Herndl et al.*, 1993; *Slezak et al.*, 2001; *Toole et al.*, 2006). This fact has been also cited as a potential explanation for the DMS summer-paradox since a reduction in a major sink may cause DMS to accumulate (*Simó and Pedros-Alió*, 1999a; *Simó*, 2001, 2004). Model results (see Figure 2.5) indicate that inhibition of bacterial sulfur uptake by UV could partly explain the cause of the deep summer maximum of DMS, although the predicted maximum is slightly deeper than in the observations and DMS values remain underestimated. However, DMS accumulation occurs in conjunction with an unrealistically large accumulation of DMSPd. This overestimate in modelled DMSPd may be due to the absence in the model of phytoplankton uptake, a new sink for DMSPd that has been recently discovered experimentally (*Vila-Costa et al.*, 2006b). The DMSPd accumulation implies a large contribution to DMS from free DMSP-lyases (1% of the DMSPd pool is converted into DMS each day). We therefore have repeated experiments B and C, but without free DMSP-lyases activity to evaluate if inhibition of bacterial sulfur uptake by UV can produce this DMS accumulation. Results (not shown) displayed a very weak increase of the deep DMS maximum in summer (much weaker than the increase observed from experiment B to experiment C, see Figure 2.5),

not enough to be the origin of the DMS summer-paradox. This result is a consequence of the fact that, although bacterial DMS uptake is reduced by the UV-induced inhibition (which tends to increse DMS), there is also a reduction of bacterial DMS production (from the associated inhibition of DMSPd uptake). The net balance of these two opposite effects is almost zero.

#### 2.3.1.4 Experiment D

The next process added to the model was consumption of DMSPd by phytoplankton. It has been reported recently that some groups of phytoplankton (diatoms and cyanobacteria) are able to take up DMSPd (*Vila-Costa et al.*, 2006b). This process may help explain the low values of DMSPd observed in the field and the strong decoupling of DMSPd to either DMSPp or DMS (*Dacey et al.*, 1998). The resulting simulations (see Figure 2.6) show an improvement in predicted DMSPd concentrations, although spring values are still overestimated relative to the observations. On the other hand, modelled DMS is totally unsatisfactory, with values clearly underestimated and showing a very weak deep summer maximum.

#### 2.3.1.5 Experiment E

The next addition to the model was a direct exudation term of DMS from phytoplankton cells as a response to UV-induced stress (*Sunda et al.*, 2002; *Toole and Siegel*, 2004). Direct DMS production by phytoplankton has been reported previously in the literature (*Vairavamurthy et al.*, 1985; *Niki et al.*, 2000; *Wolfe et al.*, 2002). This DMS production, therefore, is not routed through the DMSPd pool but comes directly from the DMSPp (in the model it is assumed that the amount of DMS exuded from the cells is immediately replaced by newly produced DMSPp). The results of this experiment, which incorporates all the mechanisms thought to be important in the sulfur cycle of the ocean, show a clear improvement over those of the previous experiments and also of existing DMSP/DMS models. Simulated DMS now shows good agreement with the observations (see Figure 2.7), with a summer maximum of about 5 $\propto$molS $m^{-3}$ at around 20m depth and winter minima of about 0.5 $\propto$molS $m^{-3}$. The predicted summer DMS maximum occurs below the surface because of the high DMS photolysis and ventilation rates occurring in the upper layers. The results suggest that phytoplankton DMS exudation may be an important factor contributing to the high summer to winter ratio of DMS concentrations observed in the field as well as explaining the strong decoupling between CHL and DMS.

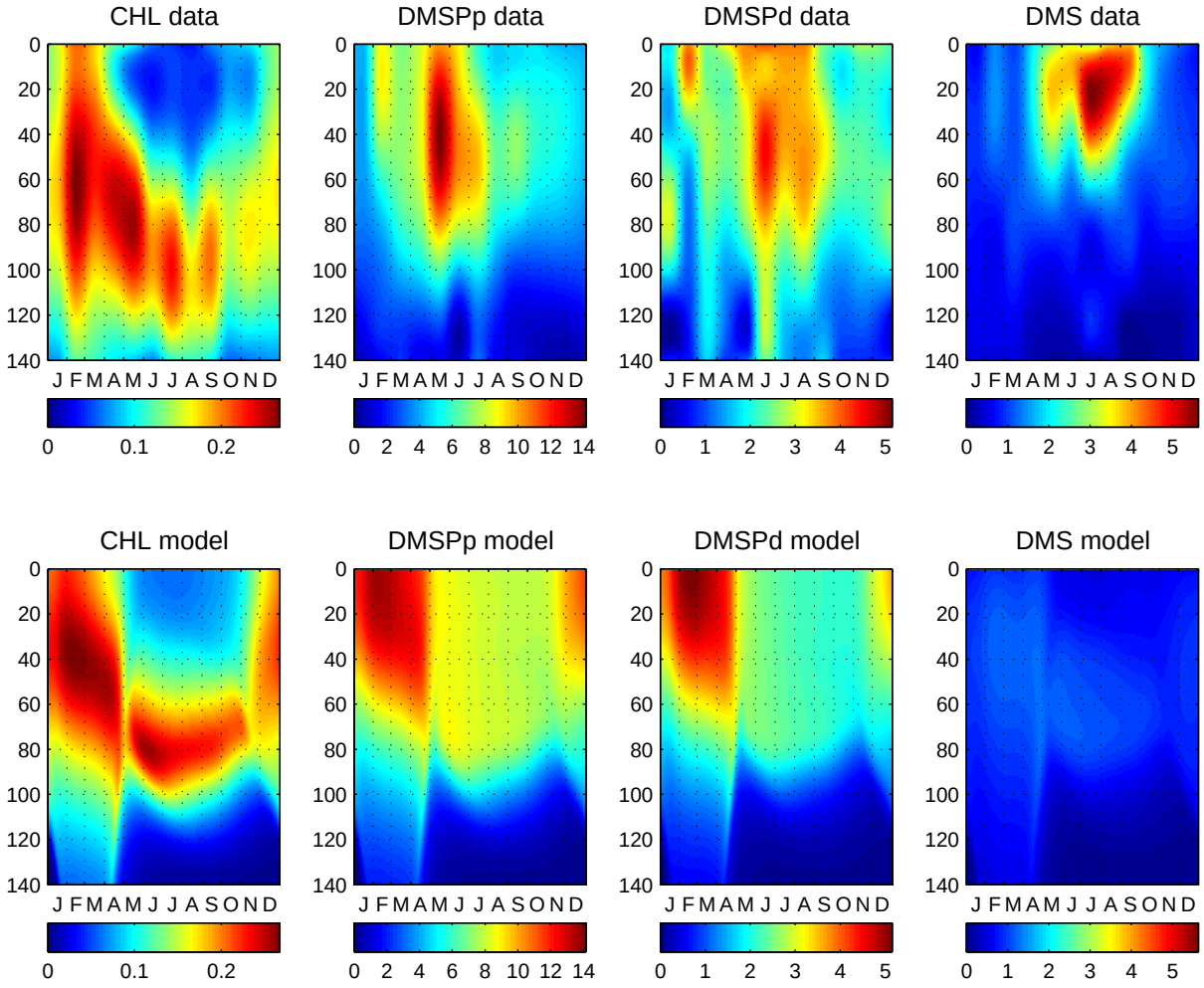


Fig. 2.3: 2D plots (time, depth) of chlorophyll-a, DMSP particulate, DMSP dissolved and DMS from climatological *in-situ* data (upper panels) and DMOS model results (lower panels) for Experiment A: *i*) no phytoplankton succession in terms of DMSP production; *ii*) no UV-induced inhibition of bacterial sulfur uptakes; *iii*) no phytoplankton uptake of DMSP dissolved; *iv*) no phytoplankton exudation of DMS due to UV stress. Units: chlorophyll-a (mg $m^{-3}$), DMSPp-DMSPd-DMS ($\propto$molS $m^{-3}$)

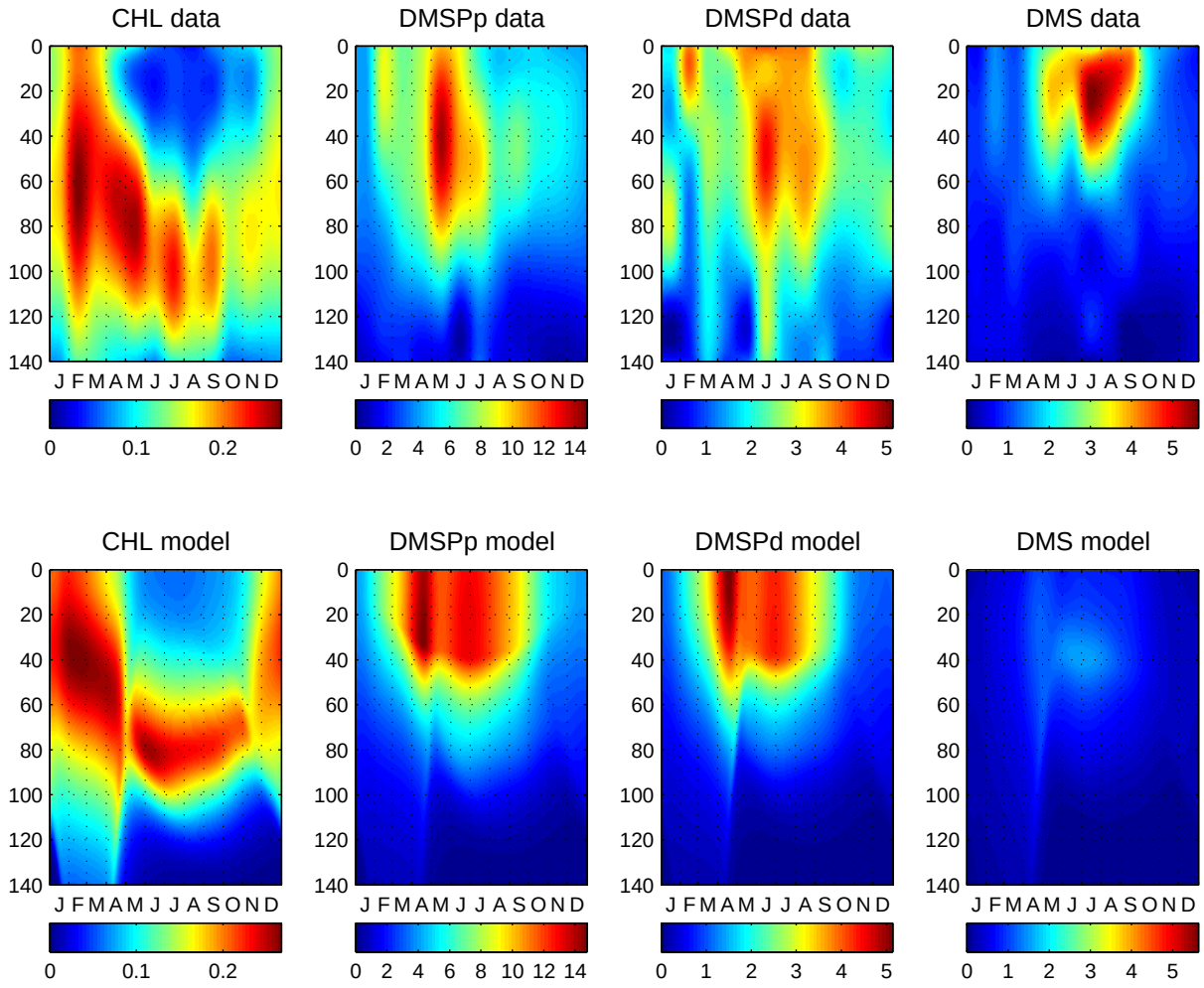


Fig. 2.4: 2D plots (time, depth) of chlorophyll-a, DMSP particulate, DMSP dissolved and DMS from climatological *in-situ* data (upper panels) and DMOS model results (lower panels) for Experiment B: *i*) yes phytoplankton succession in terms of DMSP production; *ii*) no UV-induced inhibition of bacterial sulfur uptakes; *iii*) no phytoplankton uptake of DMSP dissolved; *iv*) no phytoplankton exudation of DMS due to UV stress. Units: chlorophyll-a (mg $m^{-3}$), DMSPp-DMSPd-DMS ($\propto$molS $m^{-3}$)

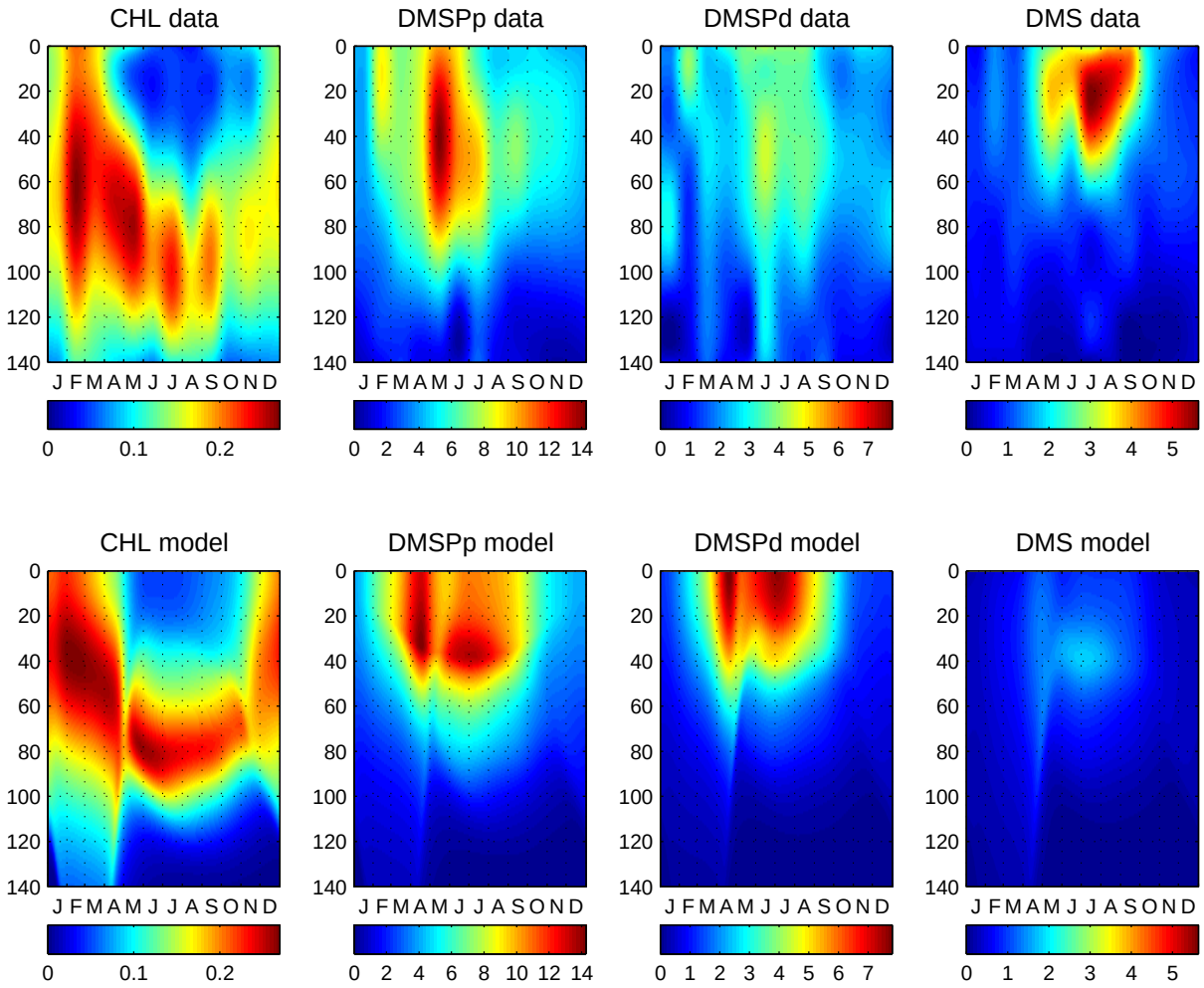


Fig. 2.5: 2D plots (time, depth) of chlorophyll-a, DMSP particulate, DMSP dissolved and DMS from climatological *in-situ* data (upper panels) and DMOS model results (lower panels) for Experiment C: *i)* yes phytoplankton succession in terms of DMSP production; *ii)* yes UV-induced inhibition of bacterial sulfur uptakes; *iii)* no phytoplankton uptake of DMSP dissolved; *iv)* no phytoplankton exudation of DMS due to UV stress. Units: chlorophyll-a (mg $m^{-3}$), DMSPp-DMSPd-DMS ($\propto$molS $m^{-3}$)

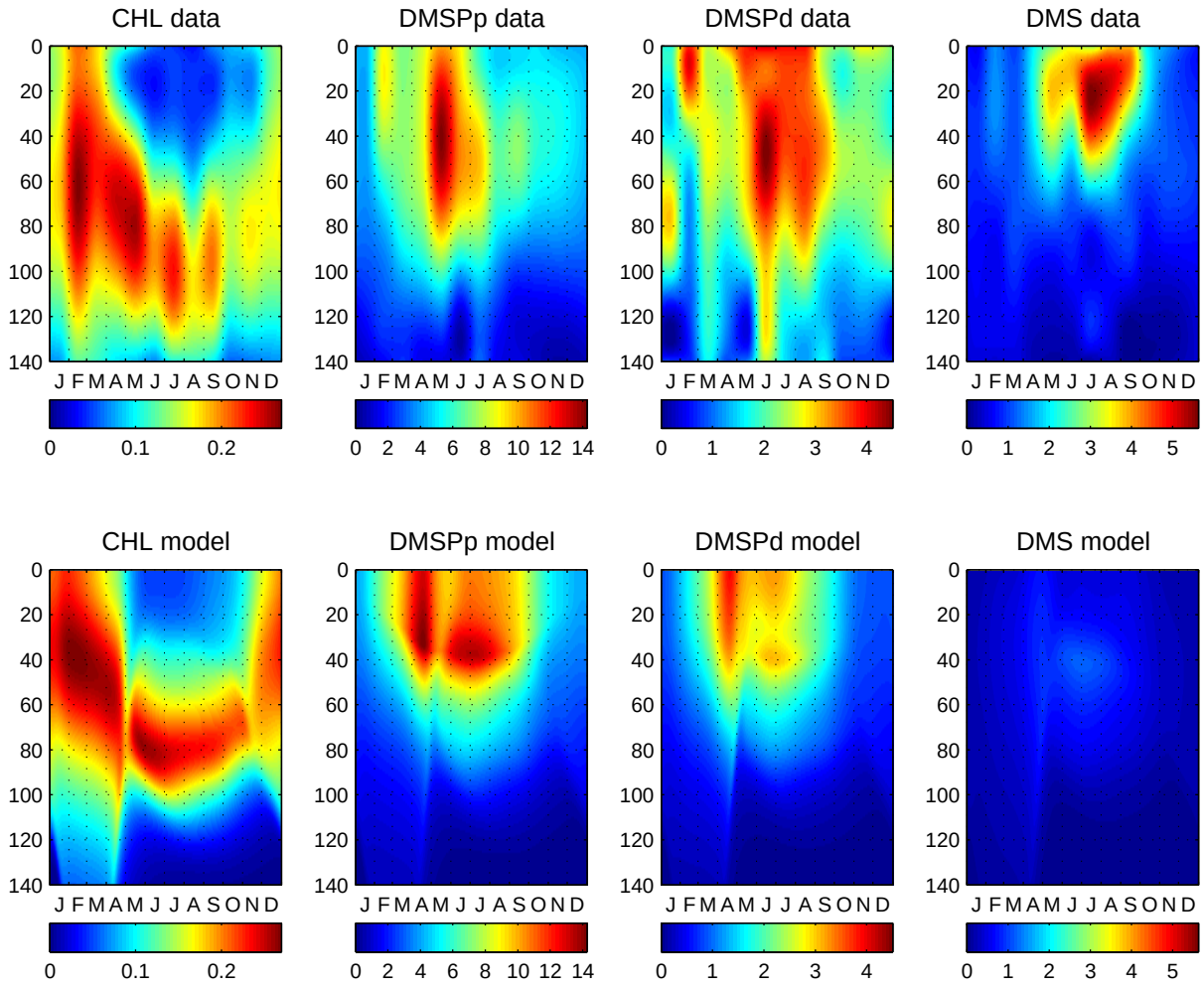


Fig. 2.6: 2D plots (time, depth) of chlorophyll-a, DMSP particulate, DMSP dissolved and DMS from climatological *in-situ* data (upper panels) and DMOS model results (lower panels) for Experiment D: *i)* yes phytoplankton succession in terms of DMSP production; *ii)* yes UV-induced inhibition of bacterial sulfur uptakes; *iii)* yes phytoplankton uptake of DMSP dissolved; *iv)* no phytoplankton exudation of DMS due to UV stress. Units: chlorophyll-a (mg $m^{-3}$), DMSPp-DMSPd-DMS ($\propto$molS $m^{-3}$)

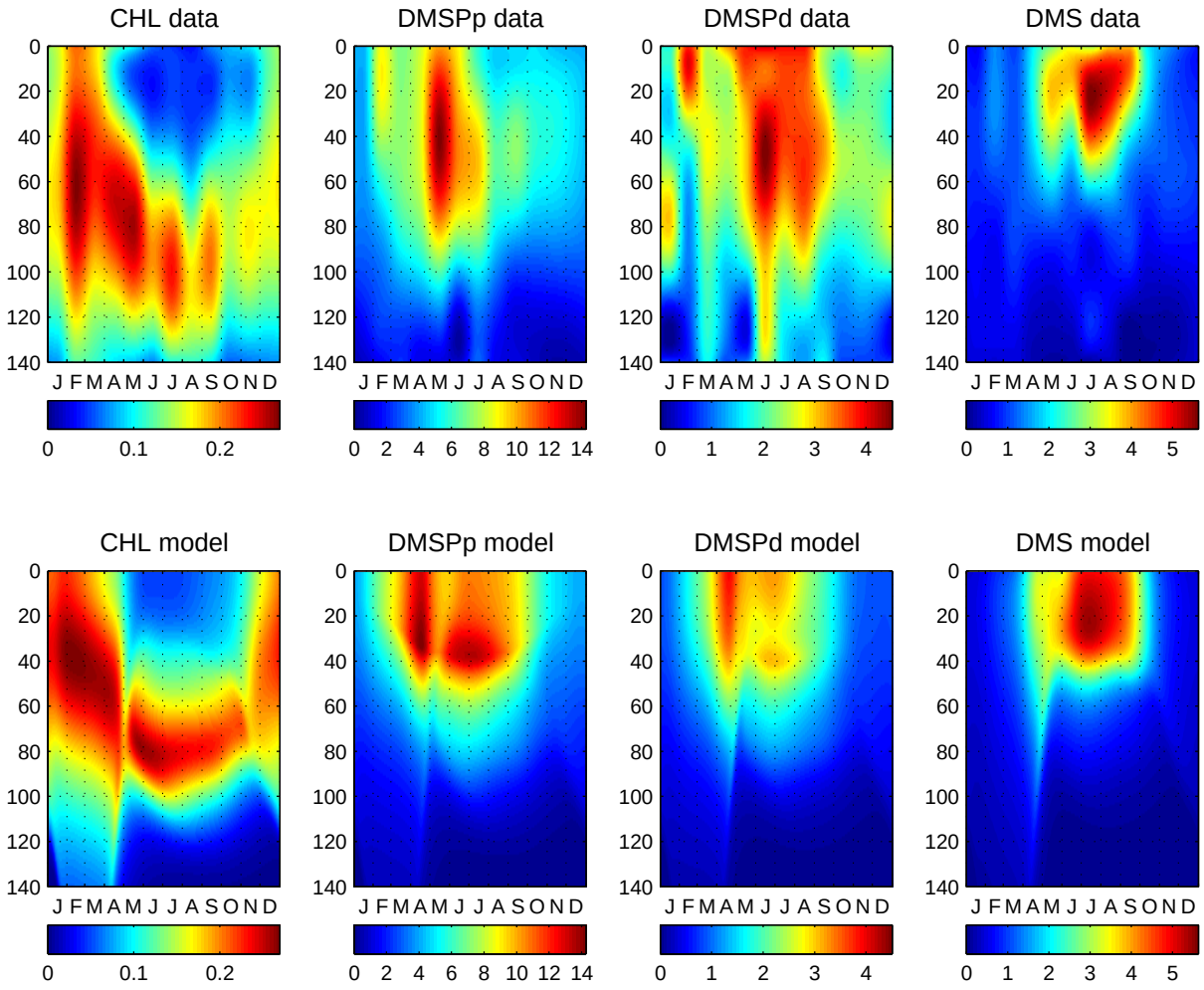


Fig. 2.7: 2D plots (time, depth) of chlorophyll-a, DMSP particulate, DMSP dissolved and DMS from climatological *in-situ* data (upper panels) and DMOS model results (lower panels) for Experiment E: *i*) yes phytoplankton succession in terms of DMSP production; *ii*) yes UV-induced inhibition of bacterial sulfur uptakes; *iii*) yes phytoplankton uptake of DMSP dissolved; *iv*) yes phytoplankton exudation of DMS due to UV stress. Units: chlorophyll-a (mg $m^{-3}$), DMSPp-DMSPd-DMS ($\propto$molS $m^{-3}$)

### 2.3.2 Further analysis of Experiment E

Results from the series of experiments described above indicate that the various mechanisms involved in the S-cycle (seasonal variations in the internal S:N quota, bacterial inhibition of sulfur uptake, exudation of DMS as well as DMSPd uptake by phytoplankton) all can play a role in driving the DMS seasonality. The direct exudation of DMS from phytoplankton cells (as a response of high UV doses) does however appear to be a major one: without this process the model is unable to realistically reproduce the observed DMS cycle and thereby explain the summer-paradox.

Monthly UML averages of CHL, DMSPp, DMSPd and DMS (data and model) are shown in Figure 2.8, along with their associated (Spearman) correlation coefficients. In general, the model is able to realistically capture both the seasonality and the absolute magnitude of these four variables. The main discrepancies between the model and the observations are that model summer DMSPp values are clearly overestimated (by as much as a factor of two in August) and that DMPSd values are slightly underestimated in the model. In this regard, however, experimentalists believe that past and current DMSPd measurements are likely to be overestimates due to filtration artifacts (*Kiene and Slezak*, 2006).

Examination of the 50-m depth integrated values for DMSPp, DMSPd, DMS and the DMS:DMSPp ratio (Figure 2.9) leads to similar conclusions. The model does a reasonably good job at reproducing the sulfur variables, although the predicted DMSPp maximum occurs one month too early and predicted DMSPp concentrations are generally too high. On the other hand, DMSPd values are underestimated in summer. Both modelled DMS and data display maxima in July, showing good agreement both in magnitude and seasonality. Due to the predictions of DMSPp being too high in August, the modelled DMS/DMSPp ratio is, however, markedly underestimated for this month.

The vertically resolved seasonal cycles of predicted sulfur fluxes in the model are shown in Figure 2.10. Bacterial uptake of DMSPd (Figure 2.10a) is highest in spring and summer (e.g., more than $\approx$1.5 $\propto$molS $m^{-3}$ $d^{-1}$ occurred at depths between 20m and 60m) coincident with high modeled bacterial biomass (see Figure 2.2) and DMSPd concentrations (see Figure 2.7). Uptake rates decline thereafter until an annual minimum is reached in winter. Phytoplankton uptake of DMSPd (Figure 2.10b) displays a similar seasonality, with an annual maximum in spring ($\approx$1.5 $\propto$molS $m^{-3}$ $d^{-1}$ in April) and a secondary maximum during summer ($\approx$1.0 $\propto$molS $m^{-3}$ $d^{-1}$) for surface waters ($<$ 30m). Bacterial uptake of DMSPd is in general higher than that of phytoplankton, and has a broader and deeper distribution (values higher than 1 $\propto$molS $m^{-3}$ $d^{-1}$ reach depths of about 80m while phytoplankton uptake does not occur deeper than 40m).

Bacterial uptake of DMS (Figure 2.10c) is highest in summer at depths between 20m and 40m, reaching values of 0.5 $\propto$molS $m^{-3}$ $d^{-1}$. In July 2004, *del Valle et al.* (2007) reported a maxi-

mum DMS consumption rate of ≈0.8 ∝molS $m^{-3}$ $d^{-1}$ around 40m depth. In surface waters in summer, bacterial uptake rates of both DMSPd and DMS (Figure 2.10a and Figure 2.10c) are reduced by almost a half due to UV-induced bacterial inhibition. Minimum bacterial DMS uptake occurs during winter due to the very low DMS concentrations. Relatively low bacterial DMS consumption rates (0.3 ∝molS $m^{-3}$ $d^{-1}$) were measured in the Sargasso Sea in May at the DCM by *Levasseur et al.* (2004). Similar rates (0.2-0.3 ∝molS $m^{-3}$ $d^{-1}$, see Figure 2.10c) are predicted in the model in May between 60-80m (the depth of modelled DCM, see Figure 2.7).

The predicted bacterial production of DMS by enzymatic cleavage of DMSPd (Figure 2.10d) follows the DMSPd uptake (Figure 2.10a) and represents approximately 8-9% of the former, in agreement with estimates for the Northern Sea (6-12%, see *Zubkov et al.* (2002)). Maximum values (higher than ≈0.15 ∝molS $m^{-3}$ $d^{-1}$) therefore are obtained in spring and summer at depths between 20m and 60m. On the other hand, DMS production from phytoplankton exudation (Figure 2.10e) displays its highest values in summer at the very surface, reaching rates of more than 1.5 ∝molS $m^{-3}$ $d^{-1}$ in July. Since this process is light-driven, the values increase exponentially towards the surface. The sum of phytoplankton exudation and bacterial DMS production gives a higher gross biological production in summer (up to 1.8 ∝molS $m^{-3}$ $d^{-1}$, not shown) in the UML. In spring, the modelled gross biological production of DMS at the surface is about 1.4-1.6 ∝molS $m^{-3}$ $d^{-1}$, a value in good agreement with in situ data from the Sargasso Sea (1.8 ∝molS $m^{-3}$ $d^{-1}$, (*Levasseur et al.*, 2004)). In a separate short-term study, where a mass balance assumption was applied to measured rates, light-mediated biological DMS production rates as high as 8 ∝molS $m^{-3}$ $d^{-1}$ were estimated by *Toole et al.* (2006). There is such a scarcity of *in-situ* measurements addressing this issue that future field work is needed. DMS photolysis (Figure 2.10f) also reaches a maximum in summer (up to 0.6 ∝molS $m^{-3}$ $d^{-1}$ in July) as a consequence of maximum DMS concentrations and light exposure. *Toole et al.* (2003) estimated maximum UML-integrated DMS photolysis rates in summer of about 10-15 ∝molS $m^{-2}$ $d^{-1}$. These estimates were based on a summer MLD of ≈20m. For this MLD value, our integrated DMS photolysis rates in summer are very similar (10-12 ∝molS $m^{-2}$ $d^{-1}$).

Model sulfur fluxes averaged over the UML are shown in Figure 2.11. Bacterial and phytoplankton uptake of DMSPd are similar in magnitude (Figure 2.11a and Figure 2.11b respectively) as are bacterial DMS consumption and DMS photolysis (Figure 2.11c and Figure 2.11f). On the other hand, predicted phytoplankton DMS exudation can be an order of magnitude higher (e.g. in summer) than bacterial production (Figure 2.11e and Figure 2.11d respectively).

Turnover rates of DMSPd and DMS due to bacterial consumption, phytoplankton DMSPd uptake, and DMS photolysis are shown in Figure 2.12. Turnover rate (or rate constant, $d^{-1}$) is the process rate (∝molS $m^{-3}$ $d^{-1}$) divided by the concentration (∝molS $m^{-3}$). Maximum turnover rates, thus lower turnover times (1/turnover rates, d), due to bacterial uptake are obtained at depth (between 20-60m in winter and 60-80m in summer) both for DMSPd and DMS (Figure 2.12a and Figure 2.12c respectively). Bacterial inhibition of sulfur uptake by UV at the surface

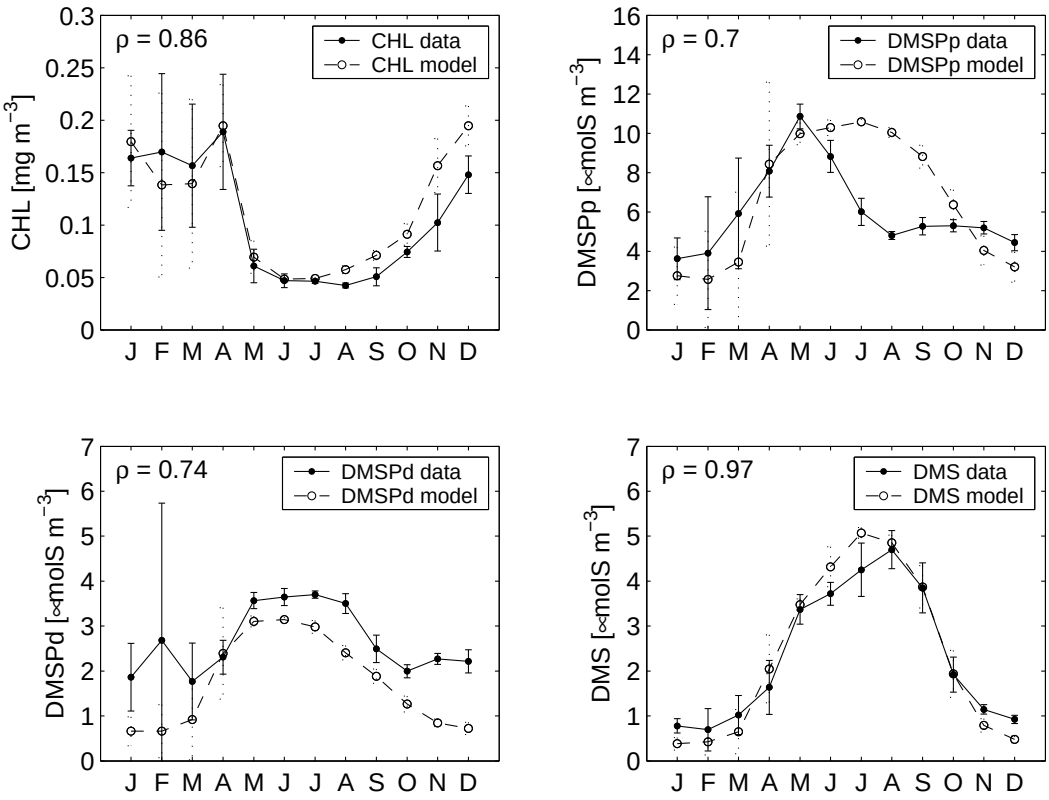


Fig. 2.8: Monthly upper mixed-layer averaged values of chlorophyll-a, DMSP particulate, DMSP dissolved and DMS for climatological *in-situ* data (solid line) and DMOS model results (dashed line) for Experiment E. Units: chlorophyll-a (mg m$^{-3}$), DMSPp-DMSPd-DMS (∝molS m$^{-3}$)

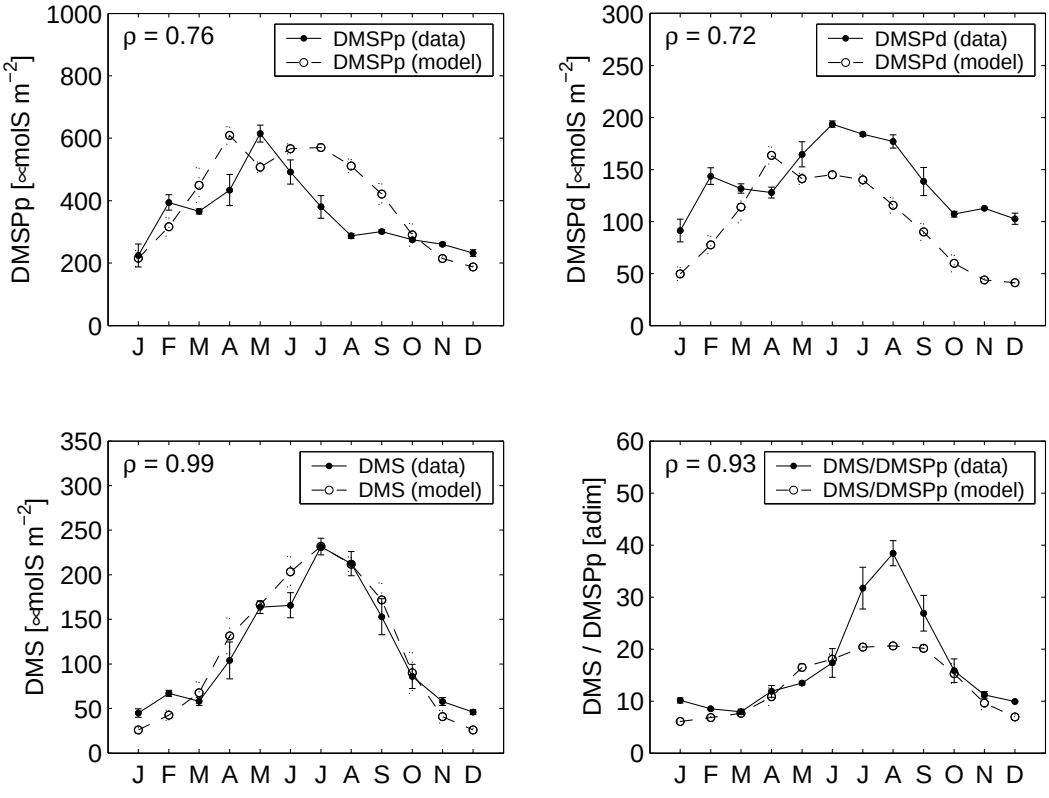


Fig. 2.9: Monthly upper 50m-integrated values of DMSP particulate, DMSP dissolved, DMS and DMSPp/DMS ratio for climatological *in-situ* data (solid line) and DMOS model results (dashed line) for Experiment E. Units: DMSPp-DMSPd-DMS (∝molS m$^{-2}$).

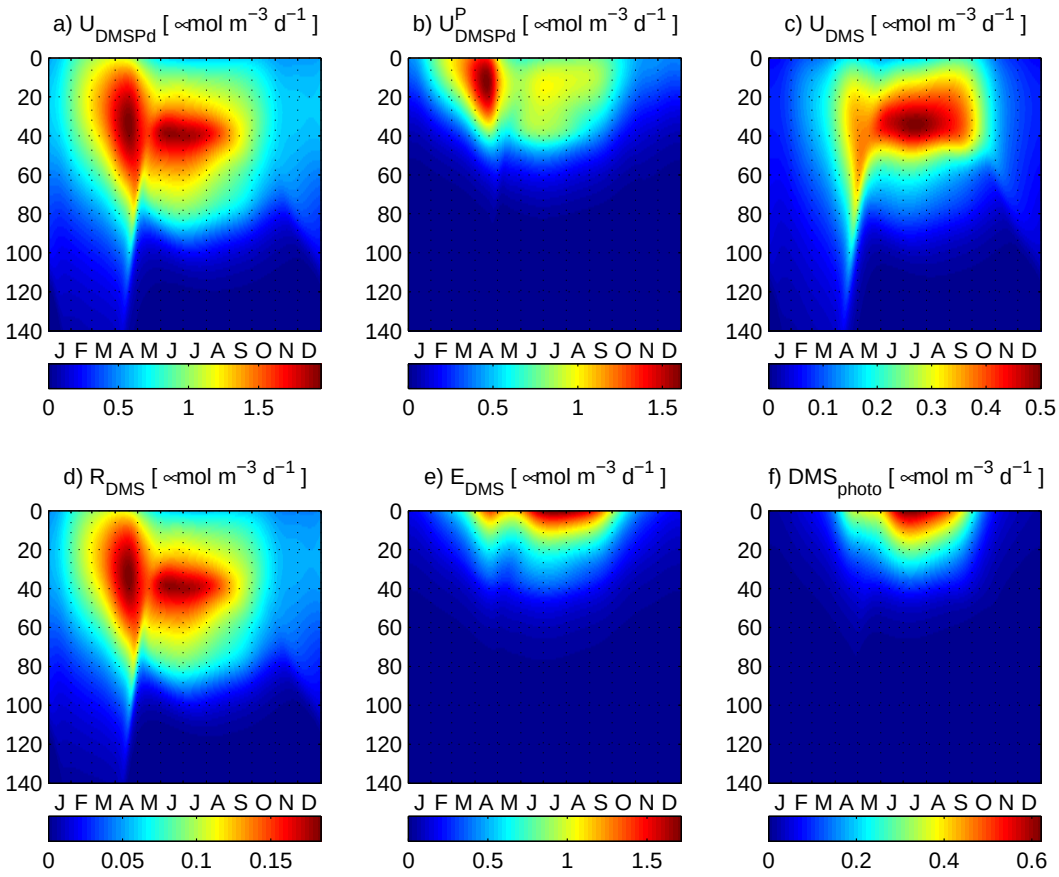


Fig. 2.10: 2D (time, depth) plots of DMOS model sulfur fluxes (∝molS $m^{-3}$ $d^{-1}$) for Experiment E: a) Bacterial uptake of DMSP dissolved. b) Phytoplankton uptake of DMSP dissolved. c) Bacterial uptake of DMS. d) Bacterial production of DMS. e) Phytoplankton production of DMS. f) Photolysis of DMS.

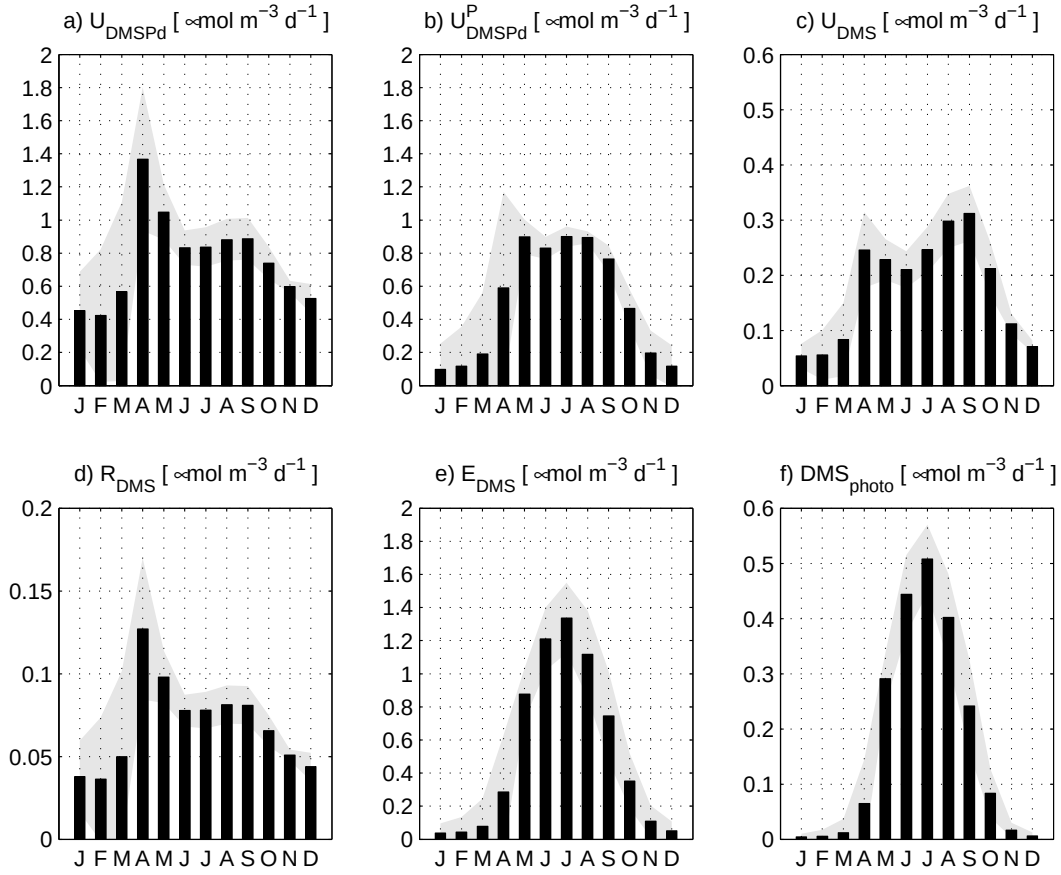


Fig. 2.11: Monthly upper mixed-layer averaged values of DMOS model sulfur fluxes (∝molS $m^{-3}$ $d^{-1}$) for Experiment E: a) Bacterial uptake of DMSP dissolved. b) Phytoplankton uptake of DMSP dissolved. c) Bacterial uptake of DMS. d) Bacterial production of DMS. e) Phytoplankton production of DMS. f) Photolysis of DMS. The gray shadow area represents the standard deviation of the averages.

is observed in summer. Turnover rates of DMS are about 20% of those for DMSPd because only this percentage of bacteria was assumed to be DMS consumers (see section 2.2.4). Thus, minimum turnover times for bacterial consumption of DMSPd and DMS are estimated as $\approx$1.5 and $\approx$6 days, respectively. Bacterial turnover rates of DMSPd and DMS have also been observed to be highest in subsurface waters of the North Sea during a coccolithophore bloom (although they were nevertheless about an order of magnitude higher than our results) (*Zubkov et al.*, 2001, 2002). For the Sargasso Sea, DMSPd and DMS turnover times have been estimated to vary between 0.4-2.8 days and $<$0.5-8 days respectively (*Ledyard and Dacey*, 1996).

Predicted rates of phytoplankton DMSPd turnover (Figure 2.12b) are of the same order of magnitude (yet slightly lower) than those of bacterial uptake (Figure 2.12a). Their vertical distribution is however very different because phytoplankton uptake depends on primary production and hence is only significant in irradiated waters ($<$ 40m). Maximum values are present in spring due to the highest primary production. Total DMSPd turnover rates (bacterial and phytoplankton uptakes plus free DMSP-lyases activity) for the upper 50m are in the range of 0.5-1.0 $d^{-1}$ (not shown), in good agreement with the values reported by *Ledyard and Dacey* (1996) for the Sargasso Sea (0.7-1.5 $d^{-1}$, see Table 2 in *Kiene et al.* (2000)). Maximum turnover rates of DMS photolysis (Figure 2.12d) are about 75% of the maximum rates of bacterial consumption (Figure 2.12c). Highest photolysis rates are, however, mainly concentrated in the upper 20m in summer, a layer and period where bacterial consumption is low. Photolysis then dominates the loss of DMS in the upper ocean, while bacterial consumption dominates at greater depths (*Toole et al.*, 2006; *Kieber et al.*, 1996).

Turnover rates averaged for the UML are shown in Figure 2.13. UML DMS turnover rates are between 0.05 and 0.15 $d^{-1}$. For a 60m mixed water column in the equatorial Pacific, *Kieber et al.* (1996) obtained bacterial DMS turnover rates of 0.04-0.66 $d^{-1}$. In the Sargasso Sea, bacterial DMS consumption rates in September were estimated to be $\approx$0.5 $\propto$molS $m^{-3}$ $d^{-1}$ (*Lefèvre et al.*, 2002, and references therein). For that month UML averaged DMS concentration from the data is about 4.0 $\propto$molS $m^{-3}$ (see Figure 2.8), giving a specific rate of 0.12 $d^{-1}$, similar in magnitude to the model results ($\approx$0.08 $d^{-1}$, see September in Figure 2.13c). An interesting feature emerging from the model results is that bacterial DMS consumption is the dominant loss term in winter and spring (Figure 2.13c), while in summer it is DMS photolysis (Figure 2.13d), as postulated previously (*Toole et al.*, 2006).

We calculated the DMS-yield (eq(2.79)) for the whole food web (total DMS production divided by total DMSP consumption) from the model sulfur fluxes, as well as the net biological production of DMS (total DMS production minus bacterial DMS consumption) averaged over the UML (see Figure 2.14). The DMS-yield (Figure 2.14a) displays a clear seasonal pattern with higher values during summer (up to $\approx$45%) and lower values in winter ($\approx$10%). For both variables the annual maximum is observed in July. These values are in the range reported in the literature (*Simó and Pedros-Alló*, 1999a). Net biological production of DMS (Figure 2.14b) follows the

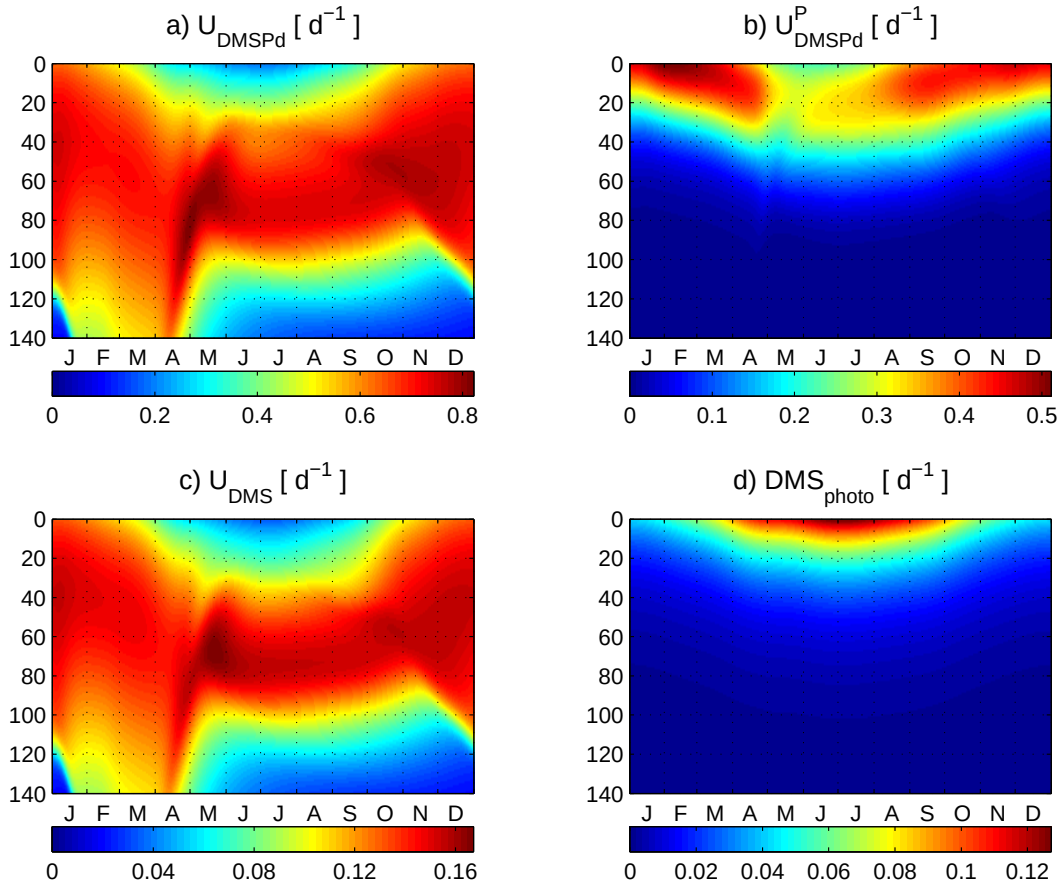


Fig. 2.12: 2D (time, depth) plots of DMOS model sulfur turnover rates ($d^{-1}$) for Experiment E: a) Bacterial uptake of DMSP dissolved. b) Phytoplankton uptake of DMSP dissolved. c) Bacterial uptake of DMS. d) Photolysis of DMS.

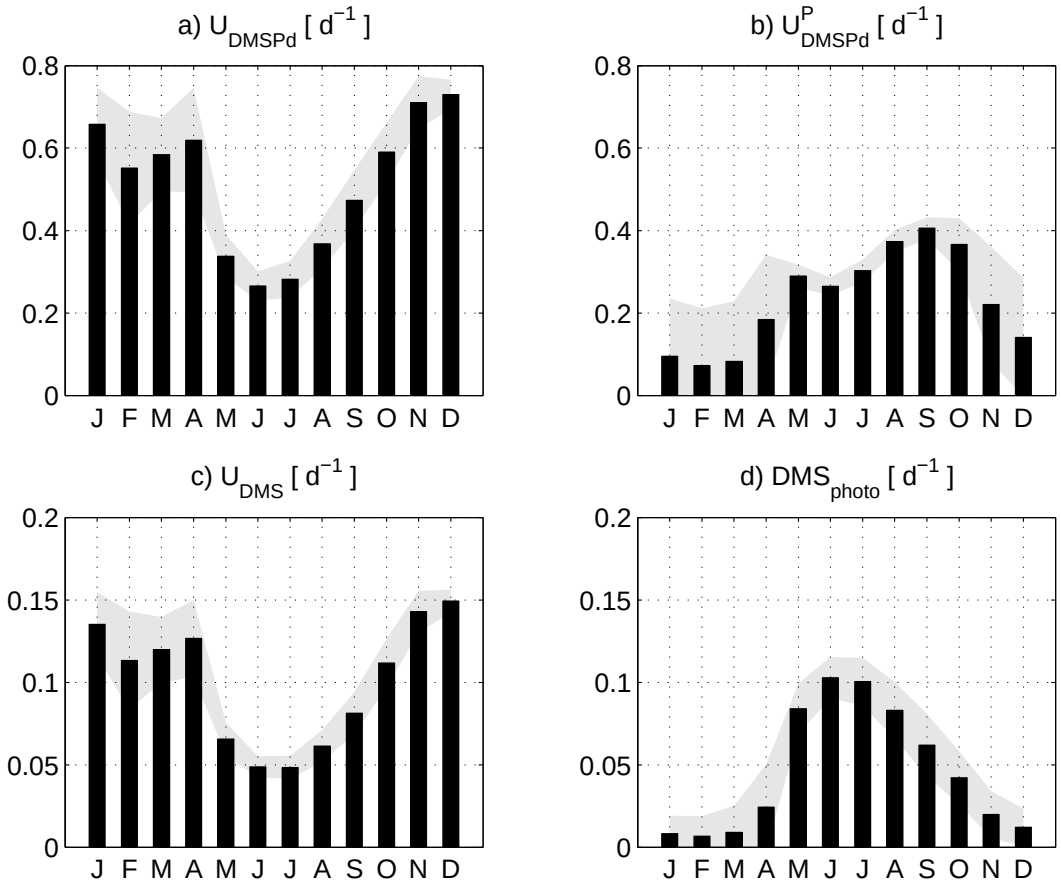


Fig. 2.13: Monthly upper mixed-layer averaged values of DMOS model sulfur turnover rates ($d^{-1}$) for Experiment E: a) Bacterial uptake of DMSP dissolved. b) Phytoplankton uptake of DMSP dissolved. c) Bacterial uptake of DMS. d) Photolysis of DMS.

same seasonality, increasing from almost zero to ≈1.2 ∝molS $m^{-3}$ $d^{-1}$ in summer. Very similar values and seasonality of net biological production of DMS were estimated by *Toole and Siegel* (2004), based on the same set of data, when using a mass-balance model (from zero in winter to 1.0-1.5 ∝molS $m^{-3}$ $d^{-1}$ in summer).

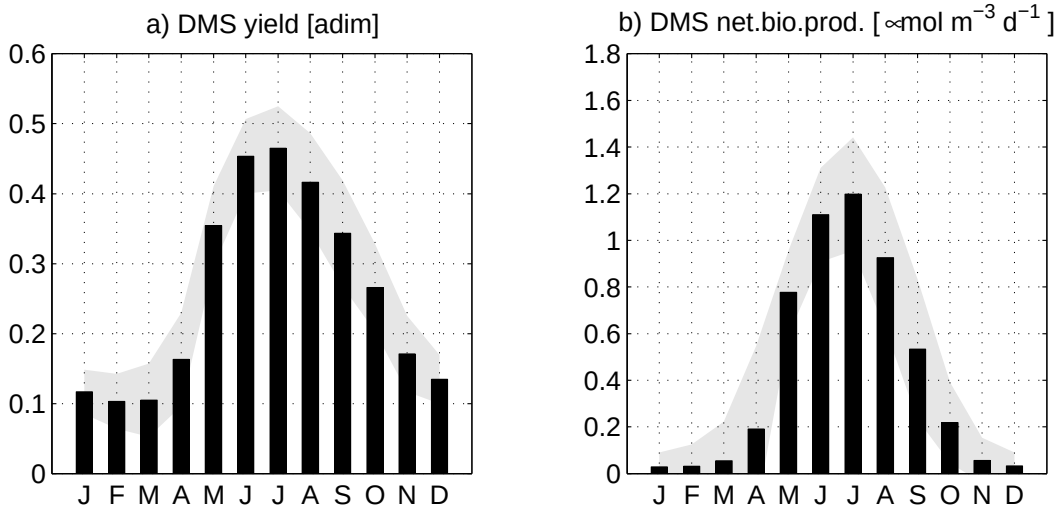


Fig. 2.14: Monthly upper mixed-layer averaged values of: a) DMS yield (DMS production / DMSP consumption). b) net biological DMS production (DMS production - bacterial uptake of DMS). The gray shadow area represents the standard deviation of the averages.

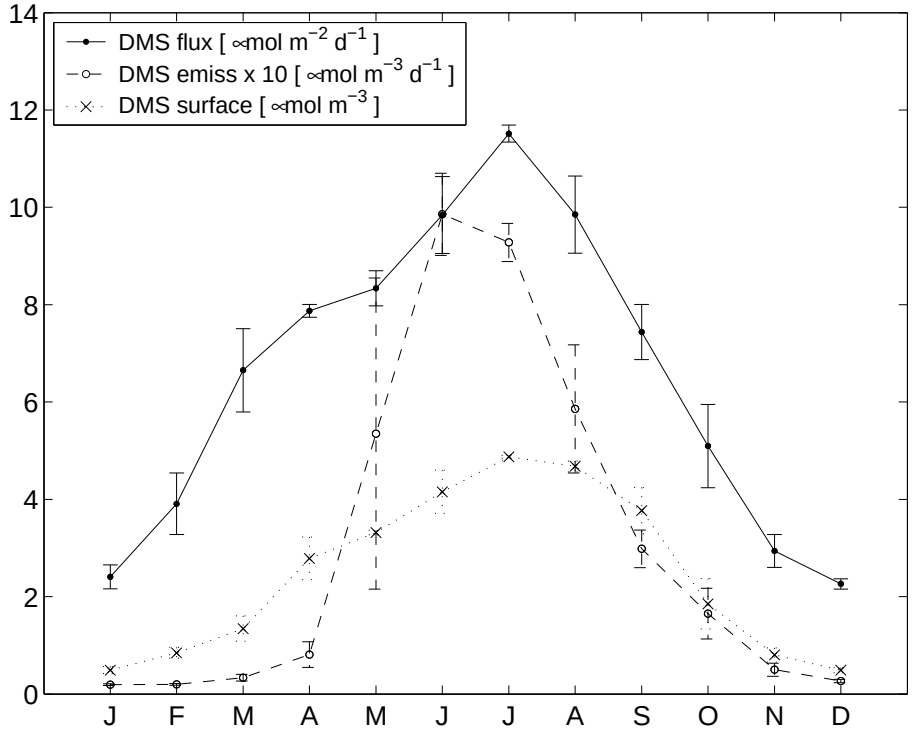


Fig. 2.15: Monthly-averaged values and standard deviation of surface DMS (∝molS $m^{-3}$, dotted line), DMS ventilation flux (∝molS $m^{-2}$ $d^{-1}$, solid line), upper mixed layer DMS ventilation (defined as DMS flux / MLD) (10*∝molS $m^{-3}$ $d^{-1}$, dashed line).

Since DMS fluxes to the atmosphere are believed to have a role in regulating climate (*Charlson et al.*, 1987; *Andreae and Crutzen*, 1997), we plotted them along with UML DMS emission rates (DMS flux divided by the MLD) and surface DMS concentrations (upper top cell grid) (see

Figure 2.15). The highest values of the three variables occur in summer (June, July, August). In particular, DMS flux to the atmosphere shows a clear maximum in July ($\approx$12 $\propto$molS $m^{-2}$ $d^{-1}$). The UML is exposed to very high doses of solar radiation during this month (because of the high solar incident radiation and very shallow MLD). If the proposed antioxidant function of DMS (*Sunda et al.*, 2002) as well as the impact of DMS on CCN and Earth albedo are shown to be important, then this higher DMS flux to the atmosphere in summer could act as a negative feedback between the ocean's ecosystems and the amount of solar radiation reaching the ocean's surface (*Charlson et al.*, 1987; *Vallina and Simó*, 2007a; *Vallina et al.*, 2007a). Maximum DMS emissions from the UML (June/July; $\approx$1.0 $\propto$molS $m^{-3}$ $d^{-1}$) are about a factor of two and four higher than the summer DMS losses by photolysis or bacterial consumption respectively ($\approx$0.5 and $\approx$0.25 $\propto$molS $m^{-3}$ $d^{-1}$; see Figure 2.11c and Figure 2.11f).

### 2.3.3 Sensitivity Analysis

In order to evaluate the sensitivity of model results to model parameters values we carried out a sensitivity analysis (SA) by increasing/decreasing each parameter by 50% in each run and comparing the results to the control simulation (experiment E, Table 2.1 with the exception of parameters $\delta_1$, $\alpha_1$ and $\phi_{inhib}^{max}$ that were lowered to 0.5 in the reference control to allow an increase of 50%). The SA index was taken from *Le Clainche et al.* (2004) and is defined as follows:

$$S_k = \frac{X_{k_{max}} - X_{k_{min}}}{X_{k_{control}}} * 100$$

where $X_{k_{control}}$, $X_{k_{max}}$ and $X_{k_{min}}$ are the annual budgets of DMSPp, DMSPd and DMS integrated over the upper 50m obtained for the 3 simulations: control (reference value of the parameter $k$), 50% increase in the parameter $k$ ($k_{max} = 1.5k$), and 50% decrease in the parameter $k$ ($k_{min} = 0.5k$) (*Le Clainche et al.*, 2004). Only those parameters which gave SA indices greater than 10% are plotted in Figure 2.16. Black bars indicate that an increase of the parameter results in an increase in the state variable, while grey bars indicate that an increase in the parameter produced a decrease in the state variable.

For DMSPp (Figure 2.16a) we observe that parameters related to zooplankton grazing have the largest effects, mainly the maximum zooplankton specific ingestion rate. This is not surprising since they directly affect the phytoplankton biomass. Another important parameter is the labile fraction of DOM produced. Other SA tests (not shown) revealed that this parameter is a key one for the nutrient pools due to the bacterial microbial loop; an increase of DOM concentrations is associated to a rise of $NO_3^=$ and $NH_4^+$ in the model, and thus to an increase of modelled phytoplankton. Bacterial hydrolysis of semilabile DOM and gross growth efficiency are also very important because they affect the amount of labile DOM (and then again the nutrient pools and phytoplankton biomass). Parameters related to zooplankton mortality are associated to DMSPp through the levels of grazing activity upon phytoplankton, while the zooplankton C:N ra-

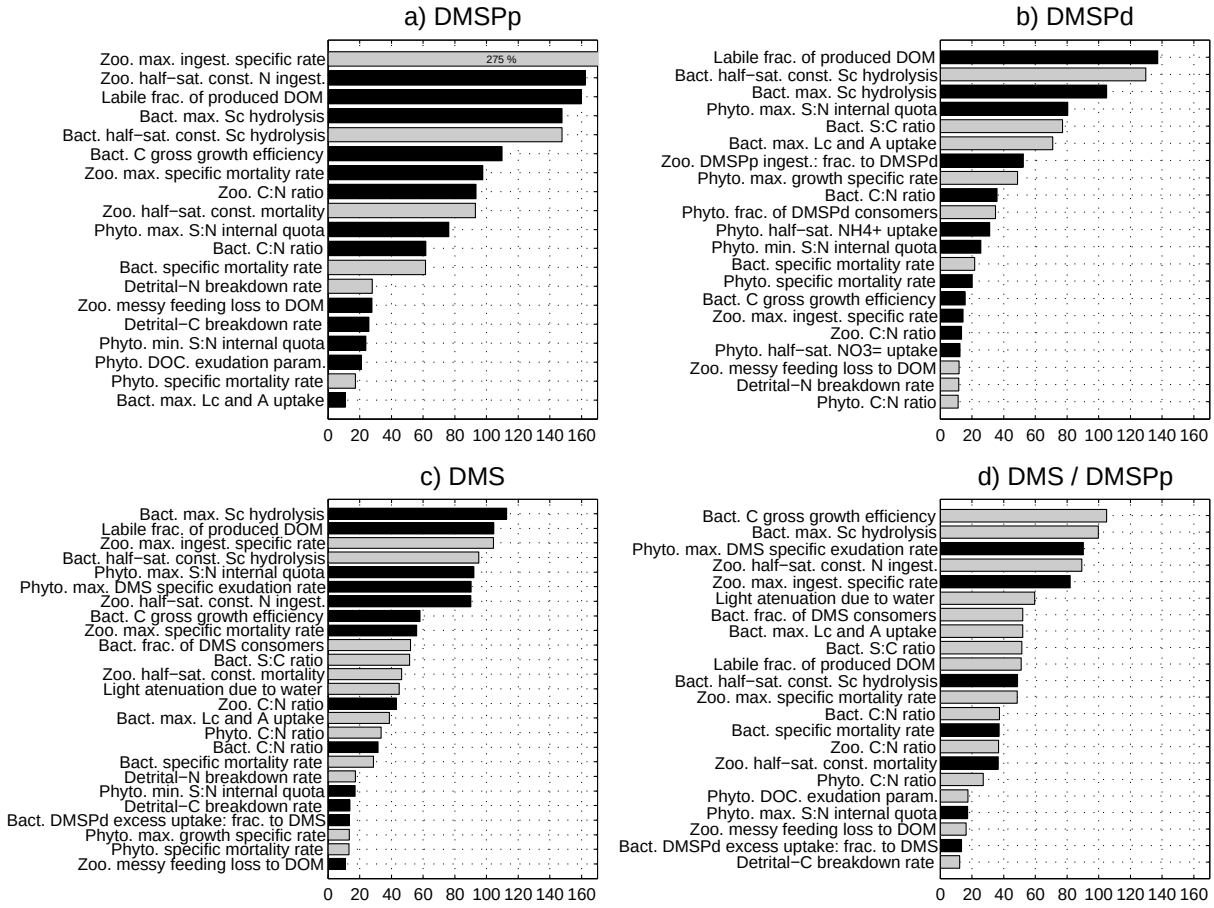


Fig. 2.16: Sensitivity Analysis indices of the DMOS model to changing parameters by ± 50%. Black bars indicate that an increase of the parameter causes an increase of the variable, while grey bars indicate that an increase of the parameter causes a decrease of the variable.

tio affects the DOC pool (and again the microbial loop). Interestingly, the maximum S:N internal quota of phytoplankton is not the most important parameter contrary to the results of *Lefèvre et al.* (2002) and *Le Clainche et al.* (2004). This difference is in part attributable to the fact that in the SA carried out by these authors they increased/reduced by 50% the minimum and maximum S:N internal ratios at the same time, while we have increased/reduced them separately. Nevertheless, these results suggest that bottom-up (nutrient availability, regulated by the microbial loop) and top-down (zooplankton grazing) processes that control phytoplanktom biomass are more important for DMSPp concentrations than the internal sulfur quota.

For DMSPd (Figure 2.16b), the 10 most sensitive parameters are related to the microbial loop, except for the maximum phytoplankton internal S:N quota (4th position), the bacterial S:C ratio (5th position), the fraction of ingested DMSPp by zoo that is recovered as DMSPd (7th) and the phytoplankton maximum specific growth rate (8th).

Regarding DMS (Figure 2.16c), we observe a set of seven parameters that have a consistently high influence (from $\approx$90% to from $\approx$110%), clearly larger than the rest ($<$60%). With the exception of the maximum phytoplankton S:N internal quota (5th position) and the maximum phytoplankton DMS exudation specific rate (6th position), all were ranked already in the top five most sensitive parameters for DMSPp (Figure 2.16a). They are related to the bottom-up and top-down processes controlling phytoplankton biomass previously cited. The parameter for the fraction of bacteria that is DMS consumers is ranked on the 10th position, which is significant since at present this is an uncertain parameter. It is followed by the bacterial S:C ratio. A higher S:C ratio implies higher sulfur requirements of bacteria (lower DMS production from DMSPd uptake) at the same time than higher DMS uptake. There is large variation in published values for the S:C molar ratio ranging from $\approx$1/50 to $\approx$1/250 (*Zubkov et al.*, 2002, and references therein). Further research is needed in order to better constrain this parameter. As expected, the light attenuation coefficient is also quite important (13th position) because any increase reduces the amount of DMS exudation by phytoplankton. On the other hand, increasing it also reduces the DMS photolysis. However, since DMS exudation by phytoplankton was about 3 times higher than DMS photolysis (see Figure 2.10), the reduction of the source term dominates.

In order to evaluate which parameters affect DMS concentrations in a way not directly related to changes in phytoplankton biomass (i.e., changes in DMSPp) the SA index was also calculated for the ratio DMS/DMSPp (Figure 2.16d). As expected the DMS/DMSPp ratio is very sensitive to the maximum phytoplankton DMS exudation rate. Significant increases of the DMS/DMSPp ratio are also observed for higher zooplankton grazing rates. On the other hand, parameters that increase bacteria concentrations (e.g., carbon gross growth efficiency, maximum DOM/$NH_4^+$ uptake, the labile fraction of DOM produced, the phytoplankton DOC exudation parameter, etc.) are associated with a decrease in the ratio. An increase of the light attenuation coefficient also produces a decrease of the DMS/DMSPp ratio.

## 2.4 Conclusion

We have presented a state-of-the-art model of the oceanic sulfur cycle which includes the various processes currently thought to be important in DMSP/DMS dynamics and which resolves explicitly DOM and bacteria dynamics within the ecosystem. Sensitivity analyses have shown that parameters related to the microbial loop have a great impact on the N/C/S-cycles, in agreement with previous conclusions reached by both modelling and experimental studies (*Spitz et al.*, 2001; *Simó et al.*, 2000). The model is able to reproduce the seasonal DMS summer-paradox observed in the Sargasso Sea and highlights that bacterial consumption of DMSPd to give DMS may not be the main process in the overall DMS budget. Field studies have also shown that DMS concentrations were not controlled by DMSPd uptake by bacteria (*Dacey et al.*, 1998; *Zubkov et al.*, 2002). Rather it seems that the key process determining DMS concentrations in the upper ocean may be direct exudation from phytoplankton cells under high UV conditions, this providing an explanation for the strong seasonal decoupling observed between chlorophyll-a and DMS over most of the ocean's surface (*Vallina et al.*, 2006; *Vallina and Simó*, 2007a). This mechanism is missing in all current models of the sulfur cycle, with the exception of the one presented here.

Our model results suggest that DMS production by phytoplankton, despite being only one among several processes that are relevant (such as light-induced increases in the S:N ratio of phytoplankton and light-induced inhibition of bacterial sulfur uptake), is a major contributor to the DMS summer-paradox. This has been previously proposed from the analysis of field data in the Sargasso Sea (*Toole and Siegel*, 2004). The fact that phytoplankton can directly produce DMS has been previously reported in the literature (*Vairavamurthy et al.*, 1985; *Niki et al.*, 2000; *Wolfe et al.*, 2002) and there is increasing experimental evidence in support of this claim (*Toole et al.*, 2006). The implication is that changes in UV levels due to shoaling of the MLD, as might occur in Global Warming scenarios, could have an impact on the oceanic DMS production, and therefore on its potential effect upon Earth climate through CCN formation. Global DMSP/DMS models should incorporate the light-mediated processes affecting DMS production included in DMOS if better estimates of surface DMS concentrations, and specially of its seasonality, are to be achieved.

## 2.5 Appendix A:

### 2.5.1 Model equations

- *Phytoplankton (mmolN $m^{-3}$) equation*

$$\frac{\partial P}{\partial t} = (1-\gamma_1)F_P - G_P - M_P - S(P) + D(P) \tag{2.1}$$

- *Zooplankton (mmolN $m^{-3}$) equation*

$$\frac{\partial Z}{\partial t} = F_Z - M_Z + D(Z) \tag{2.2}$$

- *Bacteria (mmolN $m^{-3}$) equation*

$$\frac{\partial B}{\partial t} = F_B - G_B - M_B + D(B) \tag{2.3}$$

- *Nitrates (mmolN $m^{-3}$) equation*

$$\frac{\partial N}{\partial t} = -F_P^N + \nu A + D(N) \tag{2.4}$$

- *Ammonium (mmolN $m^{-3}$) equation*

$$\frac{\partial A}{\partial t} = -F_P^A - \nu A + E_B + E_Z + \Omega_A M_Z + D(Z) \tag{2.5}$$

- *Labile DON (mmolN $m^{-3}$) equation*

$$\frac{\partial L_n}{\partial t} = \gamma_1 F_P + \delta_1[\phi G_n + \varepsilon M_P + M_B + M_{D_n} + \Omega_{dom} M_Z] + U_{S_n} - U_{L_n} + D(L_n) \tag{2.6}$$

- *Labile DOC (mmolC $m^{-3}$) equation*

$$\begin{aligned} \frac{\partial L_c}{\partial t} &= \gamma_1 \theta_{P_{c:n}} F_P + \gamma_1 E_{doc} + \delta_2(1-\gamma_1)E_{doc} \\ &+ \delta_1[\phi G_c + \varepsilon \theta_{P_{c:n}} M_P + \theta_{B_{c:n}} M_B + M_{D_c} + \Omega_{dom}\theta_{Z_{c:n}} M_Z] \\ &+ U_{S_c} - \theta_{B_{c:n}} F_B - R_B + D(L_c) \end{aligned} \tag{2.7}$$

- *Semi-labile DON (mmolN $m^{-3}$) equation*

$$\frac{\partial S_n}{\partial t} = (1-\delta_1)[\phi G_n + \varepsilon M_P + M_B + M_{D_n} + \Omega_{dom} M_Z] - U_{S_n} + D(S_n) \tag{2.8}$$

- *Semi-labile DOC (mmolC $m^{-3}$) equation*

$$\frac{\partial S_c}{\partial t} = (1-\delta_2)(1-\gamma_1)E_{doc} + (1-\delta_1)[\phi G_c + \varepsilon\theta_{P_{c:n}}M_P + \theta_{B_{c:n}}M_B + M_{D_c} + \Omega_{dom}\theta_{Z_{c:n}}M_Z] - U_{S_c} + D(S_c) \tag{2.9}$$

- *Detrital Nitrogen (mmolN $m^{-3}$) equation*

$$\frac{\partial D_n}{\partial t} = (1-\beta_n)(1-\phi)Gn + (1-\varepsilon)M_P + \Omega_{D_n}M_Z - G_{D_n} - M_{D_n} - S(D_n) + D(D_n) \tag{2.10}$$

- *Detrital Carbon (mmolC $m^{-3}$) equation*

$$\frac{\partial D_c}{\partial t} = (1-\beta_c)(1-\phi)Gc + (1-\varepsilon)\theta_{P_{c:n}}M_P + \Omega_{D_c}\theta_{Z_{c:n}}M_Z - G_{D_c} - M_{D_c} - S(D_c) + D(D_c) \tag{2.11}$$

- *Detrital $CaCO_3$ (mmolC $m^{-3}$) equation*

$$\frac{\partial D_h}{\partial t} = \theta_{Ca}\theta_{P_{c:n}}(G_P + M_P) - M_{D_h} - S(D_h) + D(D_h) \tag{2.12}$$

- *Dissolved Inorganic Carbon (mmolC $m^{-3}$) equation*

$$\frac{\partial DIC}{\partial t} = -(1+\theta_{Ca})\theta_{P_{c:n}}F_P - E_{doc} + R_B + R_Z + M_{D_h} + \Omega_{DIC}\theta_{Z_{c:n}}M_Z + F_{atm} + D(DIC) \tag{2.13}$$

- *Alkalinity (mmolC $m^{-3}$) equation*

$$\frac{\partial ALK}{\partial t} = (Q_N - Q_A)F_P - 2\theta_{Ca}\theta_{P_{c:n}}F_P + E_B + E_Z + 2M_{D_h} + \Omega_A M_Z - \nu A + D(ALK) \tag{2.14}$$

- *CHL (mg $m^{-3}$) equation*

$$\frac{\partial CHL}{\partial t} = (\rho_{chl}C_{mw}\theta_{P_{c:n}})F_P - (G_P + M_P)(CHL/P) - S(CHL) + D(CHL) \tag{2.15}$$

- *DMSPp (mmolS $m^{-3}$) equation*

$$\frac{\partial DMSPp}{\partial t} = \theta_{P_{s:n}}\frac{\partial P}{\partial t} = \theta_{P_{s:n}}[(1-\gamma_1)F_P - G_P - M_P - S(P) + D(P)] \tag{2.16}$$

- *DMSPd (mmolS $m^{-3}$) equation*

$$\frac{\partial DMSPd}{\partial t} = \theta_{P_{s:n}}[\gamma_1 F_P + \alpha_1 G_P + M_P] - U_{DMSPd} - U^P_{DMSPd} - fDMSPd + D(DMSPd) \tag{2.17}$$

- *DMS (mmolS $m^{-3}$) equation*

$$\frac{\partial DMS}{\partial t} = R_{DMS} + E_{DMS} + fDMSPd - U_{DMS} - DMS_{photo} - DMS_{emiss}(*) + D(DMS) \tag{2.18}$$

(*) This term is applied only to the top model cell.

### 2.5.2 N/C-cyles Model terms

- *Phytoplankton production ($F_P$)*

$$F_P = F_P^N + F_P^A = JQ_N P + JQ_A P = JQP \tag{2.19}$$

$$J = \propto_P R \tag{2.20}$$

$$\propto_P = \propto_P^{max} e^{(0.063(T - T_{max}))} \tag{2.21}$$

$$R = \frac{I_z}{I_s} e^{(1 - \frac{I_z}{I_s})} \leq 1 \tag{2.22}$$

$$I_z = I_0 e^{-(k_w + k_p \bar{P})z} \tag{2.23}$$

$$\bar{P} = \frac{1}{z} \int_0^z P dz \tag{2.24}$$

$$Q = Q_N + Q_A \leq 1 \tag{2.25}$$

$$Q_N = \frac{\frac{N}{k_P^N} e^{(-\psi A)}}{1 + \frac{N}{k_P^N} + \frac{A}{k_P^A}} \tag{2.26}$$

$$Q_A = \frac{\frac{A}{k_P^A}}{1 + \frac{N}{k_P^N} + \frac{A}{k_P^A}} \tag{2.27}$$

- *Phytoplankton extra-DOC exudation*

$$E_{doc} = \gamma_2 \theta_{P_{c:n}} F_P \tag{2.28}$$

- *Zooplankton grazing on phytoplankton ($G_P$), bacteria ($G_B$), detrital nitrogen ($G_{D_n}$) and detrital carbon ($G_{D_c}$)*

$$G_P = \frac{gZp_P P^2}{k_g(p_P P + p_B B + p_D D_n) + p_P P^2 + p_B B^2 + p_D D_n^2} \tag{2.29}$$

$$G_B = \frac{gZp_B B^2}{k_g(p_P P + p_B B + p_D D_n) + p_P P^2 + p_B B^2 + p_D D_n^2} \tag{2.30}$$

$$G_{D_n} = \frac{gZp_D D_n^2}{k_g(p_P P + p_B B + p_D D_n) + p_P P^2 + p_B B^2 + p_D D_n^2} \tag{2.31}$$

$$G_{D_c} = (\frac{D_c}{D_n}) G_{D_n} \tag{2.32}$$

$$G_n = G_P + G_B + G_{D_n} \tag{2.33}$$

$$G_c = \theta_{P_{c:n}} G_P + \theta_{B_{c:n}} G_B + G_{D_c} \tag{2.34}$$

- *Zooplankton production ($F_Z$) and excretion ($E_Z$)*

$$\theta_f^* = \frac{\beta_n \theta_{Z_{c:n}}}{\beta_c \omega_Z} \tag{2.35}$$

$$\theta_f = \frac{(1-\phi)G_c}{(1-\phi)G_n} \tag{2.36}$$

if $\theta_f > \theta_f^*$ (N-limitation):

$$F_Z = \beta_n (1-\phi) G_n \tag{2.37}$$

$$E_Z = 0 \tag{2.38}$$

if $\theta_f < \theta_f^*$ (C-limitation):

$$F_Z = \frac{\beta_c \omega_Z}{\theta_{Z_{c:n}}} (1-\phi) G_c \tag{2.39}$$

$$E_Z = (\frac{\beta_n}{\theta_f} - \frac{\beta_n}{\theta_f^*})(1-\phi) G_c \tag{2.40}$$

- *Zooplankton respiration*

$$R_Z = \beta_c (1-\phi) G_c - \theta_{Z_{c:n}} F_Z \tag{2.41}$$

- *Bacterial uptake of labile DOC ($U_{L_c}$), labile DON ($U_{L_n}$)*

$$U_{L_c} = \propto_B \theta_{B_{c:n}} B \frac{L_c}{k_{Lc} + L_c} \tag{2.42}$$

$$U_{L_n} = (\frac{L_n}{L_c}) U_{L_c} \tag{2.43}$$

- *Bacterial maximum potential uptake of ammonium*

$$U_A^* = \propto_B B \frac{A}{k_A + A} \tag{2.44}$$

$$\propto_B = \propto_B^{max} (1 - \phi_{inhib}) \tag{2.45}$$

$$\phi_{inhib} = \phi_{inhib}^{max} \frac{I_z}{I_{max}} \tag{2.46}$$

- *Bacterial production ($F_B$), ammonium excretion or uptake ($E_B$) and respiration ($R_B$)*

$$E_B = U_{L_n} - (\frac{\omega_B}{\theta_{B_{c:n}}}) U_{L_c} \tag{2.47}$$

if $E_B > 0$ (ammonium excretion)

if $E_B < 0$ (ammonium uptake)

if $U_A^* \geq -E_B$ (C-limitation):

$$F_B = U_{L_n} - E_B = (\frac{\omega_B}{\theta_{B_{c:n}}})U_{L_c} \tag{2.48}$$

$$R_B = (1-\omega_B)U_{L_c} \tag{2.49}$$

if $U_A^* < -E_B$ (N-limitation):

$$E_B = -U_A^* \tag{2.50}$$

$$F_B = U_{L_n} - E_B = U_{L_n} + U_A^* \tag{2.51}$$

$$R_B = (\frac{1}{\omega_B - 1})\theta_{B_{c:n}} F_B \tag{2.52}$$

- *Bacterial hydrolysis of semilabile DOC ($U_{S_c}$) and semilabile DON ($U_{S_n}$)*

$$U_{S_c} = \propto_{Sc} \theta_{B_{c:n}} B \frac{S_c}{k_{Sc} + S_c} \tag{2.53}$$

$$U_{S_n} = (\frac{S_n}{S_c})U_{S_c} \tag{2.54}$$

- *Mortality of phytplankton ($M_P$), zooplankton ($M_Z$) and bacteria ($M_B$)*

$$M_P = m_P P \tag{2.55}$$

$$M_Z = \frac{m_Z Z^2}{k_Z + Z} \tag{2.56}$$

$$M_B = m_B B \tag{2.57}$$

- *Breakdown of detrital nitrogen ($M_{D_n}$), detrital carbon ($M_{D_c}$) and detrital $CaCO_3$ ($M_{D_h}$)*

$$M_{D_n} = m_{D_n} D_n \tag{2.58}$$

$$M_{D_c} = m_{D_c} D_c \tag{2.59}$$

$$M_{D_h} = m_{D_h} D_h \tag{2.60}$$

- *Chlorophyll-a production*

$$\rho_{chl} = \frac{\theta_{chl}^m JQ}{\alpha_{chl} \theta_{chl} I_z} \tag{2.61}$$

$$\theta_{chl} = \frac{CHL}{C_{mw} \theta_{P_{c:n}} P} \tag{2.62}$$

### 2.5.3 S-cycle Model terms

- *S:N phytoplankton internal quota*

$$\theta_{P_{s:n}} = \theta^{min}_{P_{s:n}} + (\theta^{0}_{P_{s:n}} - \theta^{min}_{P_{s:n}}) \frac{min(I_z, I^*)}{I^*} \tag{2.63}$$

$$\theta^{0}_{P_{s:n}} = \theta^{max}_{P_{s:n}} - (\theta^{max}_{P_{s:n}} - \theta^{min}_{P_{s:n}}) \frac{I_{max} - I_0}{I_{max} - I_{min}} \tag{2.64}$$

- *Phytoplankton DMS exudation*

$$E_{DMS} = \gamma_s DMSPp \tag{2.65}$$

$$\gamma_s = \gamma^{max}_s \frac{Iz}{I_{max}} \frac{\propto_P}{\propto^{max}_P} \tag{2.66}$$

- *Phytoplankton DMSPd uptake*

$$U^P_{DMSPd} = \frac{DMSPd}{A} \alpha_P F^A_P + \frac{DMSPd}{N} \alpha_P F^N_P \tag{2.67}$$

- *Bacterial DMSPd and DMS uptake*

$$U_{DMSPd} = \propto_B \theta_{B_{s:c}} \theta_{B_{c:n}} B \frac{DMSPd}{k_{DMSPd} + DMSPd} \tag{2.68}$$

$$U_{DMS} = \propto_B \theta_{B_{s:c}} \theta_{B_{c:n}} \alpha_B B \frac{DMS}{k_{DMS} + DMS} \tag{2.69}$$

- *Bacterial sulfur demand*

$$U^*_{DMSPd} = \theta_{B_{s:c}} \theta_{B_{c:n}} F_B \tag{2.70}$$

- *Bacterial DMS production*

  if $U^*_{DMSPd} < U_{DMSPd}$ (no S-limitation):

$$R_{DMS} = \alpha_2 (U_{DMSPd} - U^*_{DMSPd}) \tag{2.71}$$

  if $U^*_{DMSPd} \geq U_{DMSPd}$ (S-limitation):

$$R_{DMS} = 0 \tag{2.72}$$

- *DMS photolysis*

$$DMS_{photo} = k_{photo} DMS \tag{2.73}$$

$$k_{photo} = k^{max}_{photo} \frac{Iz}{I_{max}} \tag{2.74}$$

- *DMS emission to the atmosphere*

$$DMS_{emiss} = k_{emiss} DMS \tag{2.75}$$

$$k_{emiss} = \frac{k_v \frac{24}{100}}{\Delta z} \tag{2.76}$$

$$k_v = (0.24U^2 + 0.061U)(\frac{Sc}{600})^{(-0.5)} \tag{2.77}$$

$$Sc = 2674 - 147.12(SST) + 3.726(SST^2) - 0.038(SST^3) \tag{2.78}$$

- *DMS yield*

$$DMS_{yield} = \frac{DMS_{prod.}}{DMSP_{cons.}} = \frac{E_{DMS} + R_{DMS} + fDMSPd}{E_{DMS} + U_{DMSPd} + U^P_{DMSPd} + fDMSPd} \tag{2.79}$$

### 2.5.4 Advection (sinking) and Diffusion terms

- *Phytoplankton and Detritus sinking*

$$S(X_i) = |\vec{w}_i| \frac{\partial X_i}{\partial z} \tag{2.80}$$

for $X_i$ = $P$, $D_n$, $D_c$, $D_h$ and $CHL$.

- *Turbulent diffusion*

$$D(X_i) = \frac{\partial}{\partial z}(kz \frac{\partial X_i}{\partial z}) \tag{2.81}$$

for $X_i$ = $P$, $Z$, $B$, $N$, $A$, $L_n$, $L_c$, $S_n$, $S_c$, $D_n$, $D_c$, $D_h$, $DIC$, $ALK$, $CHL$, $DMSPp$, $DMSPd$ and $DMS$.

### 2.5.5 Turbulent diffusion and temperature profiles

$$D^* = \frac{D^*_{max} + D^*_{min} e^{r(D^*_{min} - D^*_{max}) \frac{2(z^* - MLD^*)}{H^*}}}{1 + e^{r(D^*_{min} - D^*_{max}) \frac{2(z^* - MLD^*)}{H^*}}} \tag{2.82}$$

where the symbol '*' denotes normalized variables (values between 0 and 1):

$$X^* = X/H \tag{2.83}$$

$$Y^* = Y/D_{max} \tag{2.84}$$

for $X$ = $z$, $MLD$, $H$, and $Y$ = $D$, $D_{min}$, $D_{max}$. $H$ is the model vertical domain (200m) and $D$ can be either diffusion ($kz$) or sea temperature ($st$).

### 2.5.6 Numerical scheme for solving the 1D model

The general form of the model equations is:

$$\frac{\partial X_i}{\partial t} = J_i - |\vec{w}_i|\frac{\partial X_i}{\partial z} + \frac{\partial}{\partial z}(kz\frac{\partial X_i}{\partial z}) = f(X_i) \tag{2.85}$$

Where $J_i$ are the biological source/sink terms for each variable $i$ as defined above, $|\vec{w}_i|\frac{\partial X_i}{\partial z}$ is the vertical sinking (only applies to phytoplankton and detritus), and $\frac{\partial}{\partial z}(kz\frac{\partial X_i}{\partial z})$ is the vertical turbulent diffusion. The numerical scheme is implemented using a finite difference approximation. At each time step and for each vertical grid point $j$, all three terms are calculated independently to obtain $f(X_i)$. The sinking term is calculated using a first-order upwind discretization:

$$\frac{\partial X_i^j}{\partial z} = \frac{X_i^{j-1} - X_i^j}{\Delta z} \tag{2.86}$$

while the diffusion term is calculated using a second-order centered discretization:

$$\frac{\partial}{\partial z}(kz\frac{\partial X_i}{\partial z}) = \frac{kz^{j+1/2}(X_i^{j+1} - X_i^j) - kz^{j-1/2}(X_i^j - X_i^{j-1})}{(\Delta z)^2} \tag{2.87}$$

where $kz^{j+1/2} \equiv kz(z_{j+j/2})$. Finally, for each vertical grid point we then advance the solution in time from $X_i^t$ to $X_i^{t+1}$ using a forward Euler method (*Press et al.*, 1992):

$$X_i^{t+1} = X_i^t + f(X_i^t)\Delta t \tag{2.88}$$

# CHAPTER 3

# What controls cloud condensation nuclei (CCN) seasonality in the Southern Ocean?

*Men are like wines:*
*ageing sours the bad ones*
*and improve the good ones.*

*(Marcus Tullius Cicero)*

# What controls cloud condensation nuclei (CCN) seasonality in the Southern Ocean?


## ABSTRACT

A three-year time series set (from January 2002 to December 2004) of monthly means of satellite-derived chlorophyll (CHL) and cloud condensation nuclei (CCN), as well as model outputs of hydroxyl radical (OH), rainfall amount (RAIN) and wind speed (WIND) for the Southern Ocean (SO, 40°S - 60°S) is analyzed in order to explain CCN seasonality. Chlorophyll is used as a proxy for oceanic dimethylsulfide (DMS) emissions since both climatological aqueous DMS and atmospheric methanesulfonate (MSA) concentrations are tightly coupled with chorophyll seasonality over the Southern Ocean. OH is included as the main atmospheric oxidant of DMS to produce CCN, and rainfall amount as the main loss factor for CCN through aerosol scavenging. Wind speed is used as a proxy for sea salt (SS) particles production. The CCN concentration seasonality is characterized by a clear pattern of higher values during austral-summer and lower values during austral-winter. Linear and multiple regression analyses reveal high significant correlations between CCN and the product of chlorophyll and OH (in phase) and rainfall amount (in anti-phase). Also, CCN concentrations are anti-correlated with wind speed, which shows very little variability and a slight wintertime increase, in agreement with the sea salt seasonality reported in the literature. Finally, the fraction of the total aerosol optical depth contributed by small particles (ETA) exhibits a seasonality with a 3.5 fold increase from austral-winter to austral-summer. The biogenic contribution to CCN is estimated to vary between 35% (winter) and 80% (summer). Sea salt particles, although contributing an important fraction of the CCN burden, do not play a role in controlling CCN seasonality over the SO. These findings support the central role of biogenic DMS emissions in controlling not only the number but also the variability of CCN over the remote ocean.



S. M. Vallina, R. Simó, & S. Gassó (2006)
*Global Biogeochem. Cycles*, 20, GB1014, doi:10.1029/2005GB002597

## 3.1 Introduction

Since *Charlson et al.* suggested in 1987 that marine algae participate in climate regulation through the production of the cloud precursor dimethylsulfide (the CLAW hypothesis, so called after the authors' initials), much experimental effort has been invested into seeking for links between oceanic plankton and tropospheric aerosols. Many marine phytoplankton taxa produce intracellular dimethylsufoniopropionate (DMSP), the biochemical precursor of dimethylsulfide (DMS), with important physiological functions (*Stefels*, 2000; *Sunda et al.*, 2002). DMSP is partly converted to DMS by enzymatic cleavage with involvement of the whole planktonic food web (*Simó*, 2001).

In seawater, DMS undergoes bacterial consumption and photolysis, and a fraction of it is ventilated from the oceans to the atmosphere following Henry's law. The ventilation rate depends not only on aqueous DMS concentration (DMSw) but also on seawater temperature and wind speed (*Liss and Mervilat*, 1986). Once in the atmosphere DMS undergoes a sequence of oxidative reactions through interaction mainly with the hydroxyl radical (OH), giving rise to a range of products. Among them, non-sea-salt sulfate (nss-$SO_4$) and, to a lesser extent, methanesulfonate (MSA) are of particular interest because of their potential role to form cloud condensation nuclei (CCN) (*Cox*, 1997). MSA and $SO_4$ particles are highly hygroscopic and mainly occur in the submicron size fraction, ranging between 0.1 and 1 $\propto$m in diameter, which is also the optimal size range for CCN (*Ayers et al.*, 1997a, 1999; *Andreae et al.*, 1999; *Jourdain and Legrand*, 2001).

DMS emission is, by far, the largest natural source of volatile sulfur to the atmosphere (*Andreae and Crutzen*, 1997; *Simó*, 2001). Global emissions are estimated in the range of 16 to 24 TgS $yr^{-1}$ (*Kettle and Andreae*, 2000; *Chapman et al.*, 2002). Even though this represents between 25 and 35% of the estimated anthropogenic sulfur emissions (65 TgS $yr^{-1}$) (*Benkovitz et al.*, 1996) DMS accounts for essentially all nss-$SO_4$ in vast regions of the remote oceans (*Savoie and Prospero*, 1989). The Southern Ocean (SO) atmosphere is regarded as one of the most unpolluted over the world (*Buseck and Pósfai*, 1999), where the aerosol is expected to be minimally perturbed by either anthropogenic or natural ontinental sources (*Quinn et al.*, 1998; *Andreae et al.*, 1999; *Ayers and Gillett*, 2000; *Gabric et al.*, 2001; *Prospero et al.*, 2002). The SO is, therefore, the most appropriate region for testing the validity of the CLAW hypothesis, or at least some of their central statements.

Several short- and long-term observational studies carried out at sites in the SO, from temperate to Antarctic regions, have shown a strong coupling between DMS, its atmospheric oxidation products, and CCN (*Prospero et al.*, 1991; *Ayers and Gras*, 1991; *Ayers et al.*, 1997a; *Andreae et al.*, 1999; *Jourdain and Legrand*, 2001). By reviewing the large body of data collected at Cape Grim, *Ayers and Gillett* (2000) confirmed the strong seasonal coupling between DMSa, MSA and nss-$SO_4$, and also reported direct evidence for the coupling between DMS, CCN and cloud droplet numbers. Also, during the First Aerosol Characterization Experiment (ACE-

1), *Brechtel et al.* (1998) found that an increase in the number of particles in the Aitken and accumulation modes was associated with an air mass transported over warm DMS-rich waters. These findings strongly suggest a central role of oceanic DMS as a precursor of CCN in the SO, at least during the biologically productive season.

Because of the obvious geographic sparseness of atmospheric sampling stations, there is a lack of studies on regional or global scales. Optical sensors on satellites (e.g. NASA's SeaWiFS and MODIS) offer the possibility of making quasi-synoptic, reliable and with high spatial resolution simultaneous measurements of ocean and atmospheric variables at large scales. With such new methodology and data, it is possible to investigate if the connection between marine microbiota, aerosols and clouds found in local studies also holds at the larger spatial and temporal scales that are relevant for potential climate regulation.

A pioneering work on the use of satellite data for testing plankton-aerosol links has been done by *Gabric et al.* (2002) for a region of the SO south of Australia (from 40°S to 53°S and from 126°S to 148°E). They found evidence for a coupling between CHL and total aerosol optical depth (AOD) at multiple scales, from weekly to seasonal. However, they could not resolve whether this coupling was mainly due to aerosol fertilization of productivity or biogenic effects on aerosol production. Here we present a continuation of the work of *Gabric et al.* (2002) by going further in several aspects: *i*) We focus on the whole Southern Ocean (40°S - 60°S). *ii*) We use a new generation of algorithms for the derivation of CCN concentrations from the primary aerosol products of MODIS. *iii*) Two other variables are taken into account as *a-priori* important factors controlling the seasonality of CCN: the OH radical concentration in the marine boundary layer and the rainfall amount; simple and multiple linear statistical models are applied in order to test the effect of the inclusion of OH and rainfall estimates on the observed variance of CCN numbers. *iv*) The seasonality of the fine mode aerosols is also discussed.

## 3.2 Data and Methodology

### 3.2.1 Characteristics of the Study Region: Productivity, DMS and Wind

The study region covers the whole SO, defined as the area comprised between 40°S and 60°S (see Figure 3.1). The latitudinal range covers roughly 2 major water bodies: the Sub-Antarctic Zone (SAZ) (40°S-53°S) and the Antarctic Zone (AZ) (53°S-60°S) (*Curran and Jones*, 2000). We purposely exclude from our study the potential effects of the sea-ice formation and melt; with this aim, we omit latitudes south of 60°S (the Seasonal Ice Zone or SIZ), a general limit for maximum Antarctic sea-ice coverage (*Prospero et al.*, 1991; *Rasmus et al.*, 2004). The northern part of the region is flanked by the Subtropical Front (about 40°S), which is considered the upper limit of the SO (*Boyd*, 2002). In the southern part the Antarctic Polar Front (APF) is present (be-

tween 45°S - 60°S) and characterized by upwelling eddies and higher phytoplankton biomass in its southernmost edge (*Moore et al.*, 1999).

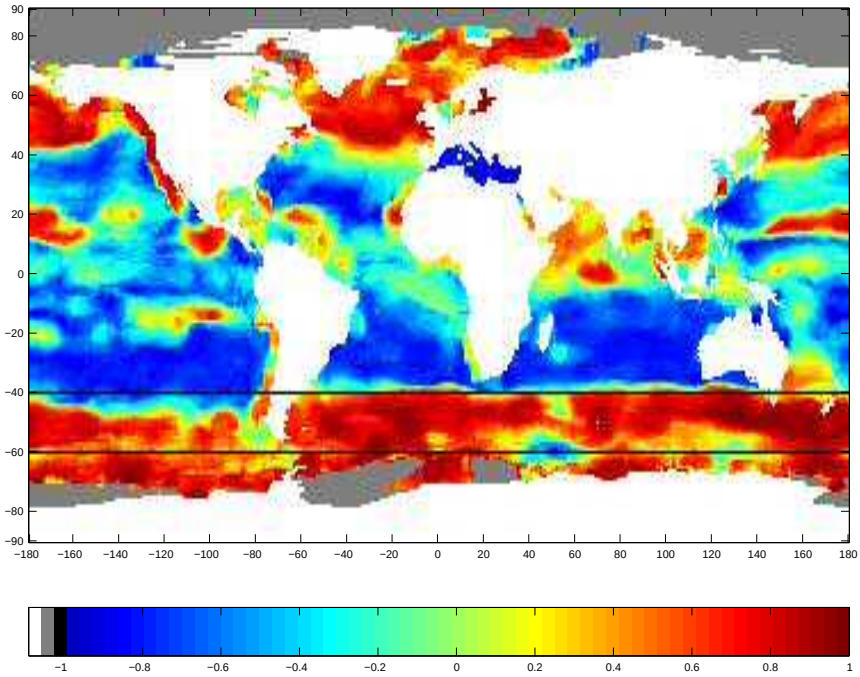


Fig. 3.1: Global map of seasonal correlations between climatological monthly aqueous DMS concentrations (from *Kettle and Andreae* (2000)) and climatological monthly CHL concentrations (from SeaWiFS, means of years 2002 to 2004). The Southern Ocean study region is the area comprised between the two black lines.

Over the year, most of the SO exhibits moderate CHL concentrations, generally less than 0.3-0.4 mg $m^{-3}$. Phytoplankton blooms that give rise to CHL concentrations higher than 1 mg $m^{-3}$ are present in shelf waters, the vicinity of major fronts, and sea-ice retreat zones (*Moore and Abbott*, 2000). CHL peaks during the summer and is depressed in winter (*Curran and Jones*, 2000; *Gabric et al.*, 2002). This seasonality is believed to be driven by the depth of the mixed layer (ML) (*Rasmus et al.*, 2004), which varies from maxima around 400 m in winter to less than 30 m in summer (*de Boyer-Montégut et al.*, 2004). In all seasons but summer, the deep mixed layer depth (MLD) imposes a severe light limitation to phytoplankton growth (probably light-iron co-limitation) (*Boyd*, 2002) even though macro-nutrient concentrations are amongst the highest of the world's oceans. During summer, phytoplankton is only limited by iron (*Boyd*, 2002).

There is compelling observational evidence that the seasonality of DMSP and DMSw concentrations, as well as DMS emission fluxes, follow the seasonality of phytoplankton in the SO (*Turner and Owens*, 1995; *Gabric et al.*, 1996; *Ayers et al.*, 1995, 1997a; *Kettle et al.*, 1999; *Curran and Jones*, 2000; *Ayers and Gillett*, 2000; *Simó and Dachs*, 2002). This is a distinct feature of the SO with respect to subtropical regions and temperate regions of the Northern Hemisphere, where maximum surface DMS concentrations occur associated with low CHL levels in highly irradiated, shallow stratified waters during summer (*Dacey et al.*, 1998; *Simó and Pedros-Alló*, 1999a; *Simó*

*and Dachs*, 2002; *Toole and Siegel*, 2004). Globally mapped, 7° x 7° running-window correlations between monthly CHL (SeaWiFS, average of 2002-2004) and DMSw (*Kettle and Andreae*, 2000) climatologies show strong positive and almost homogeneously distributed correlations over the SO region (Figure 3.1; significant correlations for $|r| > 0.5$). However, it is important to point out that the DMSw climatology is based on a compilation of DMSw measurements and they make use of an interpolation procedure to fill the large areas/seasons where no data are available. Annual time series of atmospheric DMS and MSA concentrations at Cape Grim also exhibit a pattern very similar to that of oceanic DMS and CHL (*Ayers and Gillett*, 2000). The Spearman correlation coefficient between monthly CHL (averaged for the SO over the period 2002-2004) and monthly MSA at Cape Grim (averaged over the period 1988-1996) is very high ($\rho = 0.97$; $p - val << 0.001$). Since DMS cannot be remotely sensed from satellite, and in the absence of gridded, spatially comprehensive data on DMSw simultaneous to that of CCN, we use satellite-derived CHL data, which offer such a coverage, as a proxy for DMSw. We, hereby, presume that any trends CHL might show in our analyses will be representative of those of DMSw.

The SO experiences the highest wind speeds of the globe with a persistent wind field and rich storm activity (*Yuan*, 2004). Winds flow eastward most of the time for most of the region (the 'roaring forties'), with the meridional component (mainly southward) being much weaker than the zonal component (*Gille*, 2005). Interestingly, the wind stress at 55°S shows little seasonal variability in contrast to other regions of the globe (*Gille*, 2005). On a regional average, wind speed seasonal amplitude is less than $\pm$ 10% of the annual mean (10.5 m $s^{-1}$; see Figure 3.2h). In consequence, the variability of the DMS emission flux (the source of atmospheric DMS) is driven mainly by the variability of DMSw concentrations. That is, we are using CHL as a proxy for DMS emissions.

### 3.2.2 Data Sets: Sources and Justification

The Sea-viewing Wide Field-of-view Sensor (SeaWiFS) flies on the OrbView-2 (formerly "SeaStar") platform and it measures radiances in 8 spectral bands (from 0.40 to 0.88 ∝m). SeaWiFS estimates the ocean surface CHL concentration (mg $m^{-3}$) based on the ratio between reflectance in 2 visible channels (0.49 ∝m for blue and 0.55 ∝m for green) (*Yang and Gordon*, 1997). Higher reflectance in the green channel corresponds to waters with higher CHL concentrations. The MODerate resolution Imaging Spectro-radiometer (MODIS), on board the Earth Observing System (EOS), currently has two detector in orbit (in the satellites Terra and Aqua). Both have daily global coverage with a morning and afternoon pass respectively. In this study, we used data measured by MODIS-Terra. MODIS acquires data globally at 36 spectral bands (from 0.4 to 14.5 ∝m). Several primary aerosol parameters are retrieved from MODIS daytime data over the ocean, including the fine mode fraction or ETA parameter (*Remer et al.*, 2005). ETA (being between 0 and 1) is defined as the ratio of the AOD contributed by the small mode particles (or accumulation mode) to the total AOD ($AOD_{small}/AOD_{total}$) and can thus be viewed as a

measure of the percentage of fine particles that contribute to the total aerosol burden. In this study we make use of the ETA parameter to infer the seasonality of the dominant aerosol types in the SO. Sea salt (SS) and dust mainly occur in the coarse mode particles while nss-$SO_4$ and carbonaceous aerosols occur in the accumulation mode. Because the lack of constant anthropogenic sources and minimal dust activity in the SO, SS and nss-$SO_4$ aerosols are the dominant aerosol types. Thus the seasonality of the ETA parameter allows us to infer the relative contribution of SS and nss-$SO_4$ particles for each season. We would like to note that MODIS also provide CHL estimates but it lacks the SeaWiFS capability to tilt away to avoid sunglint (the specular reflection of sunlight from the sea surface). Then SeaWiFS CHL retrievals are of higher accuracy. Either the SeaWiFS CHL data (9km x 9km resolution) and the MODIS aerosol data (1° x 1° resolution) used are available from NASA's Goddard Space Flight Center (GSFC) Distributed Active Archive Centers (DAAC).

From the primary parameters retrieved by MODIS, it is possible to derive secondary products such as column-integrated CCN numbers (in units of partic $cm^{-2}$) (*Tanré et al.*, 1999; *Gassó and Hegg*, 2003). In the present work, CCN concentrations are obtained with the derivation method described in *Gassó and Hegg* (2003). The method derives the maximum number of particles in the accumulation mode and provides an upper end estimate of the concentration of particles that may act as CCN at ≈0.2% supersaturation. The method allows for the adjustment of coefficients according to the type of aerosols that are present. Since we are focusing on the SO, the CCN algorithm coefficients (the aerosol refraction index and the aerosol density) were adjusted to be representative of the main aerosol types present in this marine remote region: SS, nss-$SO_4$ and MSA.

In order to compare the obtained column-integrated values (partic $cm^{-2}$) to *in-situ* measurements of CCN concentrations (partic $cm^{-3}$) we assume that most of the CCN occur in the marine boundary layer (MBL) (*Gassó and Hegg*, 2003). The height of the MBL varies with seasons (typically 600 m in winter and 1400 m in summer). We obtain CCN concentrations of 157 partic $cm^{-3}$ in winter and 266 partic $cm^{-3}$ in summer, which are about a factor of 2.8 higher than Cape Grim measurements of CCN at 0.23% supersaturation (55 partic $cm^{-3}$ in winter and 95 partic $cm^{-3}$ in summer (*Ayers and Gras*, 1991)). In contrast, the seasonal variability is well captured: the summer-maximum to winter-minimum ratio is about 1.7 for both satellite-derived and *in-situ* measured CCN concentrations. Similar overestimates are obtained using annual averages of CCN and an average MBL of 1000 m (225 partic $cm^{-3}$ from MODIS against 75 partic $cm^{-3}$ at Cape Grim). However, the general assumption that most of the CCN particles occur in the MBL does not seem to hold always over the SO. Summer vertical distributions of CCN obtained by *Hudson et al.* (1998) between 40°S-55°S and 135°S-160°S showed that CCN are present up to 400 mb (roughly about 7000 m). This could explain the high column-integrated values of CCN retrieved from the satellite and the apparent overestimation of the calculated concentrations based on an air column of only 1000 m. With an air column of 7000 m, satellite CCN concentrations would be ca. 53 partic $cm^{-3}$ in summer, which is lower than those mea-

sured at Cape Grim but within the range of those measured by *Hudson et al.* (1998) during the flights.

Global and regional OH concentrations in the MBL are outputs of the GEOS-CHEM model run by the Atmospheric Chemistry Modeling Group at Harvard University (*Fiore et al.*, 2003). GEOS-CHEM simulates atmospheric composition using assimilated meteorological observations from the Goddard Earth Observing System (GEOS) of the NASA Global Modeling and Assimilation Office. Including OH variability when seeking for a causal relationship between DMS and CCN seems necessary since OH is the main oxidizer of atmospheric DMS to produce CCN. Not taking in account its contribution would artificially increase the DMS weight in the statistical analysis of the CCN seasonality because OH experiences a strong reduction during the darker winter months. Surface wind speed (WIND) and rainfall amount (RAIN) were obtained from the NCEP/NCAR Reanalysis data provided by the NOAA-CIRES Climate Diagnostics Center. The NCEP/NCAR Reanalysis project uses a state-of-the-art analysis/forecast system to perform data assimilation using contemporary data. We used monthly maps of both variables at a 2.5° x 2.5° resolution. Both WIND (m $s^{-1}$) and RAIN (mm $d^{-1}$, also referred to as "precipitation rate" by NCEP) are model outputs. WIND is better constrained by contemporary data obtained from the SSM/I sensor (DMSP, NOAA). On the other hand, there are no real rainfall observations directly constraining the variable RAIN, so that it is derived solely from the model fields forced by the real atmospheric assimilated data (*Kistler et al.*, 2001).

The variables CHL, CCN, ETA, WIND, and RAIN are level 3 monthly composites for the period between January 2002 and December 2004. The multi-year time series is meant to capture the inter-annual variability. Monthly OH distributions, however, were available only for 2001. We assume that the OH inter-annual variability is low and then we have repeated three times the modeled OH annual cycle to obtain 3 years. We then calculate the mean value of each variable for each month over the whole SO area covered (36 data points). With this averaging procedure, the spatial distribution of the variables is not taken into account, with the assumption that they are rather homogeneously distributed. This is certainly not true for CHL, but it is closer to reality for OH and CCN due to the strong eastward wind conditions. Due to the faster motion of air masses than oceanic currents (and not necessarily coincident directions) any potential effect of oceanic CHL on atmospheric CCN can only be observed at spatial scales much larger than local. The choice of the monthly time frame pursues to focus on the seasonal patterns and to reduce from the statistical analysis the effect of potential time lags existing between aerosol-precursor (mainly DMS) production by the marine biota (CHL) and the formation of CCN by atmospheric oxidation of this precursor.

Since the development of a phytoplankton bloom to the rise of aqueous DMS concentrations the time lag can range from hours to days, mainly driven by algal physiological stress, cell mortality, viral activity and zooplankton grazing. During the SOIREE mission, for instance, an increase in primary production was induced by adding iron to the surface waters (*Boyd et al.*, 2000). A

significant increase in DMS concentrations was observed 5 days after the rise in *Prymnesiophyte* abundances and 2 days after the bulk CHL rise, coinciding with the response of zooplankton grazers. There is strong evidence for direct DMS exudation from phytoplankton when cells are under stressing conditions of high UV exposure and iron limitation (*Sunda et al.*, 2002) such as those encountered in the surface SO during summer. In this case there would not exist a lag between CHL and DMS. On top of that, we should add the time needed for DMS to be ventilated to the atmosphere, oxidized to $SO_2$ and subsequently to nss-$SO_4$ (gas-to-particle conversion) (*Fitzgerald*, 1991). Ventilation is rapid due to the high wind speeds, and the summer DMSa lifetime in our study region is estimated to be 12-24h (*Bates et al.*, 1998; *Mari et al.*, 1998) although in winter it is in the order of a week (*Gabric et al.*, 1996). Lifetime of $SO_2$ is normally less than 1 day (*Shon et al.*, 2001).

Taking it all together, we estimate that any time lag between CHL and CCN concentrations through DMS should be seasonally variable but in the range of few days in summer to two weeks in winter at the most. Therefore, using a time resolution of one month (monthly means) we should be able to capture most of the CHL−CCN cycle, at least in the productive season. To explore the importance of a potential lag between CHL and CCN, we repeat the statistical analysis after applying a lag of half a month to (only) the atmospheric variables: $y^* = (y_i + y_{i+1})/2$ (where $i = 1,...,36$ are months, $y_i$ is the value of either OH, CCN or RAIN for the month $i$, and $y^*$ is the lagged value).

Rainfall acts as an aerosol scavenger either by in-cloud scavenging as well as by below-cloud washout. Therefore, the two main loss factors influencing CCN concentrations are the nucleation process, which changes the status of a particle from CCN to cloud droplet, thus reducing the number of available CCN, and the washout of CCN by raindrops. Although in the SO these two processes seem to co-vary (the density of liquid water droplets in the atmosphere displays the same seasonality as the rainfall amount estimates; results not shown), in the present study we focus on the second factor only (below-cloud washout). *Nguyen et al.* (1992) found covariation between wet deposition rates of MSA and nss-$SO_4$ at Amsterdam Island (38°S, 77°E), a place not far from the northern edge of our study region and characterized by a similar DMS seasonality (*Putaud et al.*, 1992). Therefore, in the case of using MSA as a proxy for atmospheric DMS there is no need to introduce rainfall as an extra process because rain effects are already taken into account by the variables (MSA and CCN) themselves. Rather, when using a proxy for atmospheric DMS that does not undergo rain scavenging, like CHL or even DMSw, it is necessary to introduce the rain effects on CCN in the regression model if we seek to explain the CCN seasonality. We would like also to note that not only does the rainfall influence CCN concentration, but it is also influenced by the number of CCN available during cloud formation (*Albrecht*, 1989). In the presence of high numbers of CCN, due to the competition for water, the cloud droplets do not grow to larger sizes. Small cloud droplet sizes prevent rainfall and increase cloud lifetime (*Rosenfeld*, 2000; *Matsui et al.*, 2004; *Givati and Rosenfeld*, 2004).

### 3.2.3 Statistical Analyses

The monthly average time series for CHL, OH, CCN, RAIN and WIND are used to obtain statistical relationships between variables. First, for each independent variable (CHL, CHL*OH, RAIN and WIND), a simple linear regression against the dependent variable (CCN) is applied. Then, a multilinear regression model that relates CCN to CHL*OH and RAIN is developed. The $r^2$ determination coefficient is used as a measure of the degree of adjustment of the statistical models. The first equation of the multilinear model is based on the assumption that CHL is a proxy for DMS emissions and that DMSa is oxidized to CCN by the OH radical. Assuming that this effect is homogeneously distributed over the entire SO we have:

$$CCN = b * (CHL * OH) \tag{3.1}$$

Then, rainfall acts as a sink for CCN but its effect is not distributed homogeneously: local rains affect only local CCN concentrations. We thus can consider that, in a given month, only a fraction (*Srain*) of the total area (*Stot*) is under the RAIN scavenging effect, with the rest of the area being free of rainfall (*Sfree*). We also assume that CCN form a 'non-porous layer'; that is, if rainfall occurs, all CCN within the rainy region disappear. This implies that in the *Srain* area no CCN are present and the satellite is able to see only the CCN in the *Sfree* area (*CCNsat*). The second equation is therefore:

$$\begin{aligned} CCNsat = \frac{Sfree}{Sfree + Srain} * CCN = \\ = \frac{Sfree}{Stot} * CCN \end{aligned} \tag{3.2}$$

which in combination with eq(3.1) becomes:

$$CCNsat = \frac{Sfree}{Stot} * b * (CHL * OH) \tag{3.3}$$

The area fraction free of the rain scavenging effect ($\frac{Sfree}{Stot}$) is assumed to be a function of RAIN values: higher rainfall amount implies larger *Srain* areas. We call this area fraction $K(rain)$. There exists a $RAIN_{max}$ for which the whole area (*Stot*) is experiencing rain scavenging (i.e. *Sfree* =0; $K(rain)$ =0). $K(rain)$ varies between 0 and 1 and can be expressed as a function of the rainfall amount as follows:

$$K(rain) = \gamma * (RAIN_{max} - RAIN_i) \tag{3.4}$$

where $RAIN_i$ is the rainfall amount and $\gamma$ is a constant. Then, we can rewrite eq(3.3) as:

$$\begin{aligned} CCNsat &= K(rain) * b * (CHL * OH) = \\ &= \gamma * (RAIN_{max} - RAIN_i) * b * (CHL * OH) = \\ &= (\gamma * b * RAIN_{max} - \gamma * b * RAIN_i) * (CHL * OH) \end{aligned} \tag{3.5}$$

Regrouping constant terms:

$$b1 = \gamma * b * RAIN_{max} \tag{3.6}$$

and

$$b2 = \gamma * b \tag{3.7}$$

we obtain:

$$\begin{aligned} CCNsat &= (b1 - b2 * RAIN_i) * (CHL * OH) = \\ &= b1 * (CHL * OH) - b2 * RAIN_i * (CHL * OH) \end{aligned} \tag{3.8}$$

Not all *CCNsat* must be related to $CHL * OH$ (i.e. produced exclusively from DMS oxidation). Several authors have found a background level of CCN even when atmospheric MSA (an exclusive product of DMS oxidation) is almost 0, suggesting sources for CCN other than DMS, possibly SS (*Ayers and Gras*, 1991; *Andreae et al.*, 1999). To account for this background level, we need to add an intercept parameter to the above model, which leads to the final equation:

$$\begin{aligned} CCNsat = a &+ b1 * (CHL * OH) - \\ &- b2 * RAIN_i * (CHL * OH) \end{aligned} \tag{3.9}$$

Parameters $a$, $b1$ and $b2$ are obtained by a mean square fitting procedure. Conceptually, we can see the second and third terms on the right side of eq(3.9) as 'source' and 'sink' terms for CCN, respectively. The former represents the atmospheric oxidative interaction between DMS and OH radical to produce CCN; the second represents the interaction between the potential stock of CCN from DMS oxidation (using CHL*OH as a proxy) and RAIN. The source term is similar to the growth term in ecological models, where a biomass increase is the result of the interaction between the actual biomass stock and nutrient concentration, times a specific growth rate; in the same way, the loss is similar to the predation term, where prey loss is represented by the product of prey biomass and the predation rate.

This kind of model is called 'effective' models, as they are based on average data. The sum of complex non-linear processes (such as the production, emission and oxidation of biogenic DMS, or the interaction of rainfall and aerosols) is taken as a whole where individual processes

are masked and the average behavior is emphasized. Our effective model is then a first order description of the average behavior of the processes; a more complete characterization of the dynamics of the system should be obtained through the use of time dependent differential equations.

## 3.3 Results and Discussion

### 3.3.1 Linear Regressions

The 2002-2004 time series of CHL, CHL*OH, RAIN and WIND plotted against CCN, as well as their corresponding regression analyses, are shown in Figure 3.2. CHL and CCN display a strong seasonal coupling (Figure 3.2a), although in fall and early winter CHL decrease rates (slopes of the time series curves) are less pronounced than those of CCN. The Spearman correlation coefficient obtained between both variables is high ($\rho = 0.88$, $p - val << 0.001$) and equal to that obtained by *Gabric et al.* (2002) between climatological CHL and AOD (1997-2000) for a region of the SO south of Australia (from 40°S to 53°S and from 126°S to 148°E). The regression analysis also give a similar determination coefficient ($r^2 = 0.82$) to that obtained by *Ayers et al.* (1997a) between climatological monthly mean atmospheric DMS and CCN ($r^2 = 0.84$).

The linear regression gives a negative intercept value (-19.52*$10^6$ partic $cm^{-2}$; see Figure 3.2b). This fact is not in agreement with the observations at Cape Grim, where a background level not related to DMS production but most probably to SS was found at about 30-40 CCN $cm^{-3}$ (*Ayers and Gras*, 1991; *Ayers et al.*, 1997a; *Andreae et al.*, 1999). Also, the slope of the CCN *vs.* CHL regression analysis using the normalized data (values divided by its annual mean) is 1.87 (see the equation in brackets in Figure 3.2b), i.e. more than three times higher than the normalized slope obtained by *Ayers et al.* (1997a) for CCN *vs.* DMSa (0.52). A reason for this discrepancy is that CHL exhibits lower seasonal amplitude than DMSw and DMSa. A second reason would be the higher seasonal amplitude of our derived CCN compared to those measured at Cape Grim. The summer maximum to winter minimum ratio for CHL is 1.75. Based on the *Kettle and Andreae* (2000) DMSw database, the summer maximum to winter minimum ratio for DMSw over the whole SO is about 5, similar to that of DMSa at Cape Grim (*Ayers et al.*, 1995) and three times that of CHL. This reflects the differential behavior of CHL and DMS over the annual cycle: they both peak in summer but there is a higher net production of DMS per unit of CHL with respect to wintertime, probably because of the concurrence of phytoplankton succession to higher DMSP producers and plankton physiological stress due to shallow mixing, iron deficiency and high UV exposure (*Simó and Pedros-Allió*, 1999a; *Simó and Dachs*, 2002; *Sunda et al.*, 2002).

The MSA seasonal amplitude is even higher than that of the DMSa (the MSA summer maximum to winter minimum ratio is about 10 (*Andreae et al.*, 1999)). This can be regarded as an indica-

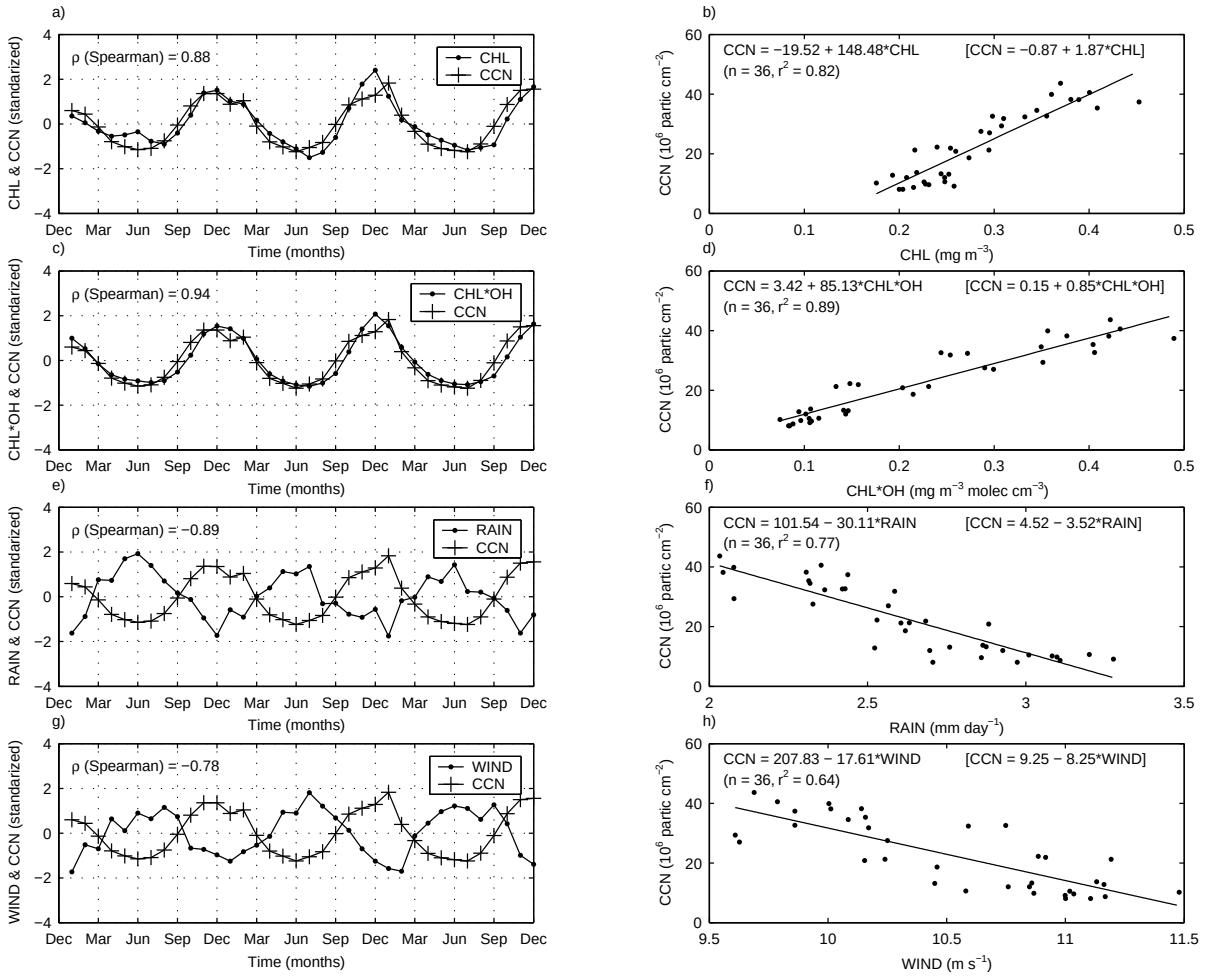


Fig. 3.2: Seasonal evolution (years 2002 to 2004) and the associated Spearman correlation coefficient of CCN against: a) chlorophyll, c) chlorophyll*hydroxyl radical e) rainfall amount, and g) wind speed (variables are presented in standardized form, i.e. subtracted the mean and divided by the standard deviation). Regression analyses of CCN against: b) chlorophyll, d) chlorophyll*hydroxyl radical f) rainfall amount, and h) wind speed. CCN values are derived from MODIS according to *Gassó and Hegg* (2003). Chlorophyll concentrations are obtained from SeaWiFS. Hydroxyl radical concentrations are outputs of the GEOS-CHEM model provided by the Atmospheric Chemistry Modeling Group at Harvard University (*Fiore et al.*, 2003). Rainfall amount and wind speeds are obtained from the NCEP/NCAR Reanalysis Project. Note the little seasonal variability of the wind speed (less than $\pm$10% of the annual mean). Equations in brackets represent the linear regressions applied to normalized data sets by dividing the individual monthly values by the annual mean.

tion that some key player(s) is (are) not represented in this correlation analysis. Most likely candidates are the main DMSa oxidant, the OH radical, which is depressed in winter (*Spivakovsky et al.*, 2000) and the main MSA loss factor, rainfall scavenging, which is enhanced in winter. Since both MSA and CCN production from DMS oxidation depend on OH concentration, the correct regression analysis should relate CCN to DMS*OH. This would increase the seasonal amplitude of the independent variable (DMS*OH) and then reduce even more the (normalized) slope. In this regard, the inclusion of the OH radical in our analysis results in a significantly better agreement between CCN and CHL*OH ($\rho = 0.94$, $p - val << 0.001$; see Figure 3.2c). At the same time we obtain a positive intercept value ($3.42*10^6$ partic $cm^{-2}$) and a (normalized) slope of 0.85 (Figure 3.2d). We can appreciate how the time series of CHL, CHL*OH and CCN agree in the inter-annual variability of their annual amplitudes, which increased slightly from Jan 2002 to Dec 2004 (see Figures 3.2a and 3.2c; CCN retrievals for Jan 2004 need to be taken with some caution because January 2004 was undersampled).

The monthly mean rainfall amount estimates used in the present study display the same seasonal pattern as the measured rainfall amounts at Cape Grim, with highest values during winter months (wet season) and minima in summer (dry season) (*Ayers and Ivey*, 1990). The time series of CCN and RAIN show a clear anti-phase trend ($\rho$ = -0.89, $p - val << 0.001$; see Figure 3.2e) that is also appreciated in the regression analysis (Figure 3.2f). However, RAIN displays also lower seasonal amplitude (winter maximum to summer minimum ratio of 1.3) than CCN (ratio of 4; see Figure 3.2f). Thus, RAIN alone can not be responsible for the CCN seasonality. It is probably the combination of the influences of CHL*OH and RAIN what dictates CCN seasonal evolution.

### 3.3.2 Multilinear Regression

While simple linear regression shows a strong coupling between CHL*OH and CCN as well as RAIN and CCN, we also made use of a more advanced multilinear regression model to describe CCN as a function of CHL, OH and RAIN. Multilinear regression allows the reconciliation of the opposite signs of the CHL*OH−CCN relationship (positive) and RAIN−CCN (negative). The model introduces RAIN as a loss process that interacts with the potential production of CCN from CHL through DMS oxidation by OH (see section 3.2).

The regression plane obtained with the multilinear regression model is plotted in Figure 3.3a along with the regression equation. Figures 3.3b and 3.3c display the distances of the data points to the plane for the '$(CHL * CHL)$' and '$RAIN * (CHL * OH)$' variables respectively. This analysis shows how CCN rise as CHL*OH increases, and decrease as RAIN goes up (Figures 3.3a, 3.3b and 3.3c). The determination coefficient is very high ($r^2 = r^2_{adj} = 0.9$; where $r^2_{adj}$ refers to the 'adjusted determination coefficient' which imposes a penalty for each additional independent variable added to explain the dependent variable *CCN* (*Ohtani*, 2000)). Thus, 90% of the variance in CCN numbers is explained with this multilinear regression model.

Looking at model parameters (see equation in Figure 3.3a) we can obtain some additional information. The intercept value is 6.34*$10^6$ partic $cm^{-2}$, i.e. twice that obtained with the linear model CCN *vs.* CHL*OH. As expected, both slopes ($b1$ and $b2$) are positive (148.06 and 30.74). This is an *a-posteriori* validation of the model: the conceptual model is not in contradiction with the data. This could seem obvious, but the way we have introduced the effect of rainfall did not necessarily have to be correct and in agreement with the observations. The fact that $b1$ is greater than $b2$ implies that the rainfall amounts present in the SO are well below the theoretical maximum rainfall amount ($RAIN_{max}$) for which all CCN should be cleared out everywhere ($Sfree = 0$, see section 3.2). We can easily check this by dividing $b1$ by $b2$, as this fraction will give us the $RAIN_{max}$ (see eq(3.6) and eq(3.7)). The $RAIN_{max}$ obtained is 4.82 mm $d^{-1}$, a value never achieved within the rainfall amount time series (Figure 3.2f). In nature, however, the $RAIN_{max}$ that corresponds to a satellite retrieval of zero CCN would be much higher or even infinite. We are able to obtain a $RAIN_{max}$ because we have assumed a linear behavior for the $K(rain)$ (see eq(3.4) in poin 3.2.3) whereas it is probably asymptotic. Nonetheless, within the range of rainfall amounts we are dealing with, such a linear approximation seems to be valid. The relative weights of the production variable '$(CHL * OH)$' and the sink variable '$RAIN * (CHL * OH)$' in determining the variability of CCN numbers can be obtained from the standardized slope values of the production and sink terms ($b1s = 1.64$ and $b2s$ = 0.71, respectively). The fact that $b1s$ is more than twice $b2s$ indicates that the production is more important than the loss to explain the seasonal CCN pattern.

### 3.3.3 Lagged correlations

Correlations lagging by half a month the atmospheric variables (see section 3.2) result in a slightly reduction of the level of association between the CHL*OH, RAIN and CCN. The determination coefficient of the linear model CCN *vs.* CHL*OH is now $r^2 = 0.83$ and the determination coefficient obtained with the multinear model becomes $r^2 = 0.86$. This may indicate that the processes of DMS production, emission and oxidation to CCN are very rapid in the SO, at least during the productive season. However, we have applied a $t$-test to the correlation coefficients of the linear model obtained with and without the lag and the differences are not statistically significant ($p - val << 0.001$).

### 3.3.4 Potential non-biogenic sources of CCN

As pointed out by *Gabric et al.* (2002), a major problem associated with monthly series analyses is the possibility of illusory correlations due to an independent seasonal variation of the studied variables. In order to assess whether this can lead to misinterpretation of our results, we need to look at all the factors that could play a controlling role in CHL, OH and CCN seasonality. As

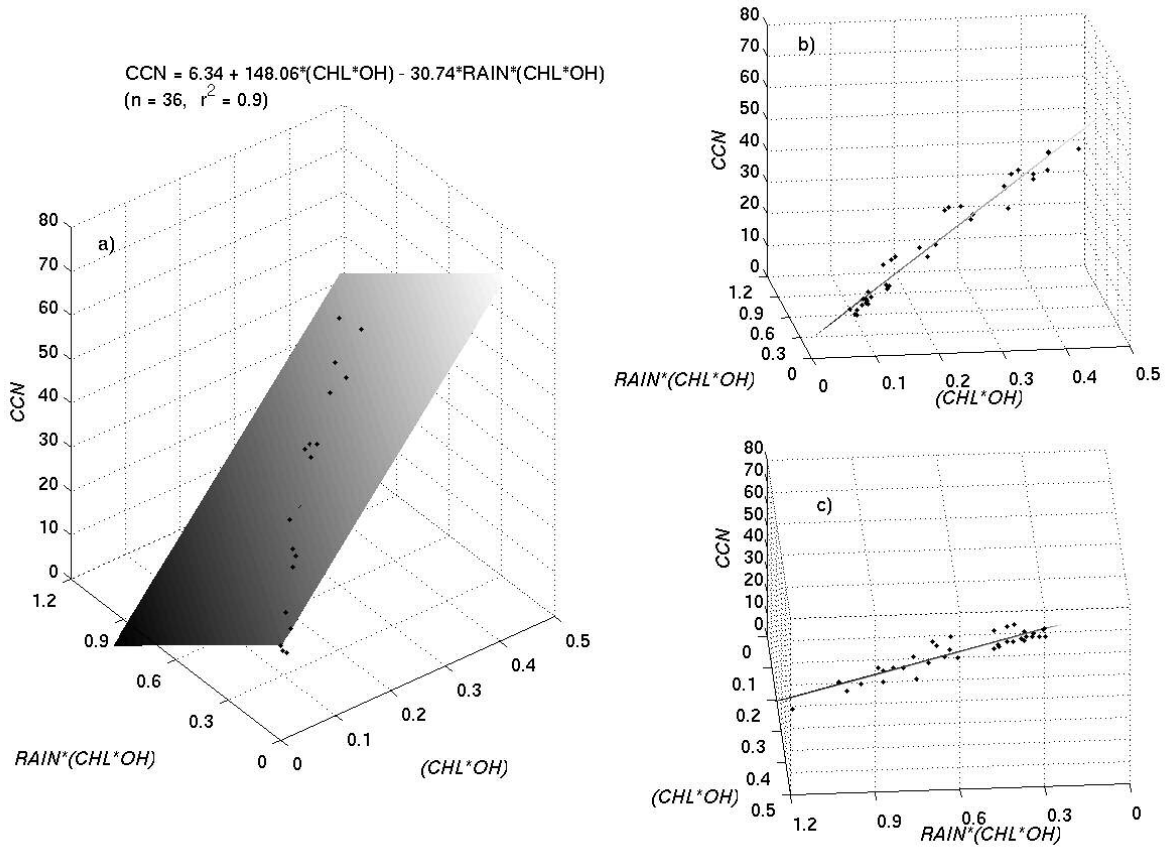


Fig. 3.3: a) Regression plane obtained for the multilinear regression model that describes CCN column-integrated concentrations (units of $10^6$ partic $cm^{-2}$) as a function of atmospheric DMS oxidation (using 'chlorophyll*hidroxyl radical' as a proxy) and rainfall washout, for 36 months between Jan 2002 and Dec 2004; b) and c) show two different points of view of the regression plane.

we have already noted, CHL seasonality in the SO is mainly governed by light. Solar radiation controls CHL evolution both directly and indirectly. The direct control is due to the higher and longer exposure to photosynthetic active radiation (PAR) during summer. The indirect effect is through the reduction of the MLD: heating of the surface ocean provokes a shoaling of the pycnocline at the same time that PAR is higher, which results in maximum CHL concentrations during summer. In this period only iron seems to be a limiting factor. OH is also driven by solar radiation, in this case by the UV radiation. Regarding the seasonality of aerosols (CCN among them), several are the potential controlling factors: *i*) DMS oxidation; *ii*) SS concentrations; *iii*) input of continental aerosols (natural or anthropogenic); *iv*) rainfall.

The day time oxidation of DMS to give nss-$SO_4$ aerosols is mediated by OH radicals. As previously mentioned, OH seasonality is coincident with DMS seasonality in the SO. Therefore, summer months would be characterized by both higher DMS emission and better efficiency in the oxidation of DMS into CCN components. In this regard, the mechanistic link proposed between DMS oxidation and nss-$SO_4$ aerosols has proved to be robust in the SO (*Andreae et al.*, 1999; *Jourdain and Legrand*, 2001). A good example is the work of *Ayers et al.* (1991) with a 17-months data series, where a strong association between DMS, MSA and nss-$SO_4$ in both signal amplitude and interannual timing of the peaks can be appreciated. However, it is important to note that although good seasonal associations have also been found between DMS oxidation products and CCN in the SO (*Ayers and Gras*, 1991; *Ayers et al.*, 1995, 1997a; *Andreae et al.*, 1999), a mechanistic link has not been completely confirmed because the relative contribution of nss-$SO_4$ to the composition of CCN is still object of discussion (*O'Dowd et al.*, 1997; *Murphy et al.*, 1998). Variable amounts of nss-$SO_4$ can be internally mixed with SS (*O'Dowd et al.*, 1997, 1999; *Alexander et al.*, 2005) bringing up more efficient CCN (*Murphy et al.*, 1998) and small SS can compete with nss-$SO_4$ for the accumulation mode (*O'Dowd et al.*, 1997; *Ghan et al.*, 1998).

SS aerosol mass concentrations are high in the SO (*Murphy et al.*, 1998; *Quinn et al.*, 1998). However, their contribution to the numbers of small aerosols is low. After a cruise across the Pacific Ocean that also traversed the SO, *McInnes et al.* (1997) reported that SS aerosols between 0.1 and 1 $\propto$m represented only 4-7% of the total number of particles in this range, but 86-100% of supermicron particles with a mean diameter of 1.5 $\propto$m. SS aerosol is formed by mechanical interaction of wind with the sea surface, particularly through bursting of air bubbles during whitecap formation and wave breaking. Thus, SS production can be qualitatively estimated from wind speed, even though the correlation between SS and wind speed in the SO is not as high as should be expected (*Andreae et al.*, 1999). As illustrated by Figure 3.2h, WIND shows little seasonal variability (values within the narrow range of 9.5-11.5 m $s^{-1}$), in agreement with what has been reported by *Gille* (2005). This contrasts with the high seasonal amplitude of CCN. Moreover, WIND seasonality is characterized by a slight increase in winter (*Ayers et al.*, 1999; *Andreae et al.*, 1999) when CCN are at their annual minimum (Figure 3.2g). All these facts are consistent with the low seasonal variability of SS reported for the SO with a slight maximum in winter (*Wangenbach et al.*, 1998; *Ayers et al.*, 1999; *Andreae et al.*, 1999; *Gong et al.*, 1997,

2002; *Grini et al.*, 2002; *Easter et al.*, 2004). Our results suggest that SS aerosol production is not responsible for the observed CCN seasonality, in agreement with the observations made at Cape Grim by *Andreae et al.* (1999), who found that CCN and SS were not correlated. It could be argued that, if SS aerosol production in the SO is rather constant throughout the year, we might expect SS aerosols follow the seasonality of the rainfall amount and be depressed during the wet season, just like CCN. The reason for this not happening is that SS aerosol production by wind friction is a very rapid process (*Andreas*, 1998; *Smirnov et al.*, 2003), and the cold fronts responsible for increases in rainfall are generally associated with local wind storms that cause higher SS production. Then the replacement of the SS washed out by rain would occur almost instantaneously, and the rain effect would not become apparent on a monthly basis. Such a hypothesis is in agreement with the modeling work of (*Grini et al.*, 2002), who showed higher wintertime SS wet deposition co-occurring with higher SS production, with a net result of slightly higher SS concentrations.

Another potential source of CCN is continental aerosols (the fine mode of dust, organic carbon in smoke and anthropogenic nss-$SO_4$). The SO is scarcely impacted by continental aerosols (*Husar et al.*, 1997; *Kaufman et al.*, 2002; *Higurashi et al.*, 2000). Anthropogenic sources of nss-$SO_4$ are mainly located in the Northern Hemisphere (*Bates et al.*, 1992), being the SO relatively free of such emissions (*Gabric et al.*, 2001). Even though a fraction of oceanic aerosols during ACE-1 contained soot (*Buseck and Pósfai*, 1999), very little soot was found by *McInnes et al.* (1997) during a ship transect from 67°S to 48°N over the Pacific Ocean, where $SO_4$ was the dominant aerosol component. Dust fluxes to the SO are also amongst the weakest of the world's oceans (*Jickells et al.*, 2005). *Gao et al.* (2001) pointed out that the SO has extremely low atmospheric concentrations of iron, reflecting little influence by dust transport throughout the year. Nonetheless, dust storm activity in south west Australia is higher in summer (*McTainsh et al.*, 1998; *Gabric et al.*, 2002). In this period, the monthly average dust storm frequency is in the range of 0.60 - 0.12, i.e. 2 to 4 dust storms per month. Such a low activity would be smoothed out in the monthly means of satellite CCN retrieval. *Herman et al.* (1997) analyzed satellite data from the Total Ozone Mapping Spectrometer (TOMS, NASA) and did not found detectable amounts of UV absorbing aerosols (e.g. dust, soot, smoke) over the SO in any month of the year. With respect to black carbon aerosols (soot and smoke), the closest sources (South America and South Africa) have their higher emissions roughly from June to September (austral-winter) (*Herman et al.*, 1997; *Kaufman et al.*, 2002). Similarly, carbon monoxide seasonality in the SO peaks in September-October and is at its minimum during January-February (*Spivakovsky et al.*, 2000) coinciding with a summer minimum in biomass burning activity (*Duncan et al.*, 2003). Thus, the potential contribution of organic carbon to the CCN burden, if any, should occur only in late winter - early spring.

### 3.3.5 Fine Mode Aerosols

Further indication of the seasonal decoupling between CCN and SS particles or dust, and support for a biogenic origin of the former, can be obtained from the study of the MODIS primary parameter ETA (the fraction of AOD accounted for by the accumulation mode, see point 3.2.2). As previously stated, SS and dust are mainly composed of coarse particles while nss-$SO_4$ belongs to the accumulation mode. Although MSA can be present in the accumulation and coarse modes (*Bates et al.* (1998) reported that during ACE-1 MSA mass was almost evenly distributed in both modes), its mass contribution to the aerosol burden is much lower than nss-$SO_4$ (*Bates et al.*, 1998; *Jourdain and Legrand*, 2001). If DMS oxidation were a major source of aerosols during summer months, the ETA parameter would be highly influenced by nss-$SO_4$ seasonality and then it should be higher in summer. On the contrary, a summer increase of SS or dust would be reflected as a decrease of the ETA parameter. Figure 3.4 shows the time evolution of ETA. It displays a marked seasonality where the contribution of the small mode particles to the total AOD increases by a factor of 3.5 in summer with respect to winter (from 13% to 45%). Therefore, although the absolute contribution of the small aerosols to the total aerosol burden is relatively low (an annual average of 30%) due to the presence of high (and almost constant) amounts of SS aerosols (*Andreae et al.*, 1999), the seasonality of the small mode aerosols is mostly driven by the biological oceanic source.

The aforementioned facts can be used to estimate the biogenic contribution to CCN numbers. If the total aerosol burden in the SO is assumed to be composed mainly of nss-$SO_4$, SS and (to a lesser extent) MSA (*Quinn et al.*, 1998), CCN would be contributed mainly by nss-$SO_4$, $SS_{small}$ and $MSA_{small}$. Then, CCN can be expresed as

$$CCN = CCN_{bio} + SS_{small} \tag{3.10}$$

(where $CCN_{bio}$ = nss-$SO_4$ + $MSA_{small}$). Assuming that the intercept value of the multilinear model corresponds to a background (and almost constant) level of SS (*Andreae et al.*, 1999) ($SS_{small}$, since CCN is contributed only by particles between 0.1 and 1 ∞m), we obtain $CCN_{bio} = CCN - SS_{small}$. $CCN_{bio}$ varies from about 3*$10^6$ partic $cm^{-2}$ in winter to 30*$10^6$ partic $cm^{-2}$ in summer. That is, a seasonal amplitude of a factor of 10, which is exactly the seasonal amplitude of MSA at Cape Grim (*Andreae et al.*, 1999). We can thus define the contribution of biogenic CCN to the total CCN as $BETA = CCN_{bio}/CCN$. The seasonal evolution of the estimated BETA is plotted in Figure 3.4. We can appreciate that the biogenic contribution to the CCN has an average value of 35% in winter months and 80% in summer (the remaining CCN being contributed by $SS_{small}$). Thus, CCN seasonality in the SO seems to be highly influenced by $CCN_{bio}$ seasonality.

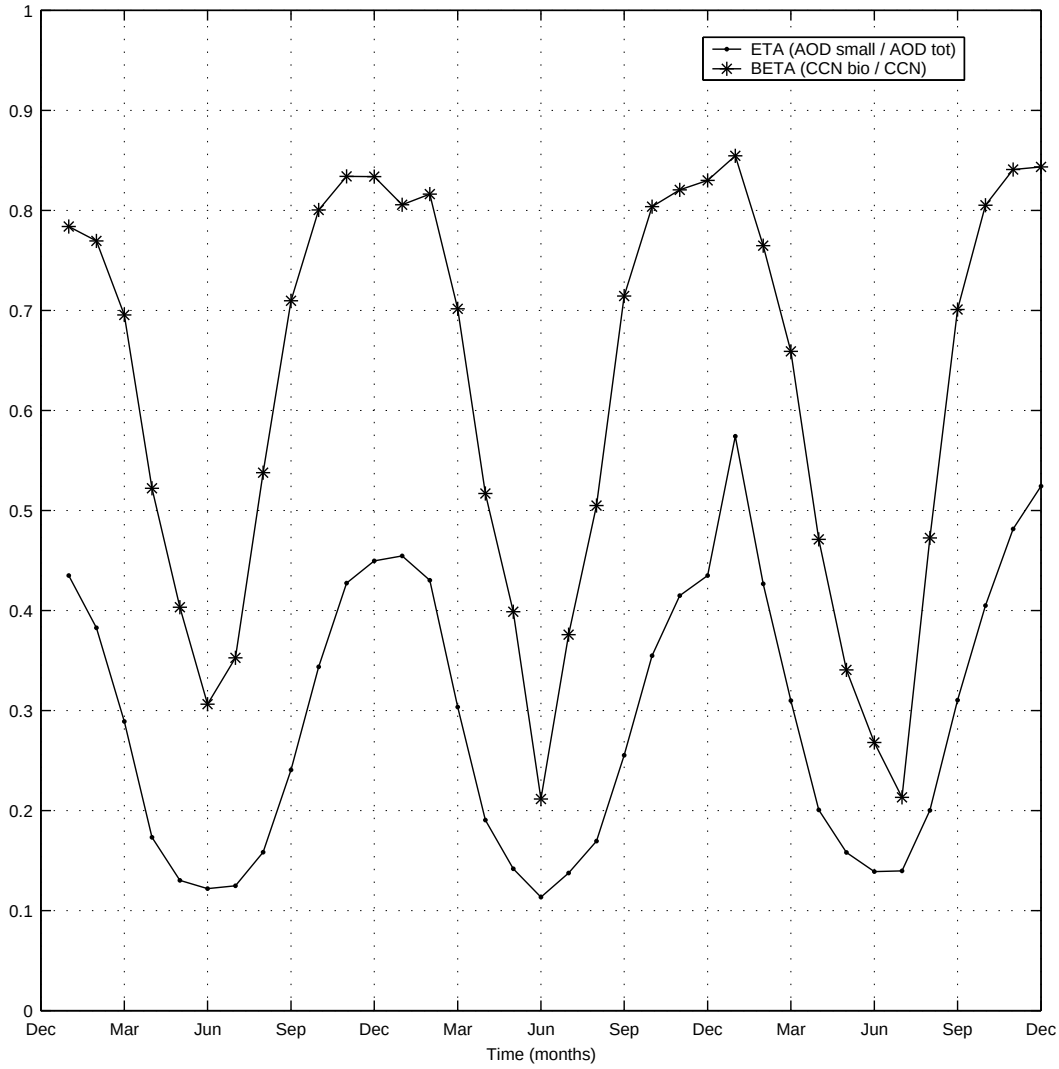


Fig. 3.4: Seasonal evolution (years 2002 to 2004) of the contribution of small mode particles to the Aerosol Optical Depth (ETA parameter = $AOD_{small}$ / $AOD_{total}$) as provided by MODIS, and seasonal evolution (years 2002 to 2004) of the estimated contribution of biogenic CCN to the total CCN burden (BETA = $CCN_{bio}$ / CCN).

## 3.4 Conclusions

We have performed statistical linear regression analyses with the aim at looking for functional relationships between monthly means of satellite-derived CCN, surface ocean CHL, OH radical and RAIN for the entire SO. Tri-annual time series (from Jan 2002 to Dec 2004) of these variables have been used to explain the seasonality of CCN in this pristine region. A multilinear regression model has revealed that the seasonal and interannual variability of potential CCN is highly explained by the variability of CHL (as a proxy for the emission of the planktonic aerosol precursor DMS), OH (as the main oxidizer of atmospheric DMS) and rainfall. This is in agreement with local experimental studies where relationships between biogenic DMS and its aerosol products have been observed, as well as with the central role of rainfall in removing atmospheric submicron aerosols. Although statistical analyses could never serve as a proof for causal relationships between variables, and other factors (like those related to atmospheric dynamics and in-cloud aerosol processing) that can influence the CCN seasonal variability cannot be ruled out, their full exploration is beyond the scope of the present study. At the present stage, our results suggest that the seasonal correlations found between CHL*OH, RAIN and CCN are not independently driven by third variables but seem to be linked through causal relationships. The main arguments for such a conclusion are: *i*) The strong association observed between CHL*OH and CCN, with some interannual association also captured; *ii*) the anti-phase association between CCN and WIND; *iii*) the low detectable influence of continentally derived aerosols on CCN numbers over the SO; *iv*) the seasonality of the ETA parameter, which shows a 3.5 times increase from winter to summer despite the high (and almost constant) contribution of SS to the total AOD. Therefore, the high determination coefficients and significance obtained with the regression models applied strongly support the hypothesis that oceanic microbiota affect CCN concentrations through the production, emission and atmospheric oxidation of DMS at large spatial scales. Given that CCN concentrations are modulated by oceanic DMS, it is very probable that cloud formation and their properties are affected too, with important implications for climate as proposed by *Charlson et al.* (1987) 18 years ago. We suggest that this kind of statistical approach, based mainly on satellite measurements and model data, should be applied to other oceanic regions and expanded to the global scale. Along with continued fieldwork, it should be very useful in future research addressing the validity of the CLAW hypothesis and its implications in Earth System functioning and Global Change.

*

CHAPTER 4

# Analysis of a potential 'Solar Radiation Dose - DMS - CCN' link from globally mapped seasonal correlations

*It's better to be quiet and thought a fool*
*than to open your mouth and remove all doubt.*

*(Groucho Marx)*

# Analysis of a potential 'Solar Radiation Dose - DMS - CCN' link from globally mapped seasonal correlations


## ABSTRACT

The CLAW postulates states that an increase in solar irradiance or in the heat flux to the ocean can trigger a biogeochemical response to counteract the associated increase in temperature and available sunlight. This natural (negative) feedback mechanism would be based on a multi-step response: first, an increase in seawater dimethylsulfide concentrations ($DMS_w$) and therefore its fluxes to the atmosphere ($DMS_{flux}$); second, an increase in the atmospheric cloud condensation nuclei (CCN) burden as a consequence of DMS oxidation to form biogenic CCN ($CCN_{bio}$); third, an increase in cloud albedo due to higher CCN numbers. Monthly global climatological fields of the solar radiation dose in the upper mixed layer (SRD), surface oceanic $DMS_w$, model outputs of hydroxyl radical concentrations (OH) and satellite-derived CCN numbers ($CCN_s$) are analyzed in order to evaluate the proposed 'Solar Radiation Dose - DMS - CCN' link from a global point of view. OH is included as the main atmospheric oxidant of the estimated $DMS_{flux}$ to produce $CCN_{bio}$. Global maps of seasonal correlations between the variables show that the solar radiation dose is highly (positively) correlated with seawater dimethylsulfide over most of the global ocean and that atmospheric DMS oxidation is highly (positively) correlated with $CCN_s$ over large regions. These couplings are stronger at high latitudes whereas the regions with negative or no correlation are located at low latitudes around the equator. However, $CCN_{bio}$ estimates for 15 regions of the global ocean show that DMS oxidation can be an important contributor to the $CCN_s$ burden only over pollution-free regions, while it would have a minor contribution over regions with high loads of continental aerosols. Globally, the mean annual contribution of $CCN_{bio}$ to total $CCN_s$ is estimated to be $\approx$30%. Our results support that an oceanic biogenic mechanism that modulates cloud formation and albedo can indeed occur, although its impact seems rather weak over regions under a strong influence of continental aerosols. Nevertheless, our approach does not fully rule out that the observed correlations are due to an independent seasonal variation of the studied variables; seasonal couplings are necessary but not sufficient conditions to prove the CLAW hypothesis.



S. M. Vallina, R. Simó, S. Gassó, C. de Boyer-Montégut, E. del Río, E. Jurado, & J. Dachs (2007)
*Global Biogeochem. Cycles*, 21, GB2004, doi:10.1029/2006GB002787

## 4.1 Introduction

One of the most important questions regarding Earth system functioning is if the biota in the global ocean respond to climate variations in ways that in turn impact climate conditions, thereby setting natural modulating mechanisms (e.g. (*Charlson et al.*, 1987; *Andreae and Crutzen*, 1997; *Miller et al.*, 2003; *Sarmiento et al.*, 2004; *Jickells et al.*, 2005)). Despite much research effort having been invested, this issue is still not fully resolved. Many mechanisms have been proposed and among them the hypothesis that the marine biota could act to modulate climate through the emission of volatile sulfur and its impact on aerosols and cloud albedo (*Charlson et al.*, 1987; *Andreae and Crutzen*, 1997) has received considerable attention. The oceans are the largest source of natural sulfur emissions to the atmosphere in the form of biogenic dimethylsulfide (DMS) (*Andreae and Crutzen*, 1997; *Simó*, 2001). Seawater DMS ($DMS_w$) follows a complex cycle where several types of organisms and chemical reactions are involved. Phytoplankton produce intracellular dimethylsulfoniopropionate (DMSP), the biochemical precursor of DMS, through enzymatic cleavage with involvement of the whole planktonic food web (*Simó*, 2001). Recent works have pointed out that, although the $DMS_w$ dynamics result from a web of biological and biogeochemical processes, they are driven mainly by physical variables (*Simó and Dachs*, 2002; *Toole and Siegel*, 2004). For example, from a global point of view, the depth of the upper mixed layer (UML) is the only variable needed to efficiently estimate $DMS_w$ surface fields over $\approx$85% of the ocean's surface (*Simó and Dachs*, 2002). Also, in the Sargasso Sea the amount of UV radiation received in the UML explains almost 80% of the $DMS_w$ seasonal variability (*Toole and Siegel*, 2004).

DMS is emitted to the atmosphere with a ventilation rate that depends on $DMS_w$ concentration as well as on seawater temperature and wind speed (*Nightingale et al.*, 2000). Once in the atmosphere DMS ($DMS_a$) undergoes a sequence of oxidative reactions through interaction mainly with the hydroxyl radical (OH) (*Savoie et al.*, 1989; *Chin et al.*, 2000; *Barrie et al.*, 2001; *Kloster et al.*, 2006), giving rise to a range of products. Among them, non-sea-salt sulfate (nss-$SO_4$) and, to a lesser extent, methanesulfonate (MSA) are of particular interest because of their potential to form cloud condensation nuclei (CCN) (*Cox*, 1997). MSA and nss-$SO_4$ particles are highly hygroscopic and usually occur in the submicron size fraction (*Ayers et al.*, 1997a, 1999; *Andreae et al.*, 1999; *Jourdain and Legrand*, 2001). On these grounds, DMS emissions are thought to be the main source of CCN in the marine troposphere remote from land (*Liss and Turner*, 1997).

CCN are believed to have a prominent role in the Earth energetic balance through both the direct scatter of solar incident radiation as well as their influence on cloud albedo and lifetime (*Twomey*, 1974; *Albrecht*, 1989; *Kaufman et al.*, 2002). The CLAW hypothesis (*Charlson et al.*, 1987) proposed that an increase in solar irradiance and/or Earth temperature could be at the origin of an increase of $DMS_w$ and its fluxes to the atmosphere. This would imply an increase in nss-$SO_4$ and, therefore, in the atmospheric CCN burden, which in turn would increase cloud albedo (Twomey or first indirect effect) and lifetime (Albrecht or second indirect effect)

then reducing the solar incident radiation and thus Earth temperature. However, recent global analyses suggest that sea surface temperature is not the driving mechanism of DMS dynamics but rather the solar radiation dose (*Vallina and Simó*, 2007a). If it can be shown that the main mechanisms and forces proposed to conform the CLAW hypothesis (DMS emission, DMS oxidation efficiency, CCN formation, solar radiation) vary seasonally, should they be in phase the hypothetical feedback would be more feasible and more efficient. If no seasonal couplings were observed between some or all of these key factors, then the feedback would be hardly observable and even hardly feasible. This is because DMS, unlike $CO_2$, is a short-lived gas that does not accumulate in the atmosphere. That is, seasonal couplings are a "necessary but not sufficient" condition for the CLAW hypothesis (*Bates et al.*, 1987). However, in present Earth conditions, the dominant sources of nss-$SO_4$ on a global scale are anthropogenic (*Lefohn et al.*, 1999; *Smith et al.*, 2001). Also, sea-salt (SS) is a dominant contributor to total aerosol mass over much of the oceans (*Heintzenberg et al.*, 2000). Both anthropogenic $SO_4$ and the small fraction of SS can be effective CCN precursors (*Dingenen et al.*, 1995; *Harrison et al.*, 1996; *O'Dowd et al.*, 1997; *Murphy et al.*, 1998; *Andreae et al.*, 2003). Other potential sources of CCN are products from biomass burning (*Ross et al.*, 2003) and maybe small dust particles (*Arimoto*, 2001), both very abundant in large regions of the globe (*Ginoux et al.*, 2001). Therefore, if a solar irradiance - DMS - CCN link exists, it should be more easily observable in oceanic regions where continental sources contribute little to aerosol seasonality.

Coincidence between the seasonalities of the solar radiation dose and $DMS_w$ has been observed at a subtropical oligotrophic ocean site (*Toole and Siegel*, 2004) as well as at a coastal site in the NW Mediterranean Sea (*Vallina and Simó*, 2007a), a feature that can be partly explained through an antioxidant function for the DMSP/DMS system in phytoplankton cells (*Sunda et al.*, 2002). Also, several authors have found seasonal couplings between DMS and CCN both at local and regional scales, mainly in unpolluted regions (*Ayers and Gras*, 1991; *Andreae et al.*, 1995, 1999; *Ayers et al.*, 1997a). However, because of the geographic sparseness of sampling stations, there is a lack of studies addressing the issue from a global point of view. Optical sensors on satellites (e.g. MODIS) offer the possibility of making quasi-synoptic measurements of atmospheric variables at a global scale, which allows the investigation of couplings between the marine biogenic sulfur emissions and the atmospheric aerosols at spatial-temporal scales relevant for potential climate regulation. As far as we know, the only previous work based on global satellite data to investigate the coupling between ocean microbiota and atmospheric aerosols is that of *Cropp et al.* (2005). Both the CLAW hypothesis as well as the Iron hypothesis (*Martin et al.*, 1994) were invoked to explain the observed positive correlations. They considered the Aerosol Optical Depth (AOD) as a surrogate of both dust particles and/or nss-$SO_4$ particles from DMS oxidation. Dust carries iron that, through deposition, has the potential to fertilize large regions of the oceans where productivity is limited by the supply of this micronutrient. Iron fertilization could in turn impact DMS production (*Boyd et al.*, 2000) and therefore atmospheric nss-$SO_4$ formation. This combined approach hampered the assessment of the influence of DMS alone on aerosols (*Cropp et al.*, 2005). The present work is based

based on a similar methodology to look at seasonal couplings but we fully focus on two of the central postulates of the CLAW hypothesis: first, if an increase (decrease) in solar irradiance could produce an increase (decrease) of $DMS_w$ over the global ocean; and second, if any increase (decrease) of $DMS_w$ can be linked to a CCN increase (decrease). We also evaluate the couplings between DMS and the fine mode aerosols since nss-$SO_4$ mainly belongs to this size fraction. Finally, the contribution of estimated biogenic CCN ($CCN_{bio}$) to total CCN numbers is evaluated region by region of the globe.

## 4.2 Data and Methodology

Since we are interested in seasonal couplings, we base all the analyses on global monthly mean climatological data for the selected variables, with a 1° x 1° spatial resolution.

### 4.2.1 Solar radiation dose and DMS data

are estimated assuming an exponential decay of the daily-averaged surface solar irradiance ($I_0$) with depth ($z$):

$$SRD = I_{uml} = \frac{1}{MLD} \int_0^{MLD} I_0 * exp(-k * z) dz \tag{4.1}$$

$I_0$ is assumed to be 50% of the daily averaged solar irradiance at the top of the atmosphere ($I_{toa}$; W $m^{-2}$) (*Kiehl and Trenberth*, 1997), which is calculated following (*Brock*, 1981). The depths of the UML (MLD) are based on the work of *de Boyer-Montégut et al.* (2004). This is the latest and most complete climatology of global MLD, based on more than 4,000,000 temperature profiles (from 1941 to 2002). We have made use of this climatology with a modification of the definition criterion: the depth of the mixed layer is calculated as the depth at which temperature departs 0.1 °C from that at 5m. We assume a general solar-radiation extinction coefficient (k) of 0.06 $m^{-1}$, which is a reasonable approximation for spectrum-centered wavelengths in open ocean waters (*Smith and Baker*, 1979; *Kieber et al.*, 1996; *Obernosterer et al.*, 2001; *Lee et al.*, 2005).

The $DMS_w$ global monthly fields are those of *Kettle and Andreae* (2000), which are based on the Global Surface Seawater DMS database, the biggest and most comprehensive compilation of $DMS_w$ measurements available at that time (about 20,000 data points). This database was used to construct a global climatology of monthly means based on inter-/extrapolation procedure to fill the large areas/seasons where no data were available (*Kettle and Andreae*, 2000). DMS emissions to the atmosphere ($DMS_{flux}$) are calculated as a function of surface wind speed and sea water temperature (SST) using the gas transfer model of *Nightingale et al.* (2000). Surface wind speed and SST data were obtained from the the NOAA-CIRES Climate Diagnostics Center. Wind speed are model outputs, from the NCEP/NCAR Reanalysis project, constrained by

contemporary data obtained from the SSM/I sensor (DMSP, NOAA) (*Kistler et al.*, 2001). SST is a climatology (1971-2000) based on field and satellite measurements (*Reynolds and Smith*, 1995).

### 4.2.2 Atmospheric Data

The MODerate resolution Imaging Spectro-radiometer (MODIS), on board the Earth Observing System (EOS), currently has two detectors in orbit (on the satellites Terra and Aqua). Both have daily global coverage with a morning and afternoon pass respectively. In this study, we use data measured by MODIS-Terra. MODIS aerosol data (1° x 1° resolution) are available from NASA's Goddard Space Flight Center (GSFC) Distributed Active Archive Centers (DAAC). MODIS acquires data globally at 36 spectral bands (from 0.4 to 14.5 $\propto$m) and it is the first satellite capable of distinguishing coarse and fine aerosols, especially over the ocean (*Ichoku et al.*, 2004). Several primary aerosol parameters are retrieved from MODIS daytime data over the ocean, including the fine mode fraction or ETA ($\eta$) parameter (*Remer et al.*, 2005). Ranging from 0 to 1, ETA is defined as the ratio of the AOD contributed by the small mode particles (or accumulation mode) to the total AOD ($AOD_{small}/AOD_{total}$) and can thus be viewed as a measure of the percentage of fine particles that contribute to the total aerosol burden. SS and dust are mainly composed of coarse particles while nss-$SO_4$ belongs to the accumulation mode (*Fitzgerald*, 1991; *Andreae et al.*, 1999). If DMS contributes significantly to the aerosol burden, the ETA parameter should be higher in regions and seasons with higher DMS oxidation. On the other hand, regions dominated by SS or dust inputs should display low ETA values.

From the primary parameters retrieved by MODIS, it is possible to derive secondary products such as column-integrated CCN numbers (in units of partic $cm^{-2}$) (*Tanré et al.*, 1999; *Gassó and Hegg*, 2003). In the present work, CCN concentrations are obtained with the derivation method described in *Gassó and Hegg* (2003). The method, which is based on atmospheric optical properties, derives the maximum number of particles in the accumulation mode and provides an upper end estimate of the concentration of particles that may act as CCN at $\approx$0.2% supersaturation. We call this satellite-based CCN estimates as $CCN_s$. The method allows for the adjustment of coefficients according to the type of aerosols that are present. Because we are interested in marine aerosols, the $CCN_s$ algorithm coefficients (the aerosol refraction index and the aerosol density) were adjusted to be representative of the main aerosol types present in marine regions: SS, nss-$SO_4$ and MSA.

Global OH concentrations in the marine boundary layer (MBL) are outputs of the GEOS-CHEM model run by the Atmospheric Chemistry Modeling Group at Harvard University (*Fiore et al.*, 2003). GEOS-CHEM simulates atmospheric composition using assimilated meteorological observations from the Goddard Earth Observing System (GEOS) of the NASA Global Modeling and Assimilation Office. Monthly OH distributions are available only for 2001.

Atmospheric MSA monthly climatologies for several locations all around the globe were obtained from the measurements of the University of Miami network of aerosol sampling stations (12 locations) (*Chin et al.*, 2000), the Australian Baseline Air Pollution Station (*Ayers and Gillett*, 2000) (Cape Grim), as well as the measurements of *Sciare et al.* (1998) (Amsterdam Island) and *Kubilay et al.* (2002) (Crete). All data correspond to aerosol-associated MSA except for Amsterdam Island, where only MSA concentrations in rainwater (for 1996) are available.

### 4.2.3 DMS oxidation

OH is the main oxidant of $DMS_a$ to produce MSA and nss-$SO_4$ through a series of reactions that occur during daytime (*Kloster et al.*, 2006). Therefore, the amount of potential biogenic CCN depends not only on the $DMS_{flux}$ but also on OH concentrations. Higher amount of OH respect to the amount of $DMS_{flux}$ would imply a higher DMS oxidation efficiency (*Gondwe et al.*, 2004). The resulting potential biogenic CCN can be characterized as follows:

$$CCN_{bio} = b * \gamma * DMS_{flux} \tag{4.2}$$

where $b$ is a unit conversion constant and $\gamma$ is a dimensionless parameter varying between 0 a 1 that gives the efficiency of DMS oxidation as function of the ratio between OH and $DMS_{flux}$ following an equation of the form:

$$\gamma = \frac{x}{k_s + x} \tag{4.3}$$

where $x = \frac{OH}{DMS_{flux}}$. In the absence of OH (or very low OH) concentrations respect to the $DMS_{flux}$, most (or at least part) of the $DMS_{flux}$ can not be converted to $CCN_{bio}$ (in this situations $\gamma$ will be low). On the other hand, if OH concentrations are in excess all the $DMS_{flux}$ can be oxidized to $CCN_{bio}$ (in this situations $\gamma$ will be close to one). The form of the equation accounts for an asymptotic behaviour; as the availability of OH for DMS oxidation (the variable $x$) increases, a higher fraction of the $DMS_{flux}$ can be converted to $CCN_{bio}$ approaching asymptotically the upper limit of gamma (for which all $DMS_{flux}$ is converted to $CCN_{bio}$). Therefore, $\gamma$ $DMS_{flux}$ gives the amount of biogenic sulfur potentially available for CCN production. The constant ($k_s$) corresponds to the value of $x$ that gives a $\gamma$ of 0.5 (a DMS oxidation efficiency of 50%). Assuming an annual-averaged DMS oxidation efficiency for the Southern Ocean (SO, defined as the area comprised between 40°S and 60°S) of 50% (*Shon et al.*, 2001), we obtained a value of $k_s$ from the annual averages of OH, $DMS_{flux}$ over the SO. In order to evaluate the potentiality of DMS oxidation as a source of biogenic aerosols, we will compare the seasonal evolution of the estimated atmospheric DMS oxidation ($\gamma DMS_{flux}$) against the seasonality of MSA (an exclusive product of DMS oxidation) in aerosols from 15 sampling stations of the world cited above. The monthly $\gamma DMS_{flux}$ series that are compared with station-based MSA series come from averaging the 49 points taken by placing a 7° x 7° window up-wind of each station.

### 4.2.4 Globally Mapped Seasonal Correlations

Three years of surface wind speed, $CCN_s$ and ETA monthly means (from January 2002 to December 2004) were combined to create a 1-year climatology for each variable. These are used to evaluate the seasonal couplings between variables of interest: SRD *vs.* $DMS_w$, $DMS_{flux}$ *vs.* OH, $\gamma DMS_{flux}$ *vs.* $CCN_s$ and ETA. The global maps of seasonal correlations are based on the following procedure: using a running window of 7° x 7° (*Sciare et al.*, 1999), we obtained for each position (latitude, longitude) of the global ocean (i.e. for every 1° x 1° grid box) time series of 12 points (months) for the pair of variables we want to analyse. Each of the 12 points of the time series is the average of the 49 values taken by the running window in a given month. Then, for every 1° x 1° grid box of the global ocean we calculate the seasonal (Spearman) correlation coefficient between the two variables (12 degrees of freedom), generating a global map of seasonal correlations (significant correlations at 95% confidence level for $|r| > 0.5$ and at 80% confidence level for $|r| > 0.4$). Prior to the global analysis all fields are smoothed with a 3° latitude x 3° longitude x 3 months running mean (*Wilson and Coles*, 2005).

## 4.3 Results and Discussion

### 4.3.1 Global maps of seasonal correlations

Figure 4.1a shows that there is a strong seasonal coupling between the solar radiation dose in the UML and oceanic $DMS_w$ concentrations, in agreement with the first postulate of the CLAW hypothesis that we are evaluating. Further, this coupling seems to be present almost everywhere in the global ocean. The areas where there is negative or no correlation are located mostly in the equatorial region. Due to the very low seasonality of these latitudes, any error or uncertainty in the monthly $DMS_w$ fields can generate a noise with higher amplitude than the underlying seasonality, thus largely affecting the correlation coefficient. These results are in agreement with recent works that have identified light as being the driving force of DMS in oligotrophic waters of the Sargasso Sea (*Toole and Siegel*, 2004) and NW Mediterranean (*Vallina and Simó*, 2007a). Long-term measurements conducted in several locations of the world have also shown that DMS generally increases in summer (*Nguyen et al.*, 1990; *Berresheim et al.*, 1991; *Ayers et al.*, 1997a,b; *Ayers and Gillett*, 2000; *Curran and Jones*, 2000; *Sciare et al.*, 2000; *Jourdain and Legrand*, 2001; *Kouvarakis and Mihalopoulos*, 2002; *Aranami and Tsunogai*, 2004; *Toole and Siegel*, 2004; *Vallina and Simó*, 2007a).

Owing to the role of the OH radical as the main DMS oxidizer to nss-$SO_4$ and MSA, any coupling or mismatch between the seasonalities of OH and the $DMS_{flux}$ will amplify or buffer the seasonal contribution of biogenic sulfur to CCN production. The seasonal coupling between $DMS_{flux}$

and OH radical is very strong over most parts of the globe (see Figure 4.1b). Therefore, summer months are characterized by both higher DMS emission and a better efficiency in the oxidation of DMS into CCN, that is, higher potential to counteract higher solar irradiances.

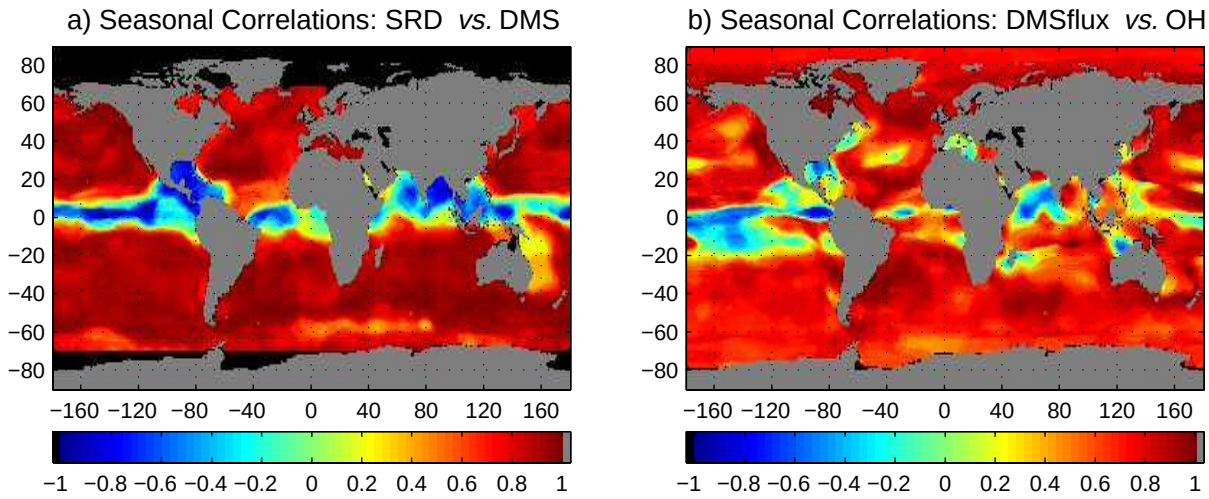


Fig. 4.1: Global map of seasonal correlations between: a) the solar radiation dose in the upper mixed layer and climatological monthly aqueous DMS concentrations (from *Kettle and Andreae* (2000)), b) the estimated DMS flux to the atmosphere (using *Nightingale et al.* (2000)) and monthly hydroxyl-radical atmospheric concentrations (from *Fiore et al.* (2003)).

Figure 4.2 displays the seasonal couplings between $\gamma DMS_{flux}$ and MSA for 15 locations of the globe. In general we observe an excellent seasonal agreement between the two variables. Therefore our DMS oxidation proxy is able to capture MSA seasonality, as it should be if DMS oxidation is fuelling MSA production. A quantitative validation with MSA is not appropriate since the biogenic nss-$SO_4$ to MSA ratio from the gas-phase DMS oxidation is very variable between regions (up to a factor of 6) because it is temperature dependent, being much lower at high latitudes (*Savoie et al.*, 2002). At Stations 5 and 13 the correlation coefficients between DMS oxidation and MSA are not significant. Station 5 is located in Japan (NE Pacific), a region subject to high levels of polluted aerosols in spring (*Husar et al.*, 1997; *Kaneyasu and Murayama*, 2000; *Tanré et al.*, 2001; *Bey et al.*, 2001; *Higurashi and Nakajima*, 2002; *Takemura et al.*, 2002; *Prospero et al.*, 2003). Therefore the observed spring peak of MSA could be related to an heterogeneous nucleation of MSA on polluted aerosols. While $DMS_a$ concentration in polluted air is generally much lower than in oceanic air masses, MSA concentrations are usually found to be also high in polluted air masses (*Berresheim et al.*, 1991; *Wylie and de Mora*, 1996), which may reflect its adsorption on pre-existing continental aerosols. On the other hand, Station 13 (American Samoa, 14.25°S - 170.5°W) is a very clean oceanic region almost free from continental influences (*Savoie et al.*, 1989, 1994). The low seasonality of this tropical location is probably the cause of the non-significant correlation. Similar results are obtained using MSA data from Fanning Island (not shown), located near the equator (3.85°N - 159.36°W). At these two locations MSA data does not show a clear seasonal cycle (*Savoie and Prospero*, 1989; *Savoie et al.*, 1994).

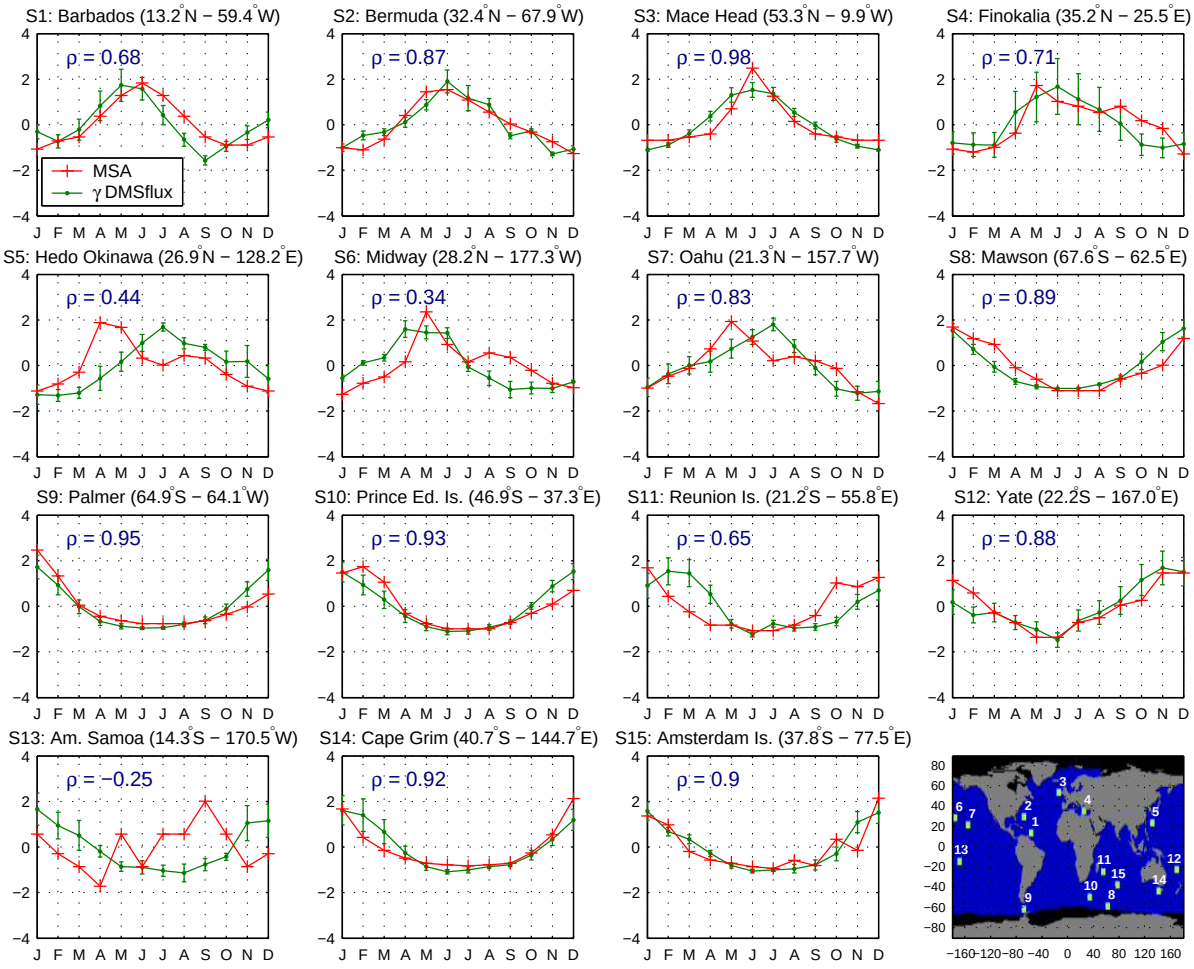


Fig. 4.2: Seasonal evolution and the associated Spearman correlation coefficient of the atmospheric DMS oxidation against monthly climatological methanesulfonate concentrations in aerosols at 15 locations of the globe. (Variables are presented in standardized form, i.e. subtracting the mean and dividing by the standard deviation).

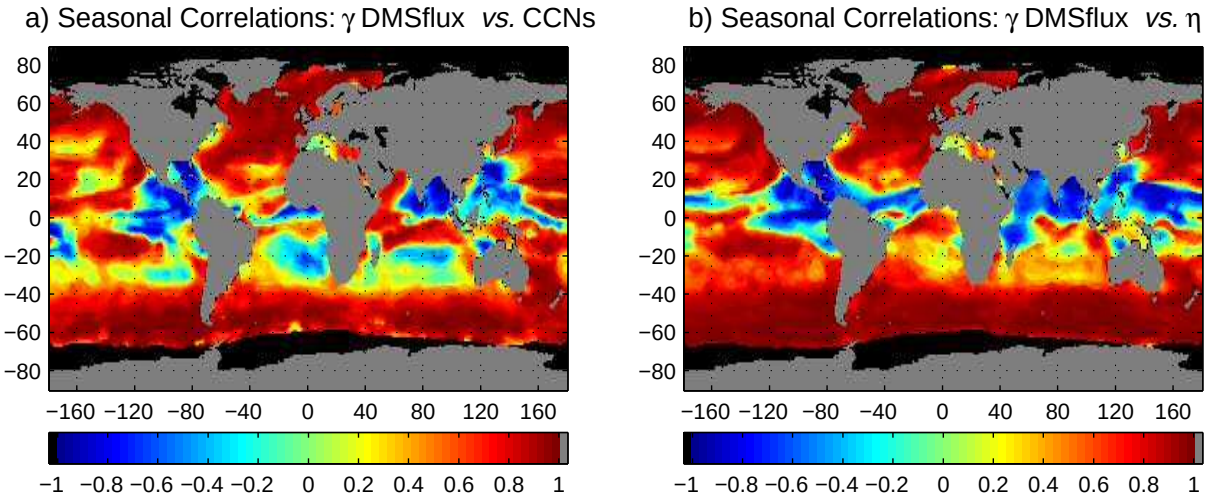


Fig. 4.3: Global map of seasonal correlations between atmospheric DMS oxidation and: a) monthly climatological (years 2002 to 2004) satellite-derived CCN concentrations (using the method of *Gassó and Hegg* (2003)), b) monthly climatological (years 2002 to 2004) satellite-derived contribution of small mode particles to the Aerosol Optical Depth (ETA parameter = $AOD_{small}$ / $AOD_{total}$) as provided by MODIS.

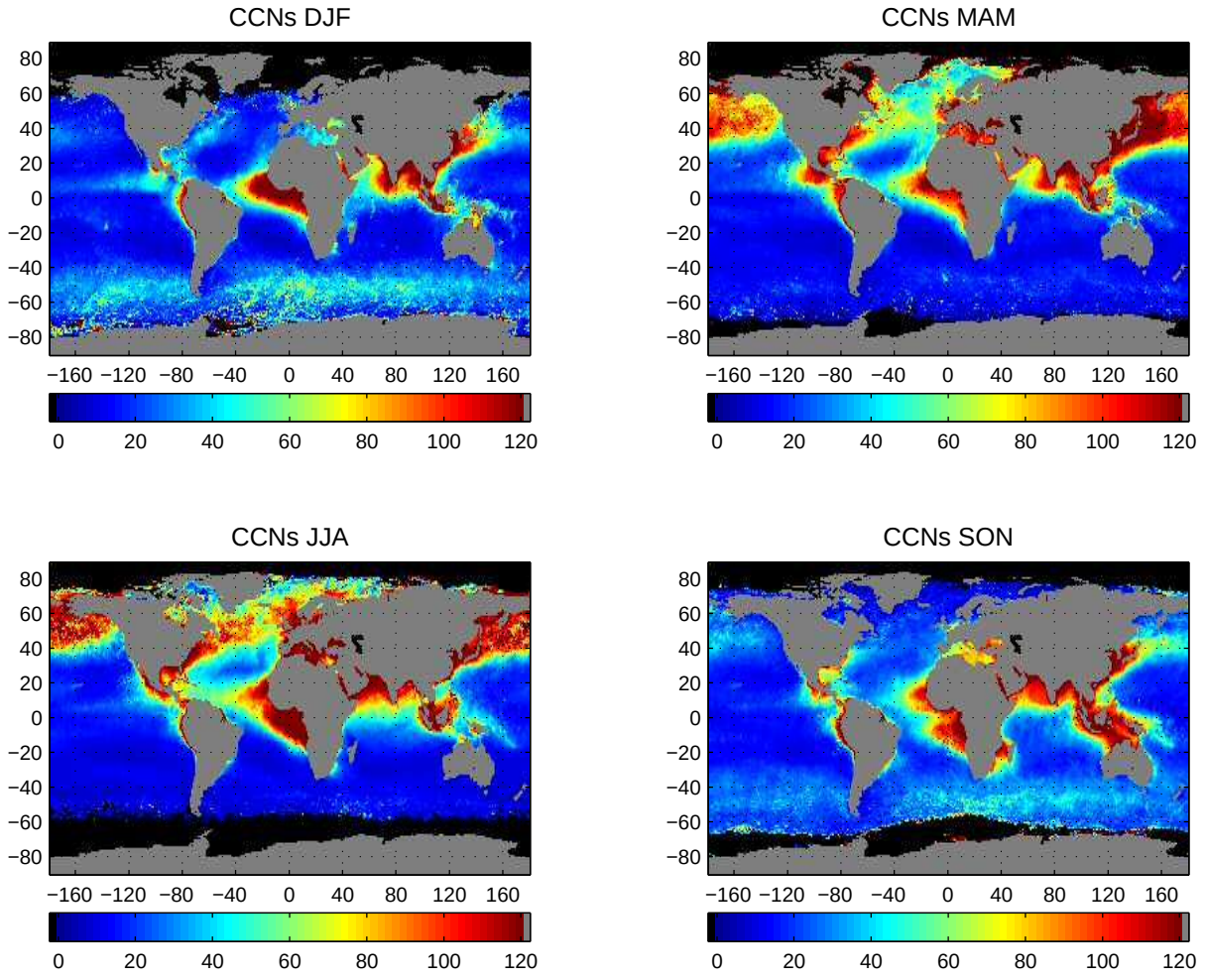


Fig. 4.4: Global maps of monthly climatological (years 2002 to 2004) satellite-derived CCN concentrations (partic $cm^{-2}$; using the method of *Gassó and Hegg* (2003)) for the four seasons. DJF: December to February; MAM: March to May; JJA: June to August; SON: September to November.

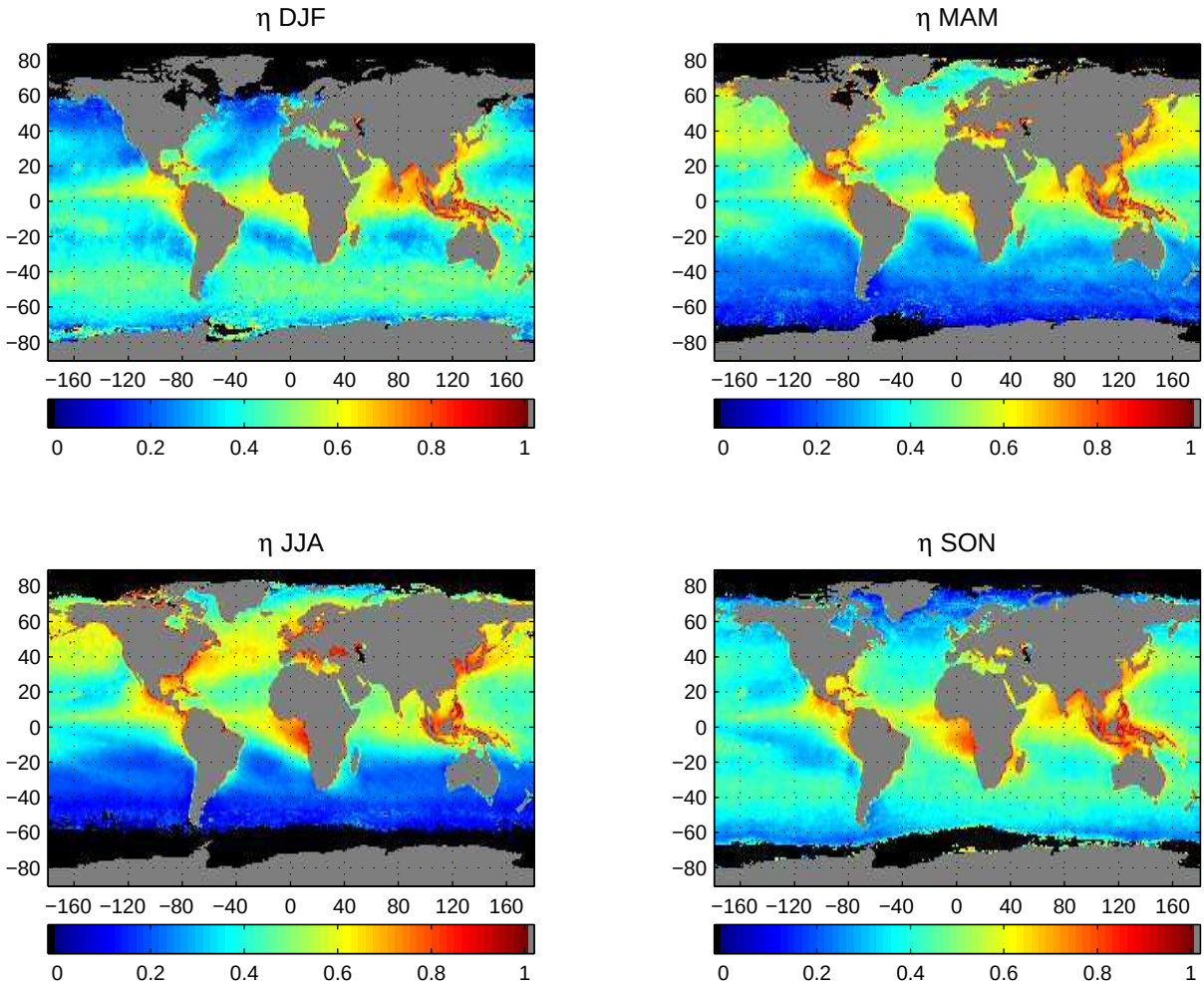


Fig. 4.5: Global maps of monthly climatological (years 2002 to 2004) satellite-derived contribution of small mode particles to the Aerosol Optical Depth (ETA parameter = $AOD_{small}$ / $AOD_{total}$) (as provided by MODIS) for the four seasons. DJF: December to February; MAM: March to May; JJA: June to August; SON: September to November.

Figures 4.3a and 4.3b show the seasonal couplings between DMS oxidation against $CCN_s$ and ETA respectively, where it can be observed that large regions of the global ocean display strong positive correlations. This is especially true, as expected, at high latitudes, where the seasonal amplitude of $DMS_w$ is higher. Of special interest is the SO (40°S - 60°S) since it is a remote region weakly impacted by continental aerosols (*Buseck and Pósfai*, 1999; *Quinn et al.*, 1998; *Andreae et al.*, 1999; *Ayers and Gillett*, 2000; *Gabric et al.*, 2001; *Prospero et al.*, 2002) where $DMS_a$ concentrations are very high in austral spring and summer (*Curran and Jones*, 2000). For example, at Cape Grim $DMS_a$ displays a strong seasonality (*Ayers et al.*, 1995). Further, summertime $SO_2$ concentrations in this pristine region are predominantly of marine origin (*Bruyn et al.*, 1998). During austral summer, a band of relatively high $CCN_s$ concentrations is clearly observed over the SO (see DJF panel of Figure 4.4). This $CCN_s$ band does not display spatial gradients coming from continents, which is a strong indication of a marine origin. SS does not seem either to be the source of this austral summer high aerosol band (*Husar et al.*, 1997; *Vallina et al.*, 2006). Its DMS-related origin is supported by the seasonality of the fine mode aerosols (Figure 4.5; see also *Vallina et al.* (2006)), field observations in the region (*Davison et al.*, 1996; *Andreae et al.*, 1999) as well as modeling works (*Yoon and Brimblecombe*, 2002; *Gondwe et al.*, 2003; *Kloster et al.*, 2006).

Strong positive correlations between DMS oxidation and $CCN_s$ (as well as ETA) are also found over oceans where nss-$SO_4$ inputs from anthropogenic sources are known to be higher than nss-$SO_4$ inputs from DMS (i.e. North Atlantic, North Pacific) (*Berresheim et al.*, 1991; *Dingenen et al.*, 1995; *Prospero*, 1996a; *Nagao et al.*, 1999; *Chin et al.*, 2000; *Aranami et al.*, 2002; *Andreae et al.*, 2003). This can be also observed through much higher $CCN_s$ numbers present in these regions during the boreal summer (JJA) compared to $CCN_s$ numbers over the SO during the austral summer (Figure 4.4). It is obvious that there is a general trend towards higher aerosol numbers in each hemispheric summer (*Husar et al.*, 1997; *Stegmann and Tindale*, 1999) (Figure 4.4). While to some extent this fact can be related to atmospheric circulation changes (e.g. the increase of aerosol loading during the boreal summer in the Caribbean Sea is due to a northern shift, following the ITCZ movement, of the dust pathway coming from Africa (*Prospero*, 1996a; *Perry et al.*, 1997; *Ginoux et al.*, 2001)) or precipitation seasonality (e.g. biomass burning usually increases during the dry season peaking in each hemispheric spring (*Lobert et al.*, 1999; *Duncan et al.*, 2003)), in some regions it is certainly related to the oxidation of $SO_2$ to form nss-$SO_4$ aerosols (*Rasch et al.*, 2000; *Chin et al.*, 2000; *Barrie et al.*, 2001). For example, in the North Atlantic, which is heavily impacted by pollution from Europe and North America (*Dingenen et al.*, 1995; *Husar et al.*, 1997; *Andreae et al.*, 2003), the levels of nss-$SO_4$ clearly increase in boreal summer, despite anthropogenic $SO_2$ emissions in these regions being fairly constant throughout the year (*Falkowski et al.*, 1992; *Smith et al.*, 2001; *Andreae et al.*, 2003) (or even slightly higher in boreal winter in Europe (*Chin et al.*, 2000; *Rasch et al.*, 2000; *Smith et al.*, 2001; *Rotstayn and Lohmann*, 2002)) and $SO_2$ concentrations display a summer minimum due to the higher oxidative efficiency to form nss-$SO_4$ (*Berresheim et al.*, 1991; *Chin et al.*, 2000; *Rasch et al.*, 2000; *Rotstayn and Lohmann*, 2002). The summertime increase of nss-$SO_4$ and $CCN_s$ in

the North Atlantic is therefore not related to the seasonality of their precursor $SO_2$ but to its increased oxidation efficiency by OH. On the other hand, in relatively pollution-free regions like Amsterdam Island (37.8°S - 77.5°E) the $SO_2$ increase in summer is probably due to a DMS origin (*Rotstayn and Lohmann*, 2002; *Kloster et al.*, 2006). We must conclude, therefore, that atmospheric oxidation efficiencies are an important actor in aerosol production. This supports that $SO_2$ (whatever its origin, anthropogenic or DMS) is indeed able to fuel new particle formation and it is responsible for a non-negligible fraction of the observed $CCN_s$.

The areas with low or negative correlations between DMS oxidation and $CCN_s$ or ETA are mostly in the equatorial to tropical regions (Figure 4.3). These are latitudes where the DMS concentration and flux show low seasonal variability, which precludes from finding significant correlations using a seasonal correlation analysis. Moreover, these are regions with high loads of continental aerosols (mostly dust and biomass burning particles) that can also contribute to satellite-retrieved $CCN_s$ numbers (Figure 4.4). For example, the very high values of $CCN_s$ observed off the tropical West Africa (see Figure 4.4) are strongly contributed by aerosols from biomass burning (*Husar et al.*, 1997; *Tanré et al.*, 2001; *Kaufman et al.*, 2002; *Duncan et al.*, 2003). This is also the case over the Pacific off Central America and the Indonesian region (*Husar et al.*, 1997; *Deuzé et al.*, 1999; *Tanré et al.*, 2001; *Duncan et al.*, 2003). This can also be observed in Figure 4.5 since biomass burning aerosols are mostly accumulation mode particles (therefore the ETA parameter is very high). Interestingly, the Arabian Sea shows a positive correlation between DMS oxidation and $CCN_s$ while it is negative between DMS oxidation and ETA. This is an indication that the observed increase of $CCN_s$ in boreal summer in this region (see the JJA panel of Figure 4.4) is not related to an increase of small aerosols but to an increase of coarser aerosols, and therefore that they do not come from DMS oxidation. This is in agreement with previous works that have found an increase of both dust from the Arabian Peninsula (at high altitudes) along with an increase of SS concentrations (at low altitudes) due to the strong winds of the SW monsoon (*Husar et al.*, 1997; *Tindale and Pease*, 1999; *Müller et al.*, 2001; *Li and Ramanathan*, 2002). A similar situation is observed in the region between off Northwestern Africa (around 10°N) and northern South America, a well known path for African dust (*Swap et al.*, 1992). Although dust and SS aerosols mainly belong to coarse particles, a fraction of them can be present in the accumulation mode (*Perry et al.*, 1997; *Murphy et al.*, 1998; *Prospero*, 1999; *Satheesh et al.*, 1999), then affecting $CCN_s$ retrieval. Therefore, in order to infer which regions could be under biogenic aerosol production it is necessary to combine the analysis of global correlation maps of DMS oxidation against $CCN_s$ as well as against the ETA parameter. An increase of biogenic $CCN_s$ should be followed by an increase of ETA.

### 4.3.2 Biogenic contribution to CCN numbers

The correlation analyses have shown that in large regions of the ocean the DMS oxidation and $CCN_s$ are seasonally coupled, but this type of analysis does not provide any quantitative infor-

mation about the contribution of biogenic $CCN_s$ to total $CCN_s$ numbers over the oceans. To obtain such information, we first focus on the SO since this is the region where CCN seasonality is believed to be driven mainly by DMS oxidation (*Ayers and Gras*, 1991; *Ayers et al.*, 1997a; *Husar et al.*, 1997; *Ayers and Gillett*, 2000; *Gondwe et al.*, 2003, 2004; *Kloster et al.*, 2006; *Vallina et al.*, 2006). We calculate the spatial mean value of $\gamma DMS_{flux}$ and $CCN_s$ for each month over the whole SO area between 40°S and 60°S (therefore obtaining 12 data points). A regression analysis $\gamma DMS_{flux}$ *vs.* $CCN_s$ is then applied in order to estimate the value of the slope $b$ of eq(4.2) for this region. Results are shown in Figure 4.6. The determination coefficient is high ($r^2 = 0.83$) and close to the value of $r^2 = 0.84$ obtained by *Ayers et al.* (1997a) using climatological $DMS_a$ and CCN from *in-situ* measurements at Cape Grim (40.7°S - 144.7°E). Further, using the normalized data (values divided by its annual mean), we obtain similar (normalized) regression coefficients to those of *Ayers et al.* (1997a). The (normalized) intercept is 0.41 (it was 0.48 at Cape Grim) and the (normalized) slope is 0.59 (it was 0.52 at Cape Grim) (see the equation in brackets in Figure 4.6).

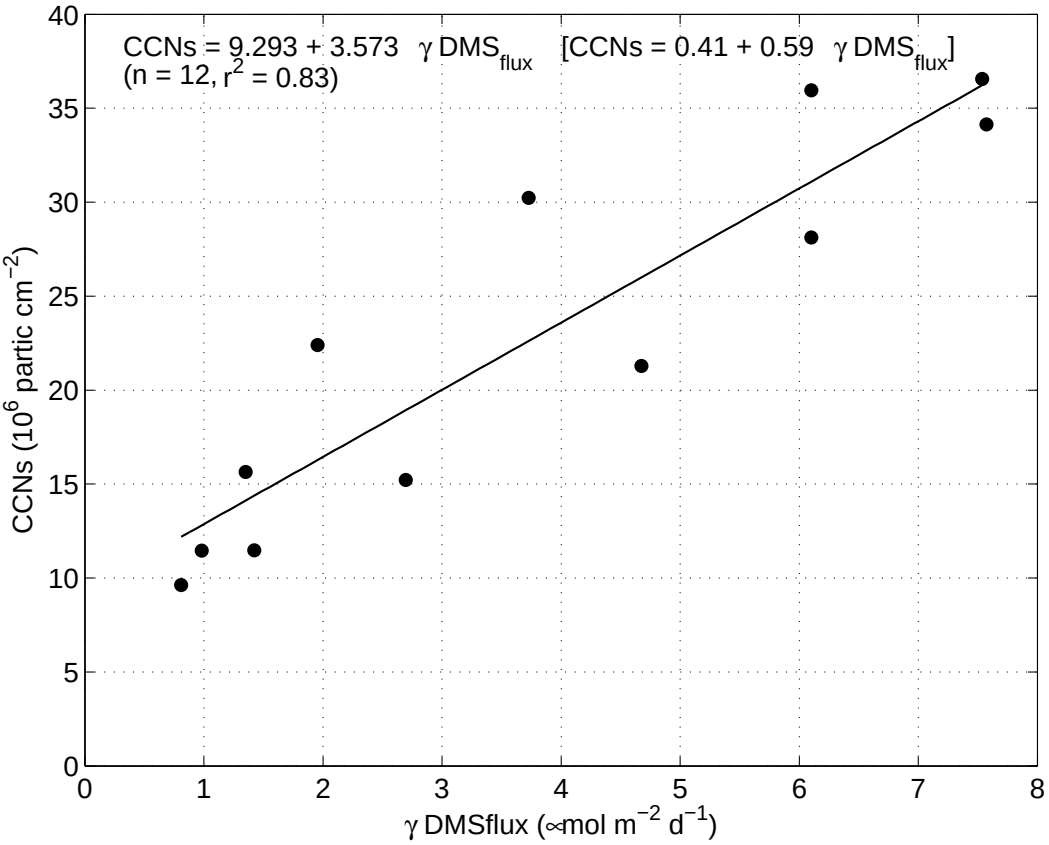


Fig. 4.6: Regression analyses of atmospheric DMS oxidation against monthly climatological (years 2002 to 2004) satellite-derived CCN concentrations (using the method of *Gassó and Hegg* (2003)) for the Southern Ocean (defined as the area comprised between 40°S and 60°S).

If over the SO CCN numbers are linked to DMS oxidation, this link between biogenic CCN and DMS must occur also over other regions, yet it could be hidden by continental CCN sources over less pristine areas. Assuming that the slope value $b$ =3.57 obtained for the SO (Figure 4.6) is valid for other regions, we apply eq(4.2) in order to estimate $CCN_{bio}$ from DMS oxidation fluxes in 15 regions of the global ocean (the value of the intercept, 9.29, is assumed to be a constant

background of SS fine mode aerosols (*Andreae et al.*, 1999) and then it is substracted to take into account only the biogenic contribution (*Vallina et al.*, 2006)). Nevertheless CCN formation is a very complex process that depends on many factors (such as aerosol composition, aerosol size and supersaturation). All these factors are certainly different for the regions in which we apply the regression derived for SO conditions. However, up to now all these processes are not well enough understood to include them into our analysis. Results are shown in Figure 4.7, where $\rho$ is the (Spearman) correlation coefficient between $CCN_{bio}$ and $CCN_s$, and $\beta = \frac{\sum CCN_{bio}}{\sum CCN_s} * 100$ is the annual contribution of biogenic derived $CCN_s$ to the total $CCN_s$.

$CCN_{bio}$ contributes annually about a 60% to the total $CCN_s$ in the SO (region 14; from about 30% in austral winter to 80% in austral summer (see also (*Vallina et al.*, 2006)), being the remaining $CCN_s$ probably small SS (*Andreae et al.*, 1999; *Vallina et al.*, 2006). However, the estimated $CCN_{bio}$ fraction for the Antarctic (region 15) is only 24%. The very low model OH concentrations present in this high latitude region give rise to very low values of $\gamma$ ($< 0.3$ for all months except for October and November with $\approx$0.55), therefore reducing the estimated DMS available for CCN production. Nevertheless, *in-situ* measurements of MSA and nss-$SO_4$ suggest that DMS plays a primary role in the atmospheric sulfur cycle over the Antarctic continent (*Savoie et al.*, 1992; *Minikin et al.*, 1998). Thus, further research is needed in this region. It has been proposed that a large fraction of $DMS_a$ is transported out of the marine boundary layer (MBL) where, in the presence of high OH and low aerosol scavenging, oxidized sulfur species accumulate and are entrained episodically back into the MBL (*Davis et al.*, 1998).

Other regions where DMS oxidation could be a significant source of CCN are the subtropical Atlantic (both hemispheres; regions 2 and 4), and the subtropical South Pacific and Indian oceans (regions 8 and 12 respectively). In the subtropical North Atlantic (region 2), although there is a good correlation between $CCN_{bio}$ and $CCN_s$ ($\rho$ = 0.72), the absolute contribution is rather moderate ($\beta$ = 38%). Only over the western part DMS may contribute up to 75% of the sulfur budget under easterly winds, although under westerly winds anthropogenic sulfur from North America dominates (*Berresheim et al.*, 1991). Also, in boreal spring and summer this region is also under the influence of supramicron particles of African dust plumes coated with $SO_4$ from Europe (*Li-Jones and Prospero*, 1998). In April at Barbados (13.15°N - 59.30°W), when dust and pollution levels are low, the dominant source of nss-$SO_4$ is ascribed to DMS and the submicron fraction dominates (up to 80%) (*Li-Jones and Prospero*, 1998). Annually, the estimated DMS contribution to the nss-$SO_4$ at Barbados and Bermuda (32.27°N - 64.87°W) is $\approx$50% and $\approx$30% respectively (*Savoie et al.*, 2002). The subtropical South Atlantic (region 4, $\beta$ = 56%) displays a seasonal $CCN_s$ maximum in September not related to $CCN_{bio}$ but to biomass burning over tropical Africa (*Husar et al.*, 1997; *Deuzé et al.*, 1999; *Goloub and Arino*, 2000; *Tanré et al.*, 2001; *Duncan et al.*, 2003; *Ross et al.*, 2003) (see also SON panel of Figure 4.4 and Figure 4.5). Nevertheless, in February-March 1991 during a ship transect along 19°S, the majority of the measured CCN contained $SO_4$ and their numbers were correlated to the $DMS_{flux}$, then supporting the hypothesis that DMS oxidation may be a source of CCN in this

region during austral summer (*Andreae et al.*, 1994). African biomass burning aerosols are also transported over Madagascar and the subtropical Southern Indian Ocean (region 12, $\beta$ = 67%) in October, the burning season in Southeastern Africa (*Rhoads et al.*, 1997; *Deuzé et al.*, 1999; *Goloub and Arino*, 2000; *Duncan et al.*, 2003) (see also SON panel of Figure 4.4 and Figure 4.5). This explains why the obtained seasonal correlations are not significant for regions 4 and 12 ($\rho$ = -0.32 and 0.31 respectively) while the biogenic contribution is significant. Over the subtropical South Pacific (region 8) $CCN_{bio}$ are significantly correlated to $CCN_s$ ($\rho$ = 0.68) and the estimated biogenic contribution is very high ($\beta$ = 99%). This is in agreement with field studies which have found that marine-derived DMS may provide essentially all of nss-$SO_4$ over the tropical South Pacific (*Savoie et al.*, 1989).

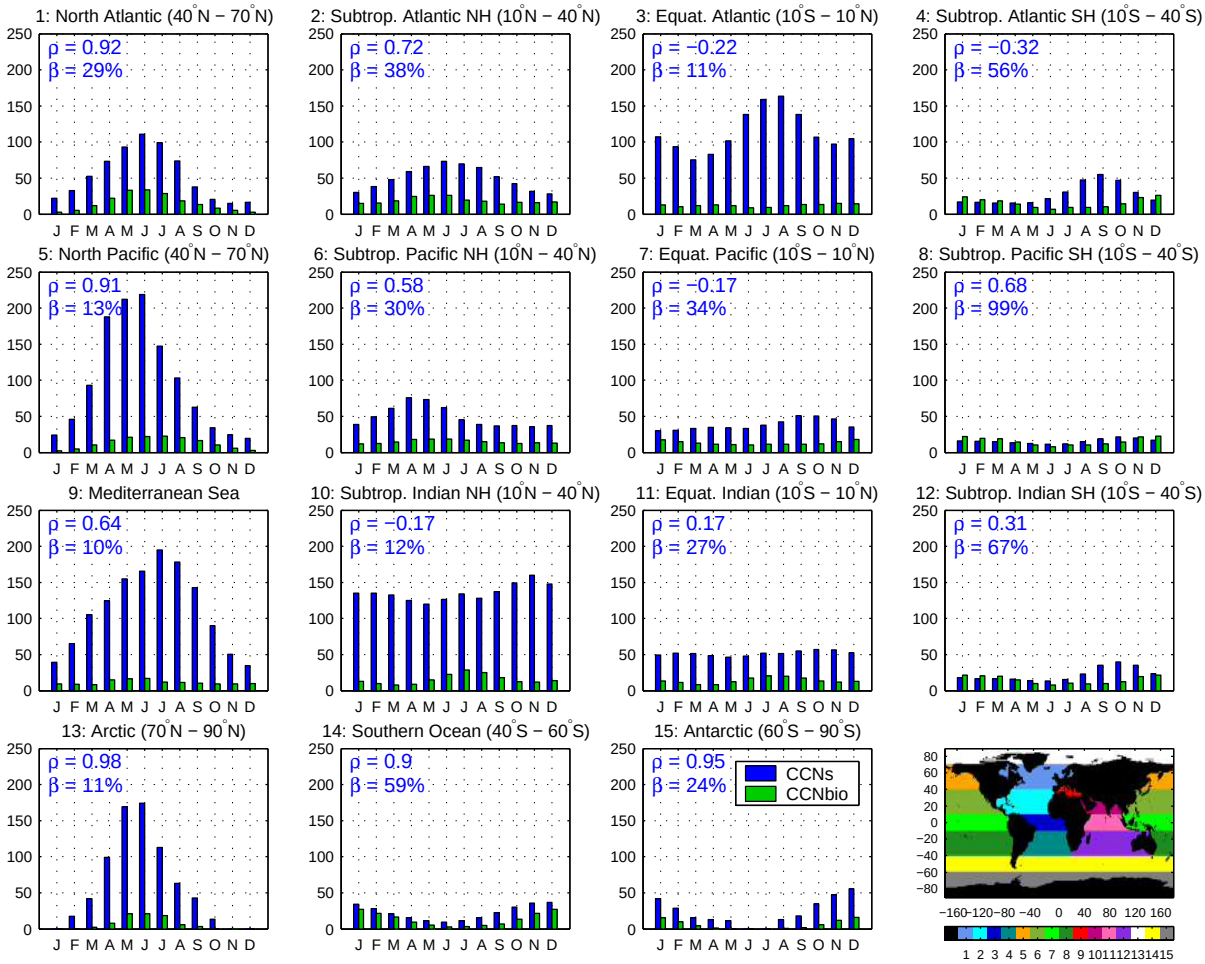


Fig. 4.7: Seasonal evolution of monthly climatological (years 2002 to 2004) satellite-derived CCN concentrations (partic $cm^{-2}$; using the method of *Gassó and Hegg* (2003)) and the estimated biogenic CCN from DMS oxidation for 15 regions of the global ocean. ($\rho$ is the Spearman correlation coefficient between $CCN_{bio}$ and $CCN_s$, and $\beta = \frac{\sum CCN_{bio}}{\sum CCN_s} * 100$ is the annual contribution of $CCN_{bio}$ to the total $CCN_s$).

In many of the regions, however, it is clear that the estimated $CCN_{bio}$ has a minor annual contribution to the total $CCN_s$. This is the case of the North Atlantic (region 1, $\beta$ = 29%), a region known for being under the influence of heavily polluted air masses from Europe and North America in spring and summer (*Dingenen et al.*, 1995; *Husar et al.*, 1997; *Fenneteaux et al.*, 1999; *Andreae et al.*, 2003). For example, at Mace Head (53.32°N - 9.85°W) the annual biogenic contribution

to nss-$SO_4$ is estimated to be less than 15% (*Savoie et al.*, 2002). In boreal spring, DMS contribution to nss-$SO_4$ is also estimated in ≈10% (*Andreae et al.*, 2003). Regarding $CCN_s$ variability ($\rho$ = 0.92), although $CCN_{bio}$ in the North Atlantic are higher in summer, they can hardly account for the full $CCN_s$ seasonality: if we subtract $CCN_{bio}$ from total $CCN_s$, the remaining (putatively anthropogenic) $CCN_s$ still have a summer-to-winter ratio of 2.25. Therefore, higher summertime oxidation of anthropogenic $SO_2$ is an important process affecting CCN seasonality over the North Atlantic. Interestingly, however, the work of *Falkowski et al.* (1992), based on satellite data analysis, identified that over the central North Atlantic the variability in cloud albedo was correlated to phytoplankton blooms rather than to anthropogenic CCN sources.

The Equatorial Atlantic (region 3, $\beta = 11\%$) is highly impacted by biomass burning and dust from Africa, and the Equatorial Indian Ocean (region 11, $\beta = 27\%$) by biomass burning from the Indonesian region. In the Equatorial Pacific (region 7), which is also impacted by biomass burning from Central America in spring (*Husar et al.*, 1997; *Deuzé et al.*, 1999; *Goloub and Arino*, 2000; *Tanré et al.*, 2001; *Kaufman et al.*, 2002; *Duncan et al.*, 2003), the estimated contribution of biogenic sulfur to $CCN_s$ numbers is a bit higher ($\beta = 34\%$). Nevertheless, in terms of sulfate aerosols, almost all nss-$SO_4$ over the Equatorial Pacific (e.g. American Samoa, Fanning Island) has been suggested to originate from the oxidation of oceanic DMS (*Savoie and Prospero*, 1989; *Savoie et al.*, 1994). Near the Christmas Islands (1.52°N - 157.2°W), DMS has also been identified as the dominant source of MBL's $SO_2$, and clear relationships between DMS, $SO_2$, OH and $H_2SO_4$ (sulfuric acid) have been observed at a daylength scale (*Davis et al.*, 1999). Also, in this region it has been demonstrated that aerosol nucleation and growth in the MBL is linked to the natural marine sulfur cycle (*Clarke et al.*, 1998).

Over the North Pacific (region 5), strong mixed plumes of polluted (mainly nss-$SO_4$ and black carbon) and dust aerosols are emitted from Asia each spring and summer (*Husar et al.*, 1997; *Nagao et al.*, 1999; *Deuzé et al.*, 1999; *Kaneyasu and Murayama*, 2000; *Higurashi and Nakajima*, 2002; *Prospero et al.*, 2002; *Aranami et al.*, 2002). These are the dominant sources of $CCN_s$ over the region, in agreement with the low beta value obtained (13%). However, in terms of sulfur, the Asian anthropogenic source is estimated to provide only about 15-25% of the nss-$SO_4$ in the North Pacific (*Savoie et al.*, 1989). For example, at Sheyma (50°N-170°E), although during spring nss-$SO_4$ is mainly from pollution, summertime nss-$SO_4$ is dominated by biogenic sources (*Savoie and Prospero*, 1989). The subtropical North Pacific (region 6, $\beta = 30\%$) is less impacted by continental aerosols although they still dominate in the northern part of the region close to the Asian continent (*Nagao et al.*, 1999) (see Figure 4.3). In this regard, over the subtropical Northwestern Pacific a positive correlation was found between $DMS_a$ and CCN in clean marine air and DMS was identified as a key factor in the production of nss-$SO_4$ and CCN (*Nagao et al.*, 1999). Also, over more open ocean locations DMS can significantly contribute to the total nss-$SO_4$ burden. For example, at Midway Island (28.22°N - 177.3°W) the annual contribution of DMS to the nss-$SO_4$ is estimated at ≈60% (*Prospero et al.*, 2003).

The Arctic (region 13, $\beta = 11\%$) is under the influence of $SO_2$ pollution from Europe and Asia (*Barrie et al.*, 1989). The subtropical North Indian Ocean (region 10, $\beta = 12\%$) is characterized by very high levels of pollution aerosols during winter (NE monsoon) and by dust and SS during summer (SW monsoon) (*Johansen et al.*, 1999; *Tindale and Pease*, 1999; *Rajeev et al.*, 2000; *Ramanathan et al.*, 2001; *Li and Ramanathan*, 2002). Nevertheless, the fraction of nss-$SO_4$ derived from DMS is significant (from ≈20% during the NE monsoon to ≈75% during the SW monsoon (*Johansen et al.*, 1999)). During the NE monsoon, the contribution to the AOD of a 20% of natural nss-$SO_4$ is estimated to be very low (about a 5%) (*Satheesh et al.*, 2002). Also, CCN properties over the Indian Ocean (North and South) differ depending on their origin: in polluted air masses, CCN particles have both a higher diameter and a higher percentage of refractory (non-volatile) material than CCN in clean marine air (see Plate 7 of *Ramanathan et al.* (2001)). Finally, the lowest $CCN_{bio}$ contribution occurs over the Mediterranean Sea (region 9, $\beta = 10\%$), a region mostly impacted by pollution from Europe and dust from Africa (*Prospero*, 1996b; *Husar et al.*, 1997; *Mihalopoulos et al.*, 1997; *Güllü et al.*, 1998; *Prospero et al.*, 2002). In terms of sulfur, the maximum contribution of DMS to the nss-$SO_4$ is also low (≈20-30% in summer (*Mihalopoulos et al.*, 1997; *Kouvarakis and Mihalopoulos*, 2002; *Kubilay et al.*, 2002; *Kouvarakis et al.*, 2002)).

Globally, the annual contribution of $CCN_{bio}$ to the total $CCN_s$ is estimated to be ≈30%. This value should be viewed as an upper end estimate since $CCN_{bio}$ losses by rain washout were not taken into account. These results are in agreement with recent global models of the sulfur cycle that estimate the contribution of DMS to the global burden of nss-$SO_4$ to be ≈20-30%. Yet, similar to our findings, it can be more than an 80-90% over the pollution-free SO in the austral summer (*Heintzenberg et al.*, 2000; *Gondwe et al.*, 2003, 2004; *Kloster et al.*, 2006). All in all, this global estimate of the oceanic biogenic contribution to CCN has to taken with some caution due to the uncertainties going along with the approach used.

### 4.3.3 Uncertainty Analysis

The estimates of the biogenic contribution to $CCN_s$ carry an associated uncertainty that arises from the various uncertainties within the approach used: the satellite retrieval of CCN, sea surface DMS concentrations, DMS oxidation in the atmosphere. To address them all we have performed an uncertainty analysis (UA) by repeating the quantitative analyses under different conditions. The importance of the satellite retrieval of $CCN_s$ has been evaluated by using an alternative set of $CCN_s$ data (MODIS algorithm, which uses a different method for CCN derivation) and comparing the results with those obtained with the modified version of the *Gassó and Hegg* (2003) algorithm used in the present study. The importance of uncertainties regarding the DMS oxidation has been addressed by increasing/decreasing the $k_s$ constant of the oxidation efficiency $\gamma$ parameter (see eq(4.3)) by 50%. The same approach has been used for the $DMS_w$ concentrations (increase/decrease by 50%). Also, we have evaluated the confidence intervals of the current estimates of the biogenic contribution to the $CCN_s$ by applying

eq(4.2) using the upper and lower limits (95% confidence intervals) of the regression parameters obtained over the SO. That is, the upper-end estimates of $CCN_{bio}$ result from using the upper slope value with the lower intercept value; the lower-end estimates of $CCN_{bio}$ result from using the lower slope value with the higher intercept value. UA results are listed in Table 1. Since the increase/decrease $DMS_w$ did not produce any change, we have omitted it.

| $CCN_{bio}$ *vs.* $CCN_s$ for: | | | | | | | | | | |
|---|---|---|---|---|---|---|---|---|---|---|
| Station | Lower estimates | | Upper estimates | | $k_s$ -50% | | $k_s$ +50% | | MODIS $CCN_s$ | |
| | $\rho$ | $\beta$ | $\rho$ | $\beta$ | $\rho$ | $\beta$ | $\rho$ | $\beta$ | $\rho$ | $\beta$ |
| 1 | 0.92 | 20% | 0.92 | 38% | 0.92 | 27% | 0.89 | 30% | 0.95 | 47% |
| 2 | 0.72 | 26% | 0.72 | 50% | 0.72 | 29% | 0.72 | 44% | 0.77 | 56% |
| 3 | -0.22 | 7% | -0.22 | 14% | -0.22 | 8% | -0.22 | 13% | -0.64 | 25% |
| 4 | -0.32 | 38% | -0.32 | 74% | -0.38 | 43% | -0.31 | 85% | 0.02 | 73% |
| 5 | 0.91 | 9% | 0.91 | 17% | 0.84 | 13% | 0.91 | 14% | 0.92 | 30% |
| 6 | 0.58 | 20% | 0.58 | 39% | 0.6 | 23% | 0.58 | 35% | 0.5 | 55% |
| 7 | -0.17 | 23% | -0.17 | 45% | -0.23 | 26% | -0.13 | 41% | 0.31 | 59% |
| 8 | 0.68 | 67% | 0.68 | 130% | 0.59 | 77% | 0.68 | 115% | 0.69 | 100% |
| 9 | 0.64 | 7% | 0.64 | 13% | 0.55 | 8% | 0.68 | 12% | 0.62 | 25% |
| 10 | -0.17 | 8% | -0.17 | 15% | -0.17 | 9% | -0.17 | 14% | 0.71 | 24% |
| 11 | 0.17 | 18% | 0.17 | 36% | 0.17 | 20% | 0.22 | 32% | 0.9 | 48% |
| 12 | 0.31 | 45% | 0.31 | 88% | 0.24 | 51% | 0.35 | 78% | 0.12 | 75% |
| 13 | 0.98 | 7% | 0.98 | 14% | 0.97 | 11% | 0.98 | 11% | 1.0 | 24% |
| 14 | 0.9 | 40% | 0.9 | 78% | 0.88 | 57% | 0.92 | 60% | 0.94 | 67% |
| 15 | 0.95 | 16% | 0.95 | 32% | 0.89 | 28% | 0.95 | 22% | 0.96 | 35% |

Table 1: Uncertity Analysis of the estimated annual biogenic contribution to total $CCN_s$ concentrations for 15 regions of the global ocean ($\beta = \frac{\sum CCN_{bio}}{\sum CCN_s} * 100$) and of the correlation coefficient ($\rho$) betweem $CCN_{bio}$ and total $CCN_s$. See text for further details.

Figure 4.8 displays the estimates of biogenic contribution to the $CCN_s$ at each region of the global ocean for all these six UA scenarios. Maximum $\beta$ estimates are given by the top of the color-bars while minimum $\beta$ estimates are given by the top of the black-bars. At each of the 15 regions, we have then 3 columns (each one with a maximum and a minimum $\beta$ value). The first column represents the results of the UA related to the $CCN_s$ data set; the second one is the UA related to the DMS oxidation parameterization; and the third one is the UA related to the regression equation (confidence intervals of the regression parameters) used to estimate CCNbio. In the first case, we obtain systematically higher biogenic contributions to CCN when using the MODIS $CCN_s$ (dark-gray bar) than with our $CCN_s$ estimates (black bar; $\beta$ values are from Figure 4.7). Similarly, an increase in the $k_s$ constant produce higher $\beta$ values in all the regions except the 13 (no change) and 15 (small decrease) (light-gray bar *vs.* black bar). The highest variability is obtained from the use of different equations (upper and lower confidence intervals) for $CCN_{bio}$ estimates (third column; white bar *vs.* black bar). The black stars denote the $\beta$ values obtained by averaging the six scenarios; they are generally very close the value obtained for the standard case (the black bar in each first column, also Figure 4.7). Therefore, although the absolute values of the biogenic contribution estimates

carry substantial uncertainty, the observed trends are robust enough. Only four regions show a dominant $CCN_{bio}$ contribution to the total $CCN_s$ numbers (more than ≈60%) and they are all located in the Southern Hemisphere (regions 4, 8, 12 and 14).

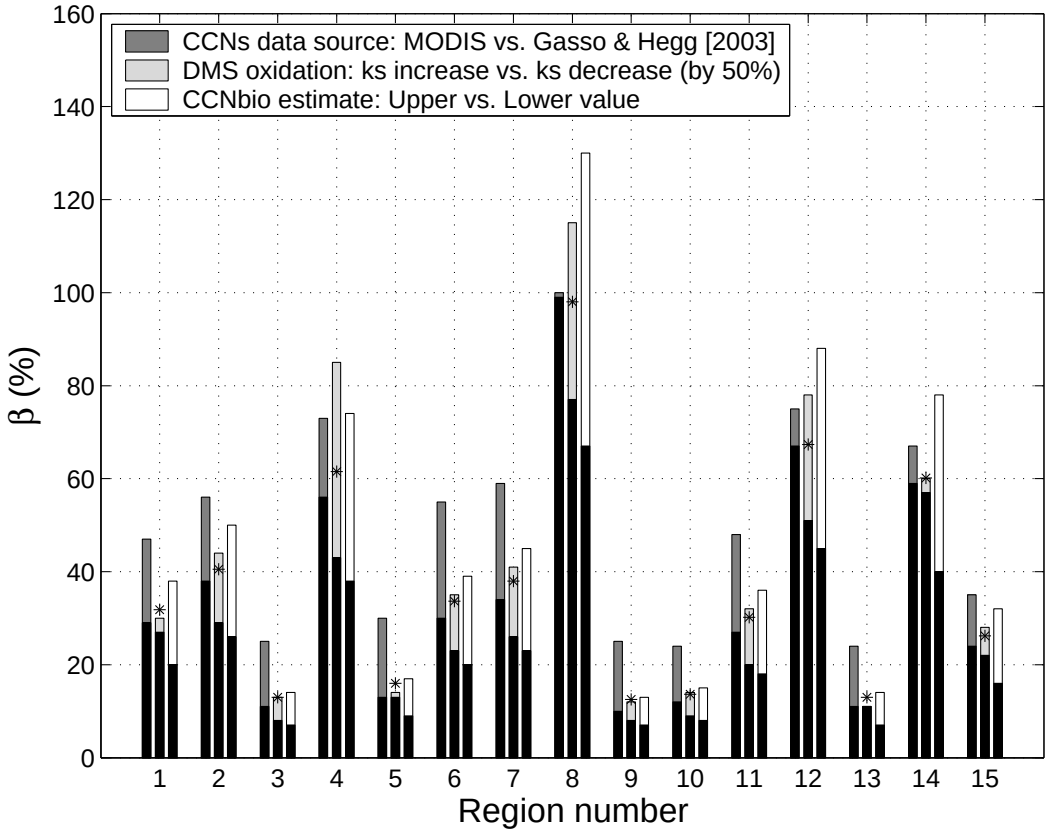


Fig. 4.8: Uncertity analysis of the estimated annual biogenic contribution to total $CCN_s$ concentrations for 15 regions of the global ocean ($\beta = \frac{\sum CCN_{bio}}{\sum CCN_s} * 100$). For each reagion, the first column represents the uncertity analysis related to the $CCN_s$ data set (MODIS algorithm *vs. Gassó and Hegg* (2003) algorithm); the second one is the uncertity analysis related to the DMS oxidation parameterization (50% $k_s$ increase *vs.* 50% $k_s$ decrease); and the third one is the uncertity analysis related to the regression equation (confidence intervals of the parameters) use to estimate CCNbio. Maximum $\beta$ estimates are given by the top of the color-bars while minimum $\beta$ estimates are given by the top of the black-bars.

## 4.4 Conclusions

Based on globally mapped seasonal correlations between climatological data, we have tested if oceanic DMS concentrations may driven by the solar radiation dose in the upper mixed layer, if DMS emissions to the atmosphere are coupled to satellite-derived CCN concentrations, and if this biogenic contribution could be significant from a regional and global perspective. While seasonal correlations are never a proof of causality, they indicate the degree to which variables move in concert and can therefore be very useful to test hypotheses of mechanistic links between the variables and, if the correlations do not show the expected couplings, reject the hypotheses. Regarding the CLAW hypothesis, the obtained results do not contradict its main two postulates: *i*) an increase (decrease) of solar irradiance can produce an increase (decrease) of seawater DMS (and then its emission to the atmosphere); *ii*) an increase

(decrease) of DMS emissions can produce an increase (decrease) of CCN. They rather support them, although the observed couplings between DMS oxidation and CCN concentrations can only be attributable to a biogenic origin over clean regions of the Southern Hemisphere. However, our approach does not fully rule out that the observed correlation are due to an independent seasonal variation of the studied variables; seasonal couplings are "necessary but not sufficient" conditions to prove the CLAW hypothesis (*Bates et al.*, 1987). Nevertheless, a sequence of observations point towards the existence of a negative feedback. Recent results have pointed out the possibility that DMS production has a protective function inside phytoplankton cells against high UV radiation (*Sunda et al.*, 2002), resulting in a constant leakage of this compound from the stressed cells into seawater. This, together with a complex web of biotic and abiotic processes, results in the accumulation of DMS in highly irradiated surface waters (*Simó and Pedros-Alló*, 1999a; *Toole and Siegel*, 2004). As solar radiation increases in summer, the subsequent increase of aqueous DMS would increase DMS emission to the atmosphere, its oxidation to nss-$SO_4$ aerosols, and CCN formation, which would reduce the level of solar radiation exposure of the surface ocean. The efficiency of this process would be enhanced if the main atmospheric DMS oxidant (the OH radical) increased also in summer, a period of maximum atmospheric vertical convection (*Barrie et al.*, 2001) that would facilitate the DMS-OH mixing and oxidation as well as a higher $SO_2$ to nss-$SO_4$ conversion efficiency (*Barrie et al.*, 2001). All these steps are globally observed: $DMS_w$, $DMS_{flux}$, OH, nss-$SO_4$ and CCN, all increase in summer. These couplings are stronger at high latitudes, probably as a consequence of the higher seasonal amplitude of the solar irradiance. However, although the DMS (hemispheric) summer increase is widespread, only in the Southern Hemisphere the estimated biogenic production of CCN from DMS oxidation significantly contributes to the total CCN. In the Northern Hemisphere, which is under very high anthropogenic influence, the biogenic contribution to CCN is minor. Over equatorial to tropical regions, other sources also dominate CCN concentrations and variability due to the low seasonality of solar irradiance and the heavy inputs of continental aerosols. From a global perspective, therefore, the contribution of biogenic CCN to the total CCN is rather moderate ($\approx$30%). However, over remote oceanic regions far from continental inputs (e.g. Southern Ocean, subtropical South Pacific), CCN seem to be strongly influenced by $CCN_{bio}$. In this regard, it is in clean air over marine regions where changes in CCN concentrations may have greater impact on cloud albedo due to the lower droplet concentrations (*Platnick and Twomey*, 1994; *Dingenen et al.*, 1995; *Liss and Turner*, 1997). Over these regions a natural biogeochemical mechanism of climate regulation (as proposed by the CLAW hypothesis) could perfectly be operating, at least on seasonal time scales. It is then plausible that in pre-industrial periods a seasonal 'Solar Radiation Dose - DMS - CCN' link was globally important.

# CHAPTER 5

# Strong relationship between DMS and the solar radiation dose over the global surface ocean

*He who seeks the truth*
*faces the risk of finding it.*

*(Manuel Vicent Villavieja)*

# Strong relationship between DMS and the solar radiation dose over the global surface ocean


## ABSTRACT

Marine biogenic dimethylsulfide (DMS) is the main natural source of tropospheric sulfur, which may play a key role in cloud formation and albedo over the remote ocean. Through a global data analysis, we found that DMS concentrations are highly positively correlated with the solar radiation dose in the upper mixed layer of the open ocean, irrespective of latitude, plankton biomass, or temperature. This is a necessary condition for the feasibility of a negative feedback in which light-attenuating DMS emissions are in turn driven by the light dose received by the pelagic ecosystem.



S. M. Vallina & R. Simó (2007)
*Science*, 315, doi:10.1126/science.1133680

## 5.1 Introduction

Oceanic biota influence climate in the long term by shaping the biogeochemical cycles of elements essential for Earth-system functioning (such as C, O, N, P, Si, and S) (*Falkowski*, 1997; *Falkowski et al.*, 1998; *Lenton and Watson*, 2000) and in the short term by exchanging climate-active gases with the atmosphere (greenhouse gases, oxidant and light scavengers, and free-radical and aerosol precursors) (*Andreae and Crutzen*, 1997; *Singh et al.*, 2001; *Chuck et al.*, 2002; *O'Dowd et al.*, 2002; *Hirsch et al.*, 2006). One of these gases is dimethylsulfide (DMS), which represents the largest natural source of atmospheric sulfur and a major precursor of hygroscopic (i.e., cloud-forming) particles in clean air over the remote oceans (*Andreae and Crutzen*, 1997; *Simó*, 2001), thereby acting to reduce the amount of solar radiation that crosses the atmosphere and is absorbed by the ocean. A 20-year-old hypothesis (*Charlson et al.*, 1987) postulated that marine plankton, cloud albedo, and solar radiation can be connected through DMS production, ventilation, and oxidation in a feedback interaction; whether this feedback would be positive or negative was uncertain.

## 5.2 Data and Methodology

### 5.2.1 Blanes Bay data

A monthly sampling of surface DMS concentrations, as well as biological and physical variables, was conducted during 2003 and part of 2004 at the Blanes Bay Microbial Observatory, located at 41.30°N, 2.48°E in the coastal northwest Mediterranean. We wanted to explore whether DMS concentrations are linked to epipelagic ecosystem exposure to solar radiation. We noted that the light exposure of an idealized seawater particle (and its associated dissolved substances and buoyant organisms) depends not only on the surface irradiance and its underwater attenuation but also on the depth of the mixed layer within which the particle is confined. Thus, we estimated (see below) the daily-averaged solar radiation received in the upper mixed layer (UML), or UML solar radiation dose (SRD), from measured data of the daily-averaged surface irradiance, the underwater light extinction coefficient, and the mixed layer depth (MLD). Pyranometer, semi-hourly total solar radiation at surface were obtained from the meteorological station of Malgrat, located 4.5 km south of Blanes Bay (data available at http://www.meteocat.com). Data were averaged over 24 hours, from 11:00 on the day before to 11:00 on the sampling day (local time). Temperature and salinity profiles were recorded in parallel to sampling for DMS. The mixed layer depth (MLD) was taken as the depth at which temperature was 0.2°C lower than that at surface. Light extinction was determined from photosynthetically active radiation (PAR) profiles measured with a LICOR radiometer in parallel to sampling for DMS.

### 5.2.2 Sargasso Sea data

A similar analysis was applied to a time series of DMS concentrations at Hydrostation S in the Sargasso Sea (*Dacey et al.*, 1998) (32.17°N, 64.50°W). Daily surface irradiances measured in Bermuda as well as MLD and extinction coefficients measured at the Bermuda Atlantic Time-Series Study (BATS) station nearby were used to estimate (see below) the UML solar radiation dose on the same days as DMS was measured. Pyranometer, minutely total solar radiation at surface were obtained from the Bermuda station of the Baseline Surface Radiation Network, World Radiation Monitoring Center, located 25 km northwest of Hydrostation S (data available at http://bsrn.ethz.ch). Daily averaged data (noon to noon) were smoothed by a running mean with a backward window of two weeks to reduce the noise caused by very short periods of heavy cloudiness that might have not occurred at Hydrostation S. Then daily averages concurrent with DMS sampling were extracted. Temperature and salinity profiles were obtained from the BATS website (http://bats.bbsr.edu/), whose study station is located 50 km southeast of Hydrostation S. MLD were calculated with a definition criterion of a 0.1°C departure with respect to the temperature at 5 m. Data were interpolated and smoothed by a running mean with a backward window of two weeks to fill gaps and reduce the noise caused by very short periods of heavy mixing that might have not occurred at Hydrostation S. Then MLD corresponding to the DMS sampling days were extracted. Light extinction was determined from depths of 99% PAR attenuation measured at the BATS station by the Bermuda Bio-Optics Project (BBOP). Data are available at http://www.icess.ucsb.edu/bbop/bbop.html.

### 5.2.3 Global data

To assess whether global DMS distributions better follow those of solar radiation or sea surface temperature (SST) than those of plankton biomass, we compiled monthly global maps of available DMS concentrations from the Global Surface Seawater (GSS) DMS database (http://saga.pmel.noaa.gov/dms/). This database includes about 30,000 individual data points collected from 1972 to 2003. No information about the corresponding in situ MLD, surface irradiances, or light extinction coefficients is available directly from the database. *de Boyer-Montégut et al.* (2004) recently constructed a comprehensive climatology of global MLD based on more than 4,000,000 temperature profiles obtained between 1941 and 2002. We made use of this climatology changing the definition criterion to a 0.1°C departure with respect to the temperature at 5 m (*Vallina et al.*, 2007a). The daily averaged solar irradiance at the top-of-the-atmosphere was calculated (*Brock*, 1981) and converted into ocean-surface irradiance considering a transmission coefficient of 0.5, that is, an atmospheric reduction by a half (*Kiehl and Trenberth*, 1997). Since we used full-spectrum irradiances, and the underwater absorption behavior strongly depends on the wavelength, to estimate the SRD a fixed light extinction of 0.06 $m^{-1}$ was considered reasonable for wavelengths of 400-500 nm (i.e., centered wavelengths in

the full solar radiation spectrum) based on experimental studies in oligo- to mesotrophic waters (*Smith and Baker*, 1979; *Kieber et al.*, 1996; *Obernosterer et al.*, 2001; *Lee et al.*, 2005). Monthly global maps of SRD were obtained from the aforementioned variables in the same way as for the local studies (see below). For chlorophyll-a (CHL) concentrations and SST, we used satellite-derived climatologies. A monthly global climatology of sea surface concentrations of CHL was constructed from 2002-2004 level 3 data from the Sea-viewing Wide Field-of-view Sensor (SeaWiFS) available at http://oceancolor.gsfc.nasa.gov/SeaWiFS/. A monthly global climatology of SST for the period 1971-2000 was obtained from the Climate Diagnostics Center (National Oceanic-Atmospheric Administration / Cooperative Institute for Research in Environmental Sciences) at http://www.cpc.noaa.gov/products/predictions/30day/SSTs/sst_clim.html (*Reynolds and Smith*, 1995).

We divided the surface of the globe into 324 boxes of 10° latitude by 20° longitude. Available DMS measurements and calculated SRD values were averaged for each month and each box. Next, we subdivided the range of SRD values (from 0 to 210 W $m^{-2}$) into spaced intervals of 15 W $m^{-2}$, and mean $\pm$ standard deviation was calculated for the box-averaged DMS concentrations corresponding to each of the intervals. Data from different latitudes and months were averaged together as long as they had a similar solar radiation dose. The highest 5% of the DMS box means were purposely not taken into account in order to exclude high DMS values associated with eutrophic coastal systems and local blooms of algae that produce very high amounts of dimethylsulfoniopropionate (DMSP), which are well-documented short-term sources of DMS that would have a disproportionately high weight on the averages. This cut-off criterion roughly corresponded to an upper limit of 10 nM (see Figure 5.1). The final number of box-month combinations used was 545, and the total number of GSS DMS data points included was about 26,400, i.e., nearly 90% of the original data.

### 5.2.4 Solar radiation dose

The daily-averaged, upper mixed layer solar radiation dose (SRD) was estimated assuming an exponential decay of the daily-averaged surface solar irradiance ($I_0$) with depth ($z$):

$$SRD = I_{uml} = \frac{1}{MLD}\int_0^{MLD} I_0 * exp(-k*z)dz = \frac{I_0}{MLD*k} * (1 - exp(-k*MLD)) \quad (5.1)$$

where MLD is the mixed layer depth (m), and $k$ is the light extinction coefficient ($m^{-1}$).

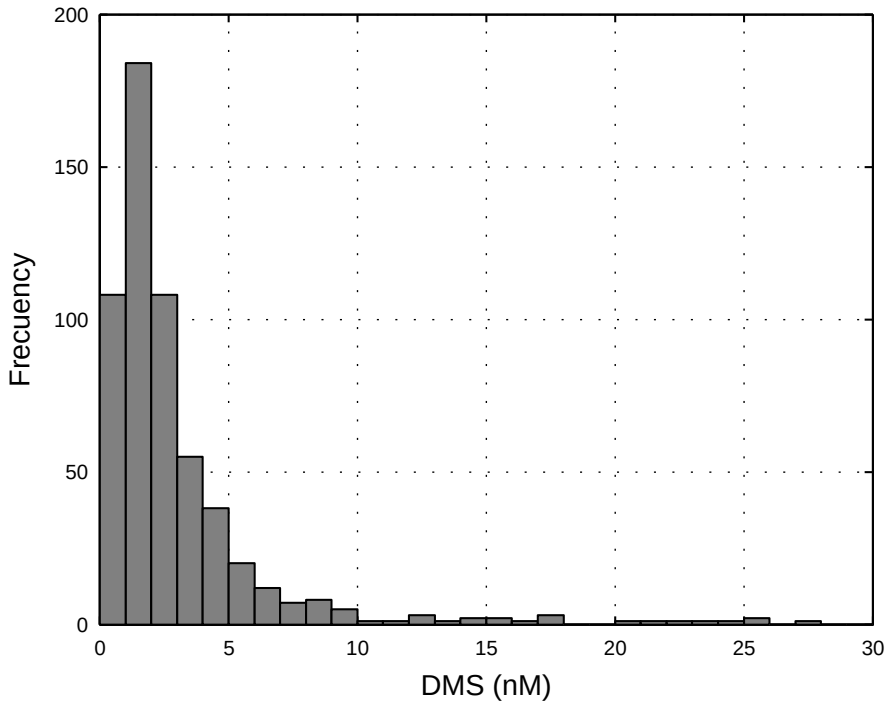


Fig. 5.1: Frequency distribution of DMS concentration box-means. Values were obtained by averaging 30,000 individual data points grouped by 10° x 20° (latitude x longitude) boxes and months. Data were obtained from the Global Sea Surface DMS Database at http://saga.pmel.noaa.gov/dms/. DMS box-mean concentrations higher than 10 nM represent 5% of the total.

## 5.3 Results and Discussion

### 5.3.1 Local analyses: Blanes Bay and Sargasso Sea

A linear regression analysis revealed that, during the period examined, the SRD accounted for 94% of the variance of monthly surface DMS concentrations (Figure 5.2). A comparison of concurrent DMS and CHL concentrations showed some inverse correlation ($\rho$=-0.51). Similary, at the Sargasso Sea the variation in the SRD explained 81% of the variance of monthly surface DMS concentrations (Figure 5.3). This is consistent with a recent work (*Toole and Siegel*, 2004) showing that the net biological production and concentration of DMS in the UML was highly correlated with the ultraviolet radiation (UVR) dose at this same study site. These authors reported an inverse correlation between UML-averaged DMS and CHL ($\rho$=-0.61).

The original plankton/sulfur/climate hypothesis postulated that a regulatory (negative) feedback would occur if positive changes in sunlight and/or temperature caused positive changes in phytoplankton production, particularly at low latitudes (*Charlson et al.*, 1987). The observation that, both in the Sargasso Sea and in the coastal Mediterranean, monthly DMS and CHL concentrations were not positively correlated but rather showed opposite patterns is not a particular case of these two stations. Away from the equatorial region, surface DMS concentrations usually peak in summer. In subtropical and low temperate regions, this maximum DMS coincides with a minimum of phytoplankton biomass. This feature has been called the

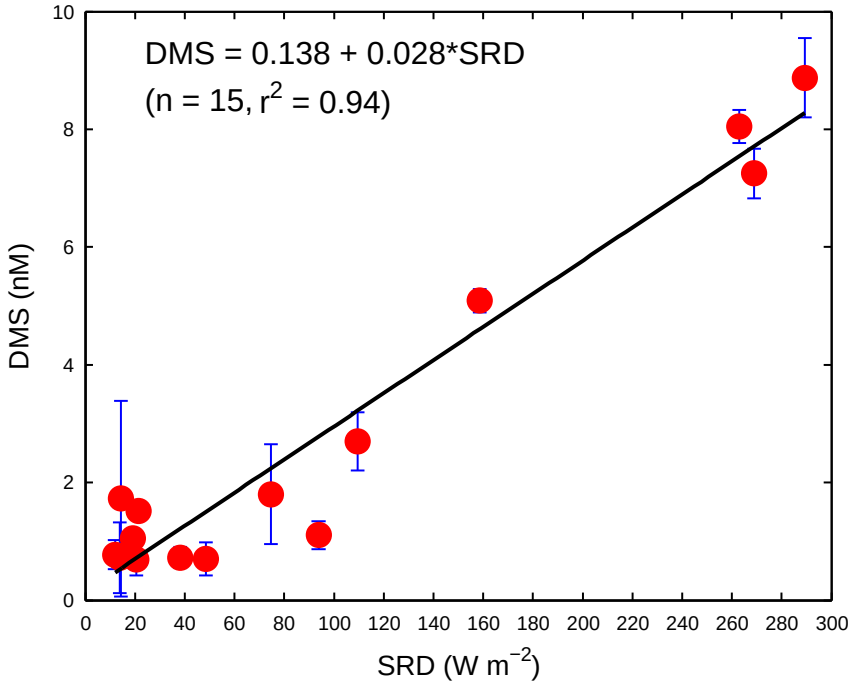


Fig. 5.2: Linear regression (n = 15, $r^2$ = 0.94) of surface DMS concentrations versus SRD in Blanes Bay (coastal northwest Mediterranean). Dots are monthly data during the period from January 2003 to April 2004. Error bars represent standard deviations of two consecutive sampling days each month. A Spearman correlation analysis of the same data gives a significant positive coefficient $\rho$ = 0.75 (P << 0.01).

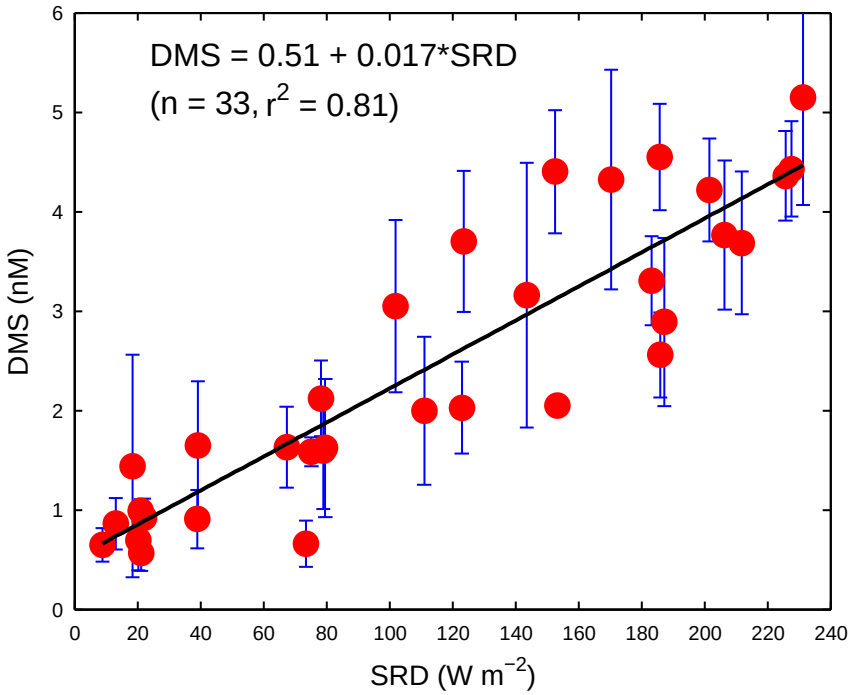


Fig. 5.3: Linear regression (n = 33, $r^2$ = 0.81) of surface (UML averaged) DMS concentrations versus the SRD in Hydrostation S (Sargasso Sea). Dots are monthly data during the period from January 1992 to November 1994. Error bars represent standard deviations of multiple sampling days each month. A Spearman correlation analysis of the same data gives a significant positive coefficient $\rho$ = 0.89 (P << 0.01). DMS data are from *Dacey et al.* (1998).

DMS summer-paradox (*Simó and Pedros-Allió*, 1999a). At high latitudes and over most of the Southern Ocean, on the other hand, the summer surface DMS maximum co-occurs with a CHL maximum, and both variables look strongly correlated (*Vallina et al.*, 2006). Such a heterogeneous behavior results in very weak global correlations between DMS and CHL (*Kettle et al.*, 1999; *Vallina et al.*, 2006).

### 5.3.2 Global analysis

Monthly latitudinal distributions of DMS, CHL, SST, and SRD show that DMS follows solar radiation dose much more closely than it follows plankton biomass or temperature (Figure 5.4). Further, consistent with the local time series, a significant positive correlation was found between averaged surface DMS concentrations and the SRD along the radiation dose range (Figure 5.5). Notably, there is a strong similarity between the slope and the intercept of the globally derived linear equation and those obtained in the Sargasso Sea (Figure 5.3). Even though the data scatter for the global relationship is quite large (shaded areas in Figure 5.5), the upper and lower contours of the scatter still show clear proportionality between DMS and the SRD.

Although upper-ocean DMS dynamics have been the object of extensive research, definitive conclusions about the main factors controlling DMS concentrations have remained elusive, and this has prevented giving an unequivocal sign for any feedback link between climate and DMS. Experimental work (*Dacey et al.*, 1998; *Simó*, 2001) has unveiled the interaction of multiple biotic and abiotic players (e.g., phytoplankton composition and physiological state, zooplankton grazing, bacterial activity and diversity, and photolysis), and solar radiation (and especially UVR) exerts a substantial but not straightforward influence on many of them (*Sunda et al.*, 2002; *Simó*, 2004; *Toole et al.*, 2006). A particularly relevant, recent hypothesis suggests that DMS leakage from the algal cell is the by-product of a sulfur-based antioxidant mechanism (*Sunda et al.*, 2002). Given that high light (high UVR) doses induce oxidative stress (i.e, DMS release) and inhibit bacterial DMS consumption as well (*Toole et al.*, 2006), DMS may accumulate in seawater. Phytoplankton succession to higher-DMSP producers in summer stratified waters, oxidative stress on these producers, and oxidative damage on DMS consumers may be concurrent reasons why DMS concentrations are higher in high-light conditions.

A recent analysis of the DMS time series in the Sargasso Sea revealed that the temporal DMS variation emerging from such a complex cycle resembles that of the local UVR, and the latter was suggested as the major driving force (*Toole and Siegel*, 2004). Whether this very same quantitative DMS-UVR relationship would be applicable to most of the global ocean was unknown but unlikely, because other local factors such as plankton abundance and community structure would be expected to have a large complementary influence. Nonetheless, a pioneering work by *Bates et al.* (1987) showed, with the few data available at the time, that the seasonally averaged DMS emission flux covaried with the seasonally averaged surface so-

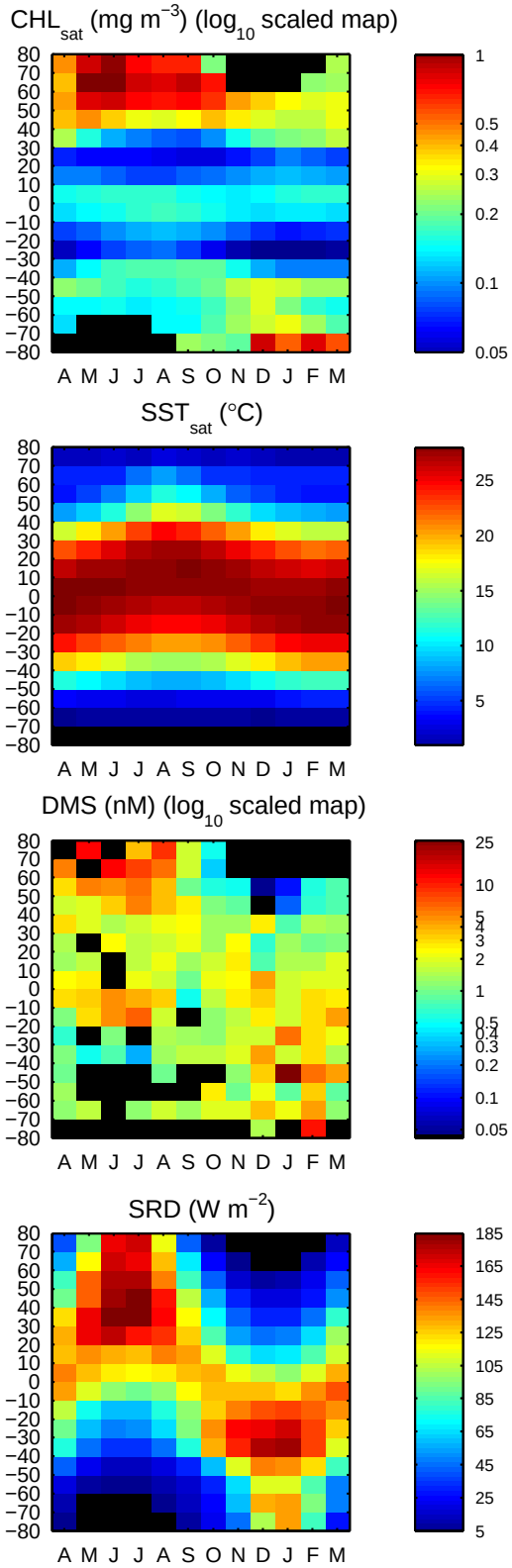


Fig. 5.4: Month (April through March) by latitude plots of climatological global distributions of satellite-derived CHL concentrations (CHLsat, Sea-Viewing Wide Field-of-View Sensor, 2002 to 2004), satellite-derived sea surface temperature (SSTsat , Climate Diagnostics Center, 1971 to 2000), surface DMS concentrations (GSS DMS database), and the SRD (calculated). All variables are monthly averaged by 10° latitude bands. Spearman coefficients ($\rho$) for the correlations between the latitude-month distributions of DMS and the other variables are DMS versus CHLsat, 0.08; DMS versus SSTsat, 0.16; DMS versus SRD, 0.56 (n = 155).

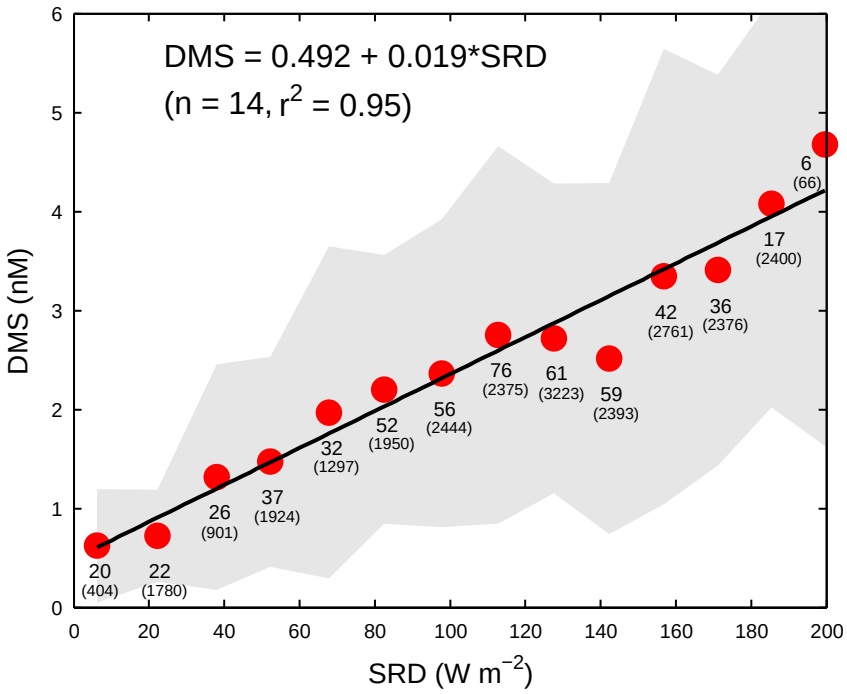


Fig. 5.5: Linear regression (n = 14, $r^2$ = 0.95) of surface DMS concentrations versus the SRD in the global open ocean. Dots are averages of 10° by 20° (latitude by longitude) box mean DMS concentrations grouped by intervals of 15 W $m^{-2}$ of SRD. The shaded area represents the standard deviation of the averages. The numbers by the data points indicate the amount of DMS box means used for each average (upper number) and the amount of original data included (number in parentheses). A Spearman correlation analysis of the 545 box means gives a significant positive coefficient $\rho$ = 0.47 (P << 0.01).

lar irradiance at different latitudes. More recently, the depth of the UML was seen to have a regulatory influence on DMS production and concentration on a global scale, and it was hypothesized that such regulation would partly occur through the effects of the MLD on plankton exposure to solar radiation (*Simó and Pedros-Allió*, 1999a; *Simó and Dachs*, 2002).

## 5.4 Conclusions

Using the most comprehensive data set available today, we show that surface DMS concentrations respond positively to the UML solar radiation dose, and this response follows the same proportionality over the global open ocean, irrespective of latitude and the large variability of, for example, temperature and trophic status. One of the challenges of today's Earth system science is to elucidate how the biosphere responds to climate in ways that in turn influence climate (*Meir et al.*, 2006), determine their operation time scale, and clarify whether these responses confer stability to the climate system in front of perturbations such as anthropogenic global environmental change. The tight coupling of DMS concentrations to the solar radiation dose that we observed is a necessary condition for the occurrence of a negative feedback between plankton and climate through the influence of the former on the radiative energy budget (*Charlson et al.*, 1987). Notably, it also provides a clue on the time scale of such feedback. The solar radiation dose of the surface ocean varies strongly over the seasonal cycle as

a consequence of the coupled variation of surface irradiance and the MLD. Our data indicate that it is at this seasonal scale that the epipelagic ecosystems respond to temporal and latitudinal changes in solar radiation by changing their production of light-attenuating volatile sulfur. Exploration of responses at time scales shorter than a month should be carried out with high-resolution measurements of DMS and solar radiation in coherent water masses. Whether this feedback will also operate efficiently at the longer time scale of anthropogenic global warming will depend on induced changes in global cloudiness, aerosol light scattering, and, most important, mixing depths in the ocean.

CHAPTER 6

# Weak response of oceanic dimethylsulfide to upper mixing shoaling induced by global warming

*Nothing is always absolutely so.*

*(Theodore Sturgeon)*

# Weak response of oceanic dimethylsulfide to upper mixing shoaling induced by global warming


## ABSTRACT

The solar radiation dose in the oceanic upper mixed layer (SRD) has recently been identified as the main climatic force driving global dimethylsulfide (DMS) dynamics and seasonality. Since DMS is suggested to exert a cooling effect on the Earth radiative budget through its involvement in the formation and optical properties of tropospheric clouds over the ocean, a positive relationship between DMS and the SRD supports the occurrence of a negative feedback between the oceanic biosphere and climate, as postulated 20 years ago. Such a natural feedback might partly counteract anthropogenic global warming through a shoaling of the mixed layer depth (MLD) and a consequent increase of the SRD and DMS concentrations and emission. By applying two globally-derived DMS diagnostic models to global fields of MLD and chlorophyll simulated with an Ocean General Circulation Model coupled to a biogeochemistry model for a 50% increase of atmospheric $CO_2$ and an unperturbed control run, we have estimated the response of the DMS-producing pelagic ocean to global warming. Our results show a net global increase in surface DMS concentrations, especially in summer. This increase, however, is so weak (globally 1.2%) that it can hardly be relevant as compared with the radiative forcing of the increase of greenhouse gases. This contrasts with the seasonal variability of DMS (1000-2000% summer-to-winter ratio). We suggest that the 'plankton - DMS - clouds - Earth albedo feedback' hypothesis is less strong a long-term thermostatic system than a seasonal mechanism that contributes to regulate the solar radiation doses reaching the Earth's biosphere.



S. M. Vallina, R. Simó, & M. Manizza (2007)
*Proc. Natl. Acad. Sci.*, 104(41), 16004-16009, doi:10.1073/pnas.0700843104

## 6.1 Introduction

Ocean-emitted dimethylsulfide (DMS) has been suggested to play a climatic role by contributing to cloud droplet condensation and thereby to cloud albedo. As such a climate-active compound, DMS was proposed as a candidate to partially counteract human-induced global warming through a global biogeochemical feedback between oceanic biosphere and climate, the so called 'CLAW hypothesis' (*Charlson et al.*, 1987). In order to quantitatively assess the feasibility and magnitude of this potential long-term climate-stabilizing response, it is important to understand which are the main factors that drive DMS dynamics: if we can estimate how they are changing due to global warming, we should be able to predict the DMS response. Early works pointed to the mutual interaction of several factors (i.e. phytoplankton community structure, zooplankton grazing, bacterial activity, etc.), over which the mixed layer depth (MLD) seems to have some kind of regulatory influence (*Simó and Pedros-Alló*, 1999a; *Simó and Dachs*, 2002). However, more recent studies have strongly suggested that solar radiation is the key factor regarding DMS dynamics, notably through its stress effects on phytoplankton and inhibitory effects on heterotrophic bacterioplankton (*Wolfe et al.*, 2002; *Sunda et al.*, 2002; *Slezak and Herndl*, 2003; *Toole and Siegel*, 2004; *Toole et al.*, 2006). One suggestion is that the enzymatic cleavage of dimethylsulfoniopropionate (DMSP) into DMS in phytoplankton is part of an antioxidant system that protects the cell from endogenous, hazardous hydroxyl (OH) radicals under high-light stressing conditions (*Sunda et al.*, 2002). This hypothesis is supported by several laboratory studies (*Hefu and Kirst*, 1997; *Stefels and van Leeuwe*, 1998; *Sunda et al.*, 2002; *Slezak and Herndl*, 2003) as well as local and global time series analyses (*Toole and Siegel*, 2004; *Vallina and Simó*, 2007a; *Vallina et al.*, 2007a; *Vila-Costa et al.*, 2008).

In this context, phytoplankton is a necessary-but-not-sufficient condition for the production of DMS. It is obvious that some phytoplankton activity needs to be present, but phytoplankton biomass proxies like chlorophyll-a (CHL) are not correlated with DMS concentrations over large scales except for high latitudes (*Vallina et al.*, 2006) and highly productive near-coastal regions (*Simó and Dachs*, 2002). In these (usually nutrient-replete) regions, the solar radiation dose in the upper mixed layer (UML) drives both phytoplankton biomass and DMS concentrations. These have been postulated to be the 'DMS bloom-regime' regions (*Toole and Siegel*, 2004). However, in subtropical and low temperate regions (which cover most of the ocean's surface) DMS is basically driven by the solar radiation dose, both increasing in summer despite CHL reduction due to nutrient depletion after water column stratification. These have been postulated to be the 'DMS stress-regime' regions (*Toole and Siegel*, 2004). Therefore, with the exception of high levels of DMS resulting from some phytoplankton blooms, most of the DMS dynamics could be predicted based purely on geophysical data (*Simó and Dachs*, 2002; *Toole and Siegel*, 2004). In support of that, recent works have found that the daily-averaged solar radiation dose received in the UML (hereafter SRD) seems to be the key factor governing DMS dynamics at all spatial scales, from the local to the global (*Vallina and Simó*, 2007a; *Vallina*

*et al.*, 2007a). These results also explained why previous diagnostic models of DMS concentrations, based basically (*Simó and Dachs*, 2002) or exclusively (*Aranami and Tsunogai*, 2004) on the MLD, work so well: the MLD might simply be a proxy of the SRD. Since MLD seasonality is related to surface irradiance (an increase on surface irradiance is usually followed by a decrease in the MLD), a multiplicative (non-linear) effect arises on the SRD. This leads to the observed non-linearity of the relationship between DMS and MLD, while DMS is linearly related to SRD.

MLD is predicted to be reduced by several meters in most regions of the ocean as a consequence of global warming, because the increase in air temperature would increase the atmosphere-to-ocean heat flux (then reinforcing water column stratification) (*Manizza*, 2006). In this regard, it has been speculated that, due to the links between MLD, SRD, and DMS, in a global warming scenario the shoaling of ocean stratification will imply an increase of DMS concentrations and its fluxes to the atmosphere (*Simó and Dachs*, 2002; *Toole and Siegel*, 2004), in support of the CLAW hypothesis. Since DMS is believed to be the main contributor to Cloud Condensation Nuclei concentrations (CCN) over marine remote regions (*Prospero et al.*, 1991; *Ayers and Gras*, 1991; *Andreae et al.*, 1995; *Ayers et al.*, 1997a; *Clarke et al.*, 1998; *Andreae et al.*, 1999; *Ayers and Gillett*, 2000; *Vallina et al.*, 2007a) and CCN numbers are related to cloud formation, cloud optical properties and lifetime (hence to the Earth albedo (*Charlson et al.*, 1987)), the anticipated DMS increase might constitute a natural negative feedback mechanism that could counteract the effects of global warming on Earth's climate (*Charlson et al.*, 1987; *Gunson et al.*, 2006). The present study seeks to estimate this (potential) DMS increase under global warming conditions by using the global relationship between DMS concentrations and the SRD (*Vallina and Simó*, 2007a) as a diagnostic model, as well as the diagnostic model proposed by *Simó and Dachs* (2002), that relates DMS to the MLD and CHL. Both diagnostic models are applied to global model outputs of MLD (from which the SRD is calculated) and CHL for the year 2061, obtained under a 50% increase in $CO_2$. A control with todays levels of $CO_2$ is run as a reference. The results are discussed in the context of the CLAW hypothesis.

## 6.2 Data and Methodology

### 6.2.1 Model data of the mixed layer depth and chlorophyll-a

Global monthly fields of MLD are outputs from the ORCA-LIM, a global version of OPA (*Timmermann et al.*, 2005). This is a three-dimensional (3D) Ocean General Circulation Model (OGCM) coupled to the LIM sea-ice model. OPA is based on primitive equations (*Madec and Imbard*, 1996; *Madec et al.*, 1999) where the vertical eddy diffusivity and viscosity coefficients are calculated by a 1.5 order turbulent kinetic energy model (*Gaspar et al.*, 1990). Sub-grid eddy induced mixing is parameterized according to *Gent and McWilliams* (1990). CHL is obtained from the coupling of PlankTOM5 to ORCA-LIM. PlakTOM5 is a biogeochemistry model based on

Plankton Functional Types (PFT) (*Le Quéré et al.*, 2005). It includes phosphorous, silicate, iron and light co-limitation and represents five PFT: mixed-phytoplankton, diatoms and coccolithophores for phytoplankton, plus meso and micro size classes for zooplankton (*Le Quéré et al.*, 2005). CHL is the sum of the chlorophyll-a of all three phytoplankton types.

### 6.2.2 Solar radiation dose

Monthly global maps of daily-averaged solar radiation dose (W $m^{-2}$) in the UML (or SRD) are estimated assuming an exponential decay of the daily-averaged surface solar irradiance ($I_0$) with depth ($z$):

$$SRD = I_{uml} = \frac{1}{MLD}\int_0^{MLD} I_0 * exp(-k*z)dz = \frac{I_0}{MLD*k} * (1 - exp(-k*MLD)) \tag{6.1}$$

$I_0$ is assumed to be 50% of the daily averaged solar irradiance at the top of the atmosphere ($I_{toa}$, W $m^{-2}$) (*Kiehl and Trenberth*, 1997), which is calculated following *Brock* (1981). We assume a general solar-radiation extinction coefficient ($k$) of 0.06 $m^{-1}$, which is a reasonable approximation for spectrum-centered wavelengths in open ocean waters (*Smith and Baker*, 1979).

### 6.2.3 DMS diagnostic models

#### 6.2.3.1 SRD-model:

$$DMS = 0.492 + 0.019 * SRD \tag{6.2}$$

#### 6.2.3.2 MLD-model:

if $CHL/MLD \geq 0.02$:

$$DMS = 0.6 + 55.8 * (CHL/MLD) \tag{6.3}$$

if $CHL/MLD < 0.02$:

$$DMS = 5.7 - Ln(MLD) \tag{6.4}$$

### 6.2.4 Control and Global Warming scenarios

We performed two parallel transient simulations (56 years, from 2005 until 2061) which differed in their atmospheric forcing $\psi$ (air temperature, wind speed, etc.): *i*) a 'control' simulation using atmospheric forcing of present day conditions $\psi_{Control} = \psi_{NCEP}$, where $\psi_{NCEP}$ is the NCEP/NCAR reanalysed atmospheric forcing (*Kistler et al.*, 2001) (56 years, from 1948 until 2004) applied to the 2005-2061 period; and *ii*) a 'global warming' simulation that makes use of an atmospheric forcing for a global warming scenario $\psi_{GW} = \psi_{Control} + \psi^*_{IPSL}$, where $\psi^*_{IPSL}$ are the atmospheric forcing anomalies from the IPSL (Institut Pierre-Simone Laplace) Earth system model simulation based on an IPCC scenario A2 (*Friedlingstein et al.*, 2001). Thus, $\psi^*_{IPSL}$ is the difference between the atmospheric output variables from a climate IPSL-A2 run with increasing $CO_2$ (56 years, from $\approx$377 ppm in 2005 to $\approx$551 ppm in 2061) and the baseline of 30-year monthly-averages (into one year climatology, from 1974 to 2004) of the same simulation. Each monthly value of the $\psi^*_{IPSL}$ anomalies was smoothed with a running-mean of 30 years to remove inter-annual variability while maintaining the seasonality (*Manizza*, 2006).

Thus we obtained estimates of the MLD and CHL under global warming ($MLD^{GW}$ and $CHL^{GW}$; $\approx$50% increase in $CO_2$ respect to 2005 levels) as well as without global warming ($MLD^{Control}$ and $CHL^{Control}$) (*Manizza*, 2006). By applying both the SRD-model and the MLD-model we obtained next, for each model, a DMS concentration estimates for the global warming scenario ($DMS^{GW}_{model}$) and the control ($DMS^{Control}_{model}$). For the SRD-model, surface solar irradiance and the light extinction coefficient are assumed to remain the same in both scenarios, so that DMS changes will only be the result of the differences between $MLD^{GW}$ and $MLD^{Control}$, which translate into differences between $SRD^{GW}$ and $SRD^{Control}$. When the MLD-model is used, either changes in MLD and CHL may result in DMS differences. The SRD-model equation does not include CHL; therefore it cannot capture changes in the bloom-regime regions due to global warming, but rather only changes in the stress-regime regions (*Vallina and Simó*, 2007a). On the other hand, the MLD-model has two empirical equations, one of which include both MLD and CHL (to be used in bloom-regime regions) while the other estimates DMS exclusively as a function of the MLD (to be used in stress-regime regions) (*Simó and Dachs*, 2002; *Toole and Siegel*, 2004). Therefore the MLD-model is expected to account for changes in both regime regions. Nevertheless, either for the GW or Control scenarios, the stress-regime clearly dominated, and DMS was estimated solely from the MLD in $\approx$90% of the ocean's surface.

### 6.2.5 Global maps of averaged DMS increase due to Global Warming

By comparing the global maps of DMS obtained for the GW and Control scenarios we calculated the DMS change due to global warming (the change in the absolute value and the percentage of change) for every 1° x 1° grid box (or pixel) of the global ocean. These esti-

mates were obtained for three periods separately: annually, from April to September, and from October to March. The changes in the absolute value (nM) were obtained as follows:

$$\Delta DMS_{Annual} = \frac{1}{12}\left(\sum_{i=Jan}^{i=Dec} DMS_i^{GW}\Delta t - \sum_{i=Jan}^{i=Dec} DMS_i^{Control}\Delta t\right) \tag{6.5}$$

$$\Delta DMS_{Apr-Sep} = \frac{1}{6}\left(\sum_{i=Apr}^{i=Sep} DMS_i^{GW}\Delta t - \sum_{i=Apr}^{i=Sep} DMS_i^{Control}\Delta t\right) \tag{6.6}$$

$$\Delta DMS_{Oct-Mar} = \frac{1}{6}\left(\sum_{i=Oct}^{i=Mar} DMS_i^{GW}\Delta t - \sum_{i=Oct}^{i=Mar} DMS_i^{Control}\Delta t\right) \tag{6.7}$$

where $\Delta t$ is one month. The percentages of DMS change were calculated by normalizing the absolute changes by the annual mean concentration of the Control scenario:

$$\Delta DMS_k^{\%} = \frac{\Delta DMS_k}{\frac{1}{12}\sum_{i=Jan}^{i=Dec} DMS_i^{Control}\Delta t} * 100 \tag{6.8}$$

where $DMS_k$ can be $DMS_{Annual}$, $DMS_{Apr-Sep}$, or $DMS_{Oct-Mar}$.

### 6.2.6 Globally averaged DMS increase due to Global Warming

Following a similar procedure, by considering the DMS change in each month and pixel along with the area covered by the pixel, the globally averaged (not spatially resolved) percentage of DMS change due to global warming was obtained for three cases: annually, summer conditions, and winter conditions. By 'summer conditions' and 'winter conditions' we mean the regions and periods with a daily-averaged solar surface irradiance higher and lower than 200 W $m^{-2}$, respectively.

## 6.3 Results and Discussion

With the aim at quantifying the (potential) future 'MLD reduction - SRD increase - DMS increase', we applied the globally-derived DMS diagnostic equations of *Vallina and Simó* (2007a) (SRD-model; see eq(6.2) in section 6.2) and *Simó and Dachs* (2002) (MLD-model; see eqs(6.3-6.4) in section 6.2) to modeled global fields of MLD and CHL obtained for 2061 (*Manizza*, 2006) under two scenarios (Global Warming *vs.* Control; see point 6.2.4).

### 6.3.1 Global validity of the DMS Diagnostic Models

In order to evaluate the validity of the DMS diagnostic models used, we have compared their results against actual data. Figure 6.1 shows the Hovmoller Diagrams (upper and middle panels) obtained both from data (Global Sea Surface -GSS- DMS database and *Kettle and Andreae* (2000)) as well as from model results (see Figure 6.1 legend), along with the global maps of seasonal correlations (*Vallina et al.*, 2006) between DMS modelled results from the control run against the *Kettle and Andreae* (2000) climatology (bottom panels). In general there is good agreement between DMS data and model estimates. However, for the control run, the SRD-model is unable of capturing the highest 10% zonally-averaged DMS values ($> \approx$4nM) while the MLD-model, since it includes the bloom-regimes, can not capture only the highest 4% zonally-averaged DMS data values ($> \approx$6nM). The correlation maps show that, with the exception of the equatorial regions (where there is almost no seasonality in the variables) the seasonality of the DMS data is very well captured by both models virtually all over the global ocean. A scatter-plot analysis between the zonally-averaged DMS values from model against data (see Figure 6.2) confirms their global validity (ie. Spearman correlation coefficients of $\approx$0.8 between MLD-model and SRD-model for the control run *vs. Kettle and Andreae* (2000); see pannels AA1 and BB2 of Figure 6.2).

### 6.3.2 DMS estimates under Global Warming

Figure 6.3 shows the global maps of estimated surface DMS concentration fields under global warming (GW) conditions for the three time periods considered, obtained with both diagnostic models. The results are fairly similar, yet some differences can be observed. Although both models display a clear seasonal pattern of higher DMS during each hemispheric summer, this seasonality is more marked in the SRD-model: $DMS^{GW}_{SRD-model}$ concentrations are slightly higher than $DMS^{GW}_{MLD-model}$ in each hemispheric summer, and vice-versa for each hemispheric winter. On the other hand, the MLD-model gives higher DMS concentrations at high latitudes due to algal blooms.

### 6.3.3 DMS increase under Global Warming

Figure 6.4 and Figure 6.5 show the global maps of the estimated increases of DMS under GW with both models. First, we notice that, although in some regions DMS decreases, there is a general increase of DMS concentrations over most of the globe. However, these increases are generally very weak, both in absolute change and in percentage of change. For example, in the case of the MLD-model, the 95% percentile from the annual maps is +0.13 nM for the absolute change and +6.3% for the percentage of change (the 5% percentile is -0.08 nM and -3.22%,

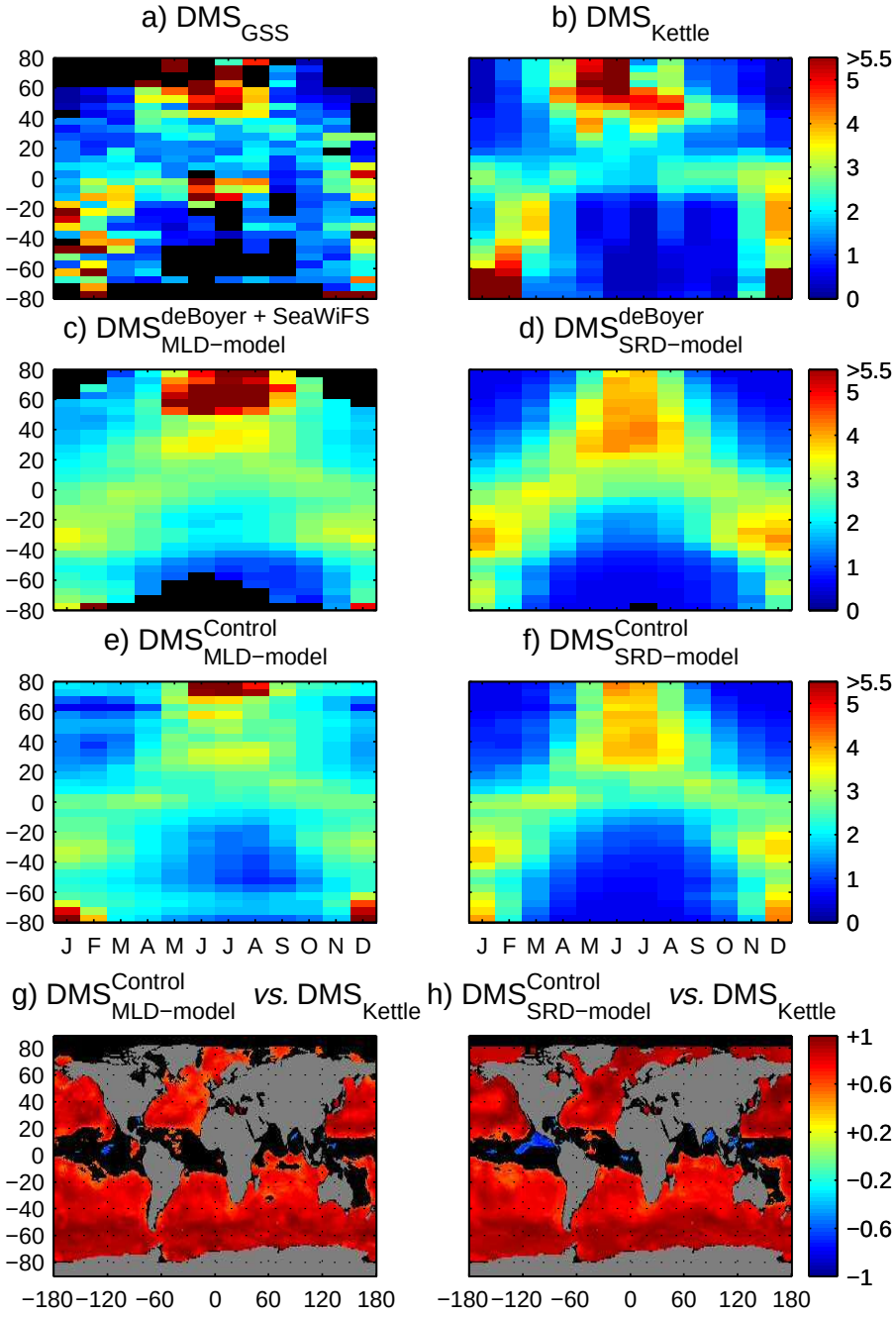


Fig. 6.1: Global DMS (nM) distributions. Panels a) to f) show the Hovmoller Diagrams for: a) GSS data; b) *Kettle and Andreae* (2000) climatology; c) present-day MLD-model (MLD from *de Boyer-Montégut et al.* (2004), CHL from a SeaWiFS 2002-2004 climatology); d) present-day SRD-model (MLD from *de Boyer-Montégut et al.* (2004)); e) MLD-model (MLD and CHL from control run); f) SRD-model (MLD from control run). The colorbar palette has been cut at 5.5nM (corresponding to the 95% percentile of zonally-averaged DMS GSS data) for the sake of visual comparison of modeled results against data. The GSS raw data (≈33,000 points) were gridded into a 180° x 360° x 12 (latitude, longitude, month) array climatology (≈5,700 points) before making the diagram. The bottom panels show the global maps of seasonal correlation (*Vallina et al.*, 2006) between modeled DMS results from the control run ( g) MLD-model; h) SRD-model ) against the *Kettle and Andreae* (2000) climatology. Only significant (95%) values are shown.

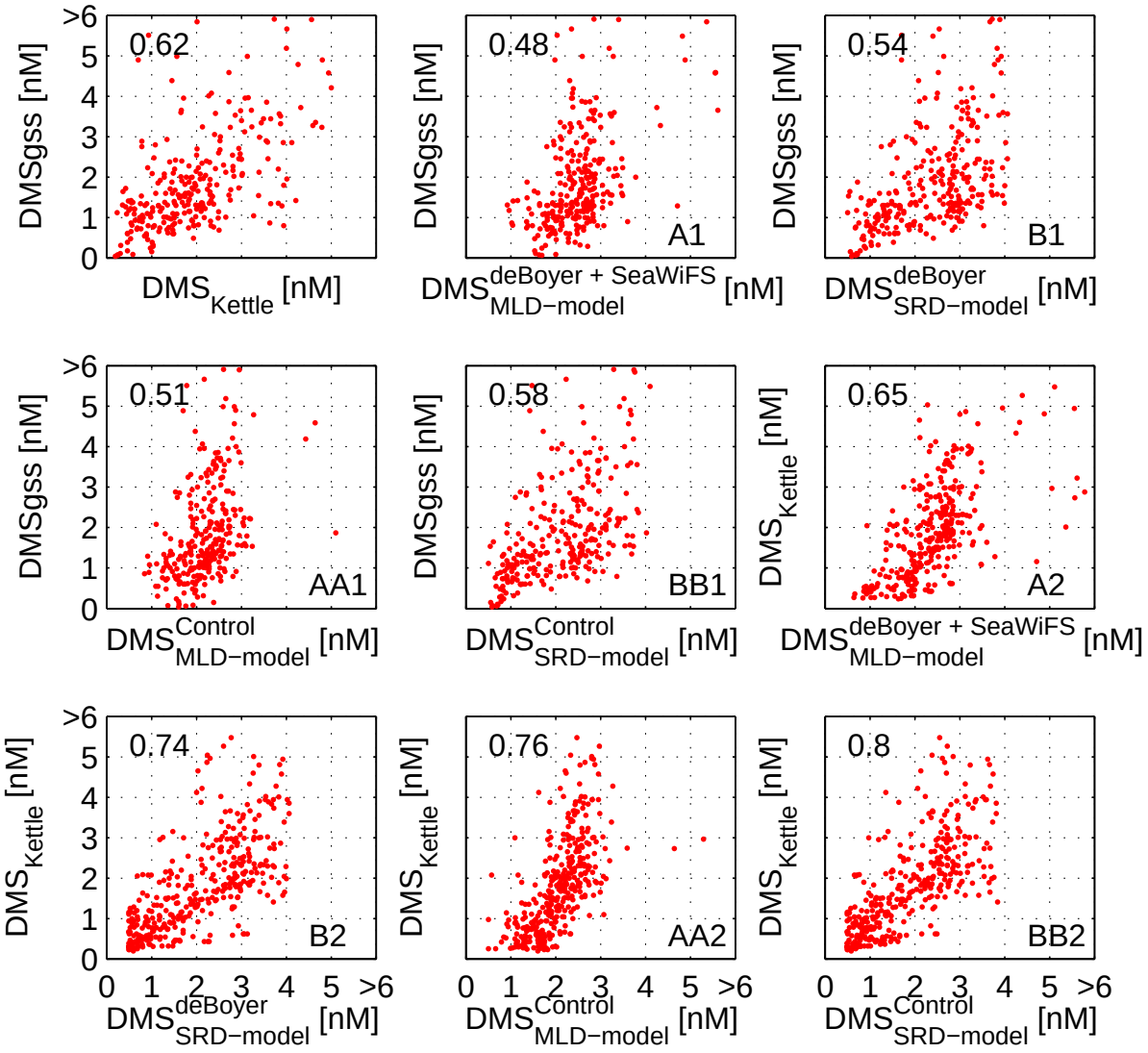


Fig. 6.2: Scatter-plots of the zonally-averaged DMS values from Figure 6.1 along with their corresponding (Spearman) correlation coefficient. For a quick visual inspection the panels were labelled on the bottom-right corner: letter refers to the diagnostic model used ('A' for MLD-model and 'B' for SRD-model); single letter refers to model results using current-day climatological data (MLD from (45) and CHL from a SeaWiFS 2002-2004 climatology) while double letter refers to the control run simulation; number refers to which data are being used to evaluate model results ('1' for GSS database and '2' for *Kettle and Andreae* (2000) climatology).

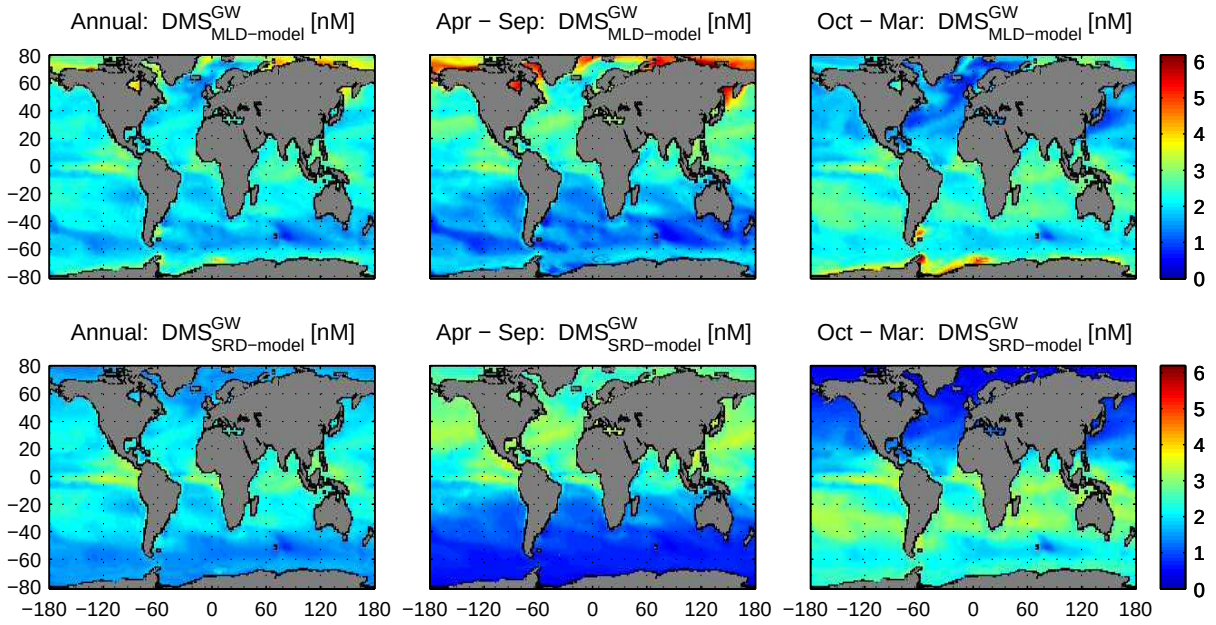


Fig. 6.3: Simulated fields of surface DMS concentrations under global warming conditions from the MLD-model (upper panels) (*Simó and Dachs*, 2002) and the SRD-model (lower panels) (*Vallina and Simó*, 2007a) for three time periods (from left to right: annual average, April-September average, October-March average).

respectively). In the case of the SRD-model these values are even lower: the 95% percentiles are +0.09 nM and +4.2% (the 5% percentiles are -0.03 nM and -1.34%). Interestingly, both models show three regions where the DMS increase is the highest: the North Atlantic between 40°N and 60°N, some zones of the equatorial Pacific, and the Southern Ocean. Overall, these results are an indication that an increase of DMS under global warming scenario due to a net reduction of the MLD seems possible and robust, but that the global strength of such response will probably be very weak. It is worth noting, however, that the predicted DMS response in tropical regions, and particularly next to the Maritime Continent, Asian equatorial Pacific (where the predicted annual increase is of the order of 10-15%), can be climatically important. This region is weakly affected by anthropogenic sulfur emissions, receives large incident solar radiation, and plays an important role in energy distribution through convection and atmospheric teleconnections (*Meehl*, 1987; *Miller et al.*, 2003). Changes in the radiative balance of this region might have ample climate implications.

A more detailed analysis reveals that the results obtained from the two diagnostic models differ markedly in the seasonality. While for the MLD-model the DMS increases are roughly equally distributed in the two time periods (Apr-Sep and Oct-Mar), the SRD-model predicts higher DMS increases in each hemispheric summer. This is important because the efficiency at which DMS is oxidized to sulfates is highly dependent on the concentration of atmospheric OH radicals (*Hynes et al.*, 1986). Since OH production is UV dependent, it displays a clear seasonality with higher values during each hemispheric summer (*Spivakovsky et al.*, 2000). Although DMS conversion into CCN is influenced also by nitrate radical DMS oxidation at night-time (*Stark et al.*, 2007) and by the presence of other aerosols, particularly over polluted regions, the central role

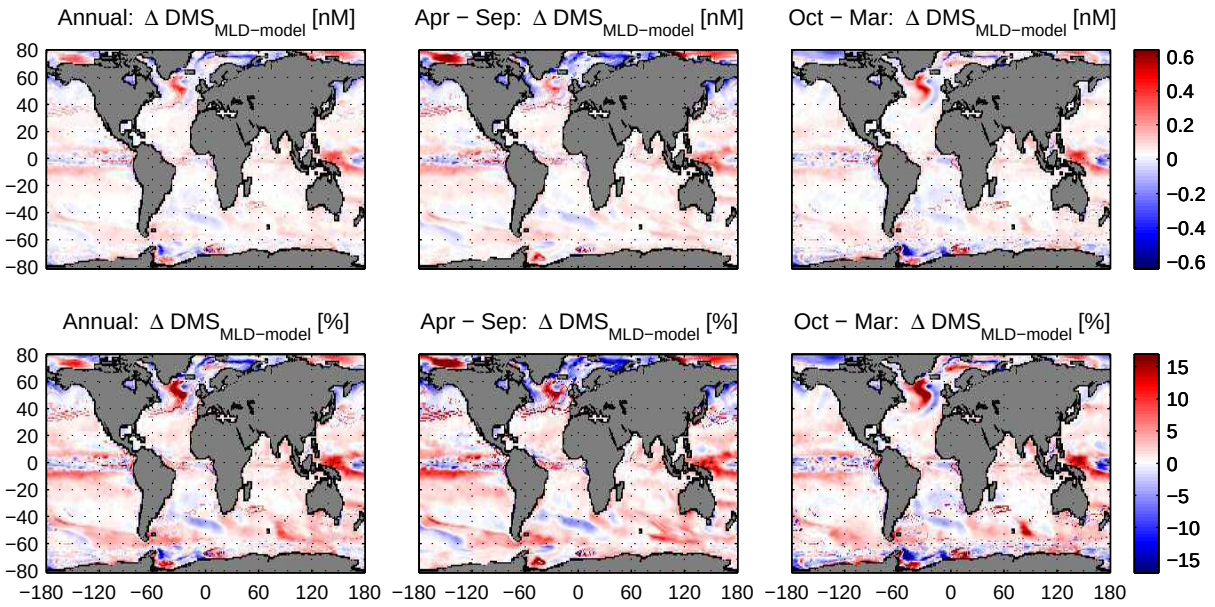


Fig. 6.4: Global maps of the estimated change of DMS under global warming obtained with the MLD-model (*Simó and Dachs*, 2002) (upper panels: averaged absolute change; bottom panels: percentage of change).

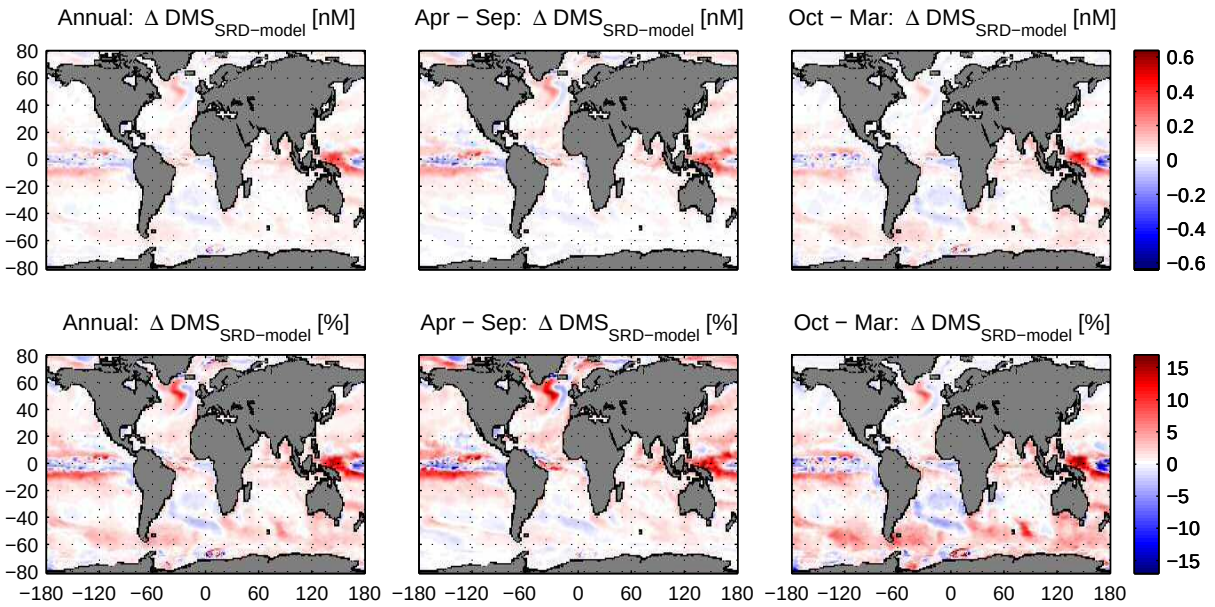


Fig. 6.5: Global maps of the estimated change of DMS under global warming obtained with the SRD-model (*Vallina and Simó*, 2007a) (upper panels: averaged absolute change; bottom panels: percentage of change).

of OH suggests that any coupling (or mismatch) between the seasonalities of DMS and OH could amplify (or buffer) the seasonal contribution of biogenic sulfur to CCN production.

Further, for DMS-derived CCN to become more effective in cooling the Earth, their increase of the cloud optical depth should co-occur with the highest solar irradiances (i.e. in each hemispheric summer). This is particularly true at high latitudes where the summer-to-winter ratio of solar incident radiation is higher. Over these regions, an increase of DMS during winter would be of little help regarding Earth cooling, because of low OH to oxidize DMS into CCN and low solar radiation to reflect back to the space. In other words, estimating the annual changes in DMS concentrations due to global warming without giving information about the season when these changes are predicted to occur results in an incomplete picture if we are to interpret our results within the context of the CLAW hypothesis.

To better quantify this difference we calculated the globally averaged (not spatially resolved) percentage of DMS change, which takes into account the area of each pixel, for three cases: annually, summer conditions, and winter conditions. Results from the two diagnostic models are shown in Figure 6.6. We can clearly observe how, although the annual average is almost identical for the two models ($\approx$1.2%), the summer-to-winter ratio is higher for the SRD-model ($\approx$0.8% in winter, $\approx$1.8% in summer) than for the MLD-model ($\approx$1.1% in winter, $\approx$1.5% in summer). As we stated previously, in the context of DMS predictions by empirical diagnostic models the MLD can be regarded as a proxy of the SRD (*Vallina and Simó*, 2007a), so, in principle the results using one or the other should have been rather similar. Why, therefore, such important differences in the seasonality of the change?. The seasonality of the MLD can be used indeed as a good (non-linear) proxy of the seasonality of SRD because, over seasonal scales, the MLD is mostly set by surface irradiance, and both concur to set the SRD. However this is not necessarily the case over the time scale of global warming. For example, a winter time reduction of the MLD at a high latitude region (e.g. the Southern Ocean) due to global warming, would hardly cause a significant increase of the regional SRD because the surface irradiance is too low. Therefore, if the driving force of the oceanic DMS production is the SRD, using simply a MLD model may over-predict the DMS increase in this scenario. This would specially be the case when estimating winter time increases due to global warming over high latitude regions.

Nevertheless, despite these differences, both models are fairly consistent in their predictions. On a global annual average, the DMS percentage of increase is $\approx$1.2%; in the summer conditions it could go up to 1.8% (Figure 6.6). Our results are consistent with other estimates of the oceanic DMS response to global warming. *Bopp et al.* (2004), based on a completely different diagnostic equation to estimate surface DMS, reported a global increase of DMS flux of 3% in a scenario of 100% increase of $CO_2$ (from $\approx$350 ppm in 1990 to $\approx$700 ppm by 2060). This DMS increase was calculated to give a global radiative forcing of -0.05 W $m^{-2}$, i.e., about 2% reduction of the estimated positive radiative forcing due to increased $CO_2$ ($\approx$ +3 W $m^{-2}$) (*Bopp et al.*, 2004). Based on a mechanistic ecosystem-DMS model, *Gabric et al.* (2001) predicted a 5% increase

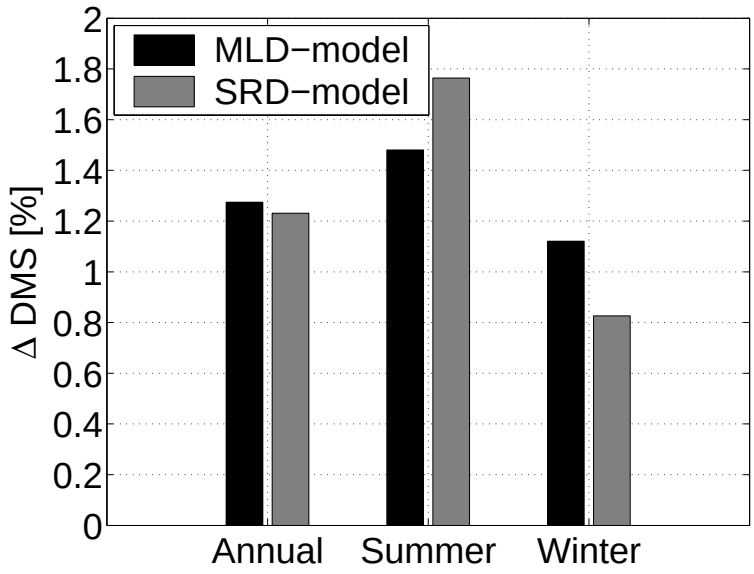


Fig. 6.6: Globally averaged percentage of DMS change under global warming obtained from the MLD-model (*Simó and Dachs*, 2002) and SRD-model (*Vallina and Simó*, 2007a) for three cases: annually, summer conditions, and winter conditions. By 'summer conditions' and 'winter conditions' we mean the regions and periods with a daily-averaged solar surface irradiance higher and lower than 200 W $m^{-2}$, respectively.

of DMS flux for a region of the Southern Ocean under a global warming scenario caused by a $CO_2$ tripling (by 2080) relative to pre-industrial levels. They estimated the associated radiative forcing to be -0.3 W $m^{-2}$, i.e., about a 4% reduction of the estimated $CO_2$ radiative forcing ($\approx$ +7 W $m^{-2}$).

Interestingly *Gabric et al.* (2004) made also use of the *Simó and Dachs* (2002) MLD-model to estimate a global DMS increase under global warming based on MLD fields simulated by the CSIRO Ocean General Circulation Model and CHL fields predicted with an ecological model of their own. They estimated a global DMS flux increase of 14%. This value, however, was highly influenced by an austral-spring DMS flux increase in the 50°S - 60°S region of $\approx$1000%. Out of this season or for any period of the year at the remaining latitudes, the DMS flux shows either a slight increase or a slight decrease (*Gabric et al.*, 2004). The way they modeled CHL was substantially different from ours and this may account for the discrepancy in the results. Their ecosystem model was applied in a zero-dimensional (OD) mode by 10° latitudinal bands, with re-calibration for each one of them. Our approach is based on a global 3D coupled physical-ecological model.

### 6.3.4 DMS and the CLAW hypothesis

When *Charlson et al.* (1987) proposed the CLAW hypothesis they postulated a global climate feedback mechanism that regulates either temperature and/or solar irradiance. However, at that time, they were not able yet to define the nature and tempo of the processes that drive DMS variability and, so, they associated DMS dynamics with long-term climate evolution (*Charl-*

*son et al.*, 1987; *Andreae and Crutzen*, 1997). But temperature and irradiance, although tightly linked, are not the same thing. Twenty years later, it starts to become clear that DMS increases with incident light (*Stefels and van Leeuwe*, 1998; *Sunda et al.*, 2002; *Toole and Siegel*, 2004; *Vallina and Simó*, 2007a) but not with temperature (*van Rijssel and Gieskes*, 2002; *Vallina and Simó*, 2007a; *Vallina*, 2008). Further, surface DMS concentrations are highly seasonal, as CCN production is (*Vallina et al.*, 2006, 2007a). For DMS to be oxidized to sulfates and produce biogenic CCN, high levels of atmospheric OH radicals are needed (*Andreae and Crutzen*, 1997). Since OH is mainly driven by UV radiation, DMS and OH are usually in phase with maxima in summer (*Vallina et al.*, 2007a). This represents an efficient seasonal mechanism for enhanced biogenic CCN formation at the time when harmful solar radiation is the highest.

On the other hand, the DMS-feedback capability as a global thermal regulator over longer time-scales such as that of global warming seems to be weak: the same mechanisms that produce 1000-2000% seasonal increases of DMS concentrations (*Toole and Siegel*, 2004; *Vallina and Simó*, 2007a) (Figure 6.3) are able to produce only a weak response to global warming conditions (1.2%; Figure 6.4, Figure 6.5 and Figure 6.6). Also, the radiative forcing of a long-lived gas like $CO_2$ is very homogeneous both in time and space (*Bopp et al.*, 2004), while CCN formation from DMS and its influence on cloud properties is regional and seasonal since both atmospheric DMS and CCN have much shorter lifetimes. Then a DMS-climate feedback would be most apparent over seasonal scale. There seems to be, therefore, a mismatch between the scales at which DMS influences climate and global warming operates.

We therefore propose a revision of the point of view on the CLAW hypothesis: rather than looking at the DMS-CCN-cloud albedo feedback as a *long-term* mechanism contributing to regulate the Earth's temperature, we should look at it as a *seasonal* mechanism contributing to regulate the solar radiation dose received by the marine pelagic biosphere.

## 6.4 Conclusions

We have estimated the DMS increase under global warming conditions (50% increase from current $CO_2$ levels) by means of two global empirically-derived diagnostic DMS models for which the mixed layer depth is a critical parameter. The goal was to evaluate if the predicted net reduction of the mixed layer depth in global warming scenarios would trigger a significant DMS increase as proposed previously (*Simó and Pedros-Alió*, 1999a; *Simó and Dachs*, 2002; *Toole and Siegel*, 2004)

Our results point towards a net global increase in surface-ocean DMS concentrations, particularly during each hemispheric summer, when a derived increase in CCN numbers and cloud albedo would be more effective in cooling the Earth because it is the period of higher incident

solar radiation. This increase, however, is weak (globally of 1.2% and only in very few places it is higher than ≈5%), so it can hardly be of much relevance to counteract global warming. This contrasts with the seasonal variability of DMS concentrations (easily 1000-2000%). Therefore we suggest that the 'DMS - CCN - cloud albedo' feedback proposed by the CLAW hypothesis does not act as a significant longer-term thermostatic mechanism in the anthropogenically-perturbed Holocene but rather as a seasonal Earth system mechanism that contributes to regulate the solar radiation dose received by the oceanic pelagic biosphere. How much this seasonal mechanism has been contributing to the global radiative balance throughout the history of the pre-industrial Earth is still uncertain (*Andreae and Crutzen*, 1997), but although a significant role is likely, it is not expected to change dramatically with the prospected manifestations of global warming within the current century. However, mechanisms other than mixed layer depth changes could also be involved in a DMS feedback loop, like changes in aeolian or riverine input of nutrients that could alter marine biology (and hence DMS production) in a global warming scenario in ways that are not captured by the seasonality of the SRD dependence. To evaluate if these effects could be of higher importance than those related to MLD changes, a fully-coupled Earth System Model including a reliable mechanistic characterization of the oceanic DMS cycle is needed.

# CHAPTER 7

# Conclusions and Perspectives

*Cross a bridge when one comes to it.*

*(Chinese quote)*

## 7.1 Summary

S. M. Vallina & R. Simó (2007), Re-visiting the CLAW hypothesis
*Environmental Chemistry*, 40(6), doi:10.1071/EN07055. (extended version)

A global negative feedback between biogenic dimethylsulfide (DMS) production by the upper-ocean ecosystems and Earth climate has been suggested to occur through the formation of cloud-forming sulfur aerosols in the troposphere and their impact on cloud albedo and the Earth radiative balance (*Charlson et al.*, 1987). The so-called CLAW hypothesis, although suggestive and not refuted by evidence hitherto, still is highly speculative and some of its main postulates remain unproven. In this study we sought to contribute to the current knowledge of the oceanic biogenic sulfur cycle and its potential impact on climate by addressing some relevant open questions regarding the CLAW hypothesis.

1) *Which is the climatic factor that drives oceanic DMS production? How does it do so?*

*Charlson et al.* (1987) proposed that increases in either sea surface temperature (SST) and/or solar irradiance may be responsible for concomitant increases of DMS concentrations. However, although both variables (temperature and solar irradiance) are closely related, clearly they are not the same thing. For example, they do not display exactly the same seasonality in the upper ocean: temperature usually peaks later than solar irradiance because heating the upper ocean requires some time. Besides, they trigger different responses from the organisms; e.g., phytoplankton photosynthesis is mainly driven by photosynthetically active radiation (PAR), although temperature affects the overall performance of phytoplankton metabolism. Solar irradiance also includes ultra-violet radiation (UVR) which has a deleterious effect on phytoplankton growth (*Perin and Lean*, 2004). The question of whether SST or solar radiation had a bigger impact on DMS production was unanswered for longtime. The analysis of a global DMS data-base as well as local DMS time-series (BATS in the Sargasso Sea and Blanes Blay in the NW Mediterranean) have revealed that it is the solar radiation dose in the upper mixed layer (or SRD) the climatic factor that seems to drive DMS dynamics (*Toole and Siegel*, 2004; *Vallina and Simó*, 2007a; *Vallina et al.*, 2007a). Further, with a spatially resolved perspective, the analysis of globally derived SRD and DMS climatologies shows that the seasonal couplings between SRD and DMS are very tight and widespread over the Global Ocean (see Chapter 4). From these results, we have been able to obtain a global predictive diagnostic equation that relates DMS concentrations to the SRD (see Chapter 5). Thus, DMS usually displays a summer maximum in surface waters, even in regions where a phytoplankton biomass proxy like chlorophyll-a (CHL) shows an annual minimum in summer (*Dacey et al.*, 1998; *Vallina et al.*, 2006; *Vila-Costa et al.*, 2008) (subtropical and low temperate regions), a feature known as the DMS summer-paradox (*Simó and Pedros-Allió*, 1999a). Over these regions phytoplankton display a summer minimum due to nutrient depletion after water column stratification, at the time when the annual DMS maximum occurs (*Vallina et al.*, 2008) (see Chapter 2).

The SRD is highly related to the ultraviolet radiation (UVR) dose in the upper mixed layer of the ocean. It has been experimentally observed that UVR can affect two of the major biological players in the oceanic sulfur cycle: *i*) heterotrophic bacterioplankton, prokariotic organisms that can be both a source and a sink for DMS; and *ii*) phytoplankton, the primary producers of dimethylsulfoniopropionate (DMSP), the DMS precursor. The question, then, is which organisms and processes the SRD may be acting upon to drive DMS dynamics. Most groups of heterotrophic bacteria take up and metabolize DMSP as a major sulfur source and bacterioplankton overall convert only a minor proportion of it into DMS (*Kiene and Linn*, 2000; *Yoch*, 2002). Some specialized bacteria are capable of degrading DMS (*Vila-Costa et al.*, 2006a; *del Valle et al.*, 2007). UVR is known to cause DNA damage and can inhibit bacterial activity (*Herndl et al.*, 1993), so it was suggested that summer time inhibition of bacterial DMS consumption (*Slezak et al.*, 2001) could contribute to the observed DMS accumulation (*Simó and Pedros-Allió*, 1999a). UVR has also been observed to produce an increase in the amounts of DMSP and DMS per cell volume in phytoplankton, and an intra-cellular DMSP/DMS conversion system has been suggested to play an antioxidant role to cope with high UVR doses (by scavenging the harmful hydroxyl radical, OH) (*Sunda et al.*, 2002). Based on a mechanistic model of an oceanic pelagic ecosystem that includes both phytoplankton and bacterioplankton, coupled to a biogenic sulfur cycle, we have suggested that bacteria, although being major players in DMS production and consumption, do not seem to to play the main role in controlling DMS seasonality (see Chapter 2). The model was applied in a one-dimensional (1D) physical frame to the Sargasso Sea, a place where the DMS summer-paradox occurs very markedly. From the analysis of several possible scenarios we conclude that phytoplankton direct production and exudation of DMS in response to solar radiation doses (i.e., UVR doses) may be the major driver of the DMS summer-paradox (*Vallina et al.*, 2008)

2) *Is oceanic DMS a globally relevant source of Cloud Condensation Nuclei?*

Several local field studies have found significant correlations between DMS, its atmospheric oxidation products, sulfates and cloud condensation nuclei (CCN), mostly over remote clean-air remote oceanic regions (*Prospero et al.*, 1991; *Ayers and Gras*, 1991; *Andreae et al.*, 1995; *Ayers et al.*, 1997a; *Clarke et al.*, 1998; *Andreae et al.*, 1999; *Ayers and Gillett*, 2000). These findings, however, lacked the spatial and temporal coverage necessary to resolve whether this DMS-CCN coupling is widespread and therefore relevant for global climate processes. Other works suggested that globally, and specially in the northern hemisphere, most of the atmospheric aerosols and CCN are not comming from DMS oxidation but from continental sources (*Charlson et al.*, 1992; *Husar et al.*, 1997; *Andreae et al.*, 2003; *Vallina et al.*, 2007a). Anthropogenic emissions of sulfur are larger than those from natural sources (*Smith et al.*, 2001; *Gondwe et al.*, 2003). Also, the small-size fraction of sea salt (SS) particles released by breaking waves has been proposed to be a dominant source of CCN over clean-air regions far from continents (*Murphy et al.*, 1998). Finally, organic aerosols of marine biogenic origin are now being seen as a further, potentially large source of CCN (*O'Dowd et al.*, 2004; *Meskhidze and Nenes*, 2006).

The analyses of satellite and model-derived global data of several oceanic and atmospheric variables suggest that DMS oxidation can indeed be a major source of CCN over oceanic regions far from continental aerosol sources (like the Southern Ocean) especially in summer (*Vallina et al.*, 2007a) (see Chapter 4). Small SS aerosols, although quantitatively important, do not seem to control CCN seasonality over the Southern Ocean (SO), a region where SS production is amongst the highest of the world due to the constant presence of strong winds. Rather, SS aerosols appear to conform a fairly constant background of CCN (*Andreae et al.*, 1999). The seasonality of wind speeds and that of the small-mode fraction of aerosols support these conclusions (*Vallina et al.*, 2006) (see Chapter 3). Over clean-air ocean regions DMS emissions seem then to control CCN seasonality and its annual contribution to CCN numbers is estimated to be higher than 60%. Over a global scale, however, the estimated current contribution of DMS to annual CCN numbers is rather moderate, of about 30% (*Vallina et al.*, 2007a). Our results suggest that DMS may therefore be contributing to CCN formation all around the globe (a biogenic source that could have been the main one in the pre-industrial Earth) but that nowadays it is rather a minor source if compared to continental sources of CCN (anthropogenic sulfates, black carbon aerosols, the fine fraction of dust particles, etc.) (*Vallina et al.*, 2007a). Further, due to the strong seasonal coupling of CHL, DMS and CCN over the SO (*Vallina et al.*, 2006), these works (*Vallina et al.*, 2006, 2007a) could not rule out the influence of biogenically driven organic aerosols on CCN (*Meskhidze and Nenes*, 2006). Since we relied on the linear regression between DMS oxidation and CCN numbers obtained for the SO to estimate the regional and global contribution of DMS-derived CCN to total CCN numbers, we were implicitly assuming that the contribution of organic aerosols is minor. Therefore, should the organic source of CCN be found important over the SO, our estimates of the DMS impact on CCN numbers would likely be overestimates.

3) *Which is the time-scale at which the suggested 'DMS - CCN - cloud albedo' feedback operates and what is its sign? Can DMS alleviate global warming?*

In their original paper *Charlson et al.* (1987) proposed that DMS emissions and their influence on CCN production, cloud albedo, and the Earth radiative balance, may be part of a long-term global thermostatic system driven by biological forces. They suggested that a 'DMS - CCN - cloud albedo' feedback could be acting as a natural cooling mechanism: an increase of Earth's temperature would increase oceanic DMS concentrations and its emission to the atmosphere, giving rise to more reflective clouds and to less amount of solar radiation reaching the surface (i.e., less global heating). They speculated that this natural feedback might also counteract anthropogenic global warming. We applied two global DMS diagnostic models, for which the mixing layer depth (MLD) is a key parameter, to global fields of MLD and CHL simulated by a biogeochemistry model embedded into an Ocean General Circulation Model for both global warming conditions (50% increase of present atmospheric $CO_2$) and non-global warming conditions (control). We obtained global maps of DMS concentrations for these two scenarios (*Vallina et al.*, 2007b) (see Chapter 6). By these means we estimated the response of

DMS to global warming. Results were fairly similar for both DMS models: a rather weak increase of DMS concentrations. Globally it was 1.2% and only in very few places the increase was higher than ≈5%. According to these results, therefore, although the sign of the feedback appears to be negative, such a low increase in DMS can hardly counteract significantly the effects of global warming since it represents less than 2% reduction of the estimated positive radiative forcing due to $CO_2$ (*Bopp et al.*, 2004).

Given that experimental evidence points to the SRD and not temperature as the climatic variable that has a large controlling effect on DMS production, the response of oceanic DMS to global temperature warming is expected to be through indirect effects: the associated shoaling of the upper mixed layer would come along with an increase of the SRD, which would cause an increase of surface DMS concentration. Our model simulations suggests that this increase would be small in a ≈50-year scenario of current warming trends (*Vallina et al.*, 2007b). This contrasts with the 1000-2000% increase in DMS concentrations observed every year in the transition from winter to summer, in response to the seasonal variability of solar radiation. We therefore suggest that the 'DMS-CCN-cloud albedo' feedback proposed by the CLAW hypothesis should not be viewed as a long-term thermostatic mechanism (at least at the time scale of anthropogenic global warming) but rather as a seasonal process that contributes to regulate the amount of solar radiation reaching the Earth's biosphere. Such a seasonal feedback is not only contributed by the seasonality of DMS emission but also by the seasonality of the main atmospheric DMS oxidant (the OH radical), which also peaks in summer (*Vallina et al.*, 2007a). The coincidence of both seasonalities greatly increases the efficiency of DMS in CCN formation in summer, when an ecosystem protection against the Sun is more needed.

This suggestion does not contradict the CLAW hypothesis, but introduces a new point of view with important implications for the mechanistic grounds of the evolution of the feedback. We can speculate that if a biosphere-climate co-evolution occurs through sulfur emission, the selective pressure onto individuals and/or ecosystems that eventually leads to more or less DMS production is to be found in the adaptation to the conditions of their season of optimal growth. Thus, plankton species and communities better adapted to grow in the highly irradiated (and generally low-nutrient) waters characteristic of the summer months are higher DMS producers than species and communities adapted to grow in lowly irradiated, nutrient richer, mixed waters. These adaptations built on physiological responses to environmental stressors (oxidative stress caused by high UVR and nutrient deficiency in both primary and secondary producers, DNA damage caused by UVR in bacteria, C and S overflow caused by N and P deficiency in primary producers) happen to affect climate in a way that reduces the environmental stressors (*Simó*, 2001, 2004; *Stefels et al.*, 2007). We do not know if such a complex negative feedback has been operating through the large environmental changes occurred over the long history of the Earth, but observational evidence indicates that it does take place every year with the change of the seasons.

## 7.2 Main uncertainties

We have inferred the connections between SRD, DMS and CCN mostly from observed seasonal couplings between the variables. Although our conclusions are well grounded and supported by previous works based on laboratory and field research, seasonal correlations are not a proof of causal links. At the most they are a 'necessary but not sufficient' condition, so that they can serve to reject hypothesis, not to prove them. Therefore, although we presented strong evidences to support causal links, our approach does not fully rule out that the observed correlations are due to an independent seasonal variation of the studied variables.

Also, even assuming that the observed relationship between the SRD and DMS concentrations reflects a causal link (and can hence be used as a diagnostic model), it is uncertain if the relationship will hold in the future. Its extrapolation into global warming scenarios, therefore, carries some associated uncertainty. Of course, the same applies to the Biogeochemistry / Ocean General Circulation Model results onto which the DMS diagnostic models were based to estimate future DMS concentrations. All in all, our results give at least a useful 'order of magnitude' estimate of the (potential) future DMS changes due to global warming.

## 7.3 Future research

The suggested mechanism of a seasonally varying phytoplankton DMS leakage (driven by SRD-induced stress) as a major factor controlling seasonal DMS dynamics is missing in other current models of the oceanic sulfur cycle. Future research should address its inclusion in 3D global DMSP/DMS models in order to obtain more realistic fields of DMS concentrations and particularly of its seasonality. More realistic global DMS fields will be helpful for atmospheric models of sulfur derived cloud-forming aerosols, and therefore in the study of present and future climate situations.

Most of DMSP/DMS models lack also of *in-situ* seasonal data of sulfur related flux rates (e.g. bacterial DMSP or DMS consumption, phytoplankton DMS production, etc.). For this reason models are poorly constrained. Future efforts should be invested to measure not only DMPS/DMS concentrations but also their flux rates within the food web and the ecosystem.

Satellite retrieval of fine atmospheric variables started to be operative about 5 years ago. Therefore the time series are still too short to evaluate longer trends in CCN concentrations and relate them to DMS production. For example, it would be important to evaluate if large-scale climate events like 'El Niño' and 'La Niña' can produce changes in either DMS and/or CCN to test causal links between them. Also, global CCN estimations from satellite-retrieved

parameters are still poorly validated with *in-situ* data, and future projects addressing this issue are required.

Finally, a step ahead to understand more in deep the suggested biosphere-climate feedback through DMS production would be the building of a fully coupled Global Earth System Model (GESM) where land, ocean, atmosphere, and ice were represented and coupled to each other. Such a model would include the interactions of ocean physics, biogeochemistry and climate, so that there would be no need to use prescribed forcings to run the model into the future since they will come up from the simulations. One of the obvious challenges for building this comprehensive model would be a realistic representation of the evolution and biogeochemical impacts of human activities. If achievable, this type of model would allow the sign and the strength of the CLAW and other Earth feedbacks to be evaluated with an unprecedented detail.

# Bibliography


Albrecht, B. A. (1989), Aerosols, cloud microphysics, and fractional cloudiness, *Science*, *245(4923)*, 1227–1230.

Alexander, B., R. J. Park, D. J. Jacob, Q. B. Li, R. M. Yantosca, J. Savarino, C. C. W. Lee, and M. H. Thiemens (2005), Sulfate formation in sea-salt aerosols: Constraints from oxygen isotopes, *J. Geophys. Res.*, *110(D10307)*, doi: 10.1029/2004JD005659.

Anderson, T. R. (1992), Modeling the influence of food C:N ratio, and respiration on growth and nitrogen excretion in marine zooplankton and bacteria, *J. Plankton Res.*, *14*, 1645–1671.

Anderson, T. R., and D. O. Hessen (1995), Carbon or nitrogen limitation of marine copepods?, *J. Plankton Res.*, *17*, 317–331.

Anderson, T. R., and P. Pondaven (2003), Non-redfield carbon and nitrogen cycling in the Sargasso Sea: pelagic imbalances and export flux, *Deep-Sea Res., Part I*, *50*, 573–591.

Anderson, T. R., and P. J. I. B. Williams (1998), Modelling the seasonal cycle of dissolved organic carbon at Station E1 in the English Channel, *Estuarine, Coastal and Shelf Science*, *46*, 93–109.

Andreae, M. O., and P. J. Crutzen (1997), Atmospheric aerosols: biogeochemical sources and role in the atmospheric chemistry, *Science*, *276*, 1052–1058.

Andreae, M. O., W. Elbert, and S. J. de Mora (1995), Biogenic sulfur emissions and aerosols over the tropical South Atlantic: 3. Atmospheric dimethylsulfide, aerosols and cloud condensation nuclei, *J. Geophys. Res.*, *100(D6)*, 11,335–11,356.

Andreae, M. O., W. Elbert, Y. Cai, and T. W. Andreae (1999), Non-sea-salt sulfate, methanesulfonate, and nitrate aerosol concentrations and size distributions at Cape Grim, Tasmania, *J. Geophys. Res.*, *104(D1)*, 21,695–21,706.

Andreae, M. O., T. W. Andreae, D. Meyerdierks, and C. Thiel (2003), Marine sulfur cycling and the atmospheric aerosol over the springtime North Atlantic, *Chemosphere*, *52*, 1321–1343.

Andreae, W. T., M. O. Andreae, and G. Schebeske (1994), Biogenic sulfur emissions and aerosols over the tropical South Atlantic: 1. Dimethylsulfide in seawater and in the atmospheric boundary layer, *J. Geophys. Res.*, *99(D11)*, 22,819–22,829.

Andreas, E. L. (1998), A new sea spray generation function for wind speeds up to 32 m/s, *J. Phys. Oceanogr.*, *28(11)*, 2175–2184.

Aranami, K., and S. Tsunogai (2004), Seasonal and regional comparison of oceanic and atmospheric dimethylsulfide in the northern North Pacific: Dilution effects on its concentration during winter, *J. Geophys. Res.*, *109, D12303*, doi: 10.1029/2003JD004288.

Aranami, K., S. Watanabe, S. Tsunogai, A. Ohki, K. Miura, and H. Kojima (2002), Chemical assessment of oceanic and terrestrial sulfur in the Marine Boundary Layer over the Northern North Pacific during summer, *J. Atmos. Chem.*, *41*, 49–66.

Archer, S. D., F. J. Gilbert, P. D. Nightingale, M. V. Zubkov, A. H. Taylor, G. C. Smith, and P. H. Burkill (2002), Transformation of dimethylsulphoniopropionate to dimethyl sulphide during summer in the North Sea with an examination of keyprocesses via a modelling approach, *Deep-Sea Res., Part II*, *49*, 3067–3101.

Arimoto, R. (2001), Eolian dust and climate: relationships to sources, tropospheric chemistry, transport and deposition, *Earth-Science Reviews*, *54*, 29–42.

Ayers, G., and J. Cainey (2007), The CLAW hypothesis: 20 years of Research, *Environmental Chemistry*, *4(6)*.

Ayers, G., and R. W. Gillett (2000), DMS and its oxidation products in the remote marine atmosphere: implications for climate and atmospheric chemistry, *Journal of Sea Research*, *43*, 275–286.

Ayers, G., and J. L. Gras (1991), Seasonal relationship between cloud condensation nuclei and aerosol methanesulphonate in marine air, *Nature*, *353*, 834–835.

Ayers, G. P., and J. P. Ivey (1990), Methanesulfonate in rainwater at Cape Grim, Tasmania, *Tellus*, *42B*, 217–222.

Ayers, G. P., J. P. Ivey, and R. W. Gillet (1991), Coherence between seasonal cycles of dimethyl sulphide, methanesulphonate and sulphate in marine air, *Nature*, *349*, 404–406.

Ayers, G. P., J. P. Ivey, and B. W. Forgan (1995), Dimethylsulfide in marine air at Cape Grim, 41°S, *J. Geophys. Res.*, *100(D10)*, 21,013–21,021.

Ayers, G. P., J. M. Cainey, R. W. Gillett, and J. P. Ivey (1997a), Atmospheric sulphur and cloud condensation nuclei in marine air in the Southern Hemisphere, *Phil. Trans. R. Soc. Lond. B*, *352*, 203–211.

Ayers, G. P., J. M. Cainey, R. W. Gillett, E. S. Saltzman, and M. Hooper (1997b), Sulfur dioxide and dimethylsulfide in marine air at Cape Grim, Tasmania, *Tellus*, *49B*, 292–299.

Ayers, G. P., R. W. Gillett, J. M. Cainey, and A. L. Dick (1999), Chloride and Bromide Loss from Sea-Salt Particle in Southern Ocean Air, *J. Atmos. Chem.*, *33*, 299–319.

Baretta, J. W., W. Ebenhöh, and P. Ruardij (1995), The European Regional Seas Ecosystem Model, a complex marine ecosystem model, *Neth. J. Sea Res*, *33*, 233–246.

Barrie, L. A., M. P. Olson, and K. K. Oikawa (1989), The flux of anthropogenic sulphur into the Arctic from mid-latitudes, *Atmos. Envir.*, *23*, 2502–2512.

Barrie, L. A., et al. (2001), A comparison of large-scale atmospheric sulphate aerosol models (COSAM): overview and highlights, *Tellus*, *53B*, 615–645.

Bates, T. S., J. R. Charlson, and R. H. Gammon (1987), Evidence for the climatic role of marine biogenic sulfur, *Nature*, *329*, 319–320.

Bates, T. S., B. K. Lamb, A. Guenther, J. Dignon, and R. E. Stoiber (1992), Sulfur emissions to the atmosphere from natural sources, *J. Atmos. Chem.*, *14*, 315–337.

Bates, T. S., R. P. Kiene, G. V. Wolfe, P. A. Matrai, F. P. Chavez, K. R. Buck, B. W. Blomquist, and R. L. Cuhel (1994), The cycling of sulfur in surface seawater of the Northeast Pacific, *J. Geophys. Res.*, *99*, 7835–7843.

Bates, T. S., V. N. Kapustin, P. K. Quinn, D. S. Covert, D. J. Coffman, C. Mari, P. A. Durkee, W. J. D. Bruyn, and E. S. Saltzman (1998), Processes controlling the distribution of aerosol particles in the lower marine boundary layer during the First Aerosol Characterization Experiment (ACE-1), *J. Geophys. Res.*, *103(D13)*, 16,369–16,383.

Benkovitz, C. M., M. T. Scholtz, J. Pacyna, L. Tarrasón, J. Dignon, E. C. Voldner, P. A. Spiro, J. A. Logan, and T. E. Graedel (1996), Global gridded inventories of anthropogenic emissions of sulfur and nitrogen, *J. Geophys. Res.*, *101(D22)*, 29,239–29,253.

Berresheim, H., M. O. Andreae, R. L. Iverson, and S. M. Li (1991), Seasonal variation of dimethylsulfide emissions and atmospheric sulfur and nitrogen species over the western north Atlantic Ocean, *Tellus*, *43B*, 353–372.

Bey, I., D. J. Jacob, J. A. Logan, and R. M. Yantosca (2001), Asian chemical outflow to the Pacific in spring: Origins, pathways, and budgets, *J. Geophys. Res., 106(D19)*, 23,097–23,113.

Bopp, L., O. Boucher, O. Aumont, S. Belviso, J. L. Dufresne, M. Pham, and P. Monfray (2004), Will marine dimethylsulfide emissions amplify or alleviate global warming? A model study, *Can. J. Fish. Aquat. Sci., 61*, 826–835.

Boyd, P. W. (2002), Environmental factors controlling phytoplankton processes in the Southern Ocean, *J. Phycol., 38*, 844–861.

Boyd, P. W., et al. (2000), Amesoscale phytoplankton bloom in the polar Southern Ocean stimulated by iron fertilization, *Nature, 407*, 695–702.

Brechtel, F. J., S. M. Kreidenweis, and H. B. Swan (1998), Air mass characteristics, aerosol particle number concentrations, and number size distributions at Macquarie Island during the First Aerosol Characterization Experiment (ACE-1), *J. Geophys. Res., 103(D13)*, 16,351–16,367.

Brimblecombe, P., and D. Shooter (1986), Photo-oxidation of dimethylsulfide in aqueous solution, *Marine Chemistry, 19*, 343–353.

Brock, T. D. (1981), Calculating solar radiation for ecological studies, *Ecologial Modelling, 14*, 1–19.

Broecker, W. S., and T. H. Peng (1982), *Tracers in the Sea*, 690pp pp., Eldigio Press, Columbia University, Palisades, New York.

Brown, C. W., and J. A. Yoder (1994), Coccolithophorid blooms in the global ocean, *J. Geophys. Res., 99(C4)*, 7467–7482.

Brugger, A., D. Slezak, I. Obernosterer, and G. J. Herndl (1998), Photolysis of dimethylsulfide in the northern Adriatic Sea: dependence on substrate concentration, irradiance and DOC concentration, *Marine Chemistry, 59*, 321–331.

Bruyn, W. J. D., T. S. Bates, J. M. Cainey, and E. S. Saltzman (1998), Shipboard measurements of dimethylsulfide and $SO_2$ southwest of Tasmania during the First Aerosol Characterization Experiment (ACE1), *J. Geophys. Res., 103(D13)*, 16,703–16,711.

Bucciarelli, E., and W. G. Sunda (2003), Influence of CO2, nitrate, phosphate, and silicate limitation on intracellular dimethylsulfoniopropionate in batch cultures of the coastal diatom *Thalassiosira pseudonana*, *Limnology and Oceanography, 48(6)*, 2256–2265.

Buseck, P. R., and M. Pósfai (1999), Aireborne minerals and related aerosol particles: Effects on climate and the environment, *Proc. Natl. Acad. Sci., 96*, 3372–3379.

Chapman, E. G., W. J. Shaw, R. C. Easter, X. Bian, and S. J. Ghan (2002), Influence of wind speed averaging on estimates of dimethylsulfide emission fluxes, *J. Geophys. Res., 107(D23)*, doi:10.1029/2001JD001564.

Charlson, R. J., J. E. Lovelock, M. O. Andreae, and S. G. Warren (1987), Oceanic phytoplankton, atmospheric sulfur, cloud albedo and climate, *Nature, 326*, 655–661.

Charlson, R. J., S. E. Schwartz, J. M. Hales, R. D. Cess, J. A. Coakley-Jr., J. E. Hansen, and D. J. Hofmann (1992), Climate forcing by anthropogenic aerosols, *Science, 255*, 423–430.

Chin, M., D. L. Savoie, B. J. Huebert, A. R. Bandy, D. C. Thornton, T. S. Bates, P. K. Quinn, E. S. Saltzman, and W. J. D. Bruyn (2000), Atmospheric sulfur cycle simulated in the global model GOCART: Comparison with field observations and regional budgets, *J. Geophys. Res., 105(D20)*, 24,689–24,712.

Chu, S., S. Elliott, M. Maltrud, J. Rodríguez, and D. J. Erickson (2004), Ecodynamic and eddy admitting simulations of dimethyl sulfide distributions in a global ocean biogeochemistry-circulation model, *Earth Interactions, 8*, 1–25.

Chuck, A. L., S. M. Turner, and P. S. Liss (2002), Direct Evidence for a Marine Source of C1 and C2 Alkyl Nitrates, *Science, 297*, 1151–1154.

Clarke, A. D., et al. (1998), Particle nucleation in the Tropical Boundary Layer and its couplings to marine sulfur sources, *Science*, *282*, 89–92.

Cox, R. A. (1997), Atmospheric sulphur and climate: What have we learned?, *Phil. Trans. R. Soc. Lond. B*, *352(1350)*, 251–254.

Cropp, R. A. (2002), *A biogeochemical modelling analysis of the potential for marine ecosystems to regulate climate by the production of dimethylsulfide*, Ph.D. thesis, Griffith University.

Cropp, R. A., J. Norbury, A. J. Gabric, and R. D. Braddock (2004), Modeling dimethylsulphide production in the upper ocean, *Global biogeochem. Cycles*, *18*, doi:10.1029/2003GB002126.

Cropp, R. A., A. J. Gabric, G. H. McTainsh, and R. D. Braddock (2005), Coupling between ocean biota and atmospheric aerosols: Dust, dimethylsulphide, or artifact?, *Global biogeochem. Cycles*, *19(GB4002)*, doi:10.1029/2004GB002436.

Curran, M. A. J., and G. B. Jones (2000), Dimethylsulfide in the Southern Ocean: Seasonality and flux, *J. Geophys. Res.*, *105(D16)*, 20,451–20,459.

Dacey, J. W. H., and S. G. Wakeham (1986), Oceanic Dimethylsulfide: Production During Zooplankton Grazing on Phytoplankton, *Science*, *233(4770)*, 1314–1316, doi:10.1126/science.233.4770.1314.

Dacey, J. W. H., F. A. Howse, A. F. Michaels, and S. G. Wakeham (1998), Temporal variability of dimethylsulfide and dimethylsulfoniopropionate in the Sargasso Sea, *Deep Sea Res., Part I*, *45*, 2085–2104.

Davis, D., G. Chen, P. Kasibhatla, A. Jefferson, D. Tanner, F. Eisele, D. Lenschow, W. Neff, and H. Berresheim (1998), DMS oxidation in the Antarctic marine boundary layer: Comparison of model simulations and field observations of DMS, DMSO, $DMSO_2$, $H_2SO_2$(g), MSA(g), and MSA(p), *J. Geophys. Res.*, *103(D1)*, 1657–1678.

Davis, D., et al. (1999), Dimethylsulfide oxidation in the equatorial Pacific: Comparison of model simulations with field observations for DMS, $SO_2$, $H_2SO_2$(g), MSA(g), MS, and NSS, *J. Geophys. Res.*, *104(D5)*, 5765–5784.

Davison, B., C. N. Hewitt, C. D. O'Dowd, J. A. Lowe, and M. H. Smith (1996), Dimethyl sulfide, methane sulfonic acid and physicochemical aerosol properties in Atlantic air from the United Kingdom to Halley Bay, *J. Geophys. Res.*, *101(D17)*, 22,855–22,867.

de Boyer-Montégut, C., G. Madec, A. S. Fischer, A. Lazar, and D. Iudicone (2004), Mixed layer depth over the Global Ocean: An examination of profile data and a profile-based climatology, *J. Geophys. Res.*, *109(C12003)*.

del Valle, D. A., D. J. Kieber, and R. P. Kiene (2007), Depth-dependent fate of biologically-consumed dimethylsulfide in the Sargasso Sea, *Marine Chemistry*, *103*, 197–208.

Denman, K. L., and M. A. P. na (1999), A coupled 1-D biological/physical model of the northeast subarctic Pacific Ocean with iron limitation, *Deep-Sea Res., Part II*, *46*, 2877–2908.

Deuzé, J. L., M. Herman, P. Goloub, D. Tanré, and A. Marchand (1999), Characterization of aerosols over ocean from POLDER/ADEOS-1, *Geophys. Res. Lett.*, *26(10)*, 1421–1424, doi:10.1029/1999GL900168.

Dingenen, R. V., F. Raes, and N. R. Jensen (1995), Evidence for anthropogenic impact on number concentration and sulfate content of cloud-processed aerosol particles over the North Atlantic, *J. Geophys. Res.*, *100(D10)*, 21,057–21,067.

DiTullio, G. R., J. Grebmeier, K. R. Arrigo, M. Lizotte, D. H. Robinson, A. Leventer, J. Barry, M. VanWoert, and R. B. Dunbar (2000), Rapid and early export of *Phaeocystis antarctica* blooms in the Ross Sea, Antarctica, *Nature*, *404*, 595–598.

Duncan, B. N., R. V. Martin, A. C. Staudt, R. Yevich, and J. A. Logan (2003), Interannual and seasonal variability of biomass burning emissions constrained by satellite observations, *J. Geophys. Res.*, *108(D2), 4100*, doi:10.1029/2002JD002378.

DuRand, M. D., R. J. Olson, and S. W. Chisholm (2001), Phytoplankton population dynamics at the Bermuda Atlantic Time-series station in the Sargasso Sea, *Deep-Sea Res., Part II*, *41*, 1983–2003.

Easter, C. R., et al. (2004), MIRAGE: Model description and evaluation of aerosols and trace gases, *J. Geophys. Res., 109(D20210)*, doi:10.1029/2004JD004571.

Eigenheer, A., W. Kuhn, and G. Radach (1996), On the sensitivity of ecosystem box model simulations on mixed-layer depth estimates, *Deep-Sea Res., Part I, 43*, 1011–1027.

Eppley, R. W. (1972), Temperature and phytoplankton growth in the sea, *Fish. Bull., 70(4)*, 1063–1085.

Falkowski, P. G. (1997), Evolution of the nitrogen cycle and its influence on the biological sequestration of CO2 in the ocean, *Nature*, *387*, 272.

Falkowski, P. G., Y. Kim, Z. Kolber, C. Wilson, C. Wirick, and R. Cess (1992), Natural versus anthropogenic factors affecting low-level cloud albedo over the North Atlantic, *Science*, *256*, 1311–1313.

Falkowski, P. G., R. T. Barber, and V. Smetacek (1998), Biogeochemical controls and feedbacks on oceanic primary production, *Science*, *281*, 200–206.

Fenneteaux, I., P. Colin, A. Etienne, H. Boudries, A. L. Dutot, P. E. Perros, and G. Toupance (1999), Influence of continental sources of oceanic air composition at the Eastern edge of the North Atlantic Ocean, TOR 1992-1995, *J. Atmos. Chem.*, *32*, 233–280.

Fiore, A. M., D. J. Jacob, H. Liu, R. M. Yantosca, T. D. Fairlie, and Q. B. Li (2003), Variability in surface ozone background over the United States: Implications for air quality policy, *J. Geophys. Res., 108(D24)*, 4787, doi:10.1029/2003JD003855.

Fitzgerald, J. W. (1991), Marine aerosols: A review, *Atmos. Envir., Part A. General Topics*, *25(3-4)*, 533–545.

Friedlingstein, P., L. Bopp, P. Ciais, J.-L. Dufresne, L. Fairhead, H. LeTreut, P. Monfray, and J. Orr (2001), Positive feedback between future climate change and the carbon cycle, *Geophysical Research Letters*, *28(8)*, 1543–1546.

Gabric, A. J., N. Murray, L. Stone, and M. Kohl (1993), Modelling the production of dimethylsulfide during a phytoplankton bloom, *J. Geophys. Res.*, *98*, 22,805–22,816.

Gabric, A. J., G. Ayers, C. N. Murray, and J. Parslow (1996), Use of remote sensing and mathematical modelling to predict the flux of dimethylsulphide to the atmosphere in the Southern Ocean, *Adv. Space Res, 18(7)*, 117–128.

Gabric, A. J., P. H. Whetton, and R. Cropp (2001), Dimethylsulphide production in the subantarctic southern ocean under enhanced greenhouse conditions, *Tellus*, *53B*, 273–287.

Gabric, A. J., R. Cropp, G. P. Ayers, G. McTainsh, and R. Braddock (2002), Coupling between cycles of phytoplankton biomass and aerosol optical depth as derived from SeaWiFS time series in the Subantartic Southern Ocean, *Geophys. Res. Lett., 29(7), 1112*, doi:10.1029/2001GL013545.

Gabric, A. J., R. Simó, R. A. Cropp, A. C. Hirst, and J. Dachs (2004), Modeling estimates of the global emission of dimethylsulfide under enhanced greenhouse conditions, *Global Biogeochem. Cycles*, *18, GB2014*, doi: 10.1029/2003GB002183.

Gabric, A. J., B. Qu, P. Matrai, and A. C. Hirst (2005), The simulated response of dimethylsulfide production in the Arctic Ocean to global warming, *Tellus*, *57B*, 391–403.

Gao, Y., Y. J. Kaufman, D. Tanré, D. Kolber, and P. G. Falkowski (2001), Seasonal distributions of aeolian iron fluxes to the Global Ocean, *Geophys. Res. Lett., 28(1)*, 29–32.

Gaspar, P., Y. Gregoris, and J. M. Lefèvre (1990), A simple kinetic energy model for simulations of the oceanic vertical mixing: Tests at station Papa and Long-Term Upper Ocean Study Site, *J. Geophys. Res., 95*, 16,17916,193.

Gassó, S., and D. A. Hegg (2003), On the retrieval of columnar aerosol mass and CCN concentration by MODIS, *J. Geophys. Res., 108(D1)*, doi:10.1029/2002JD002382.

Geider, R. J., H. MacIntyre, and T. M. Kana (1997), Dynamic model of phytoplankton growth and acclimation: responses of the balanced growth rate and the chlorophyll a: carbon ratio to light, nutrient-limitation and temperature, *Mar. Ecol. Prog. Ser., 148*, 187–200.

Gent, P. R., and J. C. McWilliams (1990), Isopycnal mixing in the ocean circulation models, *J. Phys. Oceanogr.*, *20*, 150–155.

Ghan, S. J., G. Guzman, and H. Abdul-Razzak (1998), Competition between sea salt and sulphate particles as cloud condensation nuclei, *J. Atmos. Sciences*, *55(22)*, 3340–3347.

Gille, S. T. (2005), Statistical characterization of zonal and meridonal ocean wind stress, *J. Atmos. Ocean. Tech.*, *22(9)*, 1353–1372.

Ginoux, P., M. Chin, I. Tegen, J. M. Prospero, B. Holben, O. Dubovik, and S.-J. Lin (2001), Sources and distributions of dust aerosols simulated with the GOCART model, *J. Geophys. Res.*, *106(D17)*, 20,255–20,273.

Givati, A., and D. Rosenfeld (2004), Quantifying precipitation suppression due to air pollution, *J. Appl. Met.*, *43*, 1038–1056.

Gladyshev, G. P. (1997), *Thermodynamic Theory of the Evolution of Living Beings*, Nova Scientific, New York.

Goericke, R., and N. Welschmeyer (1998), Response of Sargasso Sea phytoplankton biomass, growth rates and primary production to seasonally varying physical forcing, *Journal of Plankton Research*, *20*, 2223–2249.

Goloub, P., and O. Arino (2000), Verification of the consistency of POLDER Aerosol Index over land with ATSR-2/ERS-2 fire product, *Geophys. Res. Lett.*, *27(6)*, 899–902.

Gondwe, M., M. Krol, W. Gieskes, W. Klaassen, and H. de Baar (2003), The contribution of ocean-leaving DMS to the global atmospheric burdens of DMS, MSA, $SO_2$, and NSS $SO_4^=$, *Global Biogeochem. Cycles*, *17(2), 1056*, doi: 10.1029/2002GB001937.

Gondwe, M., M. Krol, W. Klaassen, W. Gieskes, and H. de Baar (2004), Comparison of modeled versus measured MSA:nss-$SO_{4=}$ ratios: A global analysis, *Global Biogeochem. Cycles*, *18, GB2006*, doi:10.1029/2003GB002144.

Gong, S. L., L. A. Barrie, J. M. Prospero, D. L. Savoie, G. P. Ayers, J.-P. Blanchet, and L. Spacek (1997), Modeling sea-salt aerosols in the atmosphere 2. Atmospheric concentrations and fluxes, *J. Geophys. Res.*, *102(D3)*, 3819–3830.

Gong, S. L., L. A. Barrie, and M. Lazare (2002), Canadian Aerosol Module (CAM): A size-segregated simulation of atmospheric aerosol processes for climate and air quality models 2. Global sea-salt aerosol and its budgets, *J. Geophys. Res.*, *107(D24), 4779*, doi:10.1029/2001JD002004.

González, J. M., R. P. Kiene, and M. A. Moran (1999), Transformation of Sulfur Compounds by an Abundant Lineage of Marine Bacteria in the $\alpha$-Subclass of the Class *Proteobacteria*, *Aquatic Environmental Microbiology*, *65(9)*, 3810–3819.

Grini, A., G. Myhre, J. K. Sundet, and I. S. A. Isaken (2002), Modeling the annual cycle of sea salt in the global 3D Model Oslo CTM2: Concentrations, fluxes, and radiative impact, *Journal of Climate*, *15*, 1717–1730.

Groene, T. (1995), Biogenic production and consumption of dimethylsulfide (DMS) and dimethylsulfoniopropionate (DMSP) in the marine epipelagic zone: a review, *Journal of Marine Systems*, *6*, 191–209.

Güllü, G., I. Ölmez, S. Aygün, and G. Tuncel (1998), Atmospheric trace element concentrations over the eastern Mediterranean Sea: Factors affecting temporal variability, *J. Geophys. Res.*, *103(D17)*, 21,943–21,954.

Gundersen, K., M. Heldal, S. Norland, D. A. Purdie, and A. H. Knap (2002), Elemental C, N, and P cell content of individual bacteria collected at the Bermuda Atlantic Time-Series Study (BATS) site, *Limnology and Oceanography*, *47(5)*, 1525–1530.

Gunson, J. R., S. A. Spall, T. R. Anderson, A. Jones, I. J. Totterdell, and M. J. Woodage (2006), Climate sensitivity to ocean dimethylsulphide emissions, *Geophysical Research Letters*, *33, L07701*, doi:10.1029/2005GL024982.

Harrison, R. M., J. D. Peak, and A. D. Kaye (1996), Atmospheric aerosol major ion composition and cloud condensation nuclei over the northeast Atlantic, *J. Geophys. Res.*, *101(D2)*, 4425–4434.

Hefu, Y., and G. O. Kirst (1997), Effect of UV-radiation on DMSP content and DMS formation of *Phaeocystis antarctica*, *Polar Biol.*, *18*, 402–409.

Heintzenberg, J., D. C. Covert, and R. V. Dingenen (2000), Size distribution and chemical composition of marine aerosols: a compilation and review, *Tellus*, *52B*, 1104–1122.

Herman, J. R., P. K. Bhartia, O. Torres, C. Hsu, C. Seftor, and E. Celarier (1997), Global distributions of UV-absorbing aerosols from Nimbus 7/TOMS data, *J. Geophys. Res.*, *102(D14)*, 16,911–16,922.

Herndl, G. J., G. Muller-Niklas, and J. Frick (1993), Major role of ultraviolet-B in controlling bacterioplankton growth in the surface layer of the ocean, *Nature*, *361*, 717–719, doi:10.1038/361717a0.

Higurashi, A., and T. Nakajima (2002), Detection of aerosol types over the East China Sea near Japan from four-channel satellite data, *Geophys. Res. Lett.*, *29(17), 1836*, doi:10.1029/2002GL015357.

Higurashi, A., T. Nakajima, B. N. Holben, A. Smirnov, R. Frouin, and B. Chatenet (2000), A study of global aerosol optical climatology with two channel AVHRR remote sensing, *Journal of Climate*, *13(12)*, 2011–2027.

Hirsch, A. I., A. M. Michalak, L. M. Bruhwiler, W. Peters, E. J. Dlugokencky, and P. P. Tans (2006), Inverse modeling estimates of the global nitrous oxide surface flux from 1998-2001, *Global Biogeochem. Cycles*, *20, GB1008*, doi: 10.1029/2004GB002443.

Hudson, G. J., X. Yonghong, and S. S. Yum (1998), Vertical distributions of cloud condensation nuclei spectra over the summertime Southern Ocean, *J. Geophys. Res.*, *103(D13)*, 16,609–16,624.

Husar, R. B., J. M. Prospero, and L. L. Stowe (1997), Characterization of tropospheric aerosols over the oceans with the NOAA Advanced Very High Resolution Radiometer optical thickness operational product, *J. Geophys. Res.*, *102(D14)*, 16,889–16,909.

Hynes, A. J., P. H. Wine, and D. H. Semmes (1986), Kinetics and mechanism of OH reactions with organic sulfides, *J. Phys. Chem.*, *90(17)*, 4148–4156.

Ichoku, C., Y. J. Kaufman, L. A. Remer, and R. Levy (2004), Global aerosol remote sensing from MODIS, *Advances in Space Res.*, *34*, 820–827.

Iglesias-Rodríguez, M. D., C. W. Brown, S. C. Doney, J. Kleypas, D. Kolber, Z. Kolber, P. K. Hayes, and P. G. Falkowski (2002), Representing key phytoplankton functional groups in ocean carbon cycle models: Coccolithophorids, *Global Biogeochem. Cycles*, *16(4), 1100*, doi:10.1029/2001GB001454.

Jickells, T. D., et al. (2005), Global iron connections between desert dust, ocean biogeochemistry, and climate, *Science*, *308*, 67–71.

Jodwalis, C. M., R. L. Benner, and D. L. Eslinger (2000), Modeling of dimethyl sulfide ocean mixing, biological production, and sea-to-air flux for high latitudes, *J. Geophys. Res.*, *105(D11)*, 14,387–14,399.

Johansen, A. M., R. L. Siefert, and M. R. Hoffmann (1999), Chemical characterization of ambient aerosol collected during the southwest monsoon and intermonsoon seasons over the Arabian Sea: Anions and cations, *J. Geophys. Res.*, *104(D21)*, 26,325–26,347.

Jones, A., D. L. Roberts, M. J. Woodage, and C. E. Johnson (2001), Indirect sulphate aerosol forcing in a climate model with an interactive sulphur cycle, *J. Geophys. Res.*, *106(D17)*, 20,293–20,310, doi:10.1029/2000JD000089.

Jourdain, B., and M. Legrand (2001), Seasonal variations of atmospheric dimethylsulfide, dimethylsulfoxide, sulfur dioxide, methanesulfonate, and non-sea-salt sulfate aerosols at Dumont d'Urville (coastal Antarctica) (December 1998 to July 1999), *J. Geophys. Res.*, *106(D13)*, 14,391–14,408.

Kaneyasu, N., and S. Murayama (2000), High concentrations of black carbon over middle latitudes in the North Pacific Ocean, *J. Geophys. Res.*, *105(D15)*, 19,881–19,890.

Kaufman, Y. J., D. Tanré, and O. Boucher (2002), A satellite view of aerosols in the climate system, *Nature*, *419(6903)*, 215–223.

Keller, M. D., and W. Korjeff-Bellows (1996), Physiological aspects of the production of dimethylsulfoniopropionate (DMSP) by marine phytoplankton, in *Biological and Environmental Chemistry of DMSP and Related Sulfonium Compounds*, edited by R. P. Kiene, P. T. Visscher, M. D. Keller, and G. O. Kirst, pp. 131–142, Plenum, New York.

Keller, M. D., W. K. Bellows, and R. R. L. Guillard (1989), Dimethylsulfide production in marine phytoplankton, in *Biogenic Sulfur in the Environment*, edited by E. S. Saltzman and W. J. Cooper, pp. 167–182, American Chemical Society Symposium Series No. 393, Washington, DC.

Kettle, A. J., and M. O. Andreae (2000), Flux of dimethylsulfide from the oceans: A comparison of updated data set and flux models, *J. Geophys. Res., 105 (D22)*, 26,793–26,808.

Kettle, A. J., et al. (1999), A global database of sea surface dimethylsulfide (DMS) measurements and a simple model to predict sea surface DMS as a function of latitude, longitude and month, *Global Biogeochem. Cycles*, *13*, 399–444.

Kieber, D. J., J. Jiao, R. P. Kiene, and T. S. Bates (1996), Impact of dimethylsulfide photochemistry on methyl sulfur cycling in the equatorial Pacific Ocean, *J. Geophys. Res., 101(C2)*, 3715–3722.

Kiehl, J. T., and E. Trenberth (1997), Earth's annual global mean energy budget, *Bulletin of the American Meteorological Society*, *78(2)*, 197–208.

Kiene, R. P. (1992), Dynamics of dimethylsulfide and dimethylsulfoniopropionate in oceanic water samples, *Marine Chemistry*, *37*, 29–52.

Kiene, R. P. (1993), Microbial sources and sinks for methylated sulfur compounds in the marine environment, in *Microbial Growth on C1 Compounds, Vol. 7*, edited by D. P. Kelly and J. C. Murrell, pp. 15–33, Intercept Ltd., Andover.

Kiene, R. P. (1996), Production of methanethiol from dimethylsulfoniopropionate in marine surface waters, *Marine Chemistry*, *54*, 69–83.

Kiene, R. P., and T. S. Bates (1990), Biological removal of dimethylsulfide from sea water, *Nature*, *345*, 702–705.

Kiene, R. P., and L. J. Linn (2000), The fate of dissolved dimethylsulfoniopropionate (DMSP) in seawater: Tracer studies using 35S-DMSP, *Geochimica et Cosmochimica Acta*, *64(16)*, 2797–2810.

Kiene, R. P., and D. Slezak (2006), Low dissolved DMSP concentrations in seawater revealed by small-volume gravity filtration and dialysis sampling, *Limnol. Oceanogr.: Methods*, *4*, 80–95.

Kiene, R. P., L. J. Linn, J. González, M. A. Moran, and J. A. Bruton (1999), Dimethylsulfoniopropionate and methanethiol are important precursors of methionine and protein-sulfur in marine bacterioplankton, *Aquatic Environmental Microbiology*, *65(10)*, 4549–4558.

Kiene, R. P., L. J. Linn, and J. A. Bruton (2000), New and important roles for DMSP in marine microbial communities, *Journal of Sea Research*, *43*, 209–224.

Kirst, G. O., C. Thiel, H. Wolff, J. Nothnagel, M. Wanzek, and R. Ulmke (1991), Dimethylsulfoniopropionate (DMSP) in ice algae and its possible biological role, *Marine Chemistry*, *35*, 381–388.

Kistler, R., et al. (2001), The NCEP-NCAR 50-Year Reanalysis: Monthly Means CD-ROM and Documentation, *Bull. Am. Meteo. Soc., 82(2)*, 247–267.

Kloster, S., J. Feichter, E. Maier-Reimer, K. D. Six, P. Stier, and P.Wetzel (2006), DMS cycle in the marine ocean-atmosphere system - a global model study, *Biogeosciences*, *3*, 29–51.

Kouvarakis, G., and N. Mihalopoulos (2002), Seasonal variation of dimethylsulfide in the gas phase and of methanesulfonate and non-sea-salt sulfate in the aerosol phase in the Eastern Mediterranean atmosphere, *Atmospheric Environment*, *36*, 929–928.

Kouvarakis, G., H. Bardouki, and N. Mihalopoulos (2002), Sulfur budget above the Eastern Mediterranean: relative contribution of anthropogenic and biogenic sources, *Tellus*, *54B*, 201–212.

Kubilay, N., M. Koçak, T. Çokacar, T. Oguz, G. Kouvarakis, and N. Mihalopoulos (2002), Influence of Black Sea and local biogenic activity on the seasonal variation of aerosol sulfur species in the eastern Mediterranean atmosphere, *Global Biogeochem. Cycles*, *16(4), 1079*, doi:10.1029/2002GB001880.

Langner, J., H. Rodhe, P. J. Crutzen, and P. Zimmermann (1992), Anthropogenic influence on the distribution of tropospheric sulphate aerosol, *Nature*, *359*, 712–716.

Laroche, D., A. F. Vézina, M. Levasseur, M. Gosselin, J. Stefels, M. D. Keller, P. A. Matrai, and R. L. J. Kwint (1999), DMSP synthesis and exudation in phytoplankton: a modeling aproach, *Mar. Ecol. Prog. Ser.*, *180*, 37–49.

Lawrence, M. (1993), An empirical analysis of the strength of the phytoplankton-dimethylsulfide-cloud-climate feedback cycle, *J. Geophys. Res.*, *98*, 20,663–20,763.

Le Clainche, Y., M. Levasseur, A. Vézina, J. W. H. Dacey, and F. J. Saucier (2004), Behaviour of the ocean DMS(P) pools in the Sargasso Sea viewed in a coupled physical-biogeochemical ocean model, *Can. J. Fish. Aquat. Sci.*, *61*, 788–803.

Le Quéré, C., et al. (2005), Ecosystem dynamics based on plankton functional types for global ocean biogeochemistry models, *Global Change Biology*, *11(11)*, 2016–1040.

Ledyard, K. M., and J. W. H. Dacey (1996), Microbial cycling of DMSP and DMS in coastal and oligotrophic seawater, *Limnol. Oceanogr.*, *41*, 33–40.

Lee, Z. P., K. P. Du, R. Arnone, S. C. Liew, and B. Penta (2005), Penetration of solar radiation in the upper ocean: A numerical model for oceanic and coastal waters, *J. Geophys. Res.*, *110(C09019)*, doi:10.1029/2004JC002780.

Lefèvre, M., A. Vézina, M. Levasseur, and J. W. H. Dacey (2002), A model of dimethylsulfide dynamics for the subtropical North Atlantic, *Deep Sea Res., Part I*, *49*, 2221–2239.

Lefohn, A. S., J. D. Husar, and R. B. Husar (1999), Estimating historical anthropogenic global sulfur emission patterns for the period 1850-1990, *Atmospheric Environment*, *33*, 3435–3444.

Lenton, T. M., and A. J. Watson (2000), Redfield revisited 1. Regulation of nitrate, phosphate, and oxygen in the ocean, *Global Biogeochem. Cycles*, *14*, 225–248.

Levasseur, M., M. Scarratt, S. Roy, D. Laroche, S. Michaud, G. Cantin, M. Gosselin, and A. Vézina (2004), Vertically resolved cycling of dimethylsulfoniopropionate (DMSP) and dimethylsulfide (DMS) in the Northwest Atlantic in spring, *Can. J. Fish. Aquat. Sci.*, *61*, 744–757.

Levasseur, M., et al. (1996), Production of DMSP and DMS during a mesocosm study of an Emiliania huxleyi bloom: Influence of bacteria and Calanus finmarchicus grazing, *Marine Biology*, *126(4)*, 609–618.

Levitus, S. (1982), Climatological atlas of the world, nOAA Professional Paper No. 13, U.S. Department of Commerce, Rockville.

Li, F., and V. Ramanathan (2002), Winter to summer monsoon variation of aerosol optical depth over the tropical Indian Ocean, *J. Geophys. Res.*, *107(D16), 4284*, doi:10.1029/2001JD000949.

Li-Jones, X., and J. M. Prospero (1998), Variations in the size distribution of non-sea-salt sulfate aerosol in the marine boundary layer at Barbados: Impact of African dust, *J. Geophys. Res.*, *103(D13)*, 16,073–16,084.

Liss, A. D. H. G. M. P. D. N., P. S., and S. M. Turner (1997), Marine sulphur emissions, *Phil. Trans. R. Soc. Lond. B*, *352*, 159–169.

Liss, P. S., and L. Mervilat (1986), Air-seagas exchange rates: Introduction and synthesis, in *The role of sea-air exchange in geochemical cycling*, edited by P. Buat-Menard, pp. 113–127, Reidel.

Lobert, M. J., W. C. Keene, J. A. Logan, and R. Yevich (1999), Global chlorine emissions from biomass burning: Reactive chlorine emissions inventory, *J. Geophys. Res.*, *104(D7)*, 8373–8389.

Lovelock, J. E. (1979), *Gaia: A new look at life on Earth*, 185 pp., Oxford University Press, New York.

Lovelock, J. E. (1988), *The Ages of Gaia*, 305 pp., W. W. Norton, New York.

Lovelock, J. E., and L. Margulis (1974), Atmospheric homeostasis by and for the biosphere: the Gaia hypothesis, *Tellus*, *26*, 1–44.

Madec, G., and M. Imbard (1996), A global ocean mesh to overcome the north pole singularity, *Clim. Dyn.*, *12*, 381–388.

Madec, G., P. Delecluse, M. Imbard, and C. Lévy (1999), *OPA 8.1 Ocean General Circulation Model Reference Manual*, Lab. dOcéanogr. Dyn. et de Climatol., Paris.

Malin, G. (2006), OCEANS: New Pieces for the Marine Sulfur Cycle Jigsaw, *Science*, *314*, 607–608.

Malmstrom, R. R., R. P. Kiene, and D. L. Kirchman (2004), Identification and enumeration of bacteria assimilating dimethylsulfoniopropionate (DMSP) in the North Atlantic and Gulf of Mexico, *Limnol. Oceanogr.*, *49(2)*, 597–606.

Manizza, M. (2006), Climate Change and Biogeophysics, in *Modelling phytoplankton-ligth feedback and its ocean biogeochemical implications*, Ph.D. thesis, University of East Anglia, UK, available at http://lgmacweb.env.uea.ac.uk/green_ocean/publications/manfredi/Manizza_thesis060722.pdf.

Mari, C., K. Suhre, T. S. Bates, J. E. Johnson, R. Rosset, A. R. Bandy, F. L. Eisele, R. L. M. III, and D. C. Thornton (1998), Physico-chemical modeling of the First Aerosol Characterization Experiment (ACE 1) Lagrangian B: 2. DMS emission, transport and oxidation at the mesoscale, *J. Geophys. Res.*, *103(D13)*, 16,457–16,473.

Martin, J. H., et al. (1994), Testing the iron hypothesis in ecosystems of the equatorial Pacific Ocean, *Nature*, *371*, 123–129.

Matrai, P. A., and M. Keller (1993), Dimethylsulfide in a large-scale coccolithophore bloom in the Gulf of Maine, *Cont. Shelf Res.*, *13*, 831–843.

Matrai, P. A., M. Vernet, R. Hood, A. Jennings, E. Brody, and S. Saemundsdóttir (1995), Light-dependence of carbon and sulfur production by polar clones of the genus Phaeocystis, *Journal Marine Biology*, *124(1)*, 157–167.

Matsui, T., H. Masunaga, R. Pielke, and W. Tao (2004), Impact of aerosols and atmospheric thermodynamics on cloud properties within the climate system, *Geophys. Res. Lett.*, *31(6)*, doi:10.1029/2003GL019287.

McInnes, L., D. Covert, and B. Baker (1997), The number of sea-salt, sulfate, and carbonaceous particles in the marine atmosphere: EM measurements consistent with ambient size distribution, *Tellus*, *49B*, 300–313.

McTainsh, G. H., A. W. Lynch, and E. K. Tews (1998), Climatic controls upon dust storm occurrence in eastern Australia, *Journal of Arid Environments*, *39*, 457–466.

Meehl, G. A. (1987), The tropics and their role in the global climate system, *The Geographical Journal*, *153(1)*, 21–36.

Meir, P., P. Cox, and J. Grace (2006), The influence of terrestrial ecosystems on climate, *Trends Ecol. Evol.*, *21*, 254–300.

Merzouk, A., M. Levasseur, M. G. Scarratt, S. Michaud, and M. Gosselin (2004), Influence of dinoflagellate diurnal vertical migrations on dimethylsulfoniopropionate and dimethylsulfide distribution and dynamics (St. Lawrence Estuary, Canada), *Can. J. Fish. Aquat. Sci.*, *61*, 712–720.

Merzouk, A., M. Levasseur, M. G. Scarratt, S. Michaud, and M. Gosselin (2006), Diel variations in DMSP and DMS production during vertical migration of dinoflagellates, *Can. J. Fish. Aquat. Sci.*, in press.

Meskhidze, N., and A. Nenes (2006), Phytoplankton and cloudiness in the Southern Ocean, *Science*, *314*, 1419–1423.

Mihalopoulos, N., E. Stephanou, M. Kanakidou, and S. Pilitsidis (1997), Tropospheric aerosol ionic composition in the Eastern Mediterranean region, *Tellus*, *49B*, 314–326.

Miller, A. J., et al. (2003), Potential feedbacks between Pacific Ocean ecosystems and interdecadal climate variations, *Bull. Am. Meteorol. Soc.*, *84(5)*, 617–633.

Minikin, A., M. Legrand, J. Hall, D. Wagenbach, C. Kleefeld, E. Wolff, E. C. Pasteur, and F. Ducroz (1998), Sulfur-containing species (sulfate and methanesulfonate) in coastal Antarctic aerosol and precipitation, *J. Geophys. Res., 103(D9)*, 10,975–10,990.

Moloney, C. L., M. O. Bergh, J. G. Field, and R. C. Newell (1986), The effect of sedimentation and microbial nitrogen regeneration in a plankton community: a simulation investigation, *J. of Plankton Research*, *8*, 426–445.

Moore, J. K., and M. R. Abbott (2000), Phytoplankton chlorophyll distributions and primary production in the Southern Ocean, *J. Geophys. Res., 105(C12)*, 28,709–28,722.

Moore, J. K., M. R. Abbott, and J. G. Richman (1999), Location and dynamics of the Antarctic Polar Front from satellite sea surface temperature data, *J. Geophys. Res., 104(C2)*, 3059–3073.

Müller, D., K. Franke, F. Wagner, D. Althausen, A. Ansmann, and J. Heintzenberg (2001), Vertical profiling of optical and physical particle properties over the tropical Indian Ocean with six-wavelength lidar: 1. Seasonal cycle, *J. Geophys. Res., 106(D22)*, 28,567–28,575.

Murphy, D. M., et al. (1998), Influence of sea-salt on aerosol radiative properties in the Southern Ocean marine boundary layer, *Nature*, *392*, 62–65.

Nagao, I., K. Matsumoto, and H. Tanaka (1999), Characteristics of dimethylsulfide, ozone, aerosols, and cloud condensation nuclei in air masses over the northwestern Pacific Ocean, *J. Geophys. Res., 104(D9)*, 11,675–11,693.

Nguyen, B. C., N. Mihalopoulos, and S. Belviso (1990), Seasonal variation of atmospheric dimethylsulfide at Amsterdam Island in the southern Indian Ocean, *J. Atmos. Chem., 11(1-2)*, 123–141.

Nguyen, B. C., N. Mihalopoulos, J. P. Putaud, A. Gaudry, and L. Gallet (1992), Covariations in oceanic dimethyl sulfide, its oxidation products and rain acidity at Amsterdam Island in the Southern Indian Ocean, *J. Atmos. Chem., 15*, 39–53.

Nightingale, P. D., G. Malin, C. S. Law, A. J. Watson, P. S. Liss, M. I. Liddicoat, J. Boutin, and R. C. Upstill-Goddard (2000), In situ evaluation of air-sea gas exchange parameterizations using novel conservative and volatile tracers, *Global Biogeochem. Cycles*, *14*, 373–387.

Niki, T., M. Kunugi, and A. Otsuki (2000), DMSP-lyase activity in five marine phytoplankton species: its potential importance in DMS production, *Marine Biology*, *136*, 759–764.

Novakov, T., and J. E. Penner (1993), Large contribution of organic aerosols to cloud-condensation-nuclei concentrations, *Nature*, *365*, 823–826.

Obernosterer, I., P. Ruardij, and G. J. Herndl (2001), Spatial and diurnal dynamics of dissolved organic matter (DOM) fluorescence and $H_2O_2$ and the photochemical oxygen demand of surface water DOM across the subtropical Atlantic Ocean, *Limnol. Oceanogr., 46*, 632–643.

O'Dowd, C. D., J. A. Lowe, M. H. Smith, B. Davison, C. N. Hewitt, and R. M. Harrison (1997), Biogenic sulphur emissions and inferred non-sea-salt-sulphate cloud condensation nuclei in and around Antarctica, *J. Geophys. Res., 102(D11)*, 12,839–12,854.

O'Dowd, C. D., J. A. Lowe, and M. H. Smith (1999), Coupling sea-salt and sulphate interactions and its impact on cloud droplet concentration predictions, *Geophys. Res. Lett., 26(9)*, 1311–1314.

O'Dowd, C. D., M. C. Facchini, F. Cavalli, D. Ceburnis, M. Mircea, S. Decesari, S. Fuzzi, Y. J. Yoon, and J.-P. Putaud (2004), Biogenically driven organic contribution to marine aerosol, *Nature*, *431*, 676–680.

O'Dowd, C. D., et al. (2002), Marine aerosol formation from biogenic iodine emissions, *Nature*, *417*, 632–636.

Ohtani, K. (2000), Bootstrapping $r^2$ and ajusted $r^2$ in regression analysis, *Economic Modelling*, *17*, 473–483.

Perin, S., and D. R. S. Lean (2004), The effects of ultraviolet-B radiation on freshwater ecosystems of the Artic: Influence from stratospheric ozone depletion and climate change, *Environmental Reviews*, *12*, 1–70.

Perry, K. D., T. A. Cahill, R. A. Eldred, D. D. Dutcher, and T. E. Gill (1997), Long-range transport of North African dust to the eastern United States, *J. Geophys. Res., 102(D10)*, 11,225–11,238.

Platnick, S., and S. Twomey (1994), Determining the susceptibility of cloud albedo to changes in droplet concentration with the advanced very high resolution radiometer, *J. Applied Meteorology*, *33(3)*, 334–347.

Press, W. H., B. P. Flannery, S. A. Teukolsky, and W. T. Vetterling (1992), *Numerical Recipes in FORTRAN: The Art of Scientific Computing*, 710 pp., Cambridge University Press, Cambridge, England.

Prospero, J. M. (1996a), The atmospheric transport of particles to the ocean, in *Particle Flux in the Ocean*, edited by V. Ittekkot, P. Schäfer, S. Honjo, and P. J. Depetris, pp. 20–52, John Wiley & Sons Ltd.

Prospero, J. M. (1996b), Saharan dust transport over the North Atlantic Ocean and Mediterranean: An overview, in *The impact of Desert Dust Across the Mediterranean*, edited by S. Guerzoni and R. Chester, pp. 133–151, Kluwer Academic Publishers, Netherlands.

Prospero, J. M. (1999), Long-range transport of mineral dust in the global atmosphere: Impact of African dust on the environment of the southeastern United States, *Proc. Natl. Acad. Sci.*, *96*, 3396–3403.

Prospero, J. M., D. L. Savoie, E. S. Saltzman, and R. Larsen (1991), Impact of oceanic sources of biogenic sulphur on sulphate aerosol concentrations at Mawson, Antarctica, *Nature*, *350*, 221–223.

Prospero, J. M., P. Ginoux, O. Torres, S. E. Nicholson, and T. E. Gill (2002), Environmental characterization of global sources of atmospheric soil dust identified with the Nimbus 7 Total Ozone Mapping Spectrometer (TOMS) absorbing aerosol product, *Reviews of Geophysics*, *40(1)*, 21–31.

Prospero, J. M., D. L. Savoie, and R. Arimoto (2003), Long-term record of nss-sulfate and nitrate in aerosols on Midway Island, 1981-2000: Evidence of increased (now decreasing?) anthropogenic emissions from Asia, *J. Geophys. Res.*, *108(D1), 4019*, doi:10.1029/2001JD001524.

Putaud, J. P., N. Mihalopoulos, B. C. Nguyen, and J. M. Campin (1992), Seasonal variations of atmospheric sulfur dioxide and dimethylsulfide concentrations at Amsterdam Island in the Southern Indian Ocean, *J. Atmos. Chem.*, *15*, 117–131.

Quinn, P. K., D. J. Coffman, V. N. Kapustin, and T. S. Bates (1998), Aerosol optical properties in the marine boundary layer during the First Aerosol Characterization Experiment (ACE-1) and the underlying chemical and physical aerosol properties, *J. Geophys. Res., 103(D13)*, 16,547–16,563.

Rajeev, K., V. Ramanathan, and J. Meywerk (2000), Regional aerosol distribution and its long-range transport over the Indian Ocean, *J. Geophys. Res., 105(D2)*, 2029–2043.

Ramanathan, V., et al. (2001), Indian Ocean Experiment: An integrated analysis of the climate forcing and effects of the great Indo-Asian haze, *J. Geophys. Res., 106(D22)*, 28,371–28,398.

Rasch, P. J., M. C. Barth, J. T. Kiehl, S. E. Schwartz, and C. M. Benkovitz (2000), A description of the global sulfur cycle and its controlling processes in the National Center for Atmospheric Research Community Climate Model, version 3, *J. Geophys. Res., 105(D1)*, 1367–1385.

Rasmus, K. E., W. Granéli, and S.-Å. Wängberg (2004), Optical studies in the Southern Ocean, *Deep-Sea Res., Part II*, *51*, 2583–2597.

Remer, L. A., et al. (2005), The MODIS aerosol algorithm, products and validation, *J. Atmos. Sciences*, *Special Section, 62*, 947–973.

Reynolds, R. W., and T. M. Smith (1995), A high-resolution global sea surface temperature climatology, *J. Climate*, *8*, 1571–1583.

Rhoads, K. P., P. Kelley, R. R. Dickerson, T. P. Carsey, M. Farmer, D. L. Savoie, and J. M. Prospero (1997), Composition of the troposphere over the Indian Ocean during the monsoonal transition, *J. Geophys. Res., 102(D15)*, 18,981–18,995.

Rosenfeld, D. (2000), Suppression of rain and snow by urban and industrial air pollution, *Science*, *287*, 1793–1796.

Ross, K. E., S. J. Piketh, R. T. Bruintjes, R. P. Burger, R. J. Swap, and H. J. Annegarn (2003), Spatial and seasonal variations in CCN distribution and the aerosol-CCN relationship over southern Africa, *J. Geophys. Res.*, *108(D13), 8481*, doi: 10.1029/2002JD002384.

Rotstayn, L. D., and U. Lohmann (2002), Simulation of the tropospheric sulfur cycle in a global model with a physically based cloud scheme, *J. Geophys. Res.*, *107(D21), 4592*, doi:10.1029/2002JD002128.

Sarmiento, J. L., et al. (2004), Response of ocean ecosystems to climate warming, *Global Biogeochem. Cycles*, *18, GB3003*, doi:10.1029/2003GB002134.

Satheesh, S. K., V. Ramanathan, X. Li-Jones, J. M. Lobert, I. A. Podgorny, J. M. Prospero, B. N. Holben, and N. G. Loeb (1999), A model for the natural and anthropogenic aerosols over the tropical Indian Ocean derived from Indian Ocean Experiment data, *J. Geophys. Res.*, *104(D22)*, 27,421–27,440.

Satheesh, S. K., V. Ramanathan, B. N. Holben, K. K. Moorthy, N. G. Loeb, H. Maring, J. M. Prospero, and D. Savoie (2002), Chemical, microphysical, and radiative effects of Indian Ocean aerosols, *J. Geophys. Res.*, *107(D23), 4725*, doi:10.1029/2002JD002463.

Savoie, D. L., and J. M. Prospero (1989), Comparison of oceanic and continental sources of non-sea-salt sulphate over the Pacific Ocean, *Nature*, *339*, 685–687.

Savoie, D. L., J. M. Prospero, and E. S. Saltzman (1989), Nitrate, non-seasalt sulfate and methanesulfonate over the Pacific Ocean, in *Chemical Oceanography, X*, edited by J. Riley and R. Chester, pp. 219–250, Academic Press, New York.

Savoie, D. L., J. M. Prospero, R. J. Larsen, and E. S. Saltzman (1992), Nitrogen and sulfur species in acrosols at Mawson, Antarctica, and their relationship to natural radionuclides, *J. Atmos. Chem.*, *14(1-4)*, 181–204.

Savoie, D. L., J. M. Prospero, R. Arimoto, and R. A. Duce (1994), Non-sea-salt sulfate and methanesulfonate at American Samoa, *J. Geophys. Res.*, *99(D2)*, 3587–3596.

Savoie, D. L., R. Arimoto, W. C. Keene, J. M. Prospero, R. A. Duce, and J. N. Galloway (2002), Marine biogenic and anthropogenic contributions to non-sea-salt sulfate in the marine boundary layer over the North Atlantic Ocean, *J. Geophys. Res.*, *107(D18), 4356*, doi:10.1029/2001JD000970.

Sciare, J., E. Baboukas, R. Hancy, N. Mihalopoulos, and B. C. Nguyen (1998), Seasonal variation of dimethylsulfoxide in rainwater at Amsterdam Island in the Southern Indian Ocean: Implications on the biogenic sulfur cycle, *J. Atmos. Chem.*, *30*, 229–240.

Sciare, J., N. Mihalopoulos, and B. C. Nguyen (1999), Summertime seawater concentrations of dimethylsulfide in the west Indian Ocean: Reconciliation of fluxes and spatial variability with long-term atmospheric observations, *J. Atmos. Chem.*, *32*, 357–373.

Sciare, J., N. Mihalopoulos, and F. J. Dentener (2000), Interannual variability of atmospheric dimethylsulfide in the southern Indian Ocean, *J. Geophys. Res.*, *105(D21)*, 26,369–26,377.

Shon, Z.-H., et al. (2001), Evaluation of the DMS flux and its conversion to $SO_2$ over the Southern Ocean, *Atmospheric Environment*, *35(1)*, 159–172.

Simó, R. (2001), Production of atmospheric sulfur by oceanic plankton: biogeochemical, ecological and evolutionary links, *Trends in Ecology & Evolution*, *16(6)*, 287–294.

Simó, R. (2004), From cells to globe: approaching the dynamics of DMS(P) in the ocean at multiple scales, *Can. J. Fish. Aquat. Sci.*, *61*, 673–684.

Simó, R., and J. Dachs (2002), Global ocean emission of dimethylsulfide predicted from biogeophysical data, *Global biogeochem. Cycles, 16(4)*, doi:10.1029/2001GB001829.

Simó, R., and C. Pedros-Allió (1999a), Role of vertical mixing in controlling the oceanic production of dimethyl sulphide, *Nature*, *402*, 396–399.

Simó, R., and C. Pedros-Allió (1999b), Short-term variability in the open ocean cycle of dimethylsulfide, *Global Biogeochem. Cycles*, *13*, 1173–1181.

Simó, R., C. Pedrós-Alió, G. Malin, and J. O. Grimalt (2000), Biological turnover of DMS, DMSP and DMSO in contrasting open-sea waters, *Mar. Ecol. Prog. Ser.*, *203*, 1–11.

Singh, H., Y. Chen, A. Staudt, D. Jacob, D. Blake, B. Heikes, and J. Snow (2001), Evidence from the Pacific troposphere for large global sources of oxygenated organic compounds, *Nature*, *410*, 1078–1081.

Slezak, D., and G. J. Herndl (2003), Effects of ultraviolet and visible radiation on the cellular concentrations of dimethylsulfoniopropionate (DMSP) in *Emiliania huxleyi* (strain L), *Mar. Ecol. Prog. Ser.*, *246*, 61–71.

Slezak, D., A. Brugger, and G. J. Herndl (2001), Impact of solar radiation on the biological removal of dimethylsulfoniopropionate and dimethylsulfide in marine surface waters, *Aquatic Microbial Ecology*, *25*, 87–97.

Smirnov, A., B. N. Hoben, T. F. Eck, O. Dubovik, and I. Slutsker (2003), Effect of wind speed on columnar aerosol optical properties at Midway Island, *J. Geophys. Res.*, *108(D24)*, *4802*, doi:10.1029/2003JD003879.

Smith, R. C., and K. S. Baker (1979), Penetration of UV-B and biologically effective dose-rates in natural waters, *Photochem. Photobiol.*, *29*, 311–323.

Smith, S. J., H. Pitcher, and T. M. L. Wigley (2001), Global and regional anthropogenic sulfur dioxide emissions, *Global and Planetary Change*, *29*, 99–119.

Spitz, Y. H., J. R. Moisan, and M. R. Abbott (2001), Configuring an ecosystem model using data from the Bermuda Atlantic Time Series (BATS), *Deep-Sea Res., Part II*, *48*, 1733–1768.

Spivakovsky, C. M., et al. (2000), Three-dimensional climatological distribution of tropospheric OH: Update and evaluation, *J. Geophys. Res.*, *105(D7)*, 8931–8980.

Stark, H., et al. (2007), Influence of nitrate radical on the oxidation of dimethyl sulfide in a polluted marine environment, *J. Geophys. Res.*, *112 D10S10*.

Stefels, J. (2000), Physiological aspects of the production and conversion of DMSP in marine algae and higher plants, *J. Sea Res.*, *43*, 183–197.

Stefels, J., and M. A. van Leeuwe (1998), Effects of iron and light stress on the biochemical composition of antarctic *Phaeocystis* sp. (Prymnesiophyceae): I. Intracellular DMSP concentrations, *J. Phycol.*, *34*, 486–495.

Stefels, J., M. Steinke, S. Turner, G. Malin, and S. Belviso (2007), Environmental constraints on the production and removal of the climatically active gas dimethylsulphide (DMS) and implications for ecosystem modelling, *Biogeochemistry*, *83*, 245–275.

Stegmann, P. M., and N. W. Tindale (1999), Global distribution of aerosols over the open ocean an derived from the coastal zone color scanner, *Global Biogeochem. Cycles*, *13(2)*, 383–397.

Steinberg, D. K., C. A. Carlson, N. R. Bates, R. J. Johnson, A. F. Michaels, and A. H. Knap (2001), Overview of the US JGOFS Bermuda Atlantic Time-series Study (BATS): a decade-scale look at ocean biology and biogeochemistry, *Deep-Sea Res., Part II*, *48*, 1405–1447.

Steinke, M., G. Malin, S. D. Archer, P. H. Burkill, and P. S. Liss (2002a), DMS production in a coccolithophorid bloom: evidence for the importance of dinoflagellate DMSP lyases, *Aquatic Microbial Ecology*, *26*, 259–270.

Steinke, M., G. Malin, and P. S. Liss (2002b), Trophic interactions in the sea: An ecological role for climate relevant volatiles?, *Journal of Phycology*, *38*, 630–638.

Sunda, W., D. J. Kleber, R. P. Kiene, and S. Huntsman (2002), An antioxidant function for DMSP and DMS in marine algae, *Nature*, *418*, 317–320.

Swap, R., M. Garstang, and S. Greco (1992), Saharan dust in the Amazon Basin, *Tellus*, *44B*, 133–149.

Takemura, T., I. Uno, T. Nakajima, A. Higurashi, and I. Sano (2002), Modeling study of long-range transport of Asian dust and anthropogenic aerosols from East Asia, *Geophys. Res. Lett.*, *29(24), 2158*, doi:10.1029/2002GL016251.

Tanré, D., L. A. Remer, Y. J. Kaufman, S. Mattoo, P. V. Hobbs, J. M. Livingston, P. B. Russell, and A. Smirnov (1999), Retrieval of aerosol optical thickness and size distribution over ocean from the MODIS airborne simulator during TARFOX, *J. Geophys. Res.*, *104(D2)*, 2261–2278.

Tanré, D., F. M. Bréon, J. L. Deuzé, M. Herman, P. Goloub, F. Nadal, and A. Marchand (2001), Global observations of anthropogenic aerosols from satellite, *Geophys. Res. Lett.*, *28(24)*, 4555–4558.

Timmermann, R., H. Goosse, G. Madec, T. Fichefet, C. Ethe, and V. Duliere (2005), On the representation of high latitude processes in the ORCA-LIM global coupled seaice-ocean, *Ocean Modelling*, *8*, 175–201.

Tindale, N. W., and P. P. Pease (1999), Aerosols over the Arabian Sea: Atmospheric transport pathways and concentrations of dust and sea salt, *Deep-Sea Res. II*, *46*, 1577–1595.

Toole, D. A., and D. A. Siegel (2004), Ligth-driven cycling of dimethylsulfide (DMS) in the Sargasso Sea: Closing the loop, *Geophys. Res. Lett.*, *31*, doi:10.1029/2004GL019581.

Toole, D. A., D. J. Kieber, R. P. Kiene, D. A. Siegel, and N. B. Nelson (2003), Photolysis and the dimethylsulfide (DMS) summer paradox in the Sargasso Sea, *Limnol. Oceanogr.*, *48*, 1088–1100.

Toole, D. A., D. Slezak, R. P. Kiene, D. J. Kieber, and D. A. Siegel (2006), Effects of solar radiation on dimethylsulfide cycling in the western Atlantic Ocean, *Deep-Sea Res., Part I*, *53*, 136–153.

Turner, D., and N. J. P. Owens (1995), A biogeochemical study in the Bellingshausen Sea: overview of the STERNA 1992 expedition, *Deep-Sea Res., Part II*, *42*, 907–932.

Twomey, S. (1974), Pollution and planetary albedo, *Atmos. Environ.*, *8*, 1251–1256.

Uher, G., G. Schebeske, R. G. Barlow, D. G. Cummings, R. F. C. Mantoura, S. R. Rapsomanikis, and M. O. Andreae (2000), Distribution and air-sea gas exchange of dimethyl sulphide at the European western continental margin, *Marine Chemistry*, *69*, 277–300.

Vairavamurthy, A., M. O. Andreae, and R. L. Iverson (1985), Biosynthesis of dimethylsulfide and dimethylpropiothetin by Hymenomonas carterae in relation to sulfur source and salinity variations, *Limnology and Oceanography*, *30(1)*, 59–70.

Vallina, S. M. (2008), Reply to comment by Larsen on "Analysis of a potential 'Solar Radiation Dose - DMS -CCN' link from globally mapped seasonal correlations", *Global Biogeochem. Cycles*, submitted.

Vallina, S. M., and R. Simó (2007a), Strong relationship between DMS and the solar radiation dose over the global surface ocean, *Science*, *315*, 506–508.

Vallina, S. M., and R. Simó (2007b), Re-visiting the CLAW hypothesis, *Environmental Chemistry*, *4(6)*, doi:10.1071/EN07055.

Vallina, S. M., R. Simó, and S. Gassó (2006), What controls CCN seasonality in the Southern Ocean? A statistical analysis based on satellite-derived chlorophyll and CCN and model-estimated OH radical and rainfall, *Global Biogeochem. Cycles*, *20, GB1014*, doi:10.1029/2005GB002597.

Vallina, S. M., R. Simó, S. Gassó, C. de Boyer-Montégut, E. del Río, E. Jurado, and J. Dachs (2007a), Analysis of a potential 'Solar Radiation Dose - DMS - CCN' link from globally mapped seasonal correlations, *Global Biogeochem. Cycles*, *21, GB2004*, doi:10.1029/2006GB002787.

Vallina, S. M., R. Simó, and M. Manizza (2007b), Weak response of oceanic dimethylsulfide to upper mixing shoaling induced by global warming, *Proc. Natl. Acad. Sci., 104(41)*, 16,004–16,009.

Vallina, S. M., R. Simó, T. R. Anderson, A. Gabric, R. Cropp, and J. M. Pacheco (2008), A dynamic model of oceanic sulfur (DMOS) applied to the Sargasso Sea: simulating the dimethylsulfide (DMS) summer-paradox, *J. Geophys. Res. - Biogeosciences*, *113, G01009*, doi:10.1029/2007JG000415.

van den Berg, A., S. Turner, F. van Duyl, and P. Ruardij (1996), Model structure and analysis of dimethylsulphide (DMS) production in the southern North Sea, considering phytoplankton dimethylsulphoniopropionate-(DMSP) lyase and eutrophication effects, *Mar. Ecol. Prog. Ser., 145*, 233–244.

van Rijssel, M., and W. W. C. Gieskes (2002), Temperature, light, and the dimethylsulfoniopropionate (DMSP) content of *Emiliania huxleyi* (Prymnesiophyceae), *J. Sea. Res., 48*, 17–27.

Vézina, A. (2004), Ecosystem modelling of the cycling of marine dimethylsulfide: a review of current approaches and of the potential for extrapolation to global scales, *Can. J. Fish. Aquat. Sci., 61*, 845–856.

Vila, M., R. Simó, R. P. Kiene, J. Pinhassi, J. M. González, M. A. Moran, and C. Pedrós-Alió (2004), Use of microautoradiography combined with fluorescence in situ hybridization to determine dimethylsulfoniopropionate incorporation by marine bacterioplankton taxa, *Aquatic Environmental Microbiology, 70(8)*, 4648–4657.

Vila-Costa, M. (2006), Seasonality of DMSP contribution to S and C fluxes through phytoplankton and bacterioplankton in a NW Mediterranean coastal site, in *Major players in the biogeochemical cycling of dimethylated sulfur compounds in seawater*, Ph.D. thesis, Universitat Politècnica de Catalunya, available at www.cmima.csic.es/pub/gasol/tesi_laura/MASTER_Tesi_Sense_Linies.pdf.

Vila-Costa, M., D. A. del Valle, J. M. González, D. Slezak, R. P. Kiene, O. Sánchez, and R. Simó (2006a), Phylogenetic identification and metabolism of marine dimethylsulfide-consuming bacteria, *Environmental Microbiology, 8(12)*, 2189–2200, 10.1111/j.1462-2920.2006.01102.x.

Vila-Costa, M., R. Simó, J. M. Gasol, B. Harada, D. Slezak, and R. P. Kiene (2006b), Dimethylsulfoniopropionate (DMSP) uptake by marine phytoplankton, *Science, 314*, 652–654, doi:10.1126/science.1131043.

Vila-Costa, M., R. P. Kiene, C. Alonso, J. Pertnhaler, J. Pinhassi, and R. Simó (2007), Seasonal variation of DMSP-assimilating bacteria in the coastal NW Mediterranean, *Environmental Microbiology, 9*, 2451–2463.

Vila-Costa, M., R. P. Kiene, and R. Simó (2008), Seasonal variability of the dynamics of dimethylated sulfur compounds in a NW Mediterranean site, *Limnology and Oceanography*, in press.

Volk, T. (1998), *Gaia's Body: Toward a Physiology of Earth*, Springer-Verlag.

Walsh, J., D. A. Dieterle, and J. Lenes (2001), A numerical analysis of carbon dynamics of the Southern Ocean phytoplankton community: The roles of light and grazing in effecting both sequestration of atmospheric CO2 and food availability to larval krill, *Deep-Sea Res., Part I, 48*, 1–48.

Wangenbach, D., F. Ducroz, R. Mulvaney, L. Keck, A. Minikin, M. Legrand, J. S. Hall, and E. W. Wolff (1998), Sea-salt aerosol in coastal Antarctic regions, *J. Geophys. Res., 103(D9)*, 10,961–10,974.

Wilson, C., and V. J. Coles (2005), Global climatological relationships between satellite biological and physical observations and upper ocean properties, *J. Geophys. Res., 110, C10001*, doi:10.1029/2004JC002724.

Wolfe, G. V., M. Levasseur, G. Cantin, and S. Michaud (1999), Microbial consumption and production of dimethylsulfide (DMS) in the Labrador Sea, *Aquatic Microbial Ecology, 18*, 197–205.

Wolfe, G. V., S. L. Strom, J. L. Holmes, T. Radzio, and M. B. Olson (2002), Dimethylsulfoniopropionate cleavage by marine phytoplankton in response to mechanical, chemical, or dark stress, *J. Phycol., 38*, 948–960.

Wulff, A., and S.-A. Wängberg (2004), Spatial and vertical distribution of phytoplankton pigments in the eastern Atlantic sector of the Southern Ocean, *Deep-Sea Res., Part II, 51*, 2701–2713.

Wylie, D. J., and J. de Mora (1996), Atmospheric dimethylsulfide and sulfur species in aerosol and rainwater at a coastal site in New Zealand, *J. Geophys. Res., 101(D15)*, 21,041–21,049.

Yang, H., and H. R. Gordon (1997), Remote sensing of ocean color: Assessment of the water-leaving radiance bidirectional effects on the atmospheric diffuse transmittance, *Applied Optics*, *36(30)*, 7887–7897.

Yoch, D. C. (2002), Dimethylsulfoniopropionate: Its Sources, Role in the Marine Food Web, and Biological Degradation to Dimethylsulfide, *Aquatic Environmental Microbiology*, *68(12)*, 5804–5815.

Yoch, D. C., J. H. Ansede, and K. S. Rabinowitz (1997), Evidence for intracellular and extracellular dimethylsulfoniopropionate (DMSP) lyases and DMSP uptake sites in two species of marine bacteria, *Aquatic Environmental Microbiology*, *63(8)*, 3182–3188.

Yoon, Y. J., and P. Brimblecombe (2002), Modelling the contribution of sea salt and dimethylsulfide derived aerosol to marine CCN, *Atmos. Chem. Phys.*, *2*, 17–30.

Yuan, X. (2004), High-wind-speed evaluation in the Southern Ocean, *J. Geophys. Res., 109(D13101)*, doi: 10.1029/2003JD004179.

Zubkov, M. V., B. M. Fuchs, S. D. Archer, R. P. Kiene, R. Amann, and P. H. Burkill (2001), Linking the composition of bacterioplankton to rapid turnover of dissolved dimethylsulphoniopropionate in an algal bloom in the North Sea, *Environmental Microbiology*, *3(5)*, 304–311.

Zubkov, M. V., B. M. Fuchs, S. D. Archer, R. P. Kiene, R. Amann, and P. H. Burkill (2002), Rapid turnover of dissolved DMS and DMSP by defined bacterioplankton communities in the stratified euphotic zone of the North Sea, *Deep-Sea Res., Part II*, *49*, 3017–3038.

Zubkov, M. V., L. J. Linn, R. Amann, and R. P. Kiene (2004), Temporal patterns of biological dimethylsulfide (DMS) consumption during laboratory-induced phytoplankton bloom cycles, *Mar. Ecol. Prog. Ser.*, *271*, 77–86.

# Curriculum Vitae

## Personal Details

**Name:** Sergio Manuel Vallina Fernández.
**Date of birth:** 24 March 1976.
**Place of birth:** Oviedo (Asturias), Spain.
**e-mail:** sergio.vallina@gmail.com

## Education

**1995-2000:** Degree in "Marine Sciences/Oceanography".
University of Las Palmas de Gran Canaria (ULPGC).
Canary Islands, Spain.

**2001-2002:** MSc in "Biological Oceanography and Marine Environment".
Major in "Ecosystem Modelling".
University Pierre et Marie Curie (Paris VI).
Paris, France.

**2002-2003:** MSc in "Applied Physics".
Polytechnical University of Catalonia (UPC).
Barcelona, Spain.

**2002-2006:** PhD in "Marine Sciences/Oceanography".
Polytechnical University of Catalonia (UPC).
Barcelona, Spain.

## Current Position

**2007-present:** Post Doctoral Senior Research Associate.
University of East Anglia (UEA).
Norwich, United Kingdom.

## Research Stays

**2001 (Feb - Jun):**
Laboratoire d'Océanographie Dynamique et de Climatologie (LODYC - Paris VI). France.
Supervisor: Dr. Jean Michel André.

**2002 (Jan - Jun):**
Laboratoire d'Océanographie de Villefranche-sur-Mer (LOV - Paris VI). France.
Supervisors: Dr. Antoine Sciandra & Dr. Louis Prieur.

**2002 (Aug):**
Southampton Oceanography Centre (SOC). UK.
Supervisor: Dr. Ekaterina Popova.

**2003 (Sep - Dec):**
Southampton Oceanography Centre (SOC). UK.
Supervisors: Dr. Ekaterina Popova & Dr. Tom Anderson.

**2004 (Sep - Dec):**
Griffith University - Faculty of Environmental Sciences. Australia.
Supervisors: Dr. Albert Gabric & Dr. Roger Cropp.

**2005 (Oct - Dec):**
University of East Anglia - School of Environmental Sciences. UK.
Supervisor: Dr. Corinne Le Quéré.

## Computer Skills

**Programming Languages:** Fortran, MatLab, LaTex, HTML.
**Operating Systems:** Unix/Linux, MS-DOS.

# Funding

This thesis has been funded by the Spanish "Ministry of Education and Science" (MEC) through a PhD studentship under the program "Formación de Personal Investigador" (FPI).